Journal of the OPTICAL SOCIETY of AMERICA

VOLUME 39, NUMBER 12 DECEMBER, 1949

Editorial Comment

WITH the first issue of Volume XL a new editor will assume direction of the *Journal*. The present editor, after completing the responsibility of preparing his 120th issue for the publications office, has found it necessary to request release from the position, and the Society has been extremely fortunate in securing the services of Dr. Wallace R. Brode, Associate Director of the National Bureau of Standards, to take charge of the *Journal*. The editorial offices are now in process of being moved from Cambridge to Washington.

Dr. Brode brings to his new responsibility many years of experience as a teacher, author, and editor in the field of optics, a long familiarity with the purposes and traditions of the Optical Society of America, and a wide acquaintance among its membership. He has for some time been a director of the Society and an associate editor of the *Journal*. His interest in and enthusiasm for the publication program of the Society should help to insure a continuous and healthful growth of both Society and *Journal*.

The science of optics has grown very rapidly during the past decade, and this expansion has put on the Society and its journal increasing loads as the policy was followed of publishing the results of all worthy research as promptly as possible, preferably within three months of the receipt of a manuscript. Frequently this meant increasing the size of an issue beyond the page count envisaged in the budget, and several financial squalls have been weathered only because of the foresight and wise planning of those in charge of the Society. Though membership dues and subscription rates have been raised by only nominal amounts during the decade, the page count of research results published per year has approximately trebled. This growth, coupled with the constantly rising unit costs of publication, has made necessary the most careful budgeting and the adoption of such economies as smaller type, narrower margins, cheaper paper, and more economical distribution methods. That the *Journal* fills a constantly growing need in world optics is shown by the expansion of its subscription list from less than 1400 ten years ago to nearly 3700 today.

The retiring editor has derived from his relationship with the *Journal* the great satisfaction that comes from association with an active enterprise which is obviously fulfilling a real and pressing need. During the early days of the Society there were often months when the then Editor was forced to write around to friends and colleagues for articles wherewith to bring an issue up to the respectable minimum of 32 pages. When the now retiring editor took over, it was with the burning ambition of averaging 64 pages per issue, so that the magazine could attain the dignity of such thickness that the volume number and page limits could be printed on the back. The next editor will find as one of his most pressing problems that of keeping each issue within the 96 much larger pages now allowed for in the present budget, and as the science of optics grows in breadth and importance a still larger journal will be needed.

All this is an indication of the healthy state of American optics, and the growth of optical science throughout the world. With its new editor, the *Journal of the Optical Society of America* should be better fitted than ever to fulfill its important function.

GEORGE R. HARRISON

JOURNAL OF THE OPTICAL SOCIETY OF AMERICA VOLUME 39, NUMBER 12 DECEMBER, 1949

A Frustrated Total Reflection Filter for the Infra-Red

B. H. Billings
Research Laboratory, Baird Associates, Inc., Cambridge 38, Massachusetts

and M. A. Pittman
Madison College, Harrisonburg, Virginia

(Received August 18, 1949)

The Frustrated Total Reflection filter is a transmission band pass filter. It can be constructed for any part of the spectrum for which there exist transparent materials of different indices of refraction. Measurements are shown of a filter which was designed for the rocksalt infra-red region. This filter has two oppositely polarized pass bands which, at a particular angle of incidence, are at 4½ and 5 microns, respectively. Both the pass bands are approximately $\frac{1}{16}$ of a micron wide. They can be shifted over a range of approximately half a micron by tilting the filter.

THE isolation of a narrow band of wave-lengths is often a necessary part of a scientific experiment or of an industrial instrument. If the source of the band of wave-lengths is continuous, it is necessary to use either a monochromator or a narrow band filter. Until ten years ago, only a few special filters and techniques have been available. These include reststrahlen plates,[1] the Lyot polarization filter,[2] the Christiansen filter,[3] the reflection from potassium chlorate crystals,[4] and Lippmann plates.[5] Of these, the Lyot filter, the Lippmann plate, and the Christiansen filter provide a pass band anywhere in the visible spectrum. Only the Christiansen filter has ever been manufactured for use in the infra-red. The reststrahlen plates can only be used at those few wave-lengths where nature has provided materials with a narrow metallic reflection band. The potassium chlorate crystal has narrow pass bands whose location is determined by chance. Because of this and because of their small size they are not particularly useful as filters. The Christiansen filter is not image-forming and is not particularly useful either in the infra-red or ultra-violet.

During the last decade, an increasing number of filters have been developed which can be used to isolate a narrow band and which are image-forming. The solid Fabry-Perot filter is the most popular of these filters.[6] The filter is essentially a Fabry-Perot etalon operating in the first and second order with a solid dielectric spacer. The operation of the etalon is discussed in most textbooks on optics.[7] It consists simply of two parallel plates separated by an air gap. The surfaces of the plates which face the gap are partially silvered. The action of the interferometer may be explained by assuming that at the first silvered surface the light is partly reflected and partly transmitted. The transmitted part continues to the second silvered surface where it is again partly reflected and partly transmitted. The reflected light passes back to the first surface. Part of this light is transmitted and joins with the light that was previously reflected. If these two beams are out of phase the light will be transmitted through the plates. If they are in phase, it will be reflected. For a quantitative treatment of the instrument it is necessary to consider multiple reflections between the plates.

The standard treatment ignores absorption in the film and leads to the equation

$$\frac{I}{I_0}=\frac{t^2}{t^2+4r\sin^2\delta}, \tag{1}$$

where I is the intensity of the transmitted light, I_0 the intensity of the incident light, t the transmission of the reflecting film, r its reflectivity, and δ the phase shift through dielectric layer. This phase shift is equal to $(2\pi nd/\lambda)$, where n is the index of the layer between the plates and d is its thickness. This equation has a maximum at all wave-lengths at which the optical thickness, "nd," is a whole number of half-waves.

In Fig. 1 is a family of curves of the transmission of the filter represented by Eq. (1). As the reflectivity of the boundary layers increases, the band width of the filter narrows. The peak transmission, however, stays constant. The exact behavior of a metal layer must include absorption. It has been carried through by several workers.[8] The exact treatment of the interference filter has been given by Hadley.[6]

Figure 2 shows the curves which are derived from his formulas. It is clear that the band width cannot be narrowed indefinitely without losing peak transmission to the extent that the filter is no longer useful. Similarly, if the reflectivity is lowered the filter loses its value because of the increased transmission away from the peak. Another limitation on these filters is that they are only useful in the visible part of the spectrum. The characteristics of metals are such that the filters cannot be made to operate either in the ultraviolet or infrared spectral regions. In both these regions the absorption associated with a film of given reflectivity is much higher than in the visible spectrum.

---

[1] John Strong, ***Procedures in Experimental Physics*** (Prentice-Hall, Inc., New York, 1943). Maurice Parodi, ***Recherches dans L'Infrarouge Lointain par la Methode des Rayons Restants*** (Hermann & Cie, Paris, 1938).

[2] B. Lyot, Comptes Rendus **197**, 1593 (1933).

[3] C. Christiansen, Ann. Physik u. Chemie **23**, 298 (1884); **24**, 439 (1885). E. D. McAlister, Smithsonian Misc. **93**, No. 7 (1935).

[4] R. W. Wood, ***Physical Optics*** (The Macmillan Company, New York, 1934), p. 199.

[5] See reference 4, p. 214.

[6] L. N. Hadley and D. M. Dennison, J. Opt. Soc. Am. **37**, 451–465 (1947); **38**, 483–496 (1948).

[7] See reference 4. Also, F. A. Jenkins and H. E. White, ***Fundamentals of Physical Optics*** (McGraw-Hill Book Company, Inc., New York, 1937).

[8] Thornton Fry, J. Opt. Soc. Am. **22**, 307 (1932).

The results shown in Fig. 2 are rather disappointing compared with the curves of Fig. 1. The tremendous gain to be realized by having materials of high reflectivity with low absorption makes the search for such materials particularly keen. There are actually no metals which will give any better results than those shown in Fig. 2. There are, however, three methods which have been used to achieve surfaces with high reflectivity and low absorption. All these methods give results which are better than those shown in Fig. 2.

These methods are: (1) The Frustrated Total Reflection filter which was described by Turner[9] at the Cincinnati meeting of the Optical Society. (2) The use of multiple layers of dielectric. (3) The use of multilayers of dielectric in combination with layers of silver.

THEORY OF THE FRUSTRATED TOTAL REFLECTION FILTER

This filter uses the principle of the penetration into the second medium which occurs when light is incident on a surface beyond the angle of total internal reflection. When light is sent through the base of a right angle prism it is reflected at the hypotenuse. This reflection is 100 percent if the light strikes the hypotenuse of the prism at an angle of incidence greater than the critical angle. If now a convex lens is put in contact with the hypotenuse, the light at the point of contact will not be reflected but instead will be transmitted into the lens. When the light reflected from the prism hypotenuse is observed, a black spot is seen where this penetration takes place. The size of this black spot is found to be much larger than one would expect if the light went through only where actual optical contact were achieved. In other words, the light appears to penetrate into the air space between the lens and the prism and where that air space is sufficiently thin, it is able to reach the lens surface and be transmitted. Examination of Maxwell's equations at the prism hypotenuse shows that at angles bigger than the critical angle, the light actually does penetrate into the low index medium. In this medium the amplitude drops off exponentially with the distance. If a high index surface is placed close enough to the hypotenuse so that the light amplitude has not dropped to zero, then a fraction of the incident light will be transmitted. No light will be lost in the low index layer. The surface of this low index layer thus constitutes a semitransparent reflector with no absorption loss.

The Frustrated Total Reflection filter consists of two such semitransparent reflectors. The prism hypotenuse is covered with a low index layer whose thickness is determined by the desired reflectivity. This is followed by a high index layer whose thickness determines the wave-length which will be transmitted. Another low index layer is then deposited so as to give another frustrated total reflection. Another prism is then laminated to the first prism with a material whose index is the same as the prism material. The resulting rhomb constitutes the interference filter.

The Frustrated Total Reflection filter, unlike the regular solid Fabry-Perot filter, has no inherent limitations which make it unsatisfactory for wave-lengths in the ultraviolet or infra-red. The only requirements are that the materials of which the filter is made be transparent in the desired spectral region and that the indices have the proper relationship.

In studying the Frustrated Total Reflection filter the quickest insight into its behavior is obtained by con-

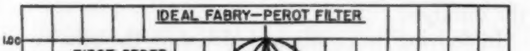

FIG. 1. Transmission as a function of wave-length and film reflectivity of an ideal Fabry-Perot filter operating in the first order.

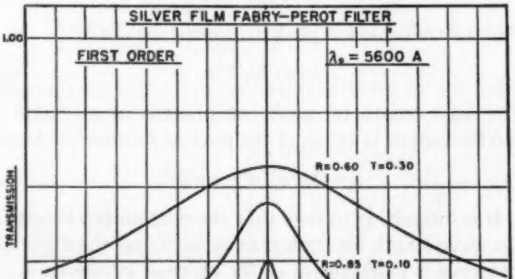

FIG. 2. Transmission as a function of wave-length and silver film reflectivity of a Fabry-Perot filter operating in the first order.

---

[9] Paul Leurgans and A. F. Turner, J. Opt. Soc. Am. 37, 983 (1947).

sidering it as a simple Fabry-Perot filter. The wave-length of peak transmission is determined by the thickness of the high index layer and the band width by the thickness of the low index layer. Equation (1) gives a good approximation to the behavior of the Fabry-Perot filter at normal incidence. When the filter is tilted the equivalent thickness of the high index layer changes and the peak transmission accordingly changes.

The change of peak transmission with angle of incidence is most easily derived by considering the behavior of the filter as arising from the interference of the light reflected from the first silver surface with light reflected from the second silver surface.

The retardation through a Fabry-Perot interference filter can be written

$$\Gamma=[2d(n^2-\sin^2\theta)^{\frac{1}{2}}]/\lambda, \tag{2}$$

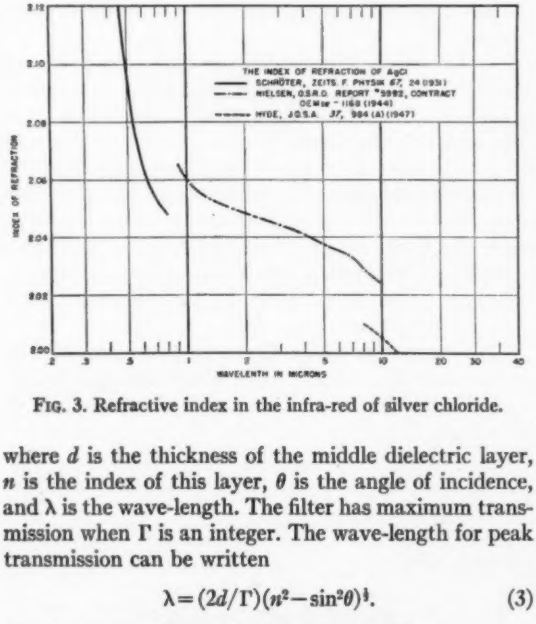

FIG. 3. Refractive index in the infra-red of silver chloride.

where d is the thickness of the middle dielectric layer, n is the index of this layer, θ is the angle of incidence, and λ is the wave-length. The filter has maximum transmission when Γ is an integer. The wave-length for peak transmission can be written

$$\lambda=(2d/\Gamma)(n^2-\sin^2\theta)^{\frac{1}{2}}. \tag{3}$$

For the transmission peak at normal incidence

$$\lambda_0=(2d/\Gamma)n. \tag{4}$$

The wave-length for peak transmission at an angle θ can be written in terms of the peak at normal incidence

$$\lambda=(\lambda_0/n)(n^2-\sin^2\theta)^{\frac{1}{2}}. \tag{5}$$

It is interesting to note that the relationship between the wave-length for peak transmission and the angle of incidence is independent of the order of interference.

Since the wave-length of peak transmission varies with the angle of incidence, it is apparent that the angular field of view of the filter, for monochromatic light, is directly related to the width of the pass band. The angular field can be considered as twice the angle through which the filter must be turned to drop the transmission by 50 percent. From Eq. (5) this can be written

$$\Theta=2\sin^{-1}\left[n\left(\frac{\lambda_0^2-\lambda_{I/2}^2}{\lambda_0^2}\right)^{\frac{1}{2}}\right], \tag{6}$$

where Θ is the angular field of view and $\lambda_{I/2}$ is the wave-length at which the transmission through the filter is one-half the transmission at the peak.

If the transmission of the filter for monochromatic light is measured in a system whose angular field of view is wider than the angular field of the filter, it will appear lower than the transmission for a collimated beam. In other words, in monochromatic light, the filter passes light over an angle Θ. Light incident at angles outside Θ is not transmitted. In a beam in which the intensity is uniformly distributed over an angle $\alpha>\Theta$, the transmission will be approximately

$$T=T_N(\Theta/\alpha), \tag{7}$$

when T_N is the transmission at normal incidence.

By the same token, the band width of a filter will appear wider if it is examined in a system of greater angular aperture than the angular field of the filter. The beam can be split into angular sections of width Θ. Each section will have a transmission peak at a different wave-length. At each wave-length the transmission will be given by Eq. (7). The apparent band width will be approximately

$$\Delta\lambda=(\alpha/\Theta)\Delta\lambda_N, \tag{8}$$

where $\Delta\lambda_N$ is the band width at normal incidence.

The same criteria which establish the angular field of view of the filter also establish the tolerance which must be placed on the homogeneity and plane parallelism of the various layers. If the low index layer is of such thickness that the filter band width is 1/1000 of the wave-length of the pass band, the high index layer must be plane parallel to within better than 1/1000 of the thickness.

In deriving the equations which show the behavior of the filter, it was considered that the phase shift through the filter depended entirely on the thickness of the high index layer. Actually, there is another additional phase difference between the light which goes directly through the high index layer and the light which is reflected from the opposite sides of this layer. This is caused by the phase change which occurs when light is reflected at a boundary. At normal incidence and with silver boundary films this additional phase shift merely means that the peak wave-length is slightly displaced from the position calculated on the basis of Eq. (1). When light goes through the filter obliquely, the phase shift on reflection becomes different for the two states of polarization. This results in splitting of the filter pass bands. This splitting can be demonstrated in the ordinary Fabry-Perot filter and has been discussed by Hadley.[8] In the Frustrated Total Reflection filter there

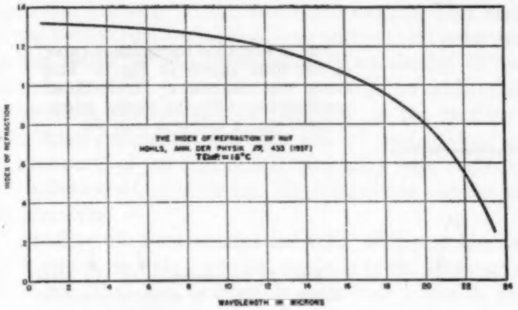

FIG. 4. Infra-red refractive index of sodium fluoride.

is also a phase shift on reflection and, as in the case of the Fabry-Perot filter, this phase shift is different for the two states of polarization. The angular shift can be calculated from the equations

$$\tan\frac{\delta_p}{2}=\frac{(\sin^2\theta-(n_1/n_0)^2)^{\frac{1}{2}}}{(n_1/n_0)^2\cos\theta};$$

$$\tan\frac{\delta_s}{2}=\frac{(\sin^2\theta-(n_1/n_0)^2)^{\frac{1}{2}}}{\cos\theta},\tag{9}$$

where δ_s is the phase shift for light polarized perpendicularly to the plane of incidence, δ_p is the phase shift for light polarized parallel to the plane of incidence, n_1 is the index of the low index layer, n_0 the index of the prism, and θ the angle of incidence. This difference in phase which takes place on total internal reflection is used in the Fresnel rhomb to convert linearly polarized light to circularly polarized light.

As a result of this phase difference all the pass bands of the Frustrated Total Reflection filter are doubled. The long wave pass band is for light polarized perpendicularly to the plane of incidence, the short wave pass band for the light polarized in the plane of incidence. Because the pass bands are thus polarized, the maximum transmission in any band is 50 percent for unpolarized light.

AN INFRA-RED FRUSTRATED TOTAL REFLECTION FILTER

It seemed interesting to attempt to construct a very narrow band filter to operate in the rocksalt infra-red region. One problem was the choice of materials for the various layers in the filter. These layers had to be of high and low index, transparent in the infra-red and easily evaporated. This last requirement was fairly difficult because few materials can be evaporate tod make smooth, thick layers. Figures 3 and 4 show the dispersion curves of AgCl and NaF which were the two materials finally selected. The indices given in these curves are for bulk materials. For evaporated layers the indices are probably different. Unfortunately, very little work has been done in determining the indices of evaporated layers, either in the visible or infra-red.

A first attempt to make the filter was made using prisms of KRS-5. Since this material has a very high index it was not possible to find a laminating liquid of the same index; accordingly, it was decided to use a laminating liquid for the low index layer. The filter was constructed with an evaporated layer of sodium fluoride of an optical thickness of 11/4 waves at 6500A and of silver chloride of an optical thickness of 11/4 waves at 6500A, followed by a layer of mineral oil for the next low index layer and as a laminating fluid. No energy was transmitted by the filter at any wave-length. It was decided that the control of the uniformity and thickness of the low index liquid layer was going to be too difficult to make this particular prism work. A prism of rocksalt was located. This was a 60° prism and was sawed in two so as to make two 30, 60, 90 prisms. The hypotenuses of these prisms were polished. A low index layer of sodium fluoride was evaporated on one of these surfaces to an optical thickness of 17/2 waves at 6500A. This was followed by a layer of silver chloride evaporated to a thickness of 23/4 waves at 6500A and a second layer of sodium fluoride. The prisms were then laminated with mineral oil. A sketch of the resulting filter is shown in Fig. 5. The predicted location of the peaks can be calculated approximately from the Fabry-Perot formulas. From Eq. (4) the wave-length peak at normal incidence for the first order is

$$\lambda_0=2dn=2\times\frac{23}{4}\times\frac{6500\times n'}{n_{6500}}.\tag{10}$$

Here n' is the index at the wave-length of the peak. Since the dispersion of AgCl is small, a good approximation is obtained simply by assuming $n'=n_{6500}$ and then getting a more exact value by using the value of n' corresponding to resulting peak wave-length. The value of n_{6500} for AgCl is found from Schröter[10] to be 2.06. The final calculation gives $\lambda_0=7.3\mu$.

From Eq. (5) the wave-length for peak transmission in the 60° filter is

$$\lambda=\frac{7.3\times n_{\mathrm{NaCl}}}{n_{\mathrm{AgCl}}}\left[\left(\frac{n_{\mathrm{AgCl}}}{n_{\mathrm{NaCl}}}\right)^2-\sin^2 60°\right]^{\frac{1}{2}}=5.6\mu.\tag{11}$$

Here all the high layer indices are divided by the index

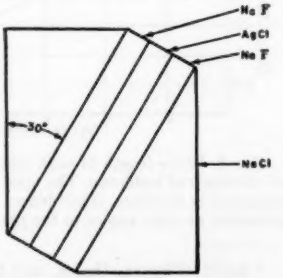

FIG. 5. Sketch of infra-red Frustrated Total Reflection filter. The rhomb has dimensions approximately $1\frac{1}{4}$ in.×$1\frac{1}{4}$ in.×2 in.

---

[10] Schröter, Zeits. f. Physik 67, 24 (1931).

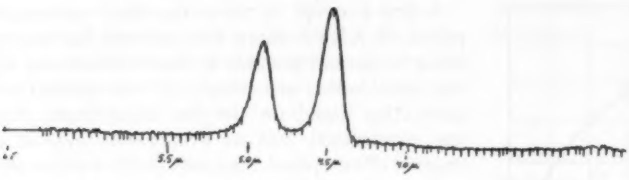

FIG. 6. Recorded transmission curve of the filter shown in Fig. 5. This curve was run on a Perkin-Elmer spectrometer with the source mirror covered with a half-inch wide slit.

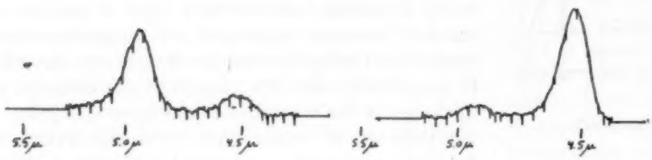

FIG. 7. Transmission of the filter shown in Fig. 5 in series with a two-plate silver chloride polarizer.

of NaCl since the filter is effectively embedded in this material. To locate the pass bands, transmission curves were run of the resulting rhomb with a Baird Associates double beam infra-red spectrometer.[11] A curve was also run to show the transmission of the mineral oil.

As predicted from the values of the thickness of the high index layer, the filter had a first-order peak at approximately 5.6μ. The prediction could probably have been made closer if the exact formula for the filter transmission had been used.

The filter was then studied with a Perkin-Elmer spectrometer in the Massachusetts Institute of Technology spectroscopy laboratory. The problem of measuring the spectral transmission of the finished filter was complicated by the dependence of band width and peak transmission on angular field of view. As a result of preliminary measurements it became apparent that the angular size of the beam was greater than the field of the filter. Accordingly, the angular size of the beam was diminished by putting a stop over one of the source mirrors. In order to avoid cutting down the energy too much, the stop was made in the form of a slit with its axis parallel to the plane of the prism hypotenuse. The slit reduced the beam width to approximately 3°.

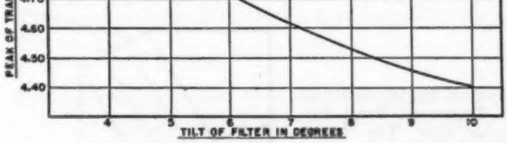

FIG. 8. Wave-length of peak transmission of filter as a function of the angle of incidence. The upper curve is for the peak which is polarized in the plane of incidence. The lower curve is for the peak polarized at right angles to the plane of incidence.

In Fig. 6 is a transmission curve of the filter. The band width of the two peaks is about 0.1μ. This seems wide for the particular thickness of the low index layer. This large width may very well be caused by the large angular beam in which the prism was examined.

To demonstrate the polarization of the bands a transmission polarizer was made of two sheets of silver chloride[12] at 63° to the beam. The use of such polarizers in the infra-red has been described by Wright[13] and by Halford.[14] Since two sheets are not sufficient to give complete polarization of the beam, neither transmission band of the filter can be completely extinguished. In Fig. 7 is shown the transmission of the filter with the polarizer first parallel and then perpendicular to the plane of incidence on the prism hypotenuse.

The variation of the transmission peak with angle of incidence was measured for both states of polarization and is shown in Fig. 8. The small size of the angular field of view is immediately apparent from this curve.

APPLICATION OF THE INFRA-RED FILTER

A most important use of the filter in the infra-red should be in problems of gas analysis. In this application one of the two pass bands of the filter is made to coincide with an absorption band of the gas to be detected. The other pass band is placed in a region where the gas has no absorption band. A polarizer is rotated in front of the filter. A beam of radiation is passed through the polarizer, the filter, a gas cell, and on to a detector such as a bolometer or thermocouple. With no gas present in the gas cell, an alternating current signal will be present in the detector because of the slight difference in radiation intensity at the two wave-lengths. This zero signal can be removed optically as with a third polarizer in the system or can be removed electronically. If the absorbing gas is present in the gas cell, an additional alternating current will be produced in the receiver. For small concentrations, this will be proportional to the amount of gas in the cell. Anything which affects both beams will not change the alternating current in the receiver.

---

[11] Baird, O'Bryan, Ogden, and Lee, "An automatic recording infra-red spectrophotometer," J. Opt. Soc. Am. 37, 754–761 (1947).

[12] Silver chloride sheets are provided by the Harshaw Chemical Company, Cleveland, Ohio.

[13] N. Wright, J. Opt. Soc. Am. 38, 69 (1948).

[14] R. Newman and R. S. Halford, Rev. Sci. Inst. 19, 270 (1948).

Another use for the infra-red filter will, perhaps, be as a means for doing spectral analysis in the long wave infra-red. It should be possible with these filters to get resolutions as high as 1000. At 300μ this is difficult to achieve by other means.

Since the pass band of the filter can be tuned over a range, perhaps 10 percent of the wave-length of the pass band, a fairly large spectral range could be covered with just a few filters.

The authors are especially indebted to Professor Richard Lord of the Massachusetts Institute of Technology for permission to use the equipment of the Massachusetts Institute of Technology spectroscopy laboratory. They are also indebted to Mr. Robert MacDonald for his help in making the measurements.

Electronics for Spectroscopists

During the week of July 23rd to 30th a summer school on "Applied Electronics for Spectroscopists," sponsored by the Photoelectric Spectrometry Group, was held at University College, Southampton, England, by arrangement with Professor E. E. Zepler (Electronic Engineering) and Professor A. M. Taylor (Physics) and their staffs. Mr. C. G. Cannon was organizer for the group.

The syllabus was designed to meet the needs of spectroscopists requiring electronic techniques, and of electronic engineers who have to design suitable equipment. Its value was confirmed by very good attendance.

Lectures and demonstrations were given by Professor Zepler, and by Messrs S. W. Punnett, T. B. Tomlinson, and G. H. Johns of the University College. Professor A. M. Taylor gave an introductory talk on the research in progress in the Physics Department which stimulated many informal discussions. Three members of the Group, Messrs P. Popper (Mitcham Works, Ltd.), J. C. O. Rochester (Sir Howard Grubb, Parsons and Company), and E. Schwarz (Hilger and Watts, Ltd.) also contributed lectures on special subjects.

A full account of the summer school will appear in the Photoelectric Spectrometry Group Bulletin and it is hoped eventually to issue the complete notes of the course in book form.

JOURNAL OF THE OPTICAL SOCIETY OF AMERICA VOLUME 39, NUMBER 12 DECEMBER, 1949

Color Correction in Optical Systems and Types of Glass*

M. Herzberger and H. Jenkins
Kodak Research Laboratories, Eastman Kodak Company, Rochester, New York

(Received August 22, 1949)

The authors suggest that the optical qualities of a transparent material are given with the help of three graphs, one a plot of the reciprocal dispersion $1/(n_F-n_C)$ against the ν-value, the other two giving two data ρ_A and ρ_h signifying the deviation of the dispersion of the glass toward the red and violet ends of the spectrum from the regular standard. A universal dispersion formula is given which permits one (a) to calculate the refractive index for any given wave-length if the above data are given; and (b) to compute the above data if the refractive index is given for four or more values.

The dispersion formula is linear with respect to the given data.

The graphs so designed permit one to estimate immediately the powers of a doublet corrected for two wave-lengths and the amount of the secondary spectrum in the red and violet ends for any two given glasses.

Testing these formulas for different types of glass and other optically important materials (fluorite, quartz, lithium fluoride, salt, etc.) shows an agreement with the measurements throughout the spectrum which is sufficient for optical calculation ($\pm 2\times 10^{-6}$).

It is well known that an achromatic lens with ordinary glasses cannot be corrected for secondary spectrum. This is one of the results of the fact that the dispersion of an ordinary optical glass is given if two of its data are given, for instance, its refractive index for D light n_D and the ν value $\nu=(n_D-1)/(n_F-n_C)$.

However, it is known that there exist optical substances, even glasses, the dispersion of which deviates from those of ordinary glasses, for example, fluorite, the short flints of various origins, and the new Eastman Kodak glasses. One of the authors has shown before that the optical properties of all these optical materials are given if four of their data are known and has suggested a dispersion formula which is linear with respect to the glass data and which has been tested throughout the visible spectrum from $\lambda=0.400$ up to infra-red wave-lengths of 1μ.

$$\mu=\mu_0+\mu_1\lambda^2+\mu_2/(\lambda^2-0.035)+\mu_3/(\lambda^2-0.035)^2. \quad (1)$$

In this formula λ is the wave-length measured in microns, $\mu=n-1$ is the refractive index of the substance diminished by 1, and μ_0, μ_1, μ_2, and μ_3 are four material constants.

Equation (1) shows that optical glass and other transparent material are given by four data. It is the attempt of the authors in this paper to select data which are easily computed and give at the same time all the necessary information about the properties of glasses for optical correction. An introductory section gives the well-known formulas for color correction of a pair of thin lenses in contact. In the second part of the paper a procedure is devised for finding four universal functions, the knowledge of which gives the desired dispersion formula. A final part contains tables showing the accuracy of the suggested dispersion formula for all types of optical glass. Three graphs are suggested in order to plot the basic data of optical glasses and rules are given on how to use these tables for information with respect to the color correction of a doublet made of a pair of glasses. The specially desirable properties of the Eastman Kodak glasses will be apparent.

1. THE COLOR CORRECTION OF A DOUBLET

Let

$$\begin{aligned}K_1&=(1/r_2-1/r_1)_1\\ K_2&=(1/r_2-1/r_1)_2\end{aligned} \quad (2)$$

be the *total curvatures* of two thin lenses (r_1 and r_2 being the first and second radii for each of the lenses). It is well known that the power of the two lenses, if in contact, is then given by

$$\Phi=(n_1-1)K_1+(n_2-1)K_2=\mu_1K_1+\mu_2K_2. \quad (3)$$

In this formula Φ, n_1, n_2, or μ_1, μ_2 are functions of the wave-length, λ. In particular, we have

$$\begin{aligned}\Phi_D&=\mu_{1D}K_1+\mu_{2D}K_2\\ \Phi_F-\Phi_C&=(\mu_{1F}-\mu_{1C})K_1+(\mu_{2F}-\mu_{2C})K_2\\ \Phi_\lambda-\Phi_D&=(\mu_{1\lambda}-\mu_{1D})K_1+(\mu_{2\lambda}-\mu_{2D})K_2,\end{aligned} \quad (4)$$

where D, F, C characterize the wave-lengths $\lambda=589.3\mu$, 486.1μ, and 656.3μ, respectively, and λ means an arbitrary wave-length.

Let us introduce Abbe's ν-value,

$$\nu=\mu_D/(\mu_F-\mu_C), \quad (5)$$

and the so-called partial dispersion, P_λ, for the wave-length λ:

$$P_\lambda=(\mu_\lambda-\mu_D)/(\mu_F-\mu_C). \quad (6)$$

Equations (4) can then be written

$$\begin{aligned}\Phi_D&=\mu_{1D}K_1+\mu_{2D}K_2\\ \Phi_F-\Phi_C&=(\mu_{1D}K_1/\nu_1)+(\mu_{2D}K_2/\nu_2)\\ \Phi_\lambda-\Phi_D&=(\mu_{1D}K_1/\nu_1)P_{1\lambda}+(\mu_{2D}K_2/\nu_2)P_{2\lambda}.\end{aligned} \quad (7)$$

Eliminating K_1 and K_2 from these formulas, we find the equation

$$\begin{vmatrix}\Phi_D & 1 & 1\\ \Phi_F-\Phi_C & 1/\nu_1 & 1/\nu_2\\ \Phi_\lambda-\Phi_D & P_1/\nu_1 & P_2/\nu_2\end{vmatrix}=0 \quad (8)$$

---

* Communication No. 1285 from the Kodak Research Laboratories.

or

$$\Phi_D(P_2-P_1)-(\Phi_F-\Phi_C)(P_2\nu_1-P_1\nu_2)+(\Phi_\lambda-\Phi_D)(\nu_1-\nu_2)=0.$$

A doublet is called achromatized if $\Phi_F-\Phi_C=0$; it shall be called *apochromatized* if we have $\Phi_\lambda=\Phi_D$, where λ is in the red or violet end of the spectrum.

We therefore have in an achromat

$$\Phi_\lambda-\Phi_D=(P_2-P_1/\nu_2-\nu_1)\Phi_D. \tag{9}$$

An apochromat for the wave-length λ is given by

$$P_2=P_1. \tag{10}$$

These are the basic formulas for a chromatic, achromatic, or apochromatic doublet consisting of two glasses. For an achromat (and therefore an apochromat), we can compute K_1 and K_2 as functions of Φ_D and obtain from

$$\begin{aligned}\Phi_D&=\mu_{1D}K_1+\mu_{2D}K_2\\ 0&=(\mu_{1D}K_1/\nu_1)+(\mu_{2D}K_2/\nu_2)\end{aligned} \tag{11}$$

the result:

$$\begin{aligned}K_1&=\Phi_D\frac{\nu_1/\mu_1}{\nu_1-\nu_2}=\frac{(1/n_F-n_C)_1}{\nu_1-\nu_2}\Phi_D=\frac{N_1}{\nu_1-\nu_2}\Phi_D\\ K_2&=\Phi_D\frac{\nu_2/\mu_2}{\nu_2-\nu_1}=\frac{(1/n_F-n_C)_2}{\nu_2-\nu_1}\Phi_D=\frac{N_2}{\nu_2-\nu_1}\Phi_D,\end{aligned} \tag{12}$$

if we use the abbreviation $1/(\mu_F-\mu_C)=N$ (reciprocal dispersion).

2. THE DISPERSION FORMULA

It is well known that for ordinary glasses the partial dispersion, P_λ, for a given wave-length λ is a linear function of ν. We therefore have for ordinary glasses

$$P_\lambda=A_1\nu+A_2, \tag{13}$$

where A_1 and A_2 are universal functions of the wave-length λ.

If we wish to include extraordinary glasses, we must replace formula (13) by

$$P_\lambda=A_1\nu+A_2+\rho_\lambda, \tag{14}$$

where ρ_λ is a function of the wave-length which is, in general, different from glass to glass. However, in the previous paper of one of the authors[1] it was found empirically that

$$\rho_\lambda=A_3\rho_A+A_4\rho_h, \tag{15}$$

where A_3 and A_4 are again universal functions of the wave-length, and ρ_A, and ρ_h are two constants, the deviations from formula (13) for the red end of the spectrum (wave-length 768.2) and the violet end of the spectrum (wave-length 404.7).

Thus, we find that

$$P_\lambda=A_1\nu+A_2+A_3\rho_A+A_4\rho_h \tag{16}$$

and, in particular,

$$\begin{aligned}P_A&=A_{1A}\nu+A_{2A}+\rho_A\\ P_h&=A_{1h}\nu+A_{2h}+\rho_h.\end{aligned} \tag{17}$$

The above formulas show that the knowledge of μ_D, ν, ρ_A, and ρ_h, or of $N=1/(\mu_F-\mu_C)$, ν, ρ_A and ρ_h is sufficient to compute the refractive index for all wave-lengths if the four universal functions A_1, A_2, A_3, and A_4 are given. For we have

$$N\mu_\lambda=[(A_1+1)\nu_D+A_2+A_3\rho_A+A_4\rho_h], \tag{18}$$

as can easily be verified with the help of (16), (5), and (6).

The problem still to be solved is to find the universal functions, A_1 to A_4. In the paper mentioned previously, formulas were given for A_1 and A_2, but the method pursued there did not give sufficiently well-determined values for A_3 and A_4, which therefore were only published in the form of a graph.

In the following section we shall describe the rather complex way in which we succeeded in arriving at a well-defined analytical representation of A_1, A_2, A_3, and A_4. It is of course obvious that the general dispersion formula (1) leads to the supposition that each A_i, as well as other functions used in this paper, have the equivalent form

$$A_i=\alpha_0+\alpha_1\lambda^2+\alpha_2/(\lambda^2-0.035)+\alpha_3/(\lambda^2-0.035)^2, \tag{19}$$

i.e., that it is given by four constants.

3. COMPUTATION OF THE UNIVERSAL FUNCTIONS, A_i

Our investigation first led us to ask how many data are sufficient to determine the refractive index as a function of the wave-length.

TABLE I.

$B_1=+17.417526$	$-18.928074\lambda^2$	$-3.958817/(\lambda^2-0.035)$	$+0.272352/(\lambda^2-0.035)^2$
$B_2=-\ 9.748519$	$+12.813951$	$+2.005768$	-0.131427
$B_3=+\ 2.381957$	$-\ 2.006448$	-0.824828	$+0.088733$
$B_4=-\ 9.050963$	$+\ 8.120572$	$+2.777877$	-0.229657
$A_1=+\ 0.001990$	$-\ 0.007841$	$+0.000867$	-0.000199
$A_2=-\ 1.320066$	$+\ 0.124839$	$+0.382922$	$+0.004920$
$A_3=-\ 8.277312$	$+10.913521$	$+1.798107$	-0.123920
$A_4=+\ 2.686801$	$-\ 2.400230$	-0.867857	$+0.090289$

---

[1] M. Herzberger, "The dispersion of optical glass," J. Opt. Soc. Am. **32**, 70–77 (1942).

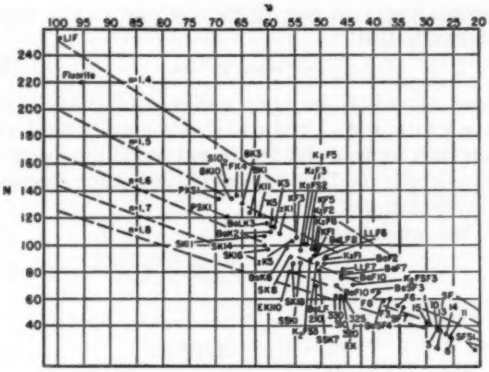

Graph I. Reciprocal dispersion plotted against ν-value. The inclined lines designate the index of refraction.

We found empirically the existence of four universal functions, B_1, B_2, B_3, and B_4 such that

$$\mu_\lambda-\mu_F=B_1(\mu_C-\mu_F)+B_2(\mu_A-\mu_F)+B_3(\mu_h-\mu_F) \quad (20)$$

or

$$\mu_\lambda=B_1\mu_C+B_2\mu_A+B_3\mu_h+B_4\mu_F$$

with

$$B_1+B_2+B_3+B_4=1.$$

The result showed good agreement with the catalog data. However, a logical analysis shows that we do not need to determine the functions B_i empirically as long as we assume that they can be given by a formula of the type (19).

This assumption made, the functions B_i are completely determined, since we know their values for four wave-lengths ($C=656.3$, $A=768.2$, $h=404.7$, $F=486.1$), since B_1 must equal 1 for $\lambda=656.3$ and 0 for the other three wave-lengths; analogously, B_2 equals 1 for $\lambda=768.2$ and 0 for the other wave-lengths, and correspondingly for B_3 and B_4.

Thus, we have obtained four universal functions, B_1, B_2, B_3, and B_4 (see Table I), which are derived theoretically without recourse to empirical material. It was gratifying to us that these functions found theoretically led to a dispersion formula, which is accurate for all optical materials.

For theoretical reasons, however, we want to obtain analytically formulas for the functions, A_1 to A_4. To find them, we proceeded in two steps. First, because of the linearity of (20), any four data are sufficient to compute μ as a function of the wave-length.

We can, for instance, choose μ_D, $\mu_F-\mu_C$, μ_A and μ_h as given data and will then obtain for μ_λ an equation equivalent to (20), namely,

$$\mu_\lambda=C_1\mu_D+C_2(\mu_F-\mu_C)+C_3\mu_A+C_4\mu_h, \quad (21)$$

where the C_i's are again well-defined functions of λ.

There are two ways to construct the functions, $C_i(\lambda)$. First, the C_i's are linear functions of the B_i's. We can construct them, as follows: Eq. (20) gives for $\lambda=D, F, C, A$, and h, respectively,

$$\begin{array}{rllll} \mu_D= & B_{1D}\mu_C & +B_{2D}\mu_A & +B_{3D}\mu_h & +B_{4D}\mu_F \\ \mu_F-\mu_C= & -\mu_C & & & +\mu_F \\ \mu_A= & & \mu_A & & \\ \mu_h= & & & \mu_h. & \end{array} \quad (22)$$

Inserting these values into (21) we find that

$$\mu_\lambda=(C_1B_{1D}-C_2)\mu_C+(C_1B_{2D}+C_3)\mu_A +(C_1B_{3D}+C_4)\mu_h+(C_1B_{4D}+C_2)\mu_F. \quad (23)$$

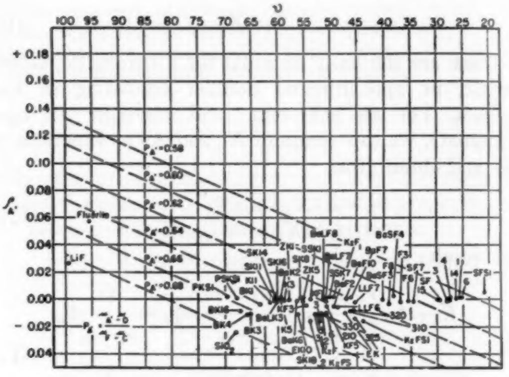

Graph II. ν-value plotted against residual partial dispersion for red end of spectrum. Inclined lines designate partial dispersion.

Comparison with (20) gives

$$\begin{aligned} B_1&=C_1B_{1D}-C_2\\ B_2&=C_1B_{2D}+C_3\\ B_3&=C_1B_{3D}+C_4\\ B_4&=C_1B_{4D}+C_2 \end{aligned} \quad (24)$$

or

$$\begin{aligned} C_1&=(B_1+B_4)/(B_{1D}+B_{4D})\\ C_2&=-B_1+C_1B_{1D}\\ C_3&=B_2-C_1B_{2D}\\ C_4&=B_3-C_1B_{3D}, \end{aligned} \quad (24a)$$

which permits us to calculate the functions, C_i, as linear functions of the B_i's.

We could, however, also calculate the function C_i directly, if we chose; for instance, C_i is the well-defined function in λ of type (1), which is 1 for D, 0 for A and h, and has the same values for F and C, respectively. Analogously, C_2 to C_4 are found. Inspection of Eq. (21) shows that the functions C_i thus constructed have the desired properties; they give a function of type (1) which reproduces D, A, h, and $(F-C)$.

Having found the C_i, we proceeded as follows to calculate the A_i: Eq. (18) is equivalent to

$$\mu_\lambda=(A_1+1)\mu_D+A_2(\mu_F-\mu_C)+A_3r_A+A_4r_h, \quad (25)$$

where

$$\begin{aligned} r_A&=\rho_A(\mu_F-\mu_C)\\ r_h&=\rho_h(\mu_F-\mu_C), \end{aligned}$$

where

$$\begin{aligned}\mu_A&=(A_{1A}+1)\mu_D+A_{2A}(\mu_F-\mu_C)+r_A\\ \mu_h&=(A_{1h}+1)\mu_D+A_{2h}(\mu_F-\mu_C)+r_h.\end{aligned}\tag{26}$$

Replacing μ_A and μ_h in (21) with the help of (26) and comparing corresponding coefficients with (25) leads to

$$\begin{aligned}A_1&=C_1+C_3(A_{1A}+1)+C_4(A_{1h}+1)-1\\ A_2&=C_2+C_3A_{2A}\qquad+C_4A_{2h}\\ A_3&=C_3\\ A_4&=C_4.\end{aligned}\tag{27}$$

Formula (26) still contains four unknown constants, A_{1A}, A_{1h}, A_{2A}, A_{2h}. The computation of these constants was undertaken in the following way:

Taking the data of 35 ordinary Schott glasses from the catalog, least-squares solutions were carried out to determine A_1 and A_2 as functions of the wave-length from the relation,

$$\mu_\lambda=(A_1+1)\mu_D+A_2(\mu_F-\mu_C).\tag{28}$$

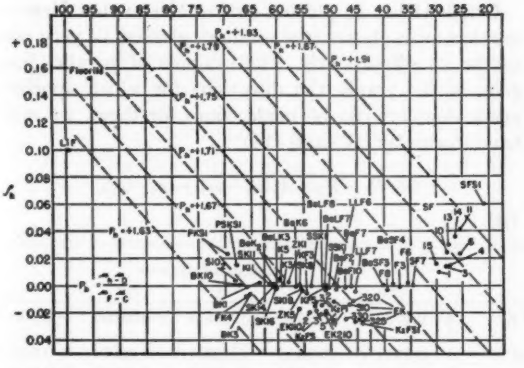

Graph III. ν-value plotted against residual partial dispersion for violet end of spectrum. Inclined lines designate partial dispersion.

We determined from these functions the four constants, A_{1A}, A_{2A}, A_{1h}, and A_{2h}. (See Table II.)

The fact that insertion of these values into the first two Eqs. of (27) reproduced A_1 and A_2, previously computed empirically, proves the consistency of the theoretical investigations.

4. ANALYSIS OF THE RESULTS

An optical glass is given by four of its constants, which we take as $N=1/\mu_F-\mu_C$, ν, ρ_A and ρ_h. We, therefore, attach three graphs wherein N is plotted against ν, ρ_A is plotted against ν, and ρ_h is plotted against ν. (Graphs I to III.)

The values of N, ν, ρ_A, and ρ_h for the glasses which we investigated are not taken from the catalog but are calculated as the mean values to fit best

$$N\mu_\lambda=(A_1+1)\nu+A_2+A_3\rho_A+A_4\rho_h,\tag{29}$$

for all the values of the index given in the catalog; in this way we are able to obtain an additional decimal for N, ν, ρ_A, and ρ_h.

We call glasses ordinary glasses if ρ_A and ρ_h are smaller than 0.005; the other glasses are called extraordinary. We see that the phosphate glasses, the SF glasses, the KzFS glasses (short flints), and the Eastman Kodak glasses are extraordinary glasses and so are fluorite and lithium fluoride. Table III gives the new catalog data and Table IV gives the deviations of the values of the index given in the catalog from the ones computed according to our method. It is obvious that

Table II.

Wave-length	B_1	B_2	B_3	B_4	(A_1+1)	A_2	A_3	A_4
h	0.0	0.0	+1.0	0.0	+0.995432	+1.971430	0.0	+1.0
G′	−0.381788	+0.155895	+0.397817	+0.828076	+0.997704	+1.408827	+0.234378	+0.414081
g	−0.383371	+0.156141	+0.373359	+0.853871	+0.997805	+1.379804	+0.238876	+0.390506
0.45	−0.342799	+0.136624	+0.213978	+0.992197	+0.998482	+1.166677	+0.250819	+0.237661
F	0.0	0.0	0.0	+1.0	+0.999531	+0.732829	+0.175843	+0.036437
0.5	+0.164271	−0.059083	−0.036481	+0.931293	+0.999754	+0.598612	+0.133568	+0.003438
e	+0.663536	−0.203894	−0.069320	+0.609678	+1.000070	+0.243079	+0.019997	−0.022927
0.55	+0.698585	−0.210798	−0.068421	+0.580634	+1.000075	+0.217939	+0.014143	−0.021810
0.*d*	+0.951915	−0.224918	−0.047524	+0.320527	+1.000007	+0.008473	−0.001168	−0.001161
D	+0.959810	−0.223231	−0.046255	+0.309676	+1.0	0.0	0.0	0.0
0.6	+1.000920	−0.208184	−0.038224	+0.245488	+0.999948	−0.051323	+0.010990	+0.007191
0.65	+1.017900	−0.033719	−0.003420	+0.019239	+0.999586	−0.246370	+0.148658	+0.034370
C	+1.0	0.0	0.0	0.0	+0.999530	−0.267174	+0.175842	+0.036438
0.7	+0.757622	+0.303761	+0.014597	−0.075979	+0.999089	−0.393543	+0.423621	+0.039435
b	+0.704479	+0.359006	+0.015243	−0.078728	+0.999013	−0.409952	+0.469037	+0.038045
0.75	+0.244397	+0.789408	+0.008563	−0.042368	+0.998505	−0.506244	+0.824935	+0.015924
A.766491[1]	+0.024134	+0.979546	+0.000948	−0.004622	+0.998301	−0.537544	+0.982975	+0.001660
A′.768195[2]	0.0	+1.0	0.0	0.0	+0.998276	−0.540634	+1.0	0.0
A.759898	−0.024370	+1.020592	−0.000976	+0.004753	+0.998254	−0.543696	+1.017139	−0.001690
0.8	−0.495862	+1.408662	−0.023100	+0.110300	+0.997858	−0.593798	+1.340860	−0.037147

[1] *A* used by Bausch and Lomb Optical Company.

[2] *A′* used by Schott and Parra Mantois. For Schott and Parra Mantois, $\mu=B_1\mu_C+B_2\mu_{A'}+B_3\mu_h+B_4\mu_F$, $\mu=(A_1+1)\mu_D+A_2(\mu_F-\mu_C)+A_3\rho_{A'}+A_4\rho_h$. For Bausch and Lomb, first compute $\mu_{A'}(768.2)$, using $\mu_{A'}(768.2)=-0.024638\mu_C+1.020881\mu_A(766.5)-0.000968\mu_h+0.004718\mu_F$. For Chance, compute A', using $\mu_{A'}=-1.962304\mu_C+2.785469\mu_b-0.042459\mu_h+0.219294\mu_F$.

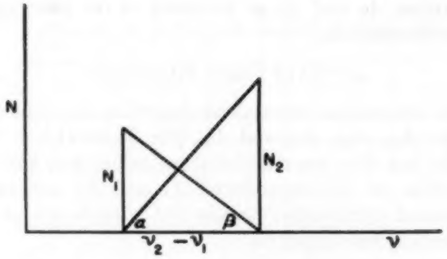

FIG. 1. Graphic illustration to show how to compute the powers of an achromatic doublet for two glasses chosen from Graph I.

the fit for all types of material is well within the accuracy needed for optical design.

In Graph I we have plotted $N=1/(\mu_F-\mu_C)$ against the ν-value. The straight lines give us constant values of n_D and can serve to estimate n_D for the glasses plotted. Formula (12) shows us how to use the graph to determine the total curvature of two lenses which give a corrected doublet. As Fig. 1 shows,

$$\begin{aligned}\tan\alpha&=N_2/(\nu_2-\nu_1)\\ \tan\beta&=N_1/(\nu_1-\nu_2).\end{aligned}\tag{30}$$

Thus, we have, substituting (30) into (12),

$$\begin{aligned}K_1&=\Phi\tan\beta,\\ K_2&=\Phi\tan\alpha,\end{aligned}\tag{31}$$

where Φ is the power of the system. We see that it is advantageous to have $\nu_2-\nu_1$ large.

The following remark may also be of interest. It seems that the glasses of the crown flint series form on the graph nearly a straight line which, however, is inclined against the line of constant refractive index. A parallel line a little above it contains the short flints. Below, we have the barium crown and the barium flint; still farther below, a parallel line of SSK glasses containing more barium; and finally, the Eastman Kodak high index glasses. Lines $\nu=$constant separate the different glass types as in other catalogs.

Graph II has ρ_A plotted against the ν-value. Here we see that most glasses (the ordinary glasses) lie very near to the coordinate axis. The systems of parallel lines give, in the graph, the directions for which apochromatic doublets can be made, since for them, we must have (formulas (10) and (14)):

$$0=P_1-P_2=A_1(\nu_1-\nu_2)+(\rho_1-\rho_2),$$

TABLE III.

		Ordinary glass							Extraordinary glass				
		μD	ν	N	$\rho A'$	ρh			μD	ν	N	$\rho A'$	ρh
BK	10	0.497753	67.0328	134.6709	−0.00839	+0.00147	FK	4	0.478214	65.9192	137.8445	−0.01091	−0.00699
	3	0.498231	65.2037	130.8705	−0.01082	−0.00631							
	1	0.510018	63.4408	124.3894	−0.00306	+0.00266	SF	1	0.717150	29.5483	41.2024	+0.00004	+0.01156
K	11	0.500056	61.6062	123.1985	−0.00207	+0.00191		3	0.739755	28.1853	38.1009	+0.00008	+0.01515
	3	0.518141	59.0295	113.9256	−0.00063	+0.00239		4	0.754957	27.5514	36.4940	+0.00044	+0.01624
	5	0.522400	59.6651	114.2134	+0.00030	+0.00546		6	0.804891	25.4769	31.6526	+0.00152	+0.02454
								10	0.728021	28.3663	38.9637	−0.00143	+0.02535
KF	3	0.514451	54.6616	106.2524	−0.00304	−0.00489		11	0.784461	25.7368	32.8083	+0.00134	+0.04203
	5	0.523009	50.9573	97.4309	−0.00488	−0.00140		13	0.740536	27.7214	37.4343	−0.00048	+0.03101
	1	0.540316	50.9451	94.2876	−0.00122	−0.00097		14	0.761578	26.5348	34.8418	+0.00087	+0.03760
ZK	1	0.533068	58.0913	108.9756	+0.00007	+0.00302		15	0.698744	30.0668	43.0298	+0.00041	+0.01741
	5	0.533657	55.4148	103.8397	+0.00181	−0.00270							
							KzF	1	0.551043	49.6423	90.0884	−0.00488	−0.01096
LLF	6	0.531620	48.8804	91.9461	−0.00596	−0.00203		2	0.529347	51.8028	97.8618	−0.00987	−0.01385
	7	0.548579	45.3951	82.7473	−0.00254	−0.00321		3	0.524021	53.1032	101.3379	−0.01071	−0.01456
F	8	0.595368	39.2310	65.8937	−0.00333	−0.00247		5	0.521211	52.7825	101.2691	−0.01056	−0.01788
	3	0.612782	36.9575	60.3110	−0.00200	+0.00006		6	0.526726	51.0700	96.9575	−0.00897	−0.01853
	6	0.636201	35.3819	55.6144	−0.00101	+0.00301	PKS	1	0.517216	69.6738	134.7093	+0.00228	+0.02318
							PSKS	1	0.558159	67.8007	121.4720	+0.00156	+0.01587
BaK	2	0.539875	59.6806	110.5454	+0.00166	+0.00442							
	6	0.574355	56.5210	98.4079	−0.00039	+0.00017	KzFS	1	0.612937	44.0351	71.8427	−0.01558	−0.02718
BaLK	3	0.518275	60.3540	116.4517	−0.00113	−0.00172		2	0.557719	53.9176	96.6751	−0.01532	−0.01906
BaLF	8	0.553518	51.3570	92.7830	+0.00115	+0.00032		3	0.575001	51.9246	90.3034	−0.01481	−0.02023
	7	0.588647	51.1694	86.9272	+0.00135	+0.00135	SFS	1	0.922486	20.9714	22.7336	+0.00536	+0.06146
BaF	2	0.569552	49.4791	86.8737	+0.00269	+0.00126	SiO_2		0.458476	68.1422	148.6277	−0.02423	+0.00446
	7	0.607895	46.2395	76.0650	+0.00128	+0.00014							
SK	11	0.563759	60.7678	107.7903	−0.00139	+0.00184	LiF		0.392082	99.3380	253.3602	+0.02762	+0.09925
	14	0.603025	60.7208	100.6937	+0.00226	+0.00093							
	16	0.620319	60.2796	97.1752	−0.00054	−0.00115	CaF_2		0.433869	95.5698	220.2735	+0.05782	+0.15232
	18	0.638433	55.4822	86.9038	−0.00012	−0.00191							
	8	0.611067	55.8675	91.4262	+0.00154	+0.00098	EK	110	0.696802	56.1850	89.6327	−0.01019	−0.01687
								210	0.734002	51.2093	69.7672	−0.01031	−0.02067
SSK	1	0.617089	54.0515	87.5911	+0.00040	+0.00041		310	0.745000	46.4353	62.3293	−0.00824	−0.01343
	7	0.618362	50.3900	81.4894	+0.00208	−0.00097		320	0.744499	45.8382	61.5692	−0.00713	−0.01097
BaF	10	0.669906	47.2001	70.4579	+0.00078	−0.00052		325	0.744500	45.5876	61.2326	−0.01335	−0.02541
BaSF	3	0.607039	40.2464	66.2996	+0.00006	+0.00127		330	0.755101	47.1990	62.5069	−0.01001	−0.02435
	4	0.651138	38.3370	58.8769	+0.00206	+0.00234							
SF	7	0.639627	34.6342	54.1475	+0.00189	+0.00182							

TABLE IV.

Residuals

Ordinary glass		A'	C	D	d	e	F	g	G'	h
BK	1	0	−1	0	0	0	+1	0	0	+1
	3	0	−1	0	+1	0	0	0	0	0
	10	0	0	0	0	0	+1	+1	−1	0
K	3	0	−1	0	+1	0	0	0	0	0
	5	0	−1	0	+1	−1	0	0	0	0
	11	0	0	−1	+1	+1	0	−1	−1	0
KF	1	0	−1	−1	0	+1	+1	−1	−1	0
	3	0	−1	0	+1	0	0	0	0	0
	5	−2	0	0	0	0	0	0	0	0
ZK	1	0	−1	0	0	0	0	0	0	0
	5	0	−1	−1	+1	0	0	−1	0	0
LLF	6	0	0	0	0	0	0	0	0	0
	7	−1	0	0	0	+1	0	−1	0	0
F	3	0	−1	+1	0	−1	0	−1	0	0
	6	+1	−2	+1	0	0	0	0	−1	+1
	8	0	−1	0	+1	0	0	0	0	0
BaK	2	0	−1	0	0	0	0	0	0	0
	6	0	−1	0	−1	0	+1	0	−1	0
BaLK	3	0	−1	0	0	0	0	−1	+1	−1
BaLF	7	0	−1	+1	0	−1	0	0	0	0
	8	+3	0	0	0	0	0	−1	+1	0
BaF	2	0	0	0	0	+1	0	−1	0	0
	7	0	−1	0	0	+1	0	0	−1	0
SK	8	0	−1	0	+1	0	0	0	0	0
	11	0	0	0	0	+1	0	0	0	0
	14	0	0	0	0	+1	+1	−1	0	0
	16	0	0	−1	0	+1	0	−1	0	0
	18	0	0	−1	+1	0	+1	−1	0	0
SSK	1	0	−1	0	+1	0	−1	0	0	0
	7	0	+1	0	0	+1	0	0	−1	0
BaF	10	0	0	−1	0	+1	+1	−1	0	0
BaSF	3	0	0	0	0	0	0	0	0	0
	4	−2	0	−1	−1	+2	0	−1	−1	0
SF	7	+1	−2	0	+1	0	0	−1	0	0

Extraordinary glass		A'	C	D	d	e	F	g	G'	h
FK	4	0	−1	+1	0	0	0	0	0	0
SF	1	+1	−2	0	0	+2	+1	−1	−1	−1
	3	+1	−3	+1	+2	0	0	−2	−1	+1
	4	+1	−2	0	+1	+1	+1	−1	0	+1
	6	+1	−3	0	+2	+1	+1	−2	−1	+1
	10	+1	−2	0	+1	0	+2	−3	−1	+1
	11	+1	−2	0	0	+2	+2	−4	−1	+1
	13	+1	−2	0	0	+1	+1	−3	0	+1
	14	+1	−2	−1	−1	+3	+1	−2	−1	+1
	15	+1	−1	0	0	+1	+2	−1	−1	+1
KzF	1	0	0	−1	+1	+1	+1	−1	0	+1
	2	0	−1	0	0	0	0	0	+1	0
	3	0	0	0	0	0	+1	0	−1	0
	5	0	0	0	0	0	+1	0	+1	+1
	6	0	0	−1	0	+1	0	0	0	0
PKS	1	0	−1	0	0	+1	0	0	0	0
PSKS	1	0	0	0	0	0	0	0	0	0
KzFS	1	0	−1	0	0	0	+1	0	+1	+2
	2	0	−1	0	0	+1	+1	−1	0	+1
	3	0	−1	+1	0	−1	0	0	0	0
Quartz		+1	−2	0	−1	+2	0	+2	−3	+1
LiF		0	0	0	0	0	0	−1	0	0
Fluorite		0	0	0	0	0	−1	−1	−2	0
EK	110	0	0	0			+1	0	−1	0
	210	0	0	0			+1	0	0	0
	310	0	0	0			0	0	0	0
	320	0	0	0			+1	−1	0	0
	325	0	0	0			+1	0	0	0
	330	0	0	0			0	−1	0	0

Units of fifth decimal place

where

$$A_1 = -0.001746, \quad \text{for } \lambda = \lambda_A$$
$$A_1 = -0.004568, \quad \text{for } \lambda = \lambda_h.$$

Using formula (9), we will be able to compute the secondary spectrum for an achromat made of two lenses.

The graph shows the significance of the deviation of fluorite in combination with K11 or EK110 which cannot be matched by any other combination of glasses. It is significant too that with respect to correcting secondary spectrum the Eastman Kodak glasses seem to be nearly as beneficial as the KzFS glasses.

To leave no possibility uninvestigated, we have tried to replace 0.035 in formula (1) by other values, for instance, 0.030 and 0.040. It seems that 0.035 is near the optimum.

The mathematical meaning of formula (1) has been evaluated elsewhere. It is based on the fact that material transparent in the visible region has an asymptote in the far-infra-red (represented by the first two members of its Taylor series), and in the near ultraviolet (represented by the first two members of its Laurent series).

It is obvious that an extension of the method to infra-red wave-lengths will be less difficult than the extension into the violet region where we are near an asymptote.

JOURNAL OF THE OPTICAL SOCIETY OF AMERICA VOLUME 39, NUMBER 12 DECEMBER, 1949

A Comparison of Photographic and Photoelectric Measurements of Atmospheric Attenuation of Brightness Contrast*

Howard S. Coleman and Harold E. Rosenberger
The Optical Research Laboratory, The University of Texas, Austin, Texas

(Received August 24, 1949)

A comparison has been made of atmospheric attenuation of brightness contrast data obtained by photographic and by photoelectric processes. The comparison involved the use of a photoelectric telephotometer and a photographic telephotometer of practically the same optical and mechanical design. Atmospheric attenuation of brightness contrast data was obtained for four practically monochromatic regions of the visible spectrum using plane objects subtending the same angle with respect to the point of observation and covering a range of approximately eight miles. The data obtained using the two types of equipment were found to be in close agreement.

INTRODUCTION

THERE are a considerable number of uses in civil and military operations for methods whereby the limitations imposed by the atmosphere on the visibility of objects can be determined. During the past twenty-five years, a number of studies have been conducted whose goal was to determine any possible functional relation between the visibility of objects and the range at which they were located with respect to an observer. For the most part the studies have been largely directed toward an attempt to verify theoretical laws which are based on assumptions that rarely if ever, simultaneously hold in nature. Even though the conditions under which the early observations were made were chosen to be as nearly in accord with the theoretical assumptions as possible, the dispersion in the experimental results was sufficiently great to cast doubt as to the value of the theoretical work under consideration. Because of the importance of atmospheric attenuation data, the Office of Naval Research established a Field Station, near Austin, Texas, designed to collect such data for the variety of weather conditions that naturally occurred. The Field Station was designed such that all of the measurements involved were to be obtained by means of a photoelectric telephotometer which has been described in a previous paper.[1] The atmospheric attenuation data obtained during the first twelve-month period indicated that under practically all conditions of the weather, the apparent brightness contrast of plane objects was attenuated exponentially with distance. This was not expected on the basis of an examination of published data in this field. A number of unsuccessful attempts have been made to show that the exponential relation could be attributed to some peculiar constraint associated with the photoelectric measuring equipment. Because of this possibility, and the fact that in some cases for which attenuation measurements are of interest, it may be necessary to use photographic processes, a comparison was made between atmospheric attenuation data obtained using photographic photometry with similar data obtained using photoelectric photometry. It is the purpose of this paper to describe

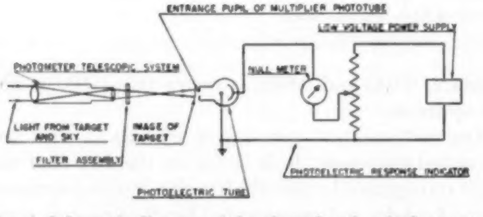
ENTRANCE PUPIL OF MULTIPLIER PHOTOTUBE
LOW VOLTAGE POWER SUPPLY
PHOTOMETER TELESCOPIC SYSTEM
NULL METER
LIGHT FROM TARGET AND SKY
IMAGE OF TARGET
FILTER ASSEMBLY
PHOTOELECTRIC RESPONSE INDICATOR
PHOTOELECTRIC TUBE

FIG. 1. Schematic diagram of the photoelectric telephotometer.

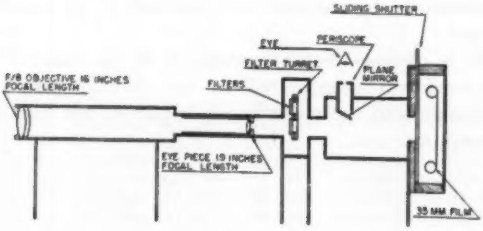

FIG. 2. Schematic diagram of the photographic telephotometer used in the University of Texas Atmospheric Optics Program.

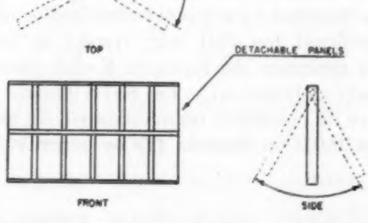

FIG. 3. Schematic diagram of the grey scale used in the University of Texas Atmospheric Optics Program.

---

* The work described in this paper was performed, in part, under terms of Task IX of Contract N6onr-266 between the ONR of the Navy Department and The University of Texas.

[1] Coleman, Morris, Rosenberger, and Walker, "A photoelectric method of measuring the atmospheric attenuation of brightness contrast along a horizontal path for the visible region of the spectrum," J. Opt. Soc. Am. 39, 515–521 (1949).

the comparison for four practically monochromatic regions of the visible spectrum.

APPARATUS AND PROCEDURE

Since a general description of the Office of Naval Research Atmospheric Optics program at The University of Texas has been presented in a previous paper,[1] only the additions to the equipment previously described will be mentioned here. The apparatus consisted essentially of two telephotometers and the black objects described in the previous paper mentioned. One of these utilizes a photoelectric tube and the other a photographic emulsion as a photo-sensitive receptor. The telephotometers are shown schematically in Figs. 1 and 2.

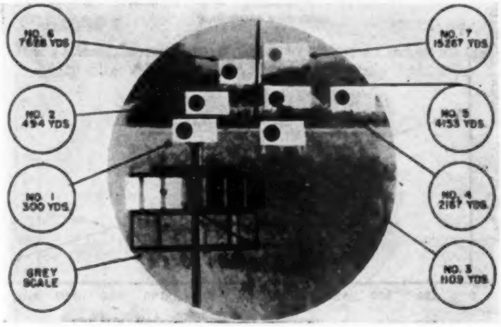

FIG. 4. Telephotograph of the University of Texas visibility targets showing the grey scale used on a day when the meteorological range was 100,000 yards (5:15 P.M., June 27, 1949).

In the case of the photographic processes such auxiliary equipment as are normally required in photographic photometry were used. For example, the form of the grey scale used is shown in Figs. 3 and 4. The elements of the grey scale are removable and their spectral reflectances were determined frequently by means of a General Electric Recording Spectrophotometer. 35-mm Super XX Film, processed in microdol developer, was used throughout the photographic photometry.

In the case of the photoelectric photometry, the characteristics of the apparatus used are shown in Figs. 5 to 10 inclusive. Figure 5 shows the linearity of the photoelectric response with flux. Figure 6 shows the spectral response of the photoelectric tube used. The spectral transmittance for the filters used in both the photographic and photoelectric photometric processes are shown in Figs. 7 to 10 inclusive.

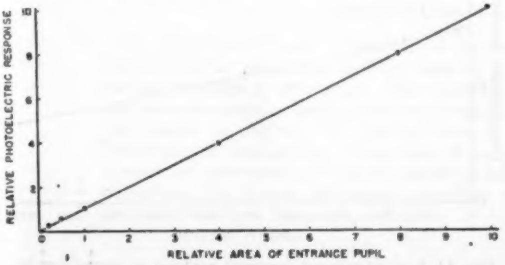

FIG. 5. Data showing linearity of telephotometer.

The procedure used in the study described in this paper consisted of simply making attenuation of brightness contrast measurements by means of the photographic and photoelectric telephotometers for each of the filters mentioned. In each case the horizon brightness along a particular direction was chosen as the background brightness for the objects being photometered. In the case of the photographic photometry, the usual type of H and D curves were prepared for the grey scale mentioned and the brightnesses of the test objects and their sky background were determined from densitometric measurements using a photoelectric densitometer. By means of the brightness data obtained using the two types of photometers, the apparent contrasts of each of the objects were calculated. The contrast data were plotted as a function of object distance for purposes of comparison.

THE DATA

Typical atmospheric attenuation data showing the comparison of the results obtained by photographic and photoelectric methods for each of the four filters mentioned, are shown in Figs. 11 to 18 inclusive. These figures show rectified plots of the logarithm of the

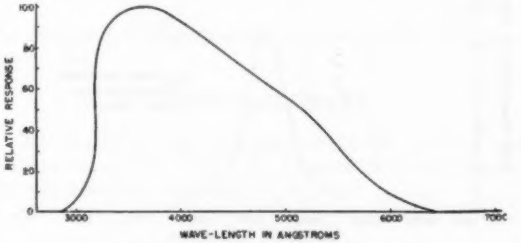

FIG. 6. Spectral response of photoelectric tube used in telephotometer.

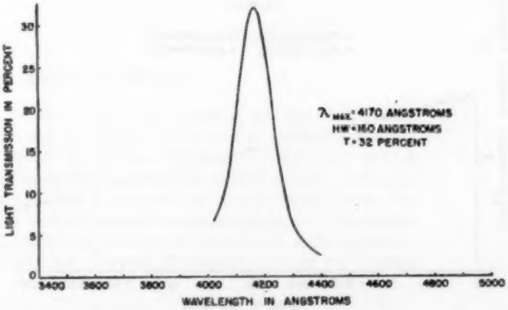

FIG. 7. Light transmission *vs.* wave-length for violet filter used in telephotometer.

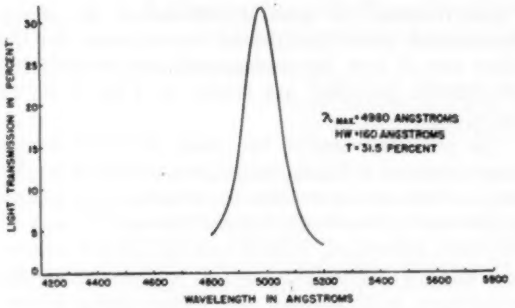

FIG. 8. Light transmission *vs.* wave-length for blue filter used in telephotometer.

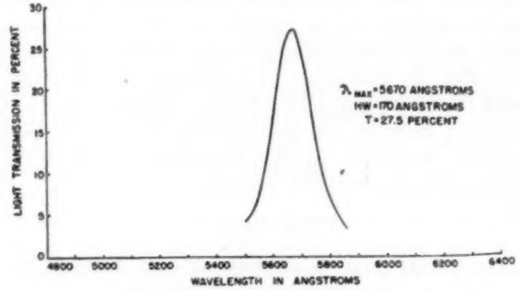

FIG. 9. Light transmission *vs.* wave-length for green filter used in telephotometer.

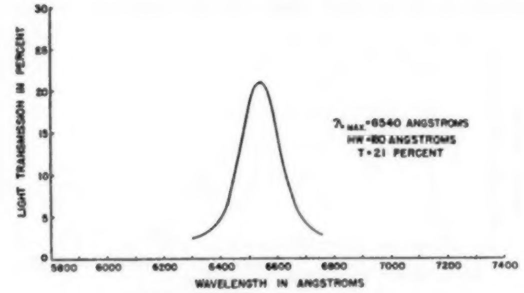

FIG. 10. Light transmission *vs.* wave-length for red filter used in telephotometer.

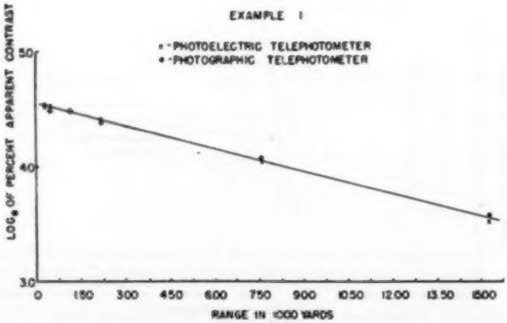

FIG. 11. Log$_e$ of percent apparent contrast *vs.* range for the violet filter (time—1631 C.S.T.; date—July 18, 1949).

apparent contrast of the object as a function of range for each of the telephotometers used and the four filters.

DISCUSSION AND CONCLUSIONS

It is evident from the study of the data presented in this paper, that the photographic and the photoelectric measurements of the attenuation of brightness contrast by the atmosphere are substantially the same. For this reason, there is little doubt as to the conclusions reached in an earlier paper concerning the simple exponential attenuation law. It is possible that one of the reasons

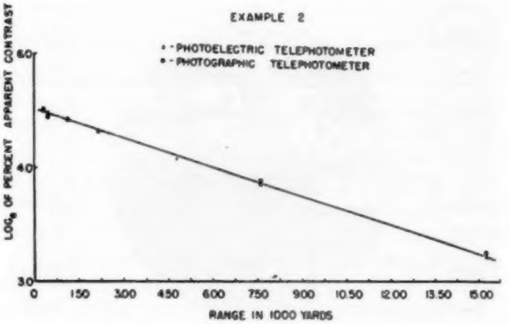

FIG. 12. Log$_e$ of percent apparent contrast *vs.* range for the violet filter (time—1724 C.S.T.; date—July 21, 1949).

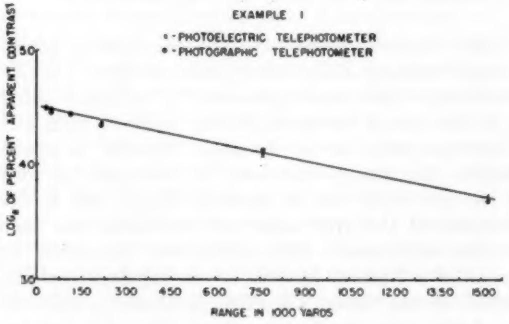

FIG. 13. Log$_e$ of percent apparent contrast *vs.* range for the blue filter (time—1701 C.S.T.; date—July 8, 1949).

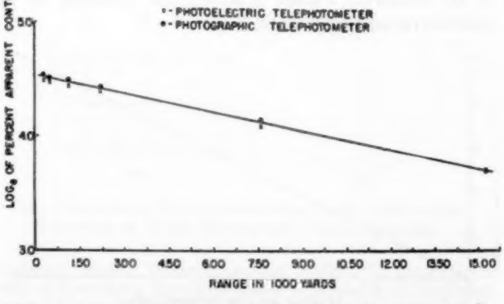

FIG. 14. Log$_e$ of percent apparent contrast *vs.* range for the blue filter (time—1614 C.S.T.; date—July 8, 1949).

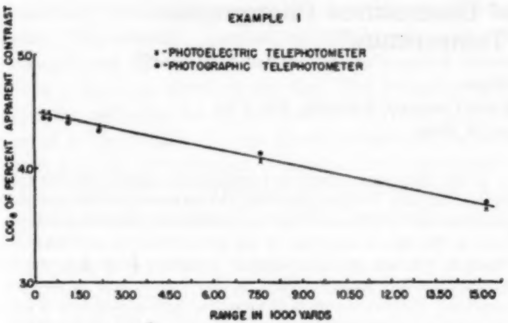

FIG. 15. Log$_e$ of percent apparent contrast *vs.* range for the green filter (time—1645 C.S.T.; date—July 8, 1949).

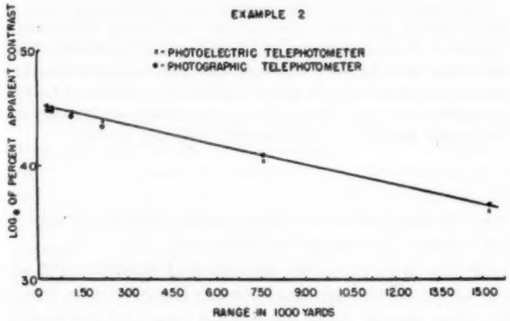

FIG. 16. Log$_e$ of percent apparent contrast *vs.* range for the green filter (time—1624 C.S.T.; date—July 8, 1949).

for the apparent failures of the exponential law found by previous investigators can be attributed to improper experimental procedures.

The results of the study described in this paper indicate that if photographic photometry is desirable for any particular atmospheric attenuation study, it can be expected to yield the same results as would

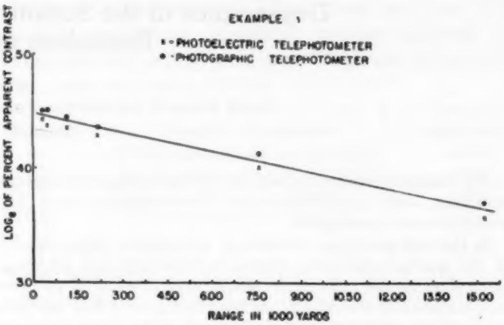

FIG. 17. Log$_e$ of percent apparent contrast *vs.* range for the red filter (time—1559 C.S.T.; date—August 13, 1949).

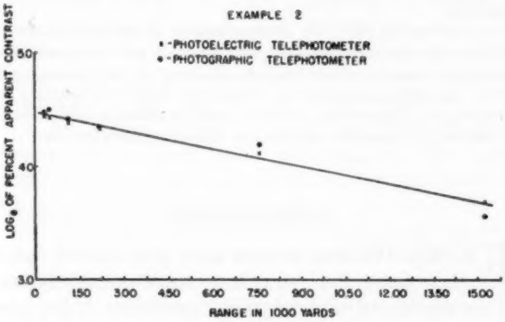

FIG. 18. Log$_e$ of percent apparent contrast *vs.* range for the red filter (time—1632 C.S.T.; date—August 13, 1949).

be obtained if photoelectric photo-sensitive receptors were used.

ACKNOWLEDGMENT

The authors wish to acknowledge the interest and assistance of Mr. Frank B. Isakson of The Office of Naval Research, Washington, D. C.

Inauguration of George Eastman House

Of considerable interest to members of the Optical Society is the recent opening of George Eastman House, a public educational institute designed to further our knowledge of the means, accomplishments, and potentialities of photography. The home built by George Eastman in Rochester, New York, will be used to house exhibits dealing with technological developments and applications of photography both past and present. In this way it is planned to make the new facility a national and international center for conferences on photography, for meetings of camera clubs and photographic organizations, for demonstrations of the most recently developed apparatus and photographic processes, and for exhibits of photographic collections. The opening ceremonies were held in the Eastman Theatre, Rochester, and at the George Eastman House, on November 9, 1949.

JOURNAL OF THE OPTICAL SOCIETY OF AMERICA VOLUME 39, NUMBER 12 DECEMBER, 1949

Dependence of the Sensitivity of Unsensitized Photographic Emulsions upon Temperature*

Martin Biltz
Kodak Research Laboratories, Eastman Kodak Company, Rochester, New York

(Received August 25, 1949)

The change in spectral sensitivity of unsensitized photographic emulsions with temperature and its connection with light-absorption are investigated.

In the first part, the influence of temperature upon the *shape* of the spectral-sensitivity curves is considered and graphs are given showing the ratio of the sensitivities at -195°C and room temperature and the ratio of the sensitivities at $+50$°C and room temperature as a function of wave-length. For pure silver bromide emulsions, these curves show a minimum at about 470 mμ and a maximum at about 500 mμ. For emulsions containing chloride or iodide, the curve shape is somewhat changed but not in its essential features.

In the second part, the *absolute* change of spectral sensitivity with temperature is discussed. The sensitivity of the basic light-sensitive material, silver bromide, is found to be comparatively little temperature-dependent. The large drop in sensitivity, on lowering the temperature, which is found in commercial emulsions, is due to the chemical sensitization becoming less effective.

In the third part, a tentative explanation is given for the results of the first part. It is assumed that the maximum of the sensitivity-ratio curves at 500 mμ is due to a different temperature-dependence in the light-absorption of the silver bromide and that of the reaction product of the chemical sensitizer with the emulsion (probably silver sulfide) which, in this region, acts as an optical sensitizer. Measurements of the spectral light-absorption of a pure silver bromide emulsion show that the decrease in sensitivity with temperature of this emulsion at 400 mμ is, at least in the main, due to decreased light-absorption and only to a smaller extent to a genuine decrease in light-sensitivity.

It is concluded from the experimental results that there exist two kinds of sensitivity specks: one kind being numerous and consisting of shallow traps, which are mainly responsible for the sensitivity of chemically non-sensitized grains and for that of the interior of chemically sensitized grains; the other kind being few in number and consisting of deep traps, which are responsible for the surface sensitivity of chemically sensitized grains.

INTRODUCTION

EXTENSIVE experiments have been carried out in these Laboratories on the temperature-dependence of the sensitivity of photographic emulsions. It has been shown that the shape of curves representing the sensitivity as a function of temperature depends to a great extent upon the exposure time used for the sensitivity measurements.[1] Furthermore, investigation of the effect of temperature on the spectral sensitivity of optically sensitized emulsions[2,3] showed that the efficiency of different dyes decreases with decreasing temperature to different degrees. Spectral-sensitivity curves of unsensitized emulsions[a] published by the Agfa Laboratories[4] established the influence of the chemical sensitizers upon the shape of these curves. Combining the experience of these two laboratories, it seemed worth while to investigate the temperature-dependence of the spectral sensitivity of unsensitized emulsions. From such experiments it was hoped to gain further insight into the mechanism of latent-image formation and into the nature of chemical sensitization.

In the first part, the influence of temperature upon the *shape* of the spectral-sensitivity curves is treated. In other words, it is considered how the ratio of the sensitivities at different temperatures *changes* with wave-length, but no attention is paid to the absolute values of these ratios. In the second part, the *absolute* change of spectral sensitivity with temperature is treated. In the third part, measurements of the spectral light-absorption of photographic emulsions are described and the results compared with those of the first two parts.

I. INFLUENCE OF TEMPERATURE UPON THE SHAPE OF THE SPECTRAL-SENSITIVITY CURVE

For measuring the spectral sensitivity, the sensitometer that is regularly employed in these Laboratories was used.[5] Intensity-scale monochromatic exposures with ten power-of-two steps are obtained. The film strips were inserted into a groove at the outside of an aluminum cylinder which was situated in an unsilvered wide-mouthed Dewar flask as described by Evans.[3] The cylinder could be heated by inserting an electric heater into it and cooled by filling it with liquid nitrogen. Strips 0.7 by 10 in. exposed at $+50$°C and at room temperature to radiation of the same wave-length were developed together, and the same was done with strips exposed at -195°C and at room temperature. Therefore, in evaluating the ratio of the sensitivities at 50° and room temperature, and at -195° and room temperature, the result cannot be falsified appreciably by

---

[*] Communication No. 1267 from the Kodak cResearh Laboratories.

[1] J. H. Webb, J. Opt. Soc. Am. **25**, 4–23 (1935); C. H. Evans and E. Hirschlaff, J. Opt. Soc. Am. **29**, 164–167 (1939).

[2] Sheppard, Wightman, and Quirk, J. Phys. Chem. **38**, 817–831 (1934).

[3] C. H. Evans, J. Opt. Soc. Am. **32**, 214–218 (1942).

[a] In this paper, "unsensitized emulsion" denotes an emulsion containing no optical sensitizer (organic dye), although it may be chemically sensitized. An emulsion is denoted as having "minimum chemical sensitization" or as being "non-sensitized," if it has not been intentionally chemically sensitized, e.g., by digestion.

[4] J. Eggert and M. Biltz, Trans. Faraday Soc. **34**, 892–901 (1938); Zeits. f. wiss. Phot. **39**, 140–155 (1940); J. Eggert and F. G. Kleinschrod, Zeits. f. wiss. Phot. **39**, 155–165, 165–174 (1940); Arens, Eggert, and Kleinschrod, Zeits. f. wiss. Phot. **42**, 33–42 (1943).

[5] C. H. Evans, J. Opt. Soc. Am. **30**, 118–127 (1940).

sensitivity variations caused by variations in development. The absolute spectral sensitivity at room temperature was determined in the regular routine fashion using 5- by 7-in. sheets of the film. The intensity of the exposing radiation for each exposure was determined by use of a thermopile. If not stated otherwise, development was for five minutes in Kodak D-19 developer at 20°C. Sensitivity is expressed as the reciprocal of the radiant density (ergs/cm^2) required to obtain a density of 0.5.

Exposure time was usually 60 sec. at 50°C and at room temperature. In some cases where longer exposure times were used, the sensitivity values were reduced to those for 60 sec. exposure time by means of reciprocity-law failure curves taken separately with white light. At −195°C, various exposure times were used ranging between 60 and 960 sec. (16 min.). Because at this temperature no reciprocity failure occurs,[1, 6] the sensitivity values obtained were independent of the exposure time.

From the experimental results, spectral-sensitivity curves were plotted in the usual manner, i.e., the logarithm of sensitivity as a function of wave-length. In order to facilitate the comparison between the curves obtained at different temperatures, sensitivity-ratio curves were plotted in addition to the sensitivity curves themselves. These curves represent the ratio of the sensitivities at different temperatures as a function of wave-length. Obviously, if the loss or gain in sensitivity with temperature is independent of wave-length, such a curve is simply a straight line parallel to the wave-length axis. Its deviation from such a line indicates a different influence of temperature upon the sensitivity at different wave-lengths.

Most easily to comprehend are the results on some very simple emulsions which were prepared especially for these measurements. All of them are pure silver bromide emulsions containing neither chloride nor iodide and no optical sensitizer. Chemical sensitization and grain size are as follows:

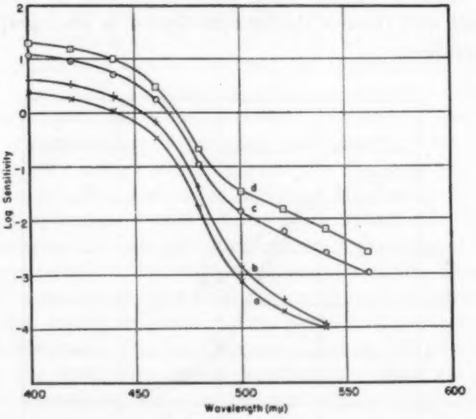

FIG. 1. Spectral sensitivity (cm^2 erg^{-1}) of pure silver bromide emulsions at room temperature. *a* = non-sensitized, average grain size 0.49μ^2; *b* = non-sensitized, average grain size 1.43μ^2; *c* = sulfur sensitized by digestion, average grain size 0.49μ^2; *d* = sulfur sensitized by digestion, average grain size 1.43μ^2.

Emulsion	Chemical sensitization	Average grain size
a	Minimum chemical sensitization	0.49μ^2
b	Minimum chemical sensitization	1.43μ^2
c	Sulfur sensitized by digestion	0.49μ^2
d	Sulfur sensitized by digestion	1.43μ^2

Spectral-sensitivity curves at room temperature of these emulsions are to be found in Fig. 1. The curves referring to emulsions with the same sensitization are parallel, the emulsions with the coarser grain having about 0.2 logarithmic unit higher sensitivity than those with the finer grain. Figure 2 shows the corresponding sensitivity curves at −195°, and Fig. 3 shows the sensitivity-ratio curves. The curves for room temperature in Fig. 1 show the shape known from previous work.[4] Starting at short wave-lengths, the sensitivity decreases, at first slowly, then more rapidly. At about 490 mμ, there occurs a break, the curve becoming flatter again toward longer wave-lengths. The appearance of a break not only in the curves for chemically sensitized emulsions but also in the curves for the emulsions which were not intentionally sensitized means that even in that case there is a considerable chemical sensitization. But quantitative differences appear: the non-sensitized emulsions show a longer steep part preceding the break, and a higher slope beyond it.

The shape of the sensitivity curves at −195° (Fig. 2) is considerably different from that of the room-temperature curves. There is not a simple parallel shift of the curves and, accordingly, the ratio curves of Fig. 3 are not straight lines parallel to the axis of the abscissas. The following features are common to all curves: Starting at 400 mμ and proceeding toward longer wave-lengths, the sensitivity ratio decreases more and more until a minimum is reached at about 470 mμ. Then the influence of temperature upon sensitivity again becomes

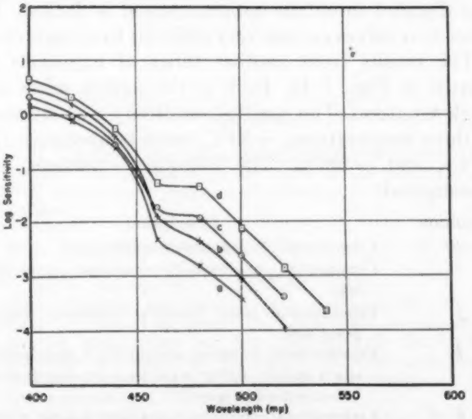

FIG. 2. Spectral sensitivity (cm^2 erg^{-1}) of pure silver bromide emulsions at −195°C. Meaning of the letters same as in Fig. 1.

---

[6] W. F. Berg and K. Mendelssohn, Proc. Roy. Soc. London **168A**, 168–175 (1938).

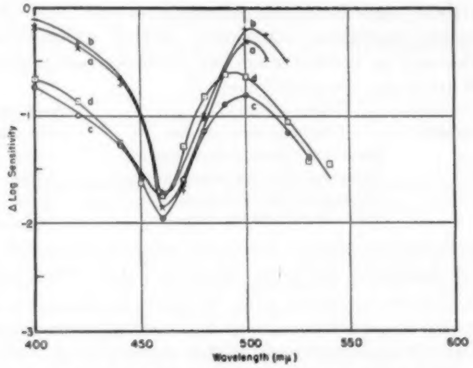

FIG. 3. Change of spectral sensitivity with temperature. Ordinate values are logarithms of the ratios of the sensitivities at −195°C and at room temperature. Meaning of the letters same as in Fig. 1.

weaker and, at 500 mμ, the change in sensitivity is about the same as at 400 mμ. At still longer wave-lengths, the sensitivity ratio decreases again, the sensitivity at −195° falling to such low values, not far beyond 500 mμ, that further measurements become impossible with reasonable exposure times. The shapes of the curves for emulsions with the same sensitization, but differing with regard to grain size, are nearly identical; those referring to emulsions with different sensitization are different insofar as the minimum at 470 mμ is flatter for the chemically sensitized emulsions.

Some further experimental material is presented in Figs. 4–6, corresponding to Figs. 1–3. The grain sizes of these emulsions are identical. The emulsions differ with respect to chemical sensitization as follows:

Emulsion	Chemical sensitization
e	Minimum chemical sensitization
f	Sulfur sensitized by digestion but below optimum speed
g	Sulfur sensitized by digestion to optimum speed.

The sensitivity-ratio curve referring to the emulsion that was digested to obtain optimum speed is flattest. The other two curves are not very different from each other.

The results from another series of emulsions are plotted in Figs. 7–16. Each of the figures refers to a single emulsion. The spectral sensitivity was measured at three temperatures, +50°C, room temperature (20–25°C), and −195°C. The following emulsions were investigated:

Emulsion	Description
h	Commercial chlorobromide emulsion
i	Commercial pure bromide emulsion, coarse grain size
j	Experimental pure bromide emulsion, medium grain size
k	Experimental emulsion containing 6 mole percent silver iodide, sulfur sensitized by digestion but below optimum speed
l	Experimental emulsion containing 6 mole percent silver iodide, sulfur sensitized by digestion to optimum speed.

An inspection of Figs. 12–16 shows that there is one feature common to all of them, namely, that the ratio curve comparing the sensitivity of an emulsion at −195°C and at room temperature bears a definite correlation to the curve comparing the sensitivity of the same emulsion at 50°C and at room temperature: The maxima in the curves of one type correspond to minima in those of the other type, and vice versa. On disregarding the more pronounced features of the −195° curves which result from the much higher temperature difference, it is observed that the maxima in the 50° curves are shifted by 10 to 20 mμ toward longer wave-lengths, compared with the minima in the −195° curves to which they correspond. The same is true for the minima.

The results of this part might be summarized as follows: The shape of the spectral-sensitivity curve of non-optically sensitized emulsions depends upon the temperature at which the sensitivity measurements are made. At low temperature (−195°C), the curve showing the sensitivity (in logarithmic units) as a function of wave-length decreases more rapidly than that at room temperature from 400 mμ toward longer wave-lengths. This rate of decrease continues up to 450 mμ for a chlorobromide emulsion, and up to 470 mμ for a pure bromide emulsion. Beyond that wave-length, the low temperature curve becomes flatter than the room-temperature curve, with the result that at about 500 mμ the separation between the room-temperature and the low temperature curves is about the same as at 400 mμ. Beyond 500 mμ the low temperature curve again becomes steeper. Analogous results are obtained for the spectral-sensitivity curves determined at +50°C.

In the third and fourth parts of this paper, an attempt is made to explain these phenomena and to connect them with those of the light-absorption in photographic emulsions.

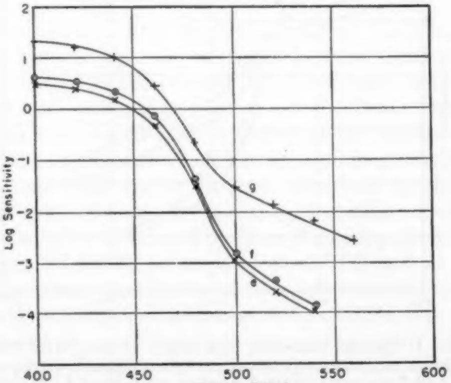

FIG. 4. Spectral sensitivity (cm^2 erg^{-1}) of pure silver bromide emulsions at room temperature. *e* = non-sensitized; *f* = sulfur sensitized by digestion below optimum speed; *g* = sulfur sensitized by digestion to optimum speed.

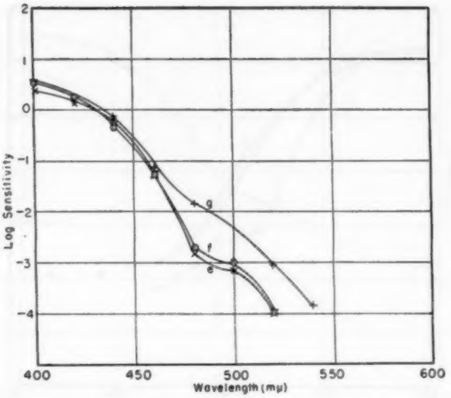

FIG. 5. Spectral sensitivity (cm^2 erg^{-1}) of pure silver bromide emulsions at −195°C. Meaning of the letters same as in Fig. 4.

II. INFLUENCE OF TEMPERATURE UPON THE ABSOLUTE VALUE OF SPECTRAL SENSITIVITY

So far, we have considered the change in the *shape* of the spectral-sensitivity curve with temperature. Now, we shall look at the change in the *absolute* values of these sensitivities. In doing so we shall restrict ourselves, for the time being, to pure silver bromide emulsions and not consider mixtures with chloride or bromide, because for the first case the conditions are simplest. Furthermore, we shall consider the measurements at room temperature and at −195° only and leave out those at +50°, since the values obtained at the latter temperature would lead to qualitatively the same conclusions but, because of their close proximity to the 25° values, would be not as suitable for a quantitative evaluation.[b]

We now inspect again Figs. 1–3, to consider the change in the absolute sensitivity values with temperature. On comparing the curves of Fig. 3 which illustrate the sensitivity loss on lowering the temperature from 25° to −195°C, there seems to be a quantitative difference between the behavior of the fine-grain and that of the corresponding coarse-grain emulsions, in that the sensitivity loss is always smaller for the coarse-grain emulsions. But, not much importance is given to these small quantitative differences, as all values refer to a density of 0.5. Because of differences in the slope of the characteristic curves of the emulsions employed, changing to another density level causes slight displacements of the sensitivity-ratio curves, parallel to the axis of the abscissas. The fact, however, that at 400 and 500 mμ the sensitivity loss is considerably higher for the sulfur-sensitized than for the non-sensitized emulsions does seem to be of fundamental importance. It was thought that this difference in behavior might correspond to a different distribution of the latent image formed in these emulsions. It has been found[7] that the sensitivity of that part of the grain which is developed by a surface developer[8] is much more dependent upon temperature than the sensitivity of the "interior" which is developed by a solvent developer after bleaching away the "surface" latent image. Although there is evidence that "surface" and "interior" refer to actual locations in the grain, there is no certainty about this, and it is safer to consider these expressions as merely distinguishing between regions accessible to two different kinds of developer.[9]

It would have required a great number of experiments to compare the sensitivity of the surface with that of the interior of the grain of several emulsions for the whole spectral region considered (400 to about 550 mμ). It turned out, however, that this was not necessary and that it was sufficient to make the comparison for one wave-length because the shape of the spectral-sensitivity curve is practically identical for the surface and the interior parts of the grain. This was expected from former experience[a, 10] but was confirmed for a pure silver bromide emulsion (Emulsion *i*): Fig. 17 shows the sensitivity-ratio curves for surface and internal development. They can be considered as being parallel within the limits of experimental error.

Figure 18 shows a comparison of external and internal sensitivity at 25° and at −195°C for the four emulsions (*a* to *d*) to which Figs. 1–3 refer. Sensitivity values are given in logarithmic units. They refer to a

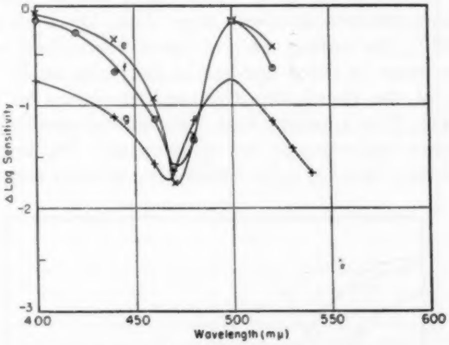

FIG. 6. Change of spectral sensitivity with temperature. Ordinate values are logarithms of the ratios of the sensitivities at −195°C and at room temperature. Meaning of the letters same as in Fig. 4.

---

[b] It might be mentioned, however, that in the short-wave-length region the sensitivity at 50° was found to be lower than at room temperature (Figs. 7–11). This is a consequence of the concept accounting for low intensity reciprocity failure, according to which the probability of thermal disintegration of the silver specks forming the latent image increases with temperature (see reference 1).

[7] Berg, Marriage, and Stevens, J. Opt. Soc. Am. **31**, 385–394 (1941).

[8] G. W. W. Stevens, Phot. J. **82**, 42–47 (1942).

[9] Keller, Maetzig, and Möglich [Ann. d. Physik (6)1, 301–316 (1947), p. 311] are of the opinion that there is not an external and an internal latent image but that there are only two kinds of development: a chemical and a physical one. Their experimental results do not seem to support this opinion sufficiently.

[a] See reference 7, p. 389, Fig. 6.

[10] It should be mentioned, however, that L. Falla [Bull. Soc. Roy. Sci. Liége **11**, 196–199 (1942)] finds much higher red-sensitivity for the deep internal image than for the surface image.

wave-length of 400 mμ, a density level of 0.5, and an exposure time of 15 sec. The development technique was the same as that used by Stevens.[8] Surface development was for three minutes at 20°C in a solution of 26 grams of sodium carbonate monohydrate in 500 cc of air-free water in which, immediately before starting the development, 12 grams of glycine had been dissolved. For the internal development, bleaching was adjusted so that just the part of the latent image which was developable by the surface developer was dissolved. For all four emulsions, bathing for three minutes at 20°C in 0.1 percent chromic acid solution was found to be appropriate. Development was for three minutes at 20°C in 500 cc of Kodak D-72 developer, to which 25 cc of a 10 percent solution of potassium bromide and 10 cc of a 30 percent solution of sodium thiosulfate had been added.

The results plotted in Fig. 18 are mean values between two measurements which agree within 0.15 logarithmic sensitivity unit. In explaining the figure, we shall consider, first, the surface sensitivity at 25°C. There we notice an increase of about 30 percent in passing from the non-sensitized fine-grain emulsion, *a*, to the corresponding coarse-grain emulsion, *b*. A similar yet smaller increase takes place in passing from the sensitized fine-grain emulsion, *c*, to the corresponding coarse-grain emulsion, *d*. A greater sensitivity increase is observed on passing from the non-sensitized emulsions, *a* and *b*, to the corresponding sensitized ones, *c* and *d*. The increase amounts to a factor of almost three for the fine-grain emulsions, *a* and *c*, and to a factor of two for the coarse-grain emulsions, *b* and *d*. There is nothing remarkable about these data. On cooling to −195°C, the surface speed of the non-sensitized emulsions drops to about one-half of the value at 25° but that of the chemically sensitized emulsions to one-fortieth. It is apparent that the chemical sensitization becomes ineffective at low temperature. The internal sensitivity behaves quite differently. At room temperature, the sensitivity of the coarse-grain emulsion is a little higher than that of the fine-grain emulsion for the non-sensitized pair (*a* and *b*), and a little lower for the sensitized pair (*c* and *d*). But these differences are minor ones. A more important fact seems to be that for the interior of the grain the chemical sensitization does not cause a speed increase but a decrease, and that, for both the non-sensitized and the sensitized emulsions, little change in internal sensitivity occurs on lowering the temperature to −195°.

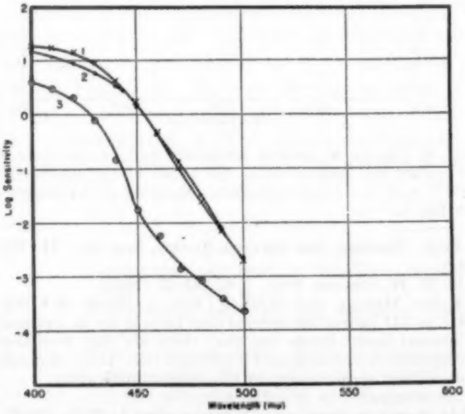

FIG. 7. Spectral sensitivity (cm² erg⁻¹) of a chlorobromide emulsion (*h*). 1, at room temperature; 2, at 50°C; 3, at −195°C.

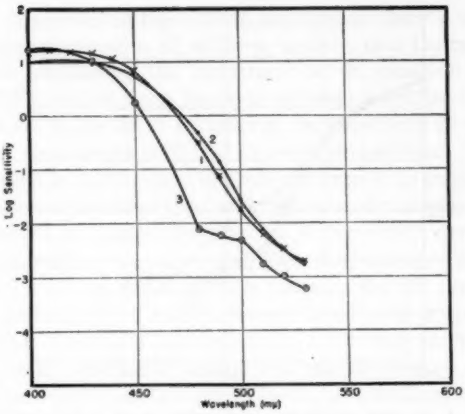

FIG. 8. Spectral sensitivity (cm² erg⁻¹) of a coarse-grain pure bromide emulsion (*i*). 1, at room temperature; 2, at 50°C; 3, at −195°C.

As has been pointed out, the sensitivity values of Fig. 18 refer to an exposure time of 15 sec. In order to demonstrate how these results change if another exposure time is chosen, reciprocity-law failure curves are given in Fig. 19. These curves are from measurements with white light, as it is known[11] that their shapes do not depend appreciably upon wave-length. They refer to 25°C. No reciprocity-law failure occurs at −195°, as was stated previously[1,6] and this was confirmed on the present emulsions by a few tests. Because the curves for the surface image are not far from horizontal, there is little influence of exposure time upon the "surface" curves of Fig. 18, within the exposure time region considered. On the other hand, the influence of exposure time upon the sensitivity of the internal image is considerable. We take, as an example, the emulsion, *a*, which, for an exposure time of 15 sec., has the same sensitivity at 25° and at −195°. With longer exposure times, the 25° sensitivity decreases while the −195° sensitivity does not change. This has the effect that, for the longer times, a sensitivity increase for the interior part of the grain is observed on lowering the temperature to −195°. On the other hand, with shorter exposure times, the 25° sensitivity increases. For an exposure time of one second it has twice its value for 15 sec., so that the internal sensitivity at −195° is only

---

[11] J. H. Webb, J. Opt. Soc. Am. 23, 316–323 (1933); M. Biltz and J. H. Webb, J. Opt. Soc. Am. 38, 561–569 (1948).

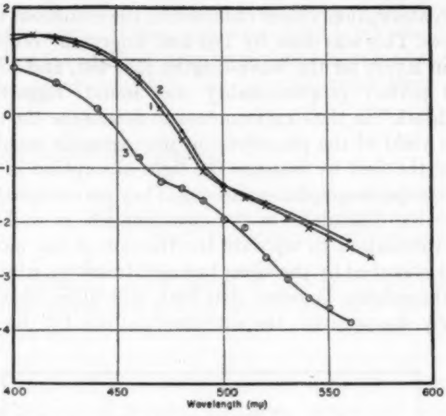

FIG. 9. Spectral sensitivity ($cm^2\ erg^{-1}$) of a medium-grain pure bromide emulsion (*j*). 1, at room temperature; 2, at 50°C; 3, at −195°C.

about one-half the sensitivity at 25°. Such changes, however, are minor, compared with the main feature, substantially higher temperature-dependence of the surface sensitivity of the chemically sensitized emulsions.

A quantitative consideration of the change in interior sensitivity with temperature will be given in the third part. It is clear, however, that the important changes in sensitivity with temperature which are observed in commercial emulsions are not due to a loss in light-sensitivity of the basic material, silver bromide, but to a loss in efficiency of the chemical sensitization. In the region of the usual exposure times, the greater part of the total sensitivity of chemically sensitized emulsions at room temperature is due to the surface, as is shown in Table I, which is derived from Fig. 18. In calculating this table we have assumed that the total sensitivity is the sum of the surface and internal sensitivities, as obtained with the development methods employed. This is certainly not correct so that the absolute values are not reliable. However, Table I permits a useful comparison between the different emulsions. The table, in connection with Figs. 18 and 19, makes it clear why with "commercial" developers, such as Kodak D-19 Developer, which develop all of the surface and part of the interior latent image, a large temperature coefficient of the sensitivity has been found on chemically sensitized emulsions.

The results of this part might be summarized as follows: On lowering the temperature from 25° to −195°C., the sensitivity of the interior of the grains of chemically non-sensitized emulsions, where the basic light-sensitive material, silver bromide, is to be found purest, decreases very little. The sensitivity of the surface of the grains of such emulsions and of the interior of chemically sensitized emulsions decreases not much more. Under the same conditions, however, a large decrease in sensitivity is found for the surface of the grains of chemically sensitized emulsions.

III. INFLUENCE OF LIGHT-ABSORPTION UPON SENSITIVITY

A. General Survey

In order to explain the results concerning the dependence of spectral sensitivity upon temperature reported in the foregoing parts, it seemed worth while to study them in conjunction with measurements on the light-absorption of silver bromide and of emulsions. Such a study is reasonable in view of the fact that, at room temperature, a close connection between spectral sensitivity and spectral light-absorption has been established. Eggert and Kleinschrod[4] considered a linear relation between the spectral sensitivity (S) of their binder-free emulsions and the extinction coefficient (E) of crystallized silver bromide in the region between 430 and 490 mμ. Their experimental results[d] are not in full agreement with this conclusion since they lead to the equation, $S=\text{const.}\times E^{0.7}$.

Actually, the comparison should be between sensitivity and absorption,[e] but in order to change values of the extinction coefficient into those of the absorption factor by calculation, an assumption has to be made about the effective thickness of the emulsion, that is, the distance traveled by the light within the turbid layer, which is greater than the distance in a clear layer of the same thickness.

In a brief note which does not contain a description of the experimental method used, Meidinger and Mucha[12] give the effective thickness at 436 mμ as about

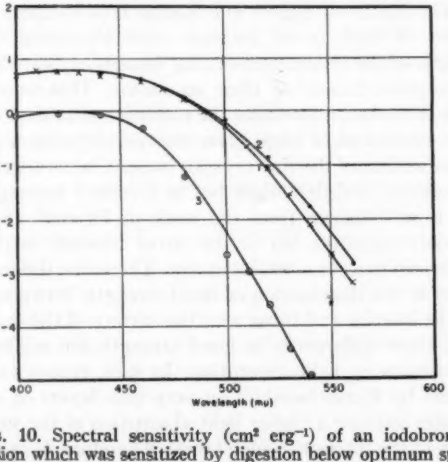

FIG. 10. Spectral sensitivity ($cm^2\ erg^{-1}$) of an iodobromide emulsion which was sensitized by digestion below optimum speed (*k*). 1, at room temperature; 2, at 50°C; 3, at −195°C.

---

[d] See reference 4, p. 171, Fig. 4.

[e] Absorptance = ratio of light absorbed to light which enters the surface = (1 − transmission factor − reflection) : (1 − reflection) $= 1 - e^{-kd}$, k extinction coefficient, d thickness. As the comparison is made with the sensitivity which is expressed in reciprocal radiant density units *incident on* not in units *entering* the layer, it is more correct to use the absorption factor instead of the absorptance. Absorption factor = ratio of light absorbed to light incident = 1 − transmission factor − reflection.

[12] W. Meidinger and H. Mucha, Physik. Zeits. 40, 239–240 (1939).

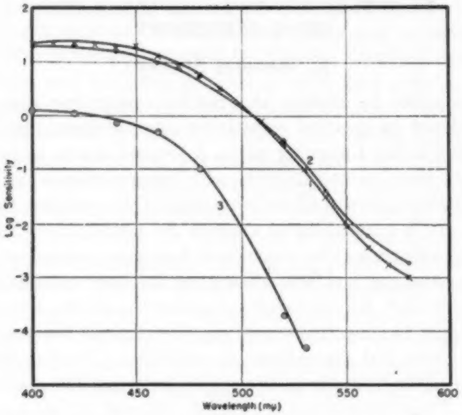

FIG. 11. Spectral sensitivity (cm² erg⁻¹) of an iodobromide emulsion which was sensitized by digestion to optimum speed (*l*). 1, at room temperature; 2, at 50°C; 3, at −195°C.

twice its real thickness for a thin Lippmann emulsion, and as about 20 times its real thickness for a coarse-grain emulsion. This factor depends upon wave-length. However, for low absorption (more correctly: absorptance) values up to about 20 percent, there is a linear proportionality between the extinction coefficient and the absorption factor so that, for a comparison between sensitivity and light-absorption, values of the absorption factor can be replaced by those of the extinction coefficient.

The results of Eggert and Kleinschrod's experiments seem to indicate an increase with increasing wave-length of the relative sensitivity (sensitivity divided by absorption factor) of their emulsions. This would be true, however, only under the condition that the extinction coefficient of large silver bromide crystals was the same as that of the tiny crystals present in photographic emulsions, and this might not be a correct assumption. As is well known from the work of Fajans[13] and his school, the silver ion in the silver bromide lattice is polarized to a considerable extent. Therefore, differences exist in the distribution of bond strength between ions in the interior and those near the surface of the crystal, and these differences in bond strength are related to differences in light-absorption. In fact, recent experiments by Barshchevskii[14] on very thin layers of silver halides indicate a higher light-absorption of the surface than of the interior of such layers. Therefore, because of the large specific surface of the silver bromide grains, their light-absorption might well be different from that of large crystals where the part played by the surface is very small.

In the face of these considerations, it would seem to be more convincing to compare the spectral sensitivity with absorption values obtained in the emulsions themselves. This was done by Toy and Edgerton[15] on single-grain layers for the wave-lengths 365, 405, and 436 mμ and perfect proportionality was found. Eggert and Noddack[16] in their experiments to determine the quantum yield of the photolysis in photographic emulsions were the first to measure the light-absorption in commercial photographic emulsions. They encountered considerable difficulties in the measurement as well as in the calculation to separate the fraction of the incident light absorbed by the silver bromide from that absorbed by the gelatin. It seems that both difficulties have now nearly disappeared, the experimental one by the creation of modern spectrophotometers, and that of separating the fractions by employing a more accurate calculating method.

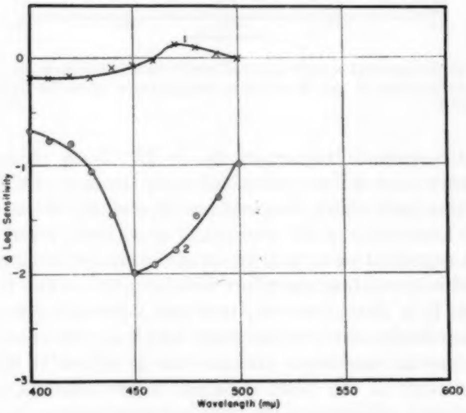

FIG. 12. Change of spectral sensitivity with temperature. Emulsion *h*. 1, ratio of the sensitivities at 50°C and at room temperature; 2, ratio of the sensitivities at −195°C and at room temperature.

A few remarks may be inserted about the latter point. In order to obtain the fraction of the incident light which is absorbed by the silver bromide, Eggert and Noddack subtracted from the measured values of the absorption factor of the photographic layer the values of the absorption factor of the gelatin, as determined from measurements on a pure gelatin layer. Weigert[17] objected to this method by pointing out that, for evaluating the absorption of mixtures, not the numerical values of absorption but the logarithmic values (extinction = −log (1−absorptance)) have to be added. Both methods are open to criticism. In a mixture of two dyes, the ratio of the fractions of the light entering the surface which are absorbed by each of them is equal to the ratio of the extinction coefficients of the dyes.[18] Therefore, for a photographic emulsion layer, the fraction, f, of the light entering its surface which is absorbed by the silver bromide, can be calculated from the formula:

---

[13] K. Fajans, *Radioelements and Isotopes. Chemical Forces and Optical Properties of Substances* (McGraw-Hill Book Company, Inc., New York, 1931).

[14] B. Barshchevskii, Proc. Acad. Sci. U.S.S.R. **65**, 25–28 (1949).

[15] F. C. Toy and H. A. Edgerton, Phil. Mag. (6)**48**, 947–961 (1924).

[16] J. Eggert and W. Noddack, Sitz. Preuss. Akad. Wiss., Physik.-math. Kl. 116–122 (1923); Zeits. f. Physik **20**, 299–314 (1923); **21**, 264 (1924); **31**, 922–941 (1925); **34**, 918–920 (1925).

[17] F. Weigert, Zeits. f. Physik **18**, 232–237 (1923); **34**, 907–917 (1925).

$$f = \text{absorptance of emulsion} \times \left[1 - \frac{\log(1-\text{absorptance of gelatin})}{\log(1-\text{absorptance of emulsion})}\right].$$

In this formula, "absorptance of gelatin" is not simply the absorptance of a gelatin layer of the same thickness as the emulsion because the light is scattered and, therefore, the distance traveled by it within the emulsion is longer than if it traveled straight through the emulsion. "Absorptance of gelatin" therefore means the absorptance of a gelatin layer of such thickness as effective in the emulsion layer, i.e., of such thickness that the light path is the same as the light path through the gelatin in the emulsion layer. It is doubtful that this formula, which is strictly true for optically clear substances, holds equally well for turbid systems, for which Beer's law does not hold. In any case, without extensive measurements and calculations, there seems to be no better way of approaching the truth.

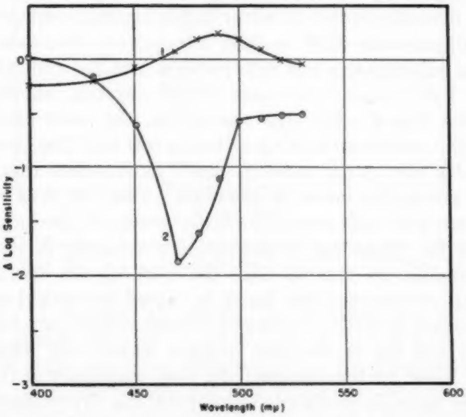

FIG. 13. Change of spectral sensitivity with temperature. Emulsion *i*. 1, ratio of the sensitivities at 50°C and room temperature; 2, ratio of the sensitivities at −195°C and room temperature.

Figure 20 gives as an example the curves for the reflection, transmission factor, absorption factor, and absorptance of the Emulsion, *j*. Figure 21 gives the corresponding curves of a clear gelatin layer of 0.914 mm thickness. For manufacturing this layer, the same gelatin was used as for the preparation of the emulsion. Reflection and transmission factors were measured with the General Electric automatic spectrophotometer, absorption factor and absorptance were calculated.[a] It is essential for calculating purposes that at long wave-lengths, where neither silver bromide nor gelatin absorbs, the absorption curves really descend to zero. This is the case with the measurements of Figs. 20 and 21. It seems reasonable to assume that the effective thickness of the gelatin layer in the emulsion is 20 to 30 μ, that is, two to three times its real thickness, in agreement with the assumption of Eggert and Kleinschrod[4] and the experimental evidence of Carroll[19] in dyed emulsions. Then, by using the formula given in the preceding paragraph, it appears that nowhere in the region between 400 and 500 mμ for bromide emulsions and between 400 and 520 mμ for iodobromide emulsions must more than 10 percent of the light absorbed by the emulsion be ascribed to gelatin absorption, and hence this fraction can be neglected for calculating purposes. In Fig. 22, the logarithms of the sensitivities of the emulsions, *a*, *c*, *k*, and *l*, are plotted as a function of the logarithms of their absorption factors. A linear relation between sensitivity and absorption factor would be indicated by a straight-line curve having an angle of 45 degrees. This is approximately true between 400 and 450 mμ for the bromide emulsions, and between 440 and 510 mμ for the iodobromide emulsions. In this limited region, therefore, the proportionality between sensitivity and absorption is confirmed by measurements of both values on the same sample. The sharp drop of the curves beyond the wave-lengths mentioned might be caused by an "inactive absorption" which so far is unexplained but, more probably, is due to an experimental error in the absorption measurements, where a small loss of light through sidewise scattering might occur.

For particles which are small compared with the wave-length of light, scattering of the light is caused by

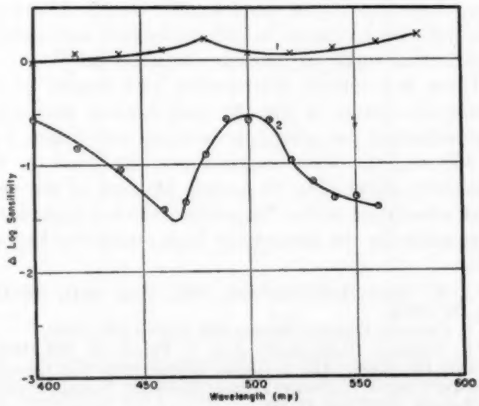

FIG. 14. Change of spectral sensitivity with temperature. Emulsion *j*. 1, ratio of the sensitivities at 50°C and at room temperature; 2, ratio of the sensitivities at −195°C and at room temperature.

---

[18] Ostwald, Luther, and Drucker, *Hand- und Hilfsbuch zur Ausführung physikochemischer Messungen* (Akademische Verlagsgesellschaft, Leipzig, 1925), fourth edition, pp. 734–735.

[19] B. H. Carroll (private communication).

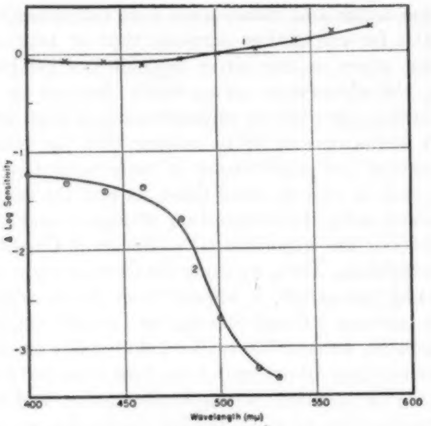

FIG. 15. Change of spectral sensitivity with temperature. Emulsion *k*. 1, ratio of the sensitivities at 50°C and at room temperature; 2, ratio of the sensitivities at −195°C and at room temperature.

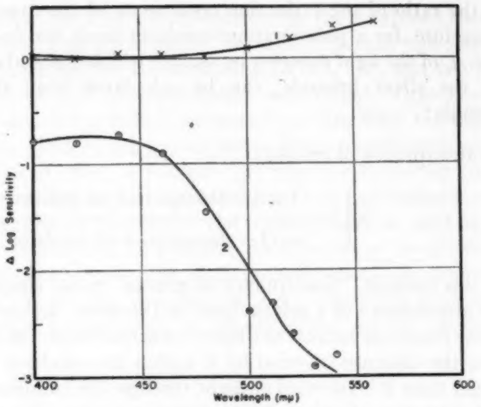

FIG. 16. Change of spectral sensitivity with temperature. Emulsion *l*. 1, ratio of the sensitivities at 50°C and at room temperature; 2, ratio of the sensitivities at −195°C and at room temperature.

diffraction only.[20] If they are not originally colored, no light-absorption takes place in such media, and hence the color of the transmitted light is complementary to that of the reflected light. With larger particles, such as are present in photographic emulsions, reflection and refraction become more important. According to Compan,[21] the dependence of the extinction coefficients of such media upon wave-length does not follow Rayleigh's formula[20] (inverse proportionality to λ^4) but that of Clausius[22] (inverse proportionality to λ^2). It is characteristic of these media that part of the transmitted radiation is not scattered, so that, on looking through them to a light source the source is seen to be quite sharp. The color of the source is shifted to the red and is complementary to the color of the scattered light.[23] It is improbable that, in such media, true, although photographically inactive, light-absorption, dependent upon wave-length, occurs. However, this question seems to be still undecided, and further experiments would be necessary to settle it.[24, 25]

There is a serious shortcoming with regard to the absorption curves of Fig. 20; they become inaccurate approximately just where our main interest begins, i.e., at 500 mμ, the wave-length where the break in the sensitivity curve (Fig. 9) occurs. Because of the very weak absorption of the "impurity" which is apparently responsible for the abnormally high sensitivity beyond 500 mμ, it has not been possible so far to measure its absorption directly with any accuracy. It can be said only qualitatively that, beyond the break, the curves of Fig. 22 will become flatter again. We are helped somewhat by measurements of Stasiw and Teltow[26] on the light-absorption of silver halide crystals containing small amounts (0.01 to 0.04 percent) of silver sulfide. This substance, when incorporated into the crystal in the right manner to form mixed crystals, shows a rather strong additional absorption, the band caused by this addition reaching as far as 600 mμ. The course of this absorption curve is much flatter than that of the absorption curve of the silver halide. As it is well known that sulfur compounds are present in the gelatin used for preparing photographic emulsions, it seems reasonable to assume that the part of the spectral sensitivity beyond the break is caused by optical sensitization by silver sulfide or a similar sulfur compound. This was the explanation brought forward by Eggert and Biltz[4] for the unexpectedly high sensitivity of their silver bromide emulsions beyond 490 mμ. By preparing emulsions containing colloidal silver in close contact with the silver bromide grain, Arens, Eggert, and Kleinschrod[4] were able to enhance greatly the sensitivity beyond 490 mμ. No attempt was made by them to decide whether the comparatively high sensitivity of plain emulsions beyond the break at 490 mμ was also caused by silver or by another "impurity."

The experimental facts discussed so far can be summarized as follows: Within a limited wave-length range, the sensitivity change is proportional to the light-absorption. Beyond this region toward longer wave-lengths, the sensitivity decreases more rapidly than the directly measured absorption, a result which may be due to faulty measurement of the absorption factor.

---

[20] J. W. Strutt (Lord Rayleigh), Phil. Mag. (4)**41**, 107–120, 274–279 (1871).

[21] P. Compan, Comptes Rendus **128**, 1226–1229 (1899).

[22] R. Clausius, Poggendorff's Ann. d. Physik **72**, 294 (1847); **76**, 161, 188 (1849); **121**, 1 (1864). Quoted from Wo. Ostwald, *Licht und Farbe in Kolloiden* (Theodor Steinkopff Verlag., Dresden and Leipzig, 1924), pp. 11, 80.

[23] E. Gretener, Zeits. f. wiss. Phot. **38**, 248–286 (1939).

[24] A complete theory of light-scattering as a function of particle size is given by J. A. Stratton, *Electromagnetic Theory* (McGraw-Hill Book Company, Inc., New York, 1941), pp. 563–573. See also reference 25.

[25] D. Sinclair and V. K. LaMer, Chem. Rev. **44**, 245–267 (1949).

[26] O. Stasiw and J. Teltow, Göttingen, Nachrichten, Math.-physik. Kl. 93–99, 100–109, 110–118 (1941); 156–163 (1944); Zeits. f. wiss. Phot. **40**, 157–165 (1941).

Proceeding to still longer wave-lengths, beyond the break in the sensitivity curve, the sensitivity is higher than would be expected from the absorption, as extrapolated from the values obtained at shorter wave-lengths. In this region, the reaction product of the chemical sensitizer with the emulsion acts as an optical sensitizer.

B. Light-Absorption and Sensitivity as a Function of Temperature

The change in light-absorption of solid compounds with temperature was investigated systematically by Koenigsberger[27] and by Koenigsberger and Kilchling.[28] For substances with steep absorption curves (extinction coefficient *vs.* wave-length), e.g., for fuchsin, they found little change of the absorption coefficient at the wave-length of maximal absorption but considerable change with temperature on the steep part of the curve: a decrease with increasing temperature in the short wave-length part, and an increase with increasing temperature in the long wave-length part. Little change was observed for substances with flat absorption curves, for example, for glass colored yellow by silver oxide. Only a few and, apparently, not very accurate measurements of the change in the light-absorption of silver bromide with temperature are known. Toy and Harrison[29] found a linear decrease of the extinction coefficient of this substance between +20° and −180°C for the wave-lengths 365, 406, and 436 mμ. Masaki[30] published spectral-absorption curves (absorption factor *vs.* wave-length) of a thin layer of clear silver bromide at 30° and 100°C. These curves (reproduced in Fig. 23) show a considerable increase in absorption at the higher temperature. As neither the thickness of the layer nor the reflection is given, it is not possible to derive values for the extinction coefficient from his data. Apparently, only a few qualitative observations on the change in light-absorption with temperature in photographic emulsions have been made so far.[31]

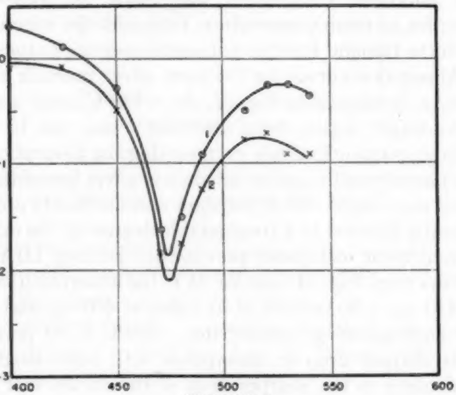

FIG. 17. Change of spectral sensitivity with temperature for the internal image (1), and the surface image (2), of Emulsion *i.*

In carrying out such measurements, we hoped to employ the General Electric automatic spectrophotometer. This instrument makes it possible to measure both the reflection and transmission factors and therefrom to calculate the absorption factor. However, this instrument is so constructed as to make it impossible to vary the temperatures of the sample over such wide limits. Therefore, the principle of Eggert and Noddack[16] was applied. The sample was held inside a photometric sphere of 15 cm diameter, near the wall, and illuminated with light of different wave-lengths from a double monochromator (Leiss) through a horizontal tube of 15 mm inner diameter, located opposite to the sample. Another horizontal tube of the same diameter formed a right angle to the first one and was directed toward the wall of the sphere. Light emerging from this tube was collected at the surface of a photo-multiplier tube (RCA 931A) arranged[32] to give a current, amplified by a factor of about one million, proportional to the illumination. This current was measured by means of a galvanometer. The sample could be pushed in and pulled out

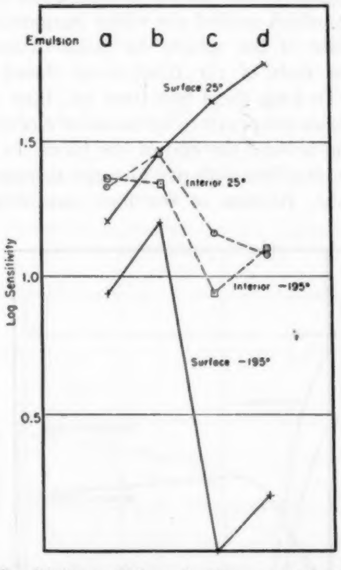

FIG. 18. Sensitivity at 400 mμ (arbitrary units) of the surface and the interior of the grains of pure silver bromide emulsions at room temperature and at −195°C. Exposure time 15 sec. Emulsions same as in Fig. 1.

---

[27] J. Koenigsberger, Ann. d. Physik (4)4, 796–810 (1901).

[28] J. Koenigsberger and K. Kilchling, Ann. d. Physik (4)28, 889–924 (1909).

[29] F. C. Toy and G. B. Harrison, Proc. Roy. Soc. London 127A, 613–628 (1930), p. 626.

[30] O. Masaki, Memoirs College of Science, Kyoto Imp. Univ. 12A, 127–134 (1929); Sci. et Ind. Photo. (2)1, 231–237 (1930).

[31] O. D. Barteneva and Yu. N. Gorokhovski, J. Tech. Phys. U.S.S.R. 14, 193–198 (1944).

[32] R. W. Engstrom, J. Opt. Soc. Am. 37, 420–431 (1947); R. Sherr, Rev. Sci. Inst. 18, 767–770 (1947).

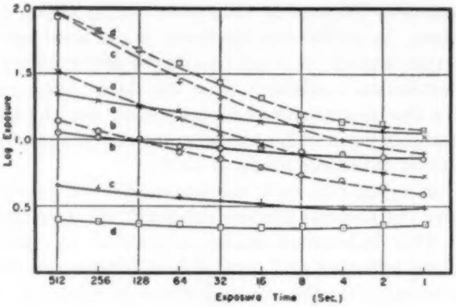

FIG. 19. Reciprocity-law failure for the surface and the internal sensitivity of pure silver bromide emulsions at room temperature. Ordinate values are logarithms of exposure (arbitrary units) to obtain density 0.5. Straight line—surface, dashes—interior. Emulsions same as in Fig. 1.

of the beam, and the galvanometer deflection was read in the two positions. The absorption was obtained as 1-(a/b), where a and b are the readings, with and without the sample in the beam. For measurements at low temperature, the under half of the sphere was dipped in liquid nitrogen. The temperature of the sample was measured with a copper-constantan thermocouple located close to it.

Considerable difficulty was encountered by the formation of ice inside the sphere. Apparently, tiny ice crystals were floating around and absorbing part of the incident light. Furthermore, condensation of oxygen took place, which spoiled the white (magnesium oxide) inner surface of the sphere. In order to avoid these effects, the ends of the tubes were closed by glass windows. To keep them free from ice, they were held at about room temperature by means of electric heating coils wound around the end of the tubes. In addition, the sphere was filled with dry nitrogen through another narrow tube. Because of the high sensitivity of the photo-multiplier tube, the level of illumination could be held so low that within several series of measurements no print-out effect occurred on the samples. The presence of the sample holder inside the sphere and of the tubes attached to it have the effect that the reflection conditions do not correspond to those of an ideal sphere. Therefore, no absolute values of the absorption factor are obtained. Calibration was made by measuring samples, at room temperature, both with the sphere and with the General Electric automatic spectrophotometer.

TABLE I. Percent of total sensitivity due to surface. (Exposure time 15 sec.)

Temperature (°C)	Emulsion *a* Non-sensitized Fine	 *b* Coarse	 *c* Chemically sensitized Fine	 *d* Coarse
+25	43	50	76	83
−195°	27	42	10	10

Absorption curves for the pure silver bromide emulsion, *a*, are shown in Fig. 24. At −140°C, only a short wave-length region, from 400 to 420 mμ, can be considered as quantitatively representing the absorption by the photolytically active substance, silver bromide. Beyond that region, the absorption measurements are apparently falsified to a considerable degree by the experimental error mentioned previously. (Section IIIA.) It follows from Fig. 24 that for 25°C the absorption factor at 420 mμ is 80 percent of its value at 400 mμ and that the corresponding number for −140°C is 55 percent. This sharper drop in absorption with wave-length is equivalent to the sharper drop of the curves in Fig. 2 (−195°) from 400 mμ toward longer wave-lengths, compared with the curves of Fig. 1 (25°), or to the downward trend of the curves of Fig. 3 toward longer wave-lengths. Thus, it appears that the change in the

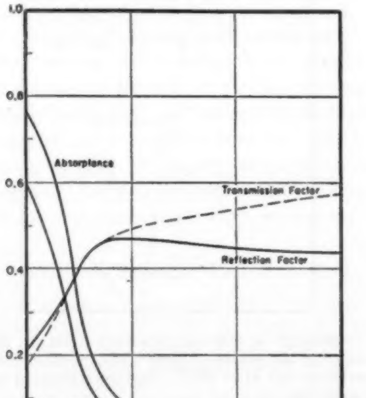

FIG. 20. Optical characteristics of Emulsion *j*.

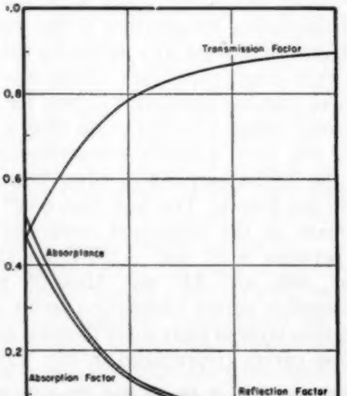

FIG. 21. Optical characteristics of a gelatin layer of 0.914 mm thickness.

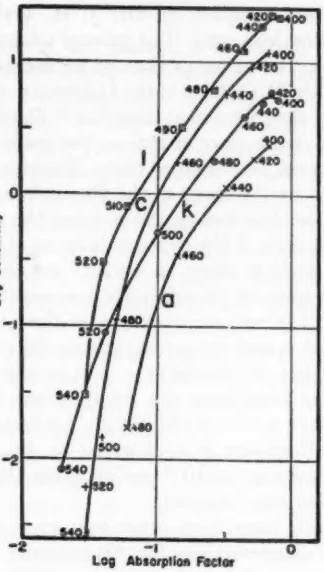

FIG. 22. Connection between sensitivity and light-absorption for Emulsions *a*, *c*, *k*, and *l* (cf. Fig. 1, 10, and 11). The numbers written beside the points are wave-lengths in mμ.

shape of the spectral-sensitivity curve between 400 and 460 mμ with temperature can be completely accounted for by the change in light-absorption.

The explanation of the peculiar shape of the sensitivity curves at −195°C (Fig. 2) beyond 460 mμ, leading to a maximum of the ratio curves (Fig. 3) at 500 mμ, is thought to be connected with the light-absorption of the reaction product of the chemical sensitizer with the emulsion which, in this region, acts as an optical sensitizer. So far, experimental proof cannot be supplied for this explanation. Figure 25(*a*) shows absorption curves for the photographically active part of a silver bromide emulsion, their numerical values being rather arbitrary but their general shape being probably close to the true shape. The solid curves refer to the silver bromide, the dashed ones to the "impurity," silver sulfide. That part of the curves which, according to the concept held in this paper, is responsible for the sensitivity, is plotted heavily. The logarithm of the ratio between the absorption values at 25° and −195°C is plotted in Fig. 25(b). The shape of this curve resembles closely that of the curves of Fig. 3.

With the sensitivity-difference curve of the chlorobromide emulsion (Fig. 12), the second maximum could not be reached because the sensitivity in the region where it is to be expected was too low to be accessible for measurement. With the curve of the coarse-grain bromide emulsion (Fig. 13), the maximum but not the second decrease could be reached, for the same reason. The break in the sensitivity curves of the iodobromide emulsions (Figs. 10 and 11) is situated so far out (at about 560 mμ) that an influence of the chemical sensitizer upon the shape of the sensitivity-difference curve can hardly be expected. Accordingly, the curves of Figs. 15 and 16 decrease monotonically, a tendency to turn back being noticeable at their ends. Additional information is necessary in order to substantiate the foregoing conceptions or to replace them by better ones.

The fact that the shape of the sensitivity-ratio curves of the non-sensitized emulsions (Fig. 3, curves *a* and *b*) is so similar to that of the sulfur-sensitized emulsions (curves *c* and *d*) seems to be at variance with the above explanation. It should be kept in mind, however, that there are only gradual differences in the chemical sensitization between the two groups. The break in the sensitivity curves, *a* and *b*, of Fig. 1 points to the presence of some chemical sensitization in these emulsions which, apparently, is sufficient to sustain the optical sensitization at low temperature.

We have digressed into consideration of the wave-length region where the reaction product of the chemical sensitizer with the emulsion acts as an optical sensitizer but we shall now go back to the more important region where the absorption by the silver bromide itself is responsible for the light-sensitivity. We turn again to Fig. 18, which shows the change in sensitivity, at 400 mμ, of the surface and of the interior of the four pure bromide emulsions, on lowering the temperature from +25° to −195°C. In order to exclude chemical sensitization so far as possible, we consider

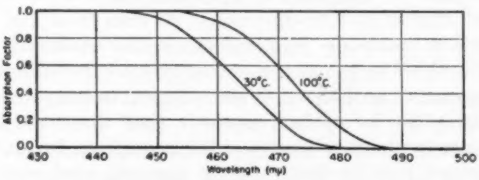

FIG. 23. Spectral light-absorption of silver bromide (according to Osamu Masaki).

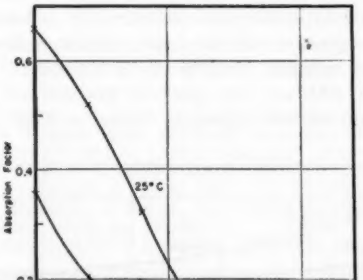

FIG. 24. Spectral light-absorption of Emulsion *a* at room temperature and at −140°C.

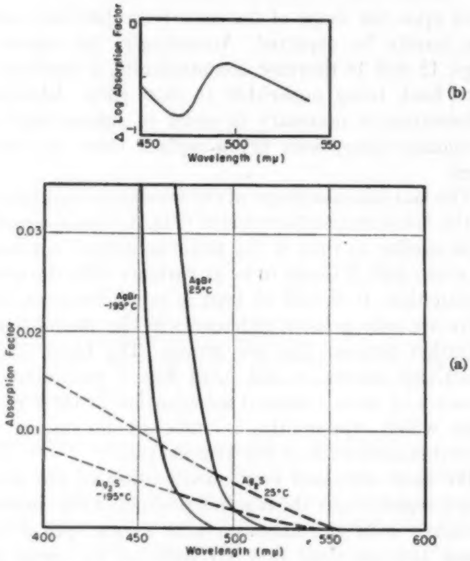

FIG. 25. Spectral light-absorption of a photographic emulsion. These are not experimental curves but are plotted with arbitrary values to illustrate the concepts of the text. (a) Spectral absorption of silver bromide and silver sulfide at room temperature and at −195°C. (b) Change in spectral absorption with temperature. The units of the axis of the ordinates are logarithms of the ratios of the absorption factors at −195° and at room temperature.

the interior of a non-sensitized emulsion, *a* or *b*, and compare the temperature-dependence of its sensitivity with that of its light-absorption. As read from Fig. 18 there is practically no difference in the sensitivity at 25° and −195°C, but this is true only for the arbitrary exposure time of 15 sec. It seems logical to compare the sensitivities for optimal exposure time where the exposure to obtain a density of 0.5 is smallest. It can be assumed that for that exposure time the sensitivity is not influenced by secondary effects. The reduction from 15 sec. to optimal exposure time was necessary only for the 25° sensitivity because, as mentioned previously, no reciprocity failure occurred at −195°.[f] Measurement of the reciprocity failure of the interior of Emulsion *a* with the ordinary reciprocity sensitometer[33] showed that at 1/2000 sec. the optimum was still not reached. To obtain shorter exposure times, a high intensity sensitometer, designed by Dr. J. H. Webb of these Laboratories, was used. The general scheme of the instrument is the same as that of an instrument made earlier by Dr. B. O'Brien of the University of Rochester, and briefly described in an abstract.[34] The method consists in moving a piece of film on the inside rim surface of a high speed bowl-shaped rotor. The exposure time is determined by the speed of the film and the size of the image in the direction of the moving film. By using a General Electric A-H6 mercury lamp as a light source, exposure times as short as 4×10^{-6} sec. could be employed, in spite of the relatively low sensitivity of the emulsions. The reciprocity curves for the internal image of Emulsion *a* and, for a comparison, the curve for the surface image of Emulsion *c* (chemically sensitized) obtained by combining the results given by the two sensitometers, are shown in Fig. 26. No flattening of the curve for Emulsion *a* is observed at short exposure times and even at 4×10^{-6} sec. exposure time the optimum has not been reached.

At present, there is no other way, except to use the sensitivity value obtained for this exposure time, under the assumption that no important sensitivity increase occurs for still shorter exposure times. The sensitivity for an exposure time of 4×10^{-6} sec. is 0.9 log unit (factor of 8) higher than for an exposure time of 15 sec. and it follows that for optimal exposure conditions the sensitivity at −195° is one-eighth that at 25°. To compare this number with the light-absorption, we turn to Fig. 27, where the absorption factor of Emulsion *a* at 400 mμ is plotted as a function of temperature. To obtain a value for −195°, an extrapolation is necessary which, in the face of the linear course of the curve, seems to be admissible. The absorption at −195° is found to be one-third that at 25°. Considering the complexity of the work involved, it is justifiable to assume that the sensitivity change is due, at least in the main, to decreased light-absorption and only to a smaller extent to a decrease of the intrinsic light-sensitivity of the silver bromide. It is obvious that the difference in temperature-dependence of the sensitivity between the surface and the interior of chemically sensitized emulsions is not due to its location but to the fact that the action of the chemical sensitizer is mainly restricted to the grain surface.

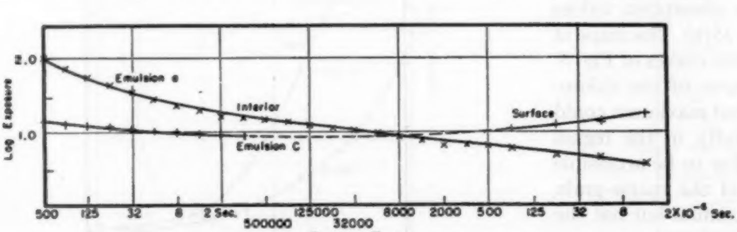

FIG. 26. Reciprocity-law failure for the internal sensitivity of Emulsion *a* and for the surface sensitivity of Emulsion *c*. Ordinate values are logarithms of exposures (arbitrary units) to obtain density 0.5.

---

[f] This has not been tested for the internal image at very short exposure times.

[33] L. A. Jones, J. Opt. Soc. Am. **7**, 305–319 (1923); J. H. Webb, J. Opt. Soc. Am. **23**, 157–169 (1933).

[34] B. O'Brien, Phys. Rev. **50**, 400–401 (1936).

IV. CONCLUSIONS

The interior of the grain of a chemically non-sensitized pure silver bromide emulsion can be considered as representing a photographic emulsion in its original state not affected by any outside (extragranular) influence. From the viewpoint of latent-image theory, it seems to be significant that this intrinsic sensitivity of the grain is so little dependent upon temperature. The important changes in sensitivity with temperature which are observed in commercial emulsions are apparently caused by secondary effects. Such a secondary effect, due to chemical sensitization, appears even at the surface of the non-sensitized emulsions which, as has been stated before, are chemically sensitized to a certain degree. Because of this sensitization, the external sensitivity changes slightly more with temperature than the internal sensitivity.

The situation is quite different for the chemically sensitized emulsions. So far, such emulsions have been examined exclusively and the large temperature coefficients of their sensitivities have served to support theories of latent-image formation. Now, it appears from our experiments, that these large temperature coefficients are due to the chemical sensitization becoming ineffective at low temperature.

The experiments and their explanations, as given in the preceding parts, lead to the following conclusions: The intrinsic sensitivity of silver bromide is due to a mechanism only slightly dependent upon temperature. This view is supported by the findings of Eggert and Kleinschrod[35] with regard to the temperature-dependence of the sensitivity of photographic emulsions to x-rays. Their experiments indicate a much smaller difference in sensitivity at room temperature and at −173°C for x-rays than for light. This is obviously due to the fact that the sensitivity to x-rays is much less affected by chemical sensitization. This also follows from experiments[36] which show that the ratio of the sensitivities of external and internal image is higher for light than for x-rays.

The temperature-dependence of the sensitivity has formed one of the important reasons for dividing the process of latent-image formation into two events, the electronic one, independent of temperature, and the ionic one, dependent upon temperature. Although this reason now seems to be invalidated to a certain degree, there is still enough other evidence to indicate the existence of two processes. Especially, it seems difficult to explain the disappearance of reciprocity failure at low temperature otherwise. Besides, the formation of electrons which are able to move freely through the lattice is indicated by the displacement of the darkening of a silver chloride crystal, on exposing it simultaneously to a light-pulse and a high electric field,[37] and the movement of silver ions through the lattice by the observations of Zimens[38] on the exchange of radioactive silver ions between a silver nitrate solution and a photographic emulsion.

Apparently, the unsensitized grain contains many imperfections which, however, are small (shallow traps). Such imperfections may consist of just a few holes where silver and bromine ions are missing. Only a small fraction of the electrons which have been liberated from bromine ions by photons are trapped there, forming an F-center, while most of these electrons combine again with the bromine atoms from which they came. The F-centers attract silver ions from the immediate neighborhood. Thus, latent-image specks are formed. They are small, as indicated by the large low intensity reciprocity-law failure which points to a high probability of their disintegration at room temperature. It is evident that this movement of silver ions over a very short distance is little dependent upon temperature.

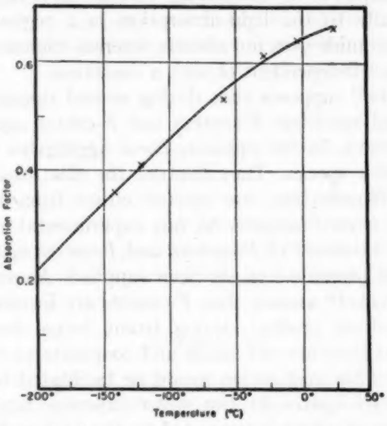

FIG. 27. Dependence of light-absorption at 400 mμ upon temperature for Emulsion *a*.

By chemical sensitization, deep electron traps are created where a greater fraction of the electrons liberated are captured.[39] There is much uncertainty about the nature of these traps. The interpretation of Stasiw and Teltow[26] was attacked and modified by Bodenstein[40] and by Mitchell,[41] but the explanations of all these authors still do not appear to be completely satisfactory. Bodenstein considers the possibility that the chemical sensitizers act like dye sensitizers. This merely reduces the problem to another, and probably even more complicated, one, which, in spite of all the experimental material[42] available, has so far found no satisfactory solution. Besides, chemical sensitizers and dye sensitizers are basically different, insofar as dye sensitizers are incapable of sensitizing unless they contribute materially to the light-absorption in a region where silver bromide does not absorb, whereas chemical sensitizers act independent of such a condition.

---

[35] J. Eggert and F. G. Kleinschrod, Zeits. f. physik. Chemie 189, 1-9 (1941).

[36] H. Sauvenier, Bull. Soc. Roy. Sci. Liége 16, 54–59 (1947); Sci. et Ind. Photo. (2)19, 305–306 (1948); H. Tellez-Plasencia, Sci. et Ind. Photo. (2)19, 45–56 (1948).

[37] J. R. Haynes, in *Preparation and Characteristics of Solid Luminescent Materials* (John Wiley and Sons, Inc., New York, 1948), Symposium held at Cornell University, October 24–26, 1946, pp. 430–431; J. R. Haynes and W. Shockley, in *Report of a Conference on Strength of Solids, held at H. H. Wills Physical Laboratory, University of Bristol, July 7–9, 1947* (The Physical Society, London, 1948), pp. 151–157.

[38] K. E. Zimens, Arkiv f. Kemi, Min. Geol. 23A, No. 16, 1–21 (1947).

[39] To explain experimental results obtained by exposing latent images, formed at −185°C, simultaneously to actinic and bleaching (infra-red) radiation at the same low temperature, W. F. Berg [Trans. Faraday Soc. 35, 445–458 (1939)] assumed that under those conditions electrons may be trapped in two ways: either in shallow and numerous traps, or in deep and relatively fewer traps. He further assumed that the shallow traps exist in the silver halide and the deep traps in the sensitivity nuclei. From the present experiments, it seems to follow that this concept is not restricted to the latent-image formation at low temperature, al-

Mitchell supposes that during second ripening with chemical sensitizer *F*-centers and *F*-center aggregates are formed. In his opinion, these aggregates are the sensitivity specks. They capture the electrons which, under illumination, are ejected either from bromide ions or from *F*-centers. So far, experimental evidence for the existence of *F*-centers and *F*-center aggregates in silver bromide has not been supplied. Anastasevich and Frenkel[43] assume that *F*-centers are formed as an intermediate product during latent image formation but that they are not stable and coagulate to colloidal silver.[e] This coagulation would be facilitated by large interstitial spaces in the silver bromide lattice the existence of which is suggested by the high mobility of silver ions in the silver bromide crystal[38,44] and the comparatively high electric conductivity of silver bromide which, at room temperature, differs from that of potassium bromide by a factor of several powers of ten.[45]

At present, it seems equally reasonable to compare the non-sensitized grains in silver bromide emulsions with either pure alkali halide crystals or crystals containing *U*-centers (KH molecules), and the chemically sensitized grains with alkali halide crystals containing *X*-centers. Such *X*-centers were found by Glaser,[46] causing additional absorption in potassium bromide crystals containing *U*-centers. He found that the formation of *F*-centers through radiation absorbed by the *U*-centers or by the long-wave-length tail of the absorption band of the alkali halide itself is not associated with a motion of electricity of measurable magnitude. This means that the electrons have to move only over very small (molecular) distances such as were postulated to exist in the unsensitized emulsions, between the *F*-centers and the silver ions attracted by them. On the other hand, formation of *F*-centers in alkali halide crystals containing *X*-centers is connected with a photoelectric current of measurable magnitude, indicating that in this case the electrons travel over considerable distances. Nothing definite is known about the nature of these *X*-centers in alkali halide crystals. Their existence, however, is further indicated by the appearance of fluorescence.

Whether the sensitivity specks formed by silver sulfide consist of holes like those in unsensitized grains, only larger and more sparsely distributed, or whether they consist of an aggregate of silver atoms, in either case, it would seem to be certain that they form deep traps. As contrasted with the shallow traps in unsensitized emulsions, most of the electrons liberated from bromine ions "fall" into them, and there is little recombination of electrons with the bromine atoms from which they originated. On the other hand, because of their limited number, silver ions have to migrate rather long distances in order to reach them, but once they have arrived they are held tightly and little low intensity reciprocity failure occurs. Lowering the temperature slows down the mobility of the silver ions on their rather long path to the charged sensitivity speck, preventing them from reaching it before it has disintegrated again.

ACKNOWLEDGMENT

The author wishes to thank Dr. R. E. Stauffer under whose supervision all the experimental emulsions and the clear gelatin layer mentioned in this paper were prepared. He also supplied the grain-size measurements. Mr. E. E. Richardson kindly supervised the reflection and transmission measurements with the automatic spectrophotometer. Furthermore, the author desires to express his gratitude to Dr. J. H. Webb for many helpful discussions.

---

though in commercial (chemically sensitized) emulsions exposed at room temperature and developed in commercial (substantially surface) developers the significance of the shallow traps is small.

[40] M. Bodenstein, Abh. Preuss. Akad. Wiss., Math.-phys. Kl. No. 19, 1–32 (1941).

[41] J. W. Mitchell, Sci. et Ind. Photo. (2)**19**, 361–369 (1948); Phil. Mag. (7)**40**, 249–268, 667–669 (1949).

[42] See, for example, the review by H. Socher, in Stenger-Staude, Vol. 3 [Akademische Verlagsgesellschaft, Leipzig, (1944)] pp. 113–139.

[43] V. S. Anastasevich and Ya. J. Frenkel, J. Exper. Theor. Phys. U.S.S.R. **11**, 127–132 (1941).

[e] In a recent note (reference 41, p. 668), Mitchell, in order to explain why coagulation of *F*-centers does not occur, assumes that they form immobile association complexes with singly charged sulfide ions. No experimental evidence is given for the existence of such complexes.

[44] W. Lehfeldt, Zeits. f. Physik **85**, 717–726 (1933).

[45] C. Tubandt, Zeits. f. anorg. Chemie **115**, 105–126 (1921).

[46] G. Glaser, Ann. d. Physik (5)**27**, 217–232 (1936).

JOURNAL OF THE OPTICAL SOCIETY OF AMERICA VOLUME 39, NUMBER 12 DECEMBER, 1949

Emissivities of Copper and Aluminum

George Best*
Department of Physics, Northwestern University, Evanston, Illinois

(Received August 29, 1949)

The total hemispherical emissivities of copper and aluminum were determined over the approximate range of temperatures from 100°C to 400°C. The material under test was formed into a hollow sphere 4.5 cm in diameter which was mounted concentrically in an evacuated spherical glass flask 28 cm in diameter. The metal sample was heated electrically from within and the flask was kept at a constant temperature by the circulation of ice water over its outer surface. Temperatures of the specimens were measured on the inner surfaces with copper-constantan thermocouples. Heat losses through the thermocouple and power leads were evaluated by a substitution method. Polishing was done mechanically using a modified metallographic procedure with levigated alumina. The emissivity of copper was found to be practically constant at 0.03 but for aluminum the value was considerably higher and showed a temperature dependence. Comparison of the results with those predicted by the theory of Davisson and Weeks shows moderate agreement for aluminum and disagreement for copper.

INTRODUCTION

THE loss of energy by a metallic surface due to its temperature alone must be considered in many heat transfer problems. Ordinarily the radiating properties of the polished surface of an opaque body are compared under the proper conditions with those of a "blackbody." The emissivity of the material is defined by such a comparison. In problems of heat transfer by radiation total hemispherical emissivities are involved since the energy is spread throughout the spectrum and is radiated in all outward directions from each element of surface.

There have been many determinations of total normal emissivities,[1] i.e., normal to the radiating surface, but few measurements of total hemispherical emissivities have been reported. Davisson and Weeks measured the latter for platinum over a wide range of temperatures using a filament-in-vacuum method,[2] and Blackman, Egerton, and Truter have made measurements on several metals at about 90°K using a method involving the evaporation of liquified gases.[3]

Davisson and Weeks derived a theoretical expression for total hemispherical emissivities of metals.[2] By taking into account the angular dependence of emission of monochromatic radiation according to Fresnel's laws, they revised the theory of Foote[4] which was developed on the basis of electromagnetic theory and the assumption of Lambert's cosine law. For a metal of resistivity ρ at an absolute temperature T they expressed the total hemispherical emissivity as

$$e_{ht}=0.752(T\rho)^{\frac{1}{2}}-0.635(T\rho)+0.674(T\rho)^{\frac{3}{2}}-0.612(T\rho)^{2}. \quad (1)$$

Their experimental results for platinum were in fair agreement with this formula.

This paper reports measurements of total hemispherical emissivities of copper and aluminum over the approximate temperature range 100°C to 400°C. It is anticipated that the work will be continued to include at least gold and silver.

APPARATUS

The apparatus consisted of a pair of concentric spheres, the inner of which was the test sample with a diameter of 4.5 cm, and the outer was a glass flask with a diameter of 28 cm. Both surfaces of the flask were coated with matt optical black and the temperature was kept constant by the circulation of ice water over the outer surface. The flask was evacuated so that the principal heat transfer was by radiation.

The metal test spheres were made of pairs of thin-walled hemispheres which were clipped together on the inside. The sphere under test was mounted concentrically around an electrical heater consisting of Chromel wire wound on a soapstone cube 1.8 cm on a side. A hole in the top of the sample permitted entry

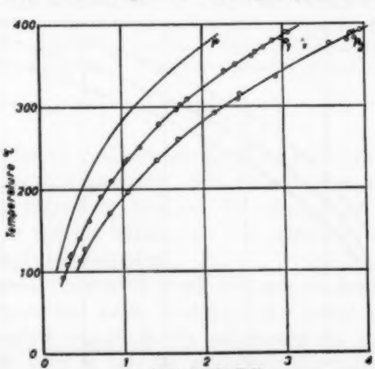

FIG. 1. Variation of copper sphere temperature with power input. P is power radiated by sphere, P_1 is power input with one set of leads, P_2 is power input with dummy leads.

---

[*] Now at Los Alamos Scientific Laboratory, Los Alamos, New Mexico.

[1] W. H. McAdams, *Heat Transmission* (McGraw-Hill Book Company, Inc., New York, 1942), p. 393.

[2] C. Davisson and J. R. Weeks, J. Opt. Soc. Am. and Rev. Sci. Inst. 8, 581 (1924).

[3] Blackman, Egerton, and Truter, Proc. Roy. Soc. (London) A194, 147 (1948).

[4] P. D. Foote, Bull. Bur. Stand. 11, 607 (1915).

of the power and thermocouple leads which also supported the sample. The leads consisted of a pair of No. 22 copper wires carrying current to the heater, two No. 30 copper wire potential leads, and two copper-constantan thermocouples of No. 30 wire for measuring the sphere temperature. The power input was determined by a voltmeter-ammeter method—a potentiometer was used for the smaller potentials. The thermocouple electromotive forces were measured with a potentiometer.

PREPARATION OF THE SAMPLE

The outer surface of each sample was polished mechanically using a modified metallographic procedure. Initial smoothing was done by hand with emery polishing paper of increasing fineness to a grit of 0000. Next, No. 600 carborundum was used on a rotating short-napped polishing cloth, the cloth being fastened over the end of a metal cylinder rather loosely so that it would conform to the shape of the sphere. Finally, levigated alumina on a cashmere wool polishing cloth mounted and rotating as above was used. Microscopic examination showed that the grains of alumina in the final polish ranged in size up to approximately five microns on a side with the predominance having dimensions less than two and one-half microns. The polished surface was rinsed several times with distilled water and alcohol and swabbed with a soft lint-free cloth to insure removal of the polishing agent. The sample was dried in a stream of nitrogen and kept in an atmosphere of nitrogen until ready for use.

EXPERIMENTAL PROCEDURE

A freshly polished sample was mounted on one of the heater assemblies, the thermocouples being cemented to the inner surface of one of the hemispheres with a conducting silver cement to provide thermal contact. The sample and heater were then placed in the large sphere and the system was evacuated. Next the temperature was raised high enough that the sample would be annealed before any data were recorded. The procedure insured a more constant crystaline state and a more uniform surface throughout a period of test. The power input was varied to obtain different sample temperatures and for each power input the system was allowed to come to thermal equilibrium. Each series of determinations was made in a cycle, i.e., from high to low and back to the initial high temperature. This gave assurance that the sample surface was unaltered.

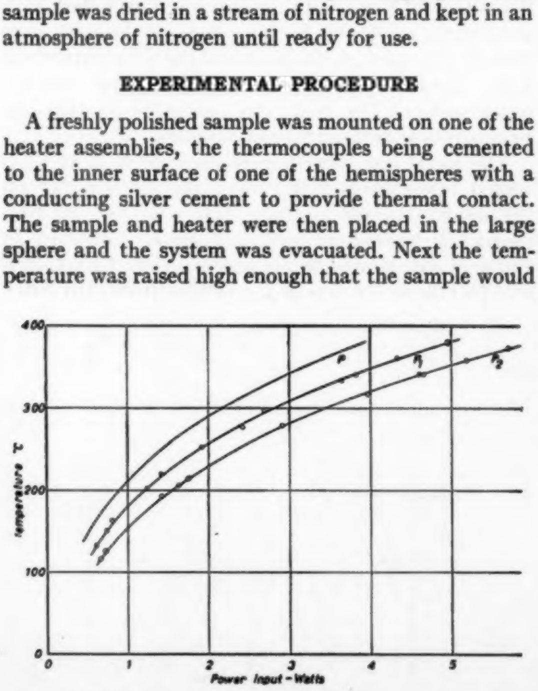

FIG. 2. Variation of aluminum sphere temperature with power input. P is power radiated by sphere, P_1 is power input with one set of leads, P_2 is power input with dummy leads.

Two sample spheres of each metal investigated were used and also two separate heater assemblies, both samples being used with both heaters. After several sets of measurements had been made for a particular metal, a hole was drilled in the bottom of one of the spheres and a set of dummy leads duplicating those entering through the top was introduced. Then another series of measurements was made with this sphere. In this manner corrections for the power loss through the leads at the various temperatures were made.

To test for the presence of an oxide layer on the surface, the copper sample was heated to 300°C in hydrogen at a pressure of one atmosphere. No change in radiating characteristics could be detected following this treatment so it was assumed that the surface of the copper was not oxidized.

COMPUTATIONS

Assuming the Stefan-Boltzmann radiation law, the net rate at which energy is transferred between two concentric spheres is

$$P=\epsilon A\sigma(T_1^4-T_2^4), \tag{2}$$

A is the area, ϵ is the emissivity of the surface of the smaller sphere, σ is the Boltzmann radiation constant, and T_1 and T_2 are the absolute temperatures of the inner and outer spheres, respectively. In this work all these quantities were either known or measured except the emissivity which was desired.

The power radiated, P, was determined by taking the difference between the power input with one set of leads, P_1, and the power input with the dummy leads inserted, P_2, and subtracting it from P_1. If we let A designate the area of the metal sphere with no holes in it, ΔA designate the area of each hole, P_L represent the power loss through one set of leads, and U be the power radiated by unit area of the sphere, then

$$P_1=(A-\Delta A)U+P_L \tag{3}$$

$$P_2=(A-2\Delta A)U+2P_L \tag{4}$$

$$P=2P_1-P_2=AU. \tag{5}$$

This means that for the power, P, determined in the above manner, the area to be used in Eq. (2) is the total area of the unpunctured sphere. The power radiated, P, along with P_1 and P_2 over the temperature range of the observations for copper and aluminum, are shown in Figs. 1 and 2, respectively.

The experimentally determined total hemispherical emissivities of copper and aluminum are plotted in Fig. 3 with the values predicted by formula (1).

EXPERIMENTAL ERRORS

The possible sources of error in this work include the determinations of the surface area of the sample, the power input, the temperatures, heat loss through the atmosphere in the flask, heat loss through the leads, and degree of polish of the surface of the metal sphere. When all of these sources are taken into consideration, the probable error in the determination of the emissivities does not exceed five percent.

DISCUSSION OF RESULTS

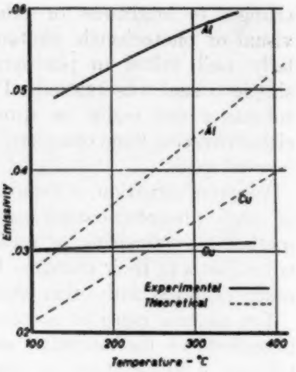

FIG. 3. Temperature dependence of total hemispherical emissivities.

Comparison of the experimental results obtained here with the theoretical values indicates that the theory may apply to aluminum but not to copper. The theoretical equation (1) is based on the assumption that the wave-length distribution of energy is in accordance with the Planck formula, however, copper exhibits selective reflection in the visible spectrum so it would be expected that some modification of the theory would be required.

JOURNAL OF THE OPTICAL SOCIETY OF AMERICA VOLUME 39, NUMBER 12 DECEMBER, 1949

The Observation of Temperature Distributions and of Thermal Radiation by Means of Non-Linear Phosphors*†

F. URBACH, N. R. NAIL, AND D. PEARLMAN
Kodak Research Laboratories, Eastman Kodak Company, Rochester, New York

(Received September 12, 1949)

It is shown that the temperature-dependence of the luminescent efficiency of numerous phosphors may be used for the observation, measurement, and recording of temperatures and temperature distributions. Remarkably high temperature-sensitivities can be obtained by exciting the phosphors under such conditions that their efficiency is far below the optimal efficiency obtainable with the same phosphors. Thus, they are used under conditions which are most unfavorable for any other practical application and for most investigations. In particular, the strong temperature-dependence of superlinear phosphors, and the variation of this dependence with the exciting intensity, have been used for the development of thermometric and thermographic methods.

Two methods are described: In the first, the surface to be observed is coated with a luminescent material and evenly illuminated with ultraviolet radiation. The temperature distribution on the surface of the object under test becomes visible as a pattern of brightness or color of the luminescent coating. This pattern can be observed visually, measured by visual or photoelectric photometry, or recorded photographically. The result may be displayed in various ways. Isotherm charts can be obtained easily by purely photographic means. In the second method, a temperature-sensitive phosphor screen is placed in the focus of a suitable optical system. An image of the distribution of the thermal radiation from the object becomes visible on the screen as a brightness pattern which is easily recorded photographically and on which measurements can be carried out. While the second method does not require any coating of the object, the first is by far the more sensitive. A number of pictures illustrating the two methods and a discussion of their performance are given.

ANY temperature-sensitive property of a material can, in principle, be used to measure temperature. There are many practical considerations which determine the choice of such properties, depending largely upon the specific uses. Under all circumstances, however, questions of sensitivity and of range will arise. The thermometric sensitivity depends upon both the temperature coefficient of a given property and upon the precision of available methods for measuring small changes of that property. We do not always realize what an ingenious method for measuring minute changes in specific volume we use whenever we read an ordinary thermometer.

The measurement of small changes in luminescent brightness is not easy. Thermometry based on such measurements would be by no means an attractive possibility were it not for some peculiar advantages. First, under certain circumstances the temperature-dependence of efficiency may be made so large that no elaborate measurement is needed. Second, while these changes in brightness or color can be measured by visual or photoelectric photometry, they are particularly well suited to photographic recording and to simple visual observation. Third, the thermometric substance can easily be spread over large surfaces, either covering them completely or in small strategically located spots.

---

* Communication No. 1261 from the Kodak Research Laboratories.

† The text of this paper is substantially as read to the Winter Meeting of the Optical Society of America, New York, February, 1949, except for the addition of the isotherms, Figs. 6 and 7.

Visual observation, or the use of photographic records, of such phosphor-coated surfaces represents a new method of estimating or measuring temperature distributions and their changes. The same results are not easily achieved with other methods of thermometry.

Let us now consider some of the characteristics of phosphors as thermometric substances. A very large number of temperature-dependence curves for a variety of phosphors have been published. A survey of these data shows that the zinc sulfide, zinc-cadmium sulfide, and zinc-cadmium selenide phosphors are among those having the strongest temperature-dependence.

Figure 1 shows some representative curves[1] which are characteristic of the temperature-dependence of this type of phosphor. The steepest parts of these curves do not represent, however, the most important region. For most applications, we are not interested in the change of brightness per degree centigrade. The sensitivity of visual and of photographic observation, and to some extent, of measurement, depends mainly upon the percentage change in brightness. This change is shown clearly if one plots the logarithm of efficiency against temperature, as has been done in Fig. 2. It is seen that in the two lower curves, the maximum slope occurs at an efficiency value which is hardly more than a few percent of the maximum efficiency. This seems to be a general rule.

This fact is undoubtedly one reason why, hitherto, neither we nor apparently others have paid much attention to the temperature-sensitivity of phosphors from a technological point of view. In order to obtain a high effective temperature-sensitivity, say, at room temperature, one would have to use a phosphor of very

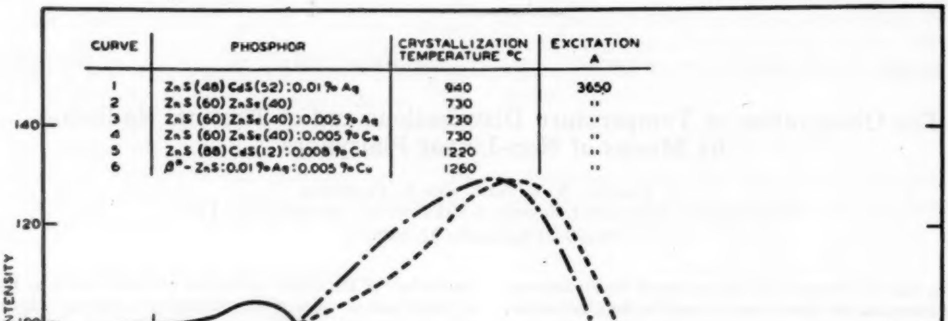
CURVE	PHOSPHOR	CRYSTALLIZATION TEMPERATURE °C	EXCITATION A
1	ZnS (48) CdS(52) : 0.01 % Ag	940	3650
2	ZnS (60) ZnSe (40)	730	"
3	ZnS (60) ZnSe (40) : 0.005 % Ag	730	"
4	ZnS (60) ZnSe (40) : 0.005 % Cu	730	"
5	ZnS (88) CdS(12) : 0.008 % Cu	1220	"
6	β* - ZnS : 0.01 % Ag : 0.005 % Cu	1260	"

FIG. 1. Dependence of luminescent intensity upon temperature (from Leverenz).

---

[1] H. W. Leverenz, R.C.A. Review 7, 238 (1947).

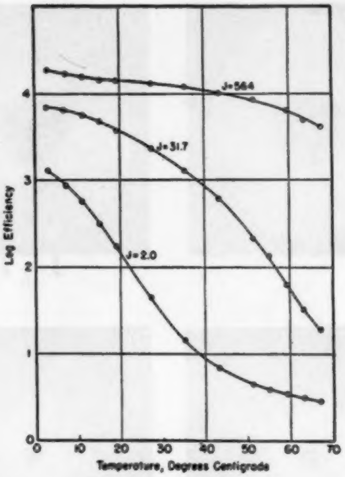

FIG. 2. Temperature-dependence of efficiency for a zinc-cadmium sulfide phosphor: 50% ZnS, 50% CdS, 2% NaCl, 400 ppm Ag, 1.0 ppm Ni. Fired at 1090°C for 30 minutes. Excited by 365 mμ.

low luminescent efficiency at that temperature. In other words, under normal conditions of use, phosphors are really not very sensitive to temperature changes.

Once this is clear, however, one finds remarkably high temperature-sensitivities in the regions of low efficiency. If high brightness is required, it can be attained by the use of strong exciting intensity.

For several reasons, we selected for this work the zinc-cadmium sulfide phosphors originally prepared for the investigation of superlinear luminescence, reported in a previous paper.[2] These phosphors make it possible to attain a very high temperature-sensitivity. The example in Fig. 2 gives about 20 percent brightness change per degree centigrade. In addition, these phosphors offer the advantages of extraordinary flexibility, owing to exactly the same group of phenomena which make them such interesting objects of research. By varying the composition of the base, the activators, and particularly the poison concentration, and by using mixtures, nearly any desired temperature-dependence curve can be obtained. This curve may be made as steep as those shown before, or very flat, depending upon whether range or sensitivity is more important. By using components of different colors, we can cover a large range and still obtain, with filters, quite high sensitivity. We cannot here describe all the possibilities in detail. One important point, the shift of the temperature curves by variation of exciting intensity, is illustrated in Fig. 2. This phenomenon provides a fine adjustment of range and sensitivity which is useful for most, and essential for some, applications.

As we stated earlier, direct measurement of temperature distributions by visual or photoelectric brightness

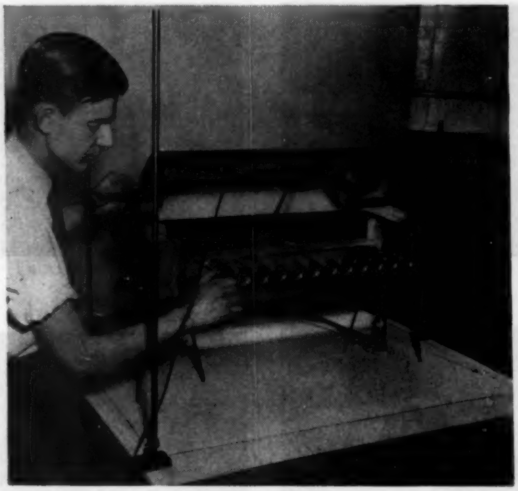

FIG. 3a. Device for calibrating temperature-sensitive phosphors (in room light).

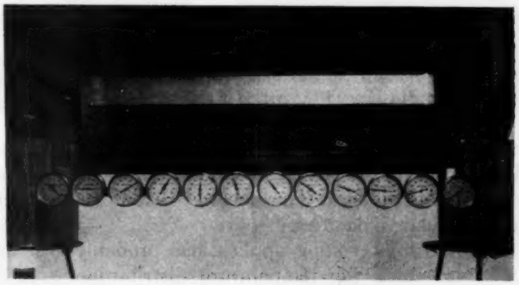

FIG. 3b. Device for calibrating temperature-sensitive phosphors (under ultraviolet radiation).

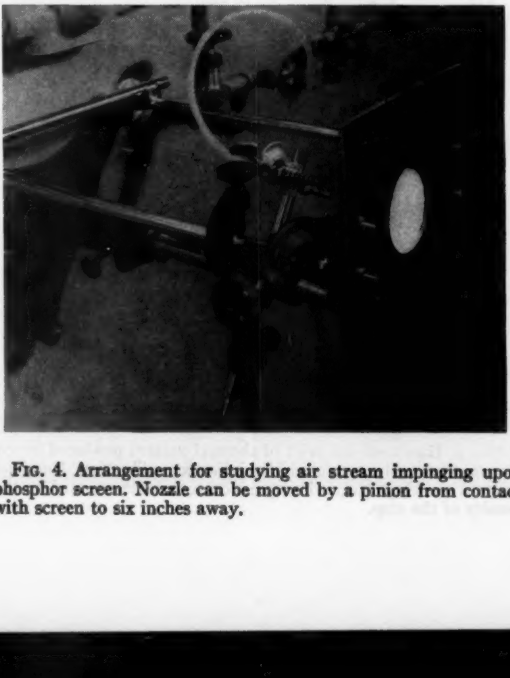

FIG. 4. Arrangement for studying air stream impinging upon phosphor screen. Nozzle can be moved by a pinion from contact with screen to six inches away.

---

[2] Nail, Urbach, and Pearlman, "New Observations on Superlinear Luminescence," J. Opt. Soc. Am. 39, 690 (1949).

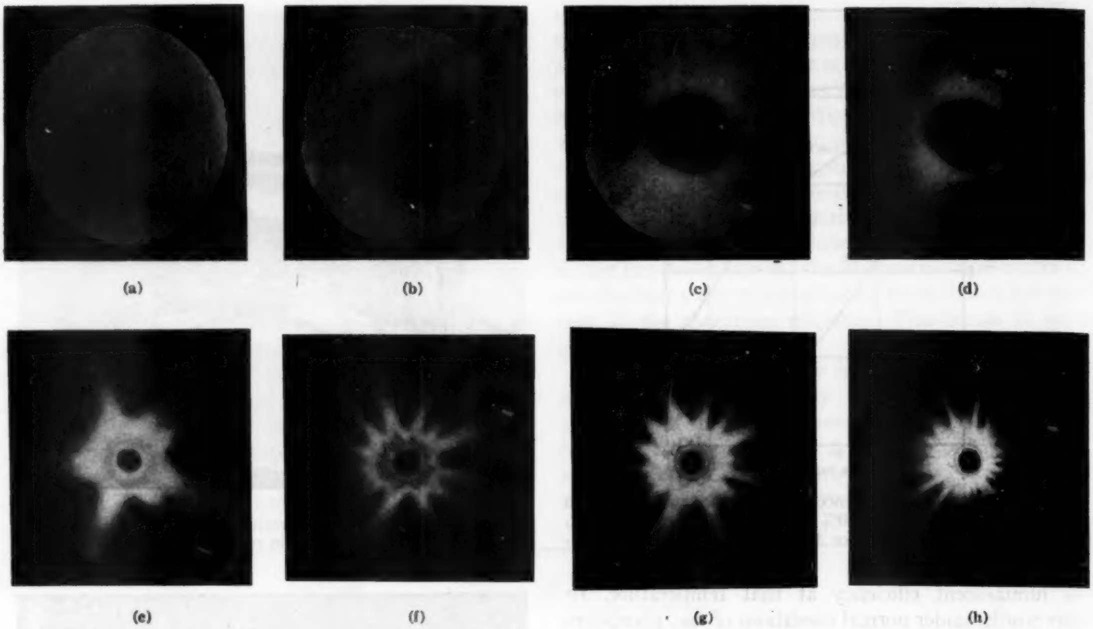

(a) (b) (c) (d)

(e) (f) (g) (h)

FIG. 5. Thermal effect of air stream impinging on back of phosphor screen. a. Phosphor screen under ultraviolet excitation. No air stream on surface. b. Air stream on. Nozzle approximately six inches from screen. c.–h. Air stream on. Nozzle moved successively closer to the screen. In Fig. 5h the nozzle is almost in contact with the screen.

measurements is perfectly possible, and often desirable. The sensitivity depends, of course, upon the photometric method used. The necessary calibrations offer no particular difficulties.

The most interesting applications probably will be those in which the temperature distribution over a surface is surveyed and quickly estimated by visual observation or is recorded photographically. A few examples are shown in Figs. 3 to 8.

The first example is a primitive but very useful arrangement. Figure 3a is a picture of two kettles filled with water. They are connected by a heavy brass bar. A set of Weston thermometers is fitted into the bar, close to the surface. A temperature-sensitive phosphor is coated on that surface and appears in a mirror mounted behind the bar. The kettle to the left is then heated, and the one to the right is filled with ice cubes (Fig. 3b). The temperature distribution thus created can be read on the thermometers and the corresponding brightness distribution can be clearly seen on the

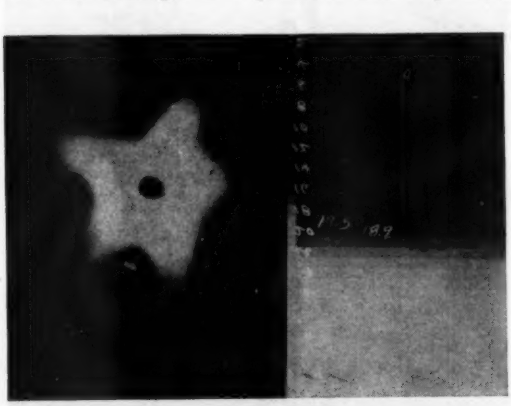

FIG. 6. High-contrast print of thermal pattern produced by air stream. Step wedge was used in printing for calibration. Numbers on steps are temperatures in degrees centigrade represented by the density of the step.

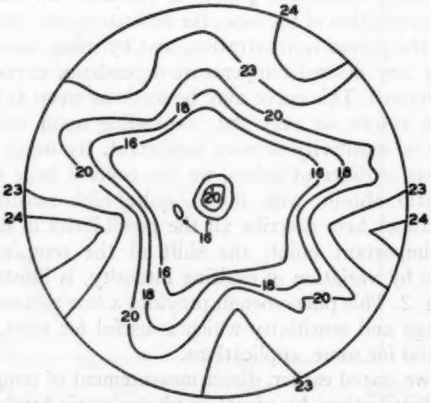

FIG. 7. Isotherms on the screen obtained from set of prints similar to that in Fig. 6. Numbers are temperatures in degrees centigrade.

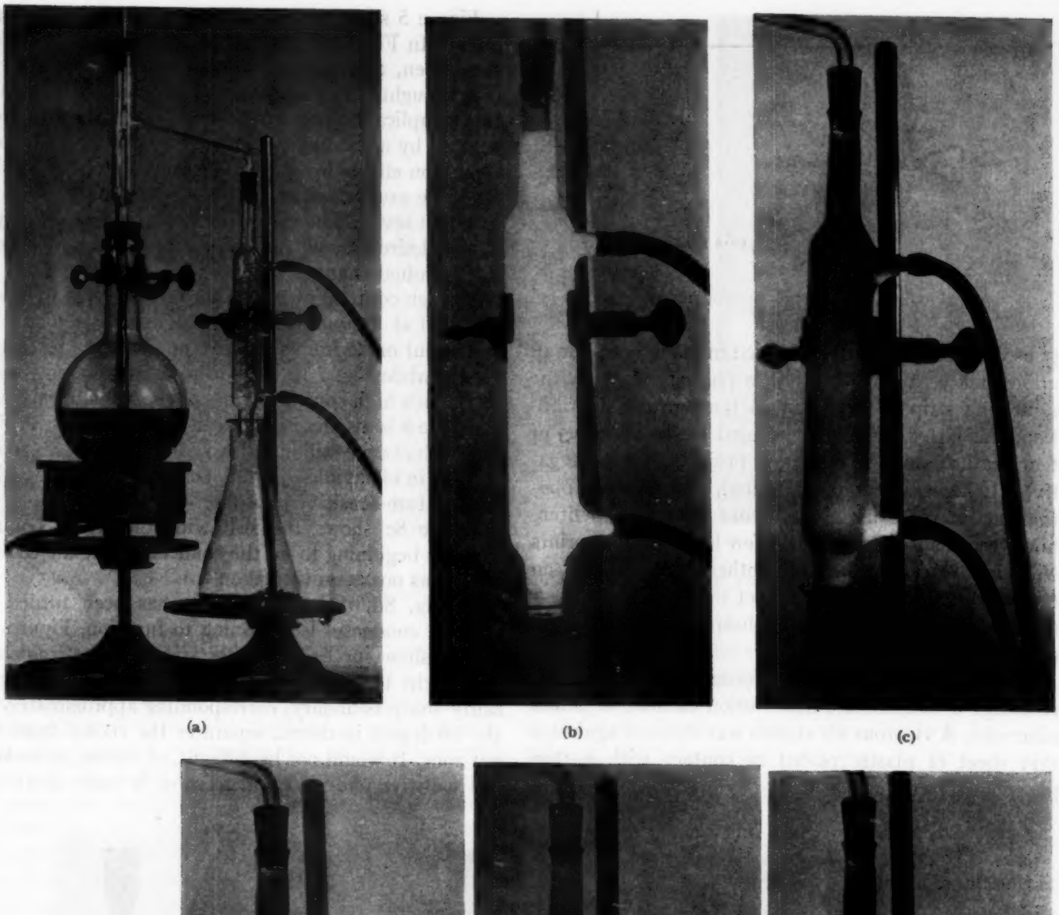

Fig. 8. Glass still. a. As seen in room light. b. Condenser coated with phosphor. Seen under ultraviolet illumination. c. Still in operation; no cooling water. d. Still in operation; cooling water on; condenser beginning to function. e.-f. Same as d, but successively later stages.

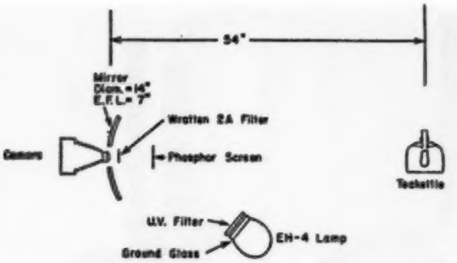

FIG. 9. Set-up for thermoradiography.

phosphor. This device can be used in many cases for an approximate calibration. If it is photographed on the same film strip as an unknown temperature distribution, the latter can be interpreted easily in terms of temperature, using a contiguous projection of the negatives. If higher precision is desired, photographic photometry may be used easily and effectively. Often, however, this is not needed. A few high contrast prints will yield reasonably precise isotherms. Instead, if no record is needed, one may project the pictures with exciting light on a superlinear phosphor, using it as a contrast amplifier.

As an example, Fig. 4 shows the arrangement used for recording a temperature distribution difficult to detect otherwise. A vigorous air stream was directed against a thin sheet of plastic placed in contact with a thin phosphor screen.

Figure 5 shows the complex patterns formed on the screen. In Fig. 5a, the nozzle is at some distance from the screen, and in the succeeding pictures of the set it is brought closer by stages. The later pictures show the complicated pattern of heating and cooling developed by a combination of friction, compression, and expansion effects in the turbulent air stream. By using the same excitation and by taking pictures of the same screen at several known temperatures, one may analyze in any desired detail the temperature distributions and their gradual change.

By high contrast printing, sets of isotherms are easily obtained at the various stages. Figure 6 is a high contrast print made from a picture similar to the picture of Fig. 5, while Fig. 7 is a set of isotherms drawn from a set of such high contrast prints of the same negative.

Figure 8 is a series of pictures of a common still. Figure 8a shows the still in ordinary light. Figure 8b shows the still in ultraviolet light, the condenser coated with a temperature-sensitive phosphor.

Figure 8c shows the still with the water boiling; steam is beginning to fill the condenser, but the cooling water has not been turned on.

In Fig. 8d, the cooling water has been turned on and the condenser is beginning to function. Figures 8e and 8f show successively later stages as the condenser is brought to normal operation. In the last picture, a fairly sharp boundary, corresponding approximately to the 80-degree isotherm, separates the cooled from the hot zone. It would not be difficult, of course, to make a less sensitive phosphor and to show in more detail the

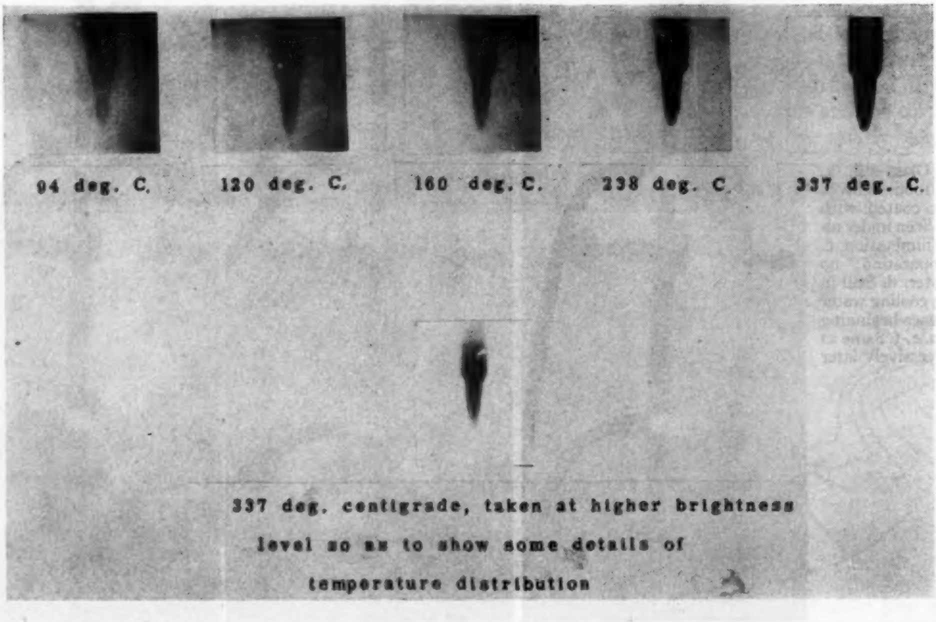
94 deg. C.
120 deg. C.
160 deg. C.
238 deg. C.
337 deg. C.
337 deg. centigrade, taken at higher brightness level so as to show some details of temperature distribution

FIG. 10. Thermoradiographs of soldering iron taken at temperatures indicated.

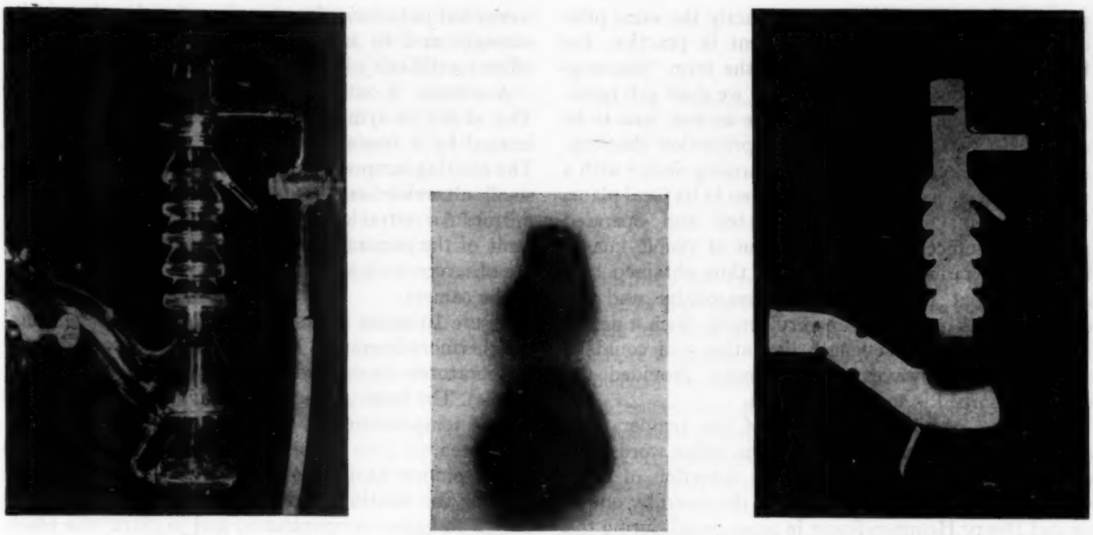
(a) (b) (c)

FIG. 11. Glass diffusion pump. a. In room light. b. Thermoradiograph of pump in operation. c. Contact-thermograph of pump in operation.

distribution of temperature in the lower part of the condenser.[3]

There are several limitations to this method. The coating of the surface to be observed or recorded is in some cases somewhat troublesome. At high temperatures, e.g., above 200°C, the stability of the coating must be taken into consideration. Sometimes the difference between the radiation properties of the coated and uncoated surface may be disturbing. This difficulty can often be overcome by coating small spots only. Some applications are possible only in a completely darkened room; others require at least a subnormal level of ambient illumination. Arranging the ultraviolet lamps properly may occasionally be difficult. For many applications, however, these difficulties will be insignificant. We believe, therefore, that the new method, for which we suggest the term "thermography," will be useful for research and development work involving thermal phenomena and also in a number of industrial processes.

The second part of this paper is devoted to another method of using the temperature-sensitivity of phos-

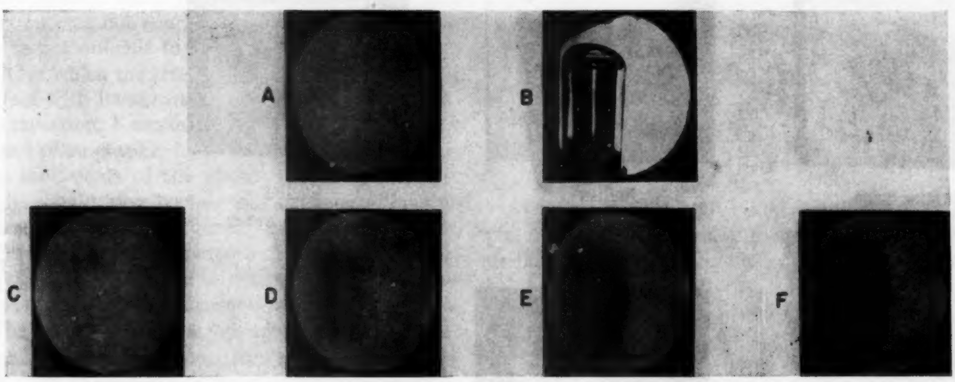

FIG. 12. Glass vacuum tube. a. Phosphor screen under ultraviolet illumination. b. Vacuum tube under room illumination. c. Thermoradiograph of tube with filament current on. d. Thermoradiograph of tube with one plate carrying rated current. e. Same as d, after several minutes of operation. f. Thermoradiograph of tube with both plates carrying rated current. Envelope of tube radiating.

---

[3] At the New York Meeting of the Society, a short motion-picture film corresponding to the sequences of Figs. 5 and 8, the latter in color, was shown.

phors which, although based on exactly the same principles as the first, is quite different in practice. For both methods, we propose to use the term "thermography." The one described thus far we shall call tentatively "contact thermography"; the second, now to be described, we shall designate as "projection thermography." We have set up an image-forming device with a temperature-sensitive phosphor screen in its focal plane. The sensitivity of properly selected and operated phosphors suffices for the formation of visible images by thermal radiation. The images thus obtained lack definition, but the sensitivity is reasonable and the device and its operation are very simple. Such a device has basically no wave-length limitation and could be applied to microwaves or ultrasonics, provided the energy absorbed is sufficiently large.

A similar possibility, the use of the temperature-sensitivity of phosphorescence, or, in other words, the use of thermoluminescence for the detection of long-wave-length thermal radiation, was discussed by one of us and Henry Hemmendinger in some detail during the war. Later, as the strong temperature-sensitivity of fluorescence became clear, it was felt that its potentialities would be worth investigating, since it would eliminate the need for cycles of excitation and observation. Since early in 1946, along with the research work on non-linear luminescence, we have experimented fairly systematically in this direction.

As indicated before, the high sensitivities needed for this application are available only at low efficiency levels. The higher the intensity required to produce a given efficiency, the higher is the brightness level in that region of low efficiency. Therefore, the best way of obtaining, with superlinear phosphors, a strong temperature-sensitivity at reasonable brightness levels is—somewhat paradoxically—to poison the phosphors quite strongly and to use very intense excitation, which offers no difficulty in this application.

A scheme of our original set-up is shown in Fig. 9. The object is symbolized by the tea kettle, which is imaged by a concave mirror on the phosphor screen. The exciting lamp was an EH-4 lamp, later replaced by small ultraviolet-emitting fluorescent lamps near the mirror. An ultraviolet-absorbing filter is arranged in front of the camera. For visual observation, the eye of the observer, or a suitable eyepiece, may take the place of the camera.

Figure 10 shows a series of projection-thermographs, or "thermoradiographs," of a soldering iron at different temperatures (measured with an attached thermocouple). The brighter spot in the picture of the iron is a spot of temperature-insensitive fluorescent material on the screen.

The picture at the bottom shows the effect of increasing the exciting intensity. The sensitivity range is shifted to higher temperatures, and in place of a black spot, the temperature distribution becomes visible in more detail.

Figure 11 shows another such thermoradiograph. Figure 11a is a picture in ordinary light of a common diffusion pump, and Fig. 11b is a thermoradiograph of the lower part, showing the hot zone of the boiler and the region where the stream of oil vapor condenses on the wall of the pump. Figure 11c is a contact-thermograph of a similar pump, coated, of course, with a temperature-sensitive phosphor.

Figure 12b shows an ordinary photograph of a two-plate rectifier tube. Figures 12c to 12f show its thermoradiographs; in Fig. 12c the heating filaments have been turned on. The tips of the filaments can just be seen

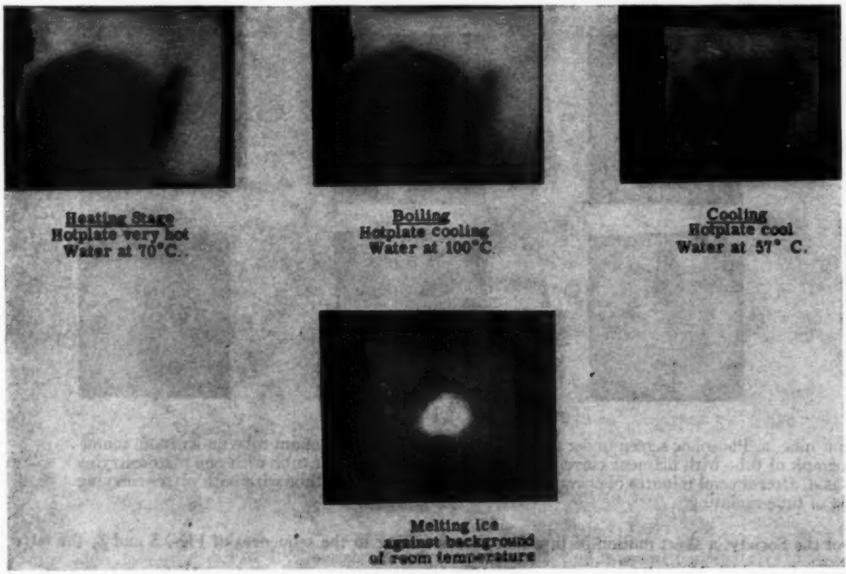

Fig. 13. Photographs by thermal radiation. All pictures taken in dark room at 28°C. Top: Hotplate and tea kettle. Bottom: Piece of ice.

projecting behind the plate. As the heating is continued, the plates become gradually visible; their heat-radiation is, to a large extent, absorbed by the glass, but as they get warmer, enough radiation of wave-length shorter than the absorption limit of the glass is generated, so that their image is obtained. Finally, the plate current is turned on, first on one plate (*D*), and then on both (*E*). A strong but blurred picture of both plates is now obtained. As heating is continued, the absorption of the glass interferes seriously; the glass envelope itself becomes warm enough to produce a strong thermoradiograph (*F*).

It is interesting to compare in principle contact thermography and projection thermography. The latter has, of course, the disadvantage of lower sensitivity and lower resolving-power, but it also has several advantages: (1) The object does not have to be coated with the phosphor and there is no need for arranging exciting lamps in a definite relation to the object. The object need not even be within the actual reach of the observer. (2) Any desired temperature range may be covered easily by changing phosphors or by varying the exciting intensity. (3) If filters eliminating the visible light are used—and such filters can now be made—the use of projection thermography is not restricted to the darkroom or to dim illumination.

On the other hand, in this technique as in contact thermography, we are not limited to qualitative observation or recording. Calibration is not difficult. It should be noted that it would be naturally a calibration in radiation units, say, erg $\text{sec.}^{-1}\ \text{cm}^{-2}$, or in equivalent temperatures of a blackbody.

The next three figures show the results obtained with objects of lower temperatures. A series of pictures taken by the radiation of a teakettle at temperatures from 100°C down to 57°C appears in Fig. 13. Although this series seemed fairly good when it was taken two years ago, it was not nearly as good as it should have been. It is not difficult to calculate approximately the temperature which the screen should assume in thermal equilibrium with its surroundings and with the image-forming radiation. Knowing approximately the physiological and photographic factors involved and the temperature coefficients of the phosphors, we found that the results should have been better. One reason for this discrepancy is the inhomogeneity of the luminescent field on the screen in the absence of a thermal object. Slight variations in exciting intensity are multiplied by factors of about three by the non-linearity of the phosphor. The coarse graininess apparent in the pictures is also partly due to non-linearity. These irregularities severely limit the minimum detectable contrast. This difficulty was overcome by taking the picture of the screen with no thermal inhomogeneity in the field. A suitable transparency from this picture is then used as a mask for visual observation, or for the printing of the thermoradiographs. With this technique, thermoradiographs of the teakettle at 47°C against a background of room temperature still show good contrast, and Fig. 14, a thermoradiograph of a human hand against a background temperature of about 27°C, illustrates the present sensitivity of this method.

FIG. 14. Thermoradiograph of human hand taken against room background of 27°C.

The detection limit for temperature differences of approximately black radiators is at present somewhere in the neighborhood of 4 to 5°C. The smallest detectable energy flux on the phosphor surface is about 500 microwatts per square centimeter. As indicated before, the sensitivity of the phosphor as a bolometer would not be high. Depending upon the method of observation or measurement used, it will be from 1/100th to 1/1000th of that of a good thermistor or Golay cell.

But, considering the complications which would be introduced in producing a reasonably detailed two-dimensional visible picture with the aid of the pointlike detectors, and comparing this complicated procedure with the simple phosphor method, it is evident where the superiority of the latter lies. It lies in the two-dimensional extension of the sensitive element, which makes possible simultaneous reception at many points, and in the fact that the response of the sensitive elements is observable directly.

The simplicity of this method is perhaps best illustrated by the fact that we never actually constructed a thermoradiographic camera, as we should have done. Whenever we wanted to make thermoradiographs, we just set up the mirror, ultraviolet lamps, and phosphor screen, and made the pictures.

The data on sensitivity, and the unsharpness of the pictures clearly show the present limitations of the new method. Within these limitations, however, this method extends effectively and with simple means, the range of visual observation and of photography far beyond the limits of ordinary infra-red photography, image tubes, and infra-red-sensitive phosphors. We hope that this method, too, will have useful applications in scientific and industrial work.

JOURNAL OF THE OPTICAL SOCIETY OF AMERICA VOLUME 39, NUMBER 12 DECEMBER, 1949

Latent-Image Distribution by X-Ray Exposures*

G. Kornfeld
Kodak Research Laboratories, Eastman Kodak Company, Rochester, New York

(Received September 1, 1949)

X-ray exposures are supposed to result in the production of a considerable amount of internal latent image. However, in a motion-picture positive emulsion hardly any internal latent image could be developed after exposure to x-rays, at the temperature of liquid nitrogen as well as at room temperature. Since the existence of a marked Herschel effect shows that a considerable number of grains carry not more than one surface center, and that of minimum size, the question arises as to where the many hundred silver atoms have gone which were produced in the grain by the absorption of one x-ray quantum. They could have disappeared by rebromination in the absence of a halogen acceptor, or they could be too finely distributed to act as development centers. A reversal of the Herschel effect at high densities, after an x-ray exposure at the temperature of liquid nitrogen, argues for the second assumption.

EXPERIMENTAL evidence[1] has been forthcoming for the favoring of internal latent-image production by x-ray exposure of various emulsions. This can be easily explained by the size of the x-ray quantum and its production of such a large amount of latent image that the formation of development centers need not take place at the sensitivity centers of the surface.[2] This would imply that the silver atoms, produced by the ionization along the paths of the secondary electrons, do not stay isolated but collect for the formation of centers. However, recent experimental evidence shows that not in every emulsion does all the silver produced by x-rays collect to form centers.

A contrast motion-picture positive emulsion was chosen which had shown a considerable Herschel effect after exposure to light (Fig. 1); for the same film, three times as much infra-red exposure was needed to produce approximately the same Herschel effect after an exposure to x-rays (Fig. 2). (The x-rays passed through a steel-step tablet and varied from 0.15A to 0.9A.) This effect, though smaller than that after light-exposure, is still very marked and implies that a large number of grains do not have more than one development center at the surface, and that these centers do not extend beyond the "critical size."[3] Since such development centers are likely to consist of less than ten atoms, the conclusion must be drawn that the several hundred silver atoms liberated in a grain by the absorption of one x-ray quantum are not contributing to the formation of surface centers and should be present in the interior of the grain.

Using the same conditions as before for the x-ray exposure (80 kilovolts, 5 minutes, step tablet), three strips were used. After the exposure, one strip was

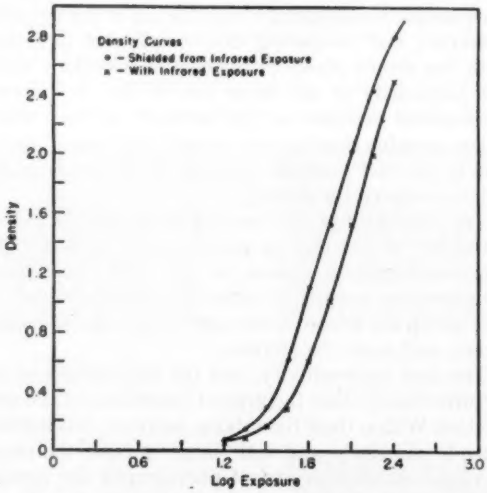

Fig. 1. Contrast motion-picture positive emulsion used throughout this investigation. Herschel effect after exposure to light. 30-minute infra-red exposure. Development in D-16. Four minutes at 68°F.

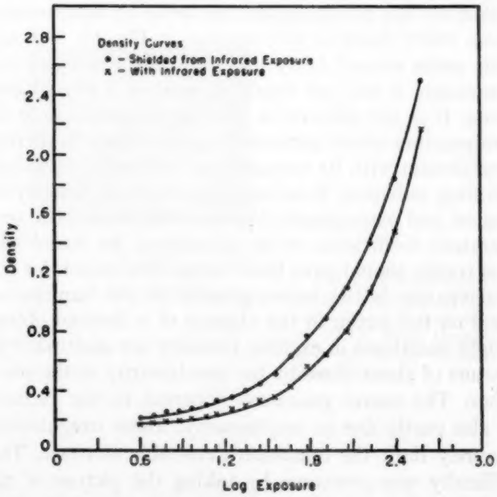

Fig. 2. Herschel effect after exposure to x-rays at room temperature for five minutes. 90-minute infra-red exposure. Development in D-16. Four minutes at 68°F.

---

* Communication No. 1287 from the Kodak Research Laboratories.

[1] A. Kempf, Zeits. f. wiss. Phot. 36, 235 (1937); H. Sauvenier, Bull. Soc. Roy. Sci. Liège 16, 54 (1947); H. Tellez-Plasencia, Sci. et Ind. Phot. 19, 451 (1948).

[2] S. E. Sheppard and A. P. H. Trivelli, Phil. Mag. 9, 787 (1931).

[3] G. Kornfeld and T. H. James, J. Opt. Soc. Am. 33, 615 (1943); G. Kornfeld, J. Opt. Soc. Am. 39, 490 (1949).

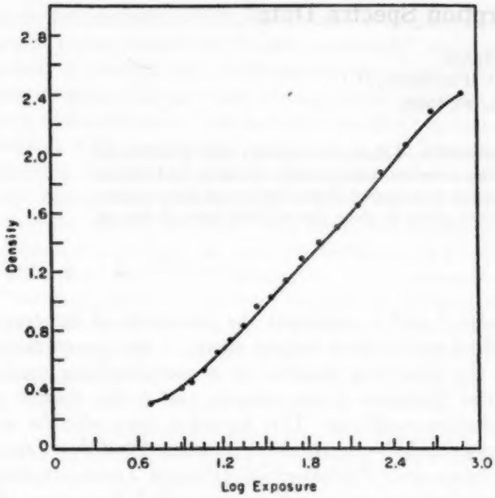

FIG. 3. Total development of latent image after five-minute x-ray exposure at room temperature.

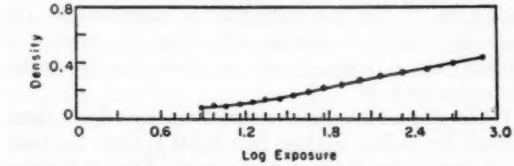

FIG. 4. Development of internal latent image after five-minute x-ray exposure at room temperature.

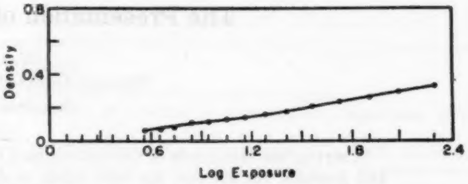

FIG. 5. Development of internal latent image after twenty-minute x-ray exposure at the temperature of liquid nitrogen.

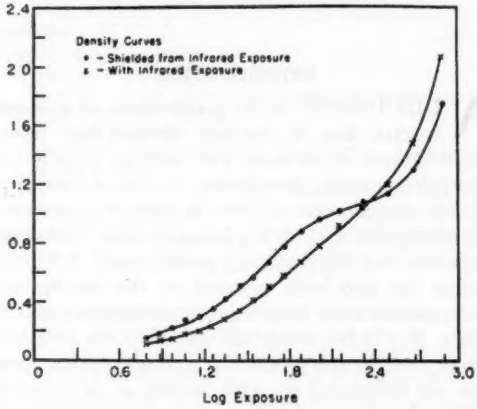

FIG. 6. Herschel effect after exposure to x-rays at the temperature of liquid nitrogen for twenty minutes. 90-minute infra-red exposure. Development in D-19. Four minutes at 68°F.

treated with a solvent developer (200 cm^3 D-19 plus 20 cm^3 of a 10 percent thiosulfate solution) for total development; the other two were bleached with ferric cyanide; one of these was then treated with the Stevens developer for the development of the internal latent image, and the other one with a surface developer, as a test that the bleach had been effective. A comparison of the density curves for the total and the internal latent image (Fig. 3 and Fig. 4) shows that the contribution of the internal latent image to the density is negligible.

This result is surprising, and even more surprising is the lack of a substantial internal latent image after an x-ray exposure which was carried out at the temperature of liquid nitrogen. The conditions for the exposure were unchanged, only the time was 4 times as long—20 minutes—instead of 5. The density curve corresponding to the internal latent image is shown in Fig. 5. It is identical with the curve in Fig. 4.

Since there is little doubt that the production of internal latent image increases at low temperatures, an explanation must be sought for the failure to find it by development, and the possibility has to be considered that it was destroyed by rebromination. However, indirect evidence for the presence of the internal silver is given by the reversal of the Herschel effect at high densities which occurs after an x-ray exposure at low temperatures. The curves in Fig. 6 show a conventional Herschel effect for low and medium temperatures which is considerably smaller than the Herschel effect found for the exposure at room temperature. But for higher densities, the curves show a reversal of the effect, which is interpreted as the increase of surface latent image produced by the Herschel effect on the internal latent image. Such a reversal was found, after exposures to visible light, by Debot, Falla, and Hautot[4] only in the solarization region, or in an emulsion where the surface latent image had been destroyed by bleaching.

The presence of internal silver, as attested by the reversal of the Herschel effect, together with the lack of any appreciable amount of developable internal image, necessitate the conclusion that, in the emulsion used, the majority of the silver produced by the deterioration of the absorbed x-ray quantum is finely dispersed and does not collect into developable centers.

ACKNOWLEDGMENTS

I wish to express my thanks to Mr. H. F. Sherwood and Mr. G. M. Corney, of the X-Ray Department of these Laboratories, who carried out the exposures to x-rays at room temperature and at the temperature of liquid nitrogen, with special precautions against any interference from scattered radiation. I also thank Dr. W. G. Lowe, of the Emulsion Research Department of these laboratories, who carried out the development of the total and internal latent image.

---

[4] A. Hautot, Bull. Soc. Roy. Sci. Liège **12**, 647 (1943).

JOURNAL OF THE OPTICAL SOCIETY OF AMERICA VOULME 39, NUMBER 12 DECEMBER, 1949

The Presentation of Absorption Spectra Data*

WALLACE R. BRODE
National Bureau of Standards, Washington, D. C.

(Received September 19, 1949)

A survey has been made of the systems used for the presentation of absorption spectra data in textbooks and journals. An attempt has been made to determine the accepted nomenclature systems, and recommendations have been made where there is some uncertainty as to proper or desirable form of presentation. Examples of data and graphical relation of values have been given to show the relative form of data as presented by different systems.

INTRODUCTION

A DISCUSSION of the presentation of absorption spectra data is logically divided into separate considerations of ordinate and abscissa notation and absorption spectra description. In the following discussion consideration will first be given to transmission and absorption and then a consideration wave-length, frequency and wave number presentation. A brief discussion has also been included on the description of spectrophotometric properties of compounds and materials. It will be noted that the methods and terminology used in the presentation of absorption spectra data are influenced by such factors as (a) precedent and previous usage, (b) the technical concepts involved in the data to be presented, (c) the notation prescribed by instrument producers and standard references, textbooks or data forms, (d) the editorial policies and practices of technical journals and book publishers, and (e) the personal desires of the scientist or accords obtained by groups of research workers.

TRANSMISSION AND ABSORPTION

Nearly a century ago Bunsen and Roscoe[1] outlined the general theory of absorption of radiant energy, which has usually been reproduced in what is known as the Bunsen absorption equation (Fig. 1):[2] $I=I_0 10^{-kcd}$ where I and I_0 represent the intensities of the transmitted and incident radiant energy, c the concentration of the absorbing material in a non-absorbing media, d the thickness of the sample, and k the *Bunsen* or *extinction coefficient*. This equation may also be expressed as $kcd=\log_{10}I_0/I=1/T$, where $T=I/I_0=$ *Transmittance* and $T\times 100=\%T$ (Percent transmittance). The observed value, which was called *Extinction* (E) was given as $E=kcd$, where c is expressed in grams per liter, d in centimeters and k is known as the specific extinction. If the concentration is expressed as the molecular weight in grams (M), then the term k is replaced by ϵ (epsilon) and is known as the molar extinction $\epsilon=k\cdot M$.

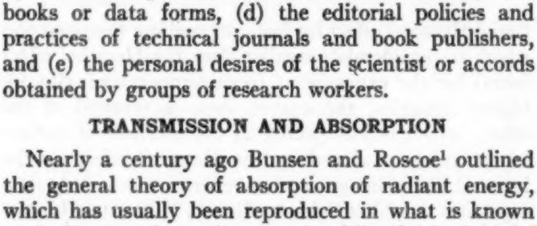

FIG. 1. Graphical indication of transmission terms.

While there have been some deviations from these symbols by various authors (see Table I) there has been no change in the fundamental theory. The conformity to this general law of absorption with respect to certain parts of the equation has given rise to such "*laws*" as *Beer's Law*[3,4] which denotes the conformation with respect to changes in concentration, c, and *Bouguer's* or *Lambert's Law*[5] which denotes conformation with respect to thickness, d, changes. Conformation to both of these changes might be expressed as merely the conformation with the *absorption law*. Variations from these laws are the result of chemical and physical changes, such as association, dissociation, tautomeric shifts, fluorescence, or colloidal phenomena, which are in themselves non-conformity to the concept of the concentration being defined as a true solution of a single molecular state.

The large number of symbols and terms in use today and the lack of uniformity in recent publications (see Tables III and V) indicates the necessity for some study of the cause for this variation and if possible some recommendations to improve the uniformity of notation. About fifty years ago, Kayser[6] in his *Handbuch der Spektroscopie* noted that it would be "desirable if

---

[*] Presented as an invited paper at the Detroit meeting of the Optical Society of America, October 22, 1948, and revised in respect to discussion presentations on the same subject before the Society of Applied Spectroscopy in New York, December 7, 1948, and the 9th Pittsburgh Conference on Spectroscopy, February 18, 1949.

[1] R. Bunsen and H. E. Roscoe, Pogg. Ann. Physik **101**, 235 (1857).

[2] Variations in the earlier absorption equations, such as the use of natural logarithmic formulas and the inclusion of the concentration factor in the extinction constant, have been omitted in this discussion.

[3] A. Beer, Pogg. Ann. Physik **86**, 78 (1852).

[4] A. C. Hardy and F. M. Young, J. Opt. Soc. Am. **38**, 854 (1948).

[5] Lambert (1760), reprinted in Ostwald's *Klassiker der exakten Wissenschaften*, No. 32.

[6] H. Kayser, *Handbuch der Spektroscopie* (I. Hirzel, Leipzig, 1905), Vol. 3, p. 14.

the uncertain usage of different notations in absorption spectra papers should be brought to an end," yet comparison of present day publications with those in the time in which Kayser was writing would indicate as much non-conformity now as there was fifty years ago. There is still considerable confusion in the literature regarding the definition of intensity, extinction coefficient, absorption coefficient, density, absorption index, and other similar terms so that many textbooks and technical articles precede their discussions with a table of absorption spectra definitions.

The development of research instruments or methods usually involves the initial conception of the theory and instrumentation in the hands of the physicist or instrumental designer. In the practical application of the instrument or theory to research problems, however, the principal users may be chemists, biologists, ceramists, medical research workers, or others to whom the theory or instrument may be applicable. This often results in instrument graduation and nomenclature which may have been developed in a highly technical atmosphere finding their principal users in an applied atmosphere where the observed values are interpreted as functions of molecular structure, concentration, reaction condition or identity, without a full knowledge of the significance of either the theory of observation or nomenclature as applied to the observed values.

In the consideration of the physical concepts of absorption spectra theory as affecting the application of this method to biological, chemical and physical studies in characterization, analysis and chemical control, it is not essential to consider seriously those effects which are adequately compensated or controlled by instrumental and technical methods. The effect to be measured or recorded, if it is a ratio of sample values to standard or reference values, may be obtained as the ratio of several physical properties, with the same final result. For example, in the determination of the transmittance of a solution, one may insert the solvent in the instrument, adjust the instrument reading to zero and then measure the transmittance of the material directly by replacing the solvent cell with the solution cell: or one may make separate transmittance readings on both solution and solvent and take the ratio of these to obtain the transmittancy of the solution, the transmittancy of the solution being equivalent to the transmittance of the material in solution.

From the applied biological and chemical point of view, it is the transmittance and absorbance of the dissolved material which is of primary importance and it is accepted as axiomatic that, unless data specifically indicates otherwise, correction has been made for solvent and cell absorption, source intensity, and receiver or instrumental characteristics. It is, however, essential that data on concentration, solvent, and cell thickness as well as other influencing factors of importance such as *pH*, temperature, density, etc., should be given in the presentation of the data.

TABLE I.*

Transmission

I = Transmitted intensity of radiant energy.

I_0 = Intensity of incident (or transmitted comparison) radiant energy.

T = *Transmittance* = I/I_0 (*Transmittancy* is used to indicate relative transmittance if I_0 is the transmitted comparison radiant energy).

t = *Transmissivity*, (T^{-cd}) is the Transmittance for a unit concentration and thickness.

$\%T$ = *percent transmittance* = $T\times 100$.

Absorption

Absorption law: $I=I_0 10^{-kcd}$.

A = *Absorbance* = $kcd=\log_{10} I_0/I$.

k = *Absorptivity* = A/cd (specific absorbance or absorbance per unit concentration and thickness).

ϵ = *Molar Absorptivity* = $k\cdot M$.

c = concentration in grams per liter, d = thickness of cell in cm, M = molecular weight.

* *General* The suffix *-ion* is used to indicate a process, as in the case of *conduction* or *calibration; -or* or *-er* to indicate a device as in *generator* or *absorber; -ance* to indicate a measurable quantity of a property such as *resistance* or *conductance;* and *-ity* to indicate a specific property of the measured substance such as *density* and *conductivity.*

PROPOSED SYSTEM OF ABSORPTION NOTATION AND SURVEY OF PRESENT PRACTICE

The system of notation in Table I is proposed so as to define the various terms under discussion and permit an intercomparison of other methods of presentation (Tables II and III). The terminology recommended in Table I has been prepared with respect to the requirements of the principal users of absorption spectra data (chemists and biologists) and hence considerations of a technical or theoretical nature have in some cases been made secondary to those of simplification and ease of application. To avoid confusion, the proposed system represents a compromise between some of the present day proposed systems, and the common usage and practice over a long period of time. In the notes to some of the terms there have been included some of the expressions of limited application for special application or reference.

Notes on Tables I, II and III

I The symbol *I* and the term *intensity* have had an almost universal adoption (see Table II) until recently as the representation for intensity of radiant energy. It is obviously not practical to use in applied spectrophotometry a separate system of symbols such as *I*, *J*, *U*, *P*, *F*, etc., and names such as power, intensity, energy, flux, etc., which are dependent on the instrument, source or receiver, if the final recorded data is a ratio which is corrected for such differences as may exist in the above quantities, especially since these quantities are determined as spectral values. It should be noted in Table II that *I* and *J* are used interchangeably in German notation hence the proposal[7] that *I* be used for *Luminous Intensity* and *J* for *Radiant Intensity*

---

[7] H. K. Hughes *et al.*, "*Letter symbols for physics*" (A.S.M.E., New York, 1948).

TABLE II. Notation for absorption and transmission as used in textbooks.†

	Terms								
Authority	I	I_0	T	D	A	K	ϵ	C	d
German									
Kayser	J	J_0	T	—	—	K	ϵ	c	d
Beer	J	J_0	—	—	—	K	ϵ	c	x
Joos	I	I_0	—	—	—	—	ϵ	c	d
Lowe	J	J_0	A	—	—	K	ϵ	c	d
Abderhalden	J_p	J	—	D	—	—	ϵ	c	p
Lange	I	I_0	—	—	E	—	α	c	s
Thiel	I	I_0	T	—	—	—	ϵ	c	d
Schiebe	I	I_0	T	—	—	K	ϵ	c	d
Heilmeyer	I	I_0	T	—	E	ϵ_0	ϵ_m	c	d
Weigert	I	I_0	T	D	E	K	ϵ	c	d
Mohler	I	I_0	T	—	E	K	ϵ	c	d
Ley	J	J_0	T	—	E	K	ϵ	c	d
Seith and Ruthardt	I_d	I_0	T	—	E	K	—	c	s
French									
Fabry	I	I_0		D					
Ramart-Lucas	I	I_0	T						
Lecomte	I_1	I_0	T	—	K	—	ϵ	c	d
Henri	I	I_0	T	—	K	—	ϵ	c	l
English									
Twyman	I	I_0	T	d	d	K	ϵ	c	l
Lothian	I	I_0	t	d	d	E	ϵ	c	l
Heilmeyer	I	I_0	T	—	—	K	ϵ	c	d
Morton	I	I_0	T	—	E	K	ε	c	d
Judd-Lewis	I	I_0	T	—	—	—	ϵ	c	d
Bowen	I	I_0	T	—	—	—	ϵ	c	d
Watson	I	I_0	—	—	—	K	—	c	d
American									
Brode	I	I_0	T	D	E	K	ϵ	c	d
Gibb	I	I_0	T	D	E	K	ϵ	c	d
Harrison	I^a	I_0	T^a	D	K	k	ϵ	c	X
Sawyer	I	I_0	T	—	—	—	—	—	—
West-Weissberger	I	I_0	T	—	D	—	ϵ	c	d
Mellon	I	I_0	T	D	—	K	mk	c	b
Barnes	I	I_0	T	—	—	K	—	c	X
Snell	I_2	I_1	T	D	K	k	$\mathfrak{e}$	c	l
Heinrich	J	J_0	T	—	K	k	ϵ	c	d
Brode-Berl	I	I_0	T	D	A	K	ϵ	c	d
Compendia									
Lasareff	I	I_0	—	—	K	—	—	c	d
Ellinger	J	J_0	—	—	$\mathfrak{e}_s$	k	$\mathfrak{e}$	c	d
Tab. Ann. de Const.	I	I_0	T_r	—	E	K	ϵ	C_s	d
Landolt Bornstein	I	I_0	T	D	$\log I_0/I$	K	ϵ	c	d
Int. Crit. Tables	J	J_0	T	—	—	K	ϵ	c	l
Nomenclature studies									
N.B.S.*	I	I_0	T_i, T_s	—	A_i, A_s	a_i, a_s	a_m	c	b
Hughes ('47)	P	P_0	τ	—	A	—	a	c	l
Hughes ('48)	P	P_0	τ	—	A	—	a	c	b
Mellon	I	I_0	τ	—	A_s	a_s	a_m	c	b
Rosenbaum	P	P_0	τ	—	A	a		c	b
Brode—(Table I)	I	I_0	T	D	A	K	ϵ	c	d

† References to the authority cited here with the exception of the later group can be found in the bibliography section of W. R. Brode, *Chemical Spectroscopy* (John Wiley and Sons, Inc., New York, 1943), second edition.

* See reference 8.

would not be a satisfactory discrimination among German speaking scientists.

T *Transmittance* is almost universally indicated by *T*. A recent suggestion[7] has been made to use τ (Greek tau); however, this does not appear to be an essential change and it is extremely difficult to differentiate between τ and t in both manuscript and type form.

There has been a tendency to use *Transmission* for the name of this term but as indicated above it would be consistent with our general scientific nomenclature to use the suffix *-ance* for the quantity and *-ion* for the process.

Transmittancy has been used to describe the relative transmittance of two samples; however, for characterization of materials one is concerned with the transmittance of a compound in solution, rather than the transmittancy of the compound and solvent compared with the solvent. Instruments and recording forms should read in transmittance even though transmittancy may be read and recorded. The transmittance recorded should indicate method of observation if correction has not been made for solvent and cell. *Transmissivity*, *t*, is sometimes used to indicate specific transmittance.

%T Percent seems to be preferred as one word by scientists but is seldom so accepted by publishers. The use of the symbol *%T* in lieu of the term is a partial solution to this problem.

The principal use of *Transmittance* is in color description in the visible spectrum, where this method of presentation serves to emphasize the color or transmitted portions. Transmittance has a disadvantage in that curves are not additive to determine proportional effects in mixtures or the influence or impurity materials.

O *Opacitance* is defined as $1/T$ or I_0/I. It is seldom used in the description of absorption spectra data.

k *Absorptivity* is generally indicated by the symbol *k*, although a number of other symbols have been used for this value including α, a, E, K, etc., and it has been called specific extinction, absorption coefficient, specific absorption, etc. The use of *a* is to be particularly discouraged since it is easily confused with *A* for absorbance. Many people write their capital and small *a* alike except for size and when used alone they could not be differentiated apart. The same argument may be used against the use of capital and lower case *K* as symbols for different terms.

d The symbol for cell thickness has been variously given as *d*, *l*, *x*, *b*, etc., but accepted practice by a

TABLE III. Absorption and transmission notation as used in current technical journals (approximately 1000 articles in 1946 to 1949).‡

Names	No. times used	Symbols	No. times used
Extinction	45	$\log I_0/I$	24
Extinction coefficient	31	D	18
Specific extinction	12	E	41
Molar extinction	5	$E^{1\%}{}_{1\,\mathrm{cm}}$	70
Molar extinction coefficient	11	E mol	6
Molar absorption coefficient	12	*A	14
*Absorbance	20	ϵ	87
Specific absorption coeff.	28	*$\epsilon\times10^{-2}$	10
Density	12	*$\epsilon\times10^{-3}$	110
Optical density	78	$\epsilon\times10^{-4}$	35
−Log transmittancy	10	K	10
Transmission	142	k	14
Transmittancy	53	$\log k$	8
*Transmittance	78	*$\log A$	18
*Per cent	28	$\log E$	21
Per cent	160	*$\log\epsilon$	180
		T	42
		*$\%T$	143

‡ Terms and symbols infrequently used have not been included. More than one system may be used in a single paper or graph. In 1949 approximately 15 percent of all articles in the J. Am. Chem. Soc. (200 out of 1300 as estimated from the first 9 months) contained absorption spectra data, as compared with a 5 percent absorption spectra content in 1936 in the same Journal. *Note:* In Tables III and V the notation used on absorption spectrographical forms has been recorded, rather than the notation used in the written text, since the former are usually more representative of the research workers' ideas of presentation.

* Indicates recommended notation.

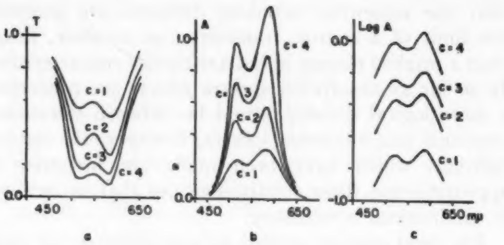

FIG. 2. Comparison of transmittance (a), absorbance (b), and log absorbance (c) presentation of absorption spectra data.

majority of observers would indicate a slight preference for *d*. Some texts give *d* in cm when dealing with solutions but in mm when dealing with solids. It would seem desirable to consistently express *d* in cm only.

c *c* is the universal symbol for concentration, although not all texts agree on whether it represents grams per liter or gram moles per liter and some used it for either expression. It is recommended that it be used as grams per liter.

A Absorbance as a term and its symbol *A* are relatively new in absorption spectra notation and are the only real departure from the more accepted nomenclature of the past. The previous symbol and term for this has varied although a preference would appear to be slightly in favor of extinction and *E*. To be consistent with the process of ***absorption***, the name ***absorbance*** is preferred over extinctance. There is confusion in the literature as to the use of *E* for absorbance or molar absorptivity, the latter is usually indicated by the Greek letter epsilon, ϵ, and this is often confused with the script *E*. In the gradual evolution through which our nomenclature is passing it is not unlikely that *E* may replace ε as the symbol for molar absorptivity. There is still some question as to whether *A* should be called Absorptance or Absorbance but the preference among spectroscopists seems to be in favor of Absorbance. (Fig. 2.)

$A^{1\%}{}_{1\,\mathrm{cm}}$ The expression $A^{1\%}{}_{1\,\mathrm{cm}}$ is recommended for use in lieu of the $E^{1\%}{}_{1\,\mathrm{cm}}$ which is extensively used in the description of biological preparations and their assay by spectrophotometric methods. This expression and a similar expression of $p\cdot p\cdot m$ (indicating parts per million) in place of % are not very popular with theoretical experts but find support among analysts who measure and report concentrations in these forms.

ϵ (***Epsilon***) ϵ, is almost universally used for molar absorptivity. A majority of the absorption spectra curves appearing in chemical publications which characterize pure compounds, use epsilon as the ordinate. It is, however, given variously as ϵ, ε, or *E* and to partially eliminate the confusion with the *E* as formerly used for *Extinction* (now known as Absorbance) it has been suggested that this latter use of *E* be discouraged. A study of Table II and III will indicate the ϵ has been used consistently for a definite absorption property to a greater degree and extent than any other absorption designation. It should be recognized that the use of ϵ or $\log\epsilon$ as ordinate is merely an indication that a molar quantity is involved in the calculated concentration and that the actual ordinate values are still absorbance or log absorbance values. The use of $\log A$ and $\log\epsilon$-recording, while eliminating the additive character of the curves, provides a better comparison of weak and intense bands identification. The $\log A$ curves also possess a shape which is independent of concentration which may be of assistance in the identification of pure compounds of unknown structure. Where *A*- or ϵ-values of considerable size are recorded and $\log A$ or $\log\epsilon$ are not desirable forms to present the data on account of a desire to maintain the additive concentration notation, it is suggested that $A\times10^{-2}$ or $\epsilon\times10^{-2}$ be used.

TABLE IV. Wave-length units for recording absorption spectra.

Unit	Size of unit	Range (from left to right)	Region
1. Angstroms	meter $\times10^{-10}$	1000 to 1A	Far or extreme-ultraviolet
2. mμ	meter $\times10^{-9}$	1500 to 100 mμ	Ultraviolet and visible
3. mμ	meter $\times10^{-9}$	400 to 750 mμ	Visible (color description)
4. μ	meter $\times10^{-6}$	1 to 200μ	Infra-red and far-infra-red
5. cm	meter $\times10^{-2}$	0.1 to 100 cm	Microwave

In the proposed system of nomenclature no attempt has been made to include terms which may be essential to the theoretical worker but may serve only to confuse the applied analyst. Among such terms are:

$\alpha=1-T=$ *Absorptance*
$O=1/T=$ *Opacitance* (or Opacity),
$D=\log_{10}I_0/I=$ *Density* (same as ***Absorbance*** but applied to non-specular determinations such as photographic blackening)
$\mu=1/cd\cdot\ln I_0/I=$ *absorption coefficient*
$\gamma=\lambda/4\pi d\cdot\ln I_0/I=$ *absorption index.*

Special terms and symbols for internal transmittance, external reflectance, etc., as used in precise spectro-

3	30	250	400	750	1500f	Frequency (ν)
100	1000	8333	13333	25000	50000 cm^{-1}	Wave number (ν′)
		Infra-red				
Far	Middle	Near	Visible		Ultraviolet	Spectral region
				Electronic		
Rotational Pure rotation spectra	Rotation-vibrational Rotation superimposed on vibrational spectra			Rotation and vibration superimposed on electronic spectra		Origin of spectra
100	10	1.2	0.7	0.4	0.2μ	Wave-length (λ)

FIG. 3. Radiant energy spectrum.

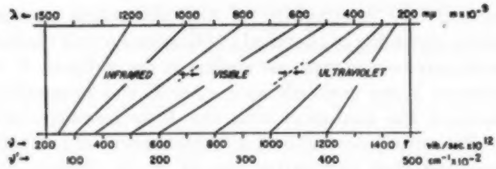

FIG. 4. Wave-length-frequency relation in near infra-red, visible and ultraviolet region.

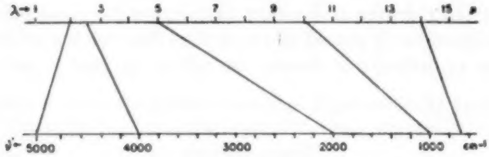

FIG. 5. Wave-length-frequency relation in infra-red region.

photometry and colorimetry have not been included in this discussion.[8]

WAVE-LENGTH, WAVE NUMBER, AND FREQUENCY

From the basic theory of wave motion it is obvious that there are three methods of denoting wave characteristics; (a) the length of the wave (*wave-length* (λ)), (b) the number of waves or cycles in a unit distance (*wave number* (ν^1)), and (c) the number of waves or cycles passing a point in space in a unit time (*frequency* (ν)). The relation between these units may be expressed as

$$1/\text{wave-length} = \text{wave number} = \text{frequency}/\text{speed of light},$$

or

$$1/\lambda = \nu' = \nu/c.$$

A condensed arrangement of the radiant energy spectrum (Fig. 3) shows the relation of these three systems of notation and the principal spectral regions which are included in a general consideration of absorption spectra data presentation. It is to be noted that the spectral regions are not sharply defined and that the somewhat nebulous divisions are generally the limit of a source, transmitter or receiver, rather than a marked change in radiant energy characteristics. In so far as absorption spectra effects are concerned, a more logical division would be between *vibrational*, *rotational* and *electronic* spectra, however, the natural divisions which have been made are fortunate in approximating these subdivisions, so that no revision in subdivisions is necessary.

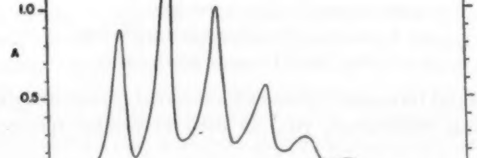

FIG. 6. Ultraviolet spectrum of benzene in isooctane. Conc. 0.432 g. per liter; cell thickness 1.0 cm.

The term *near* as applied to *near-ultraviolet* or *near-infra-red* should denote that portion of the indicated spectral region which is just beyond the limits of the visible spectrum. *Near-infra-red* is generally accepted as that extension of the spectrum, beyond the red sensitive threshold of the eye, to which the photoemissive cell or photographic plate is sensitive. This includes approximately the region from 750 to 1500 mμ. The *near-ultraviolet* is that extension of the spectrum beyond the violet sensitive threshold of the eye which is transmitted by ordinary glass. This includes approximately the region from 400 to 300 mμ.

TABLE V. Wave-length, wave number, and frequency notation in applied technical literature (nearly 1000 articles from 1946 to 1949) for absorption spectra description. (Numbers indicate number of times used, * indicates authors recommended notation (see Tables IV and VI); (see ‡ note to Table III).

Names	No. times used	Symbols	No. times used
*Ultraviolet	270	*λ	124
Ultra violet	120	**A*	12
Ultra-violet	30	Å	52
		AU and *IA*	16
*Infrared	310	*mμ	438
Infra red	30	μμ	14
Infra-red	90	*μ	280
		mmμ	6
*Wavelength	96	*ν	28
Wave length	370	**f*	16
Wave-length	16	*ν'	12
		1/λ	2
*Wavenumber	8	$\bar{\nu}$	4
Wave number	60	σ	2
Wave-number	10	mm^{-1}	16
		*cm^{-1}	106
*Frequency	44	*$cm^{-1} \times 10^{-2}$ or 10^{-3}	10
		mm^{-1}	4

The term *far* as applied to ultraviolet and infra-red spectra should denote the spectral region beyond the range of the usual recording or transmitting system. The *far-ultraviolet* region is the shorter wave-length region beyond the 200 mμ cut-off of the transmission of quartz and the limit of the usual gelatin photographic emulsion. The *far-infra-red* region is the longer wave-length region beyond the 25μ cut-off of the KBr prism and the start of the pure rotational spectral region.

Between these two fringe designations of near and far regions are the usual extended regions over which ultraviolet and infra-red absorption spectra observations are made. It is recommended that these regions, 400 to 200 mμ in the ultraviolet and 0.75 to 25μ in the infra-red be designated merely as the *ultraviolet* and

---

[8] *Terminology and symbols for use in ultraviolet, visible, and infrared absorptometry*, Letter Circular LC 857, National Bureau of Standards, May 19, 1947; K. S. Gibson, *Colorimetry*, Nat. Bur. Stand. Circular No. 484 (in press).

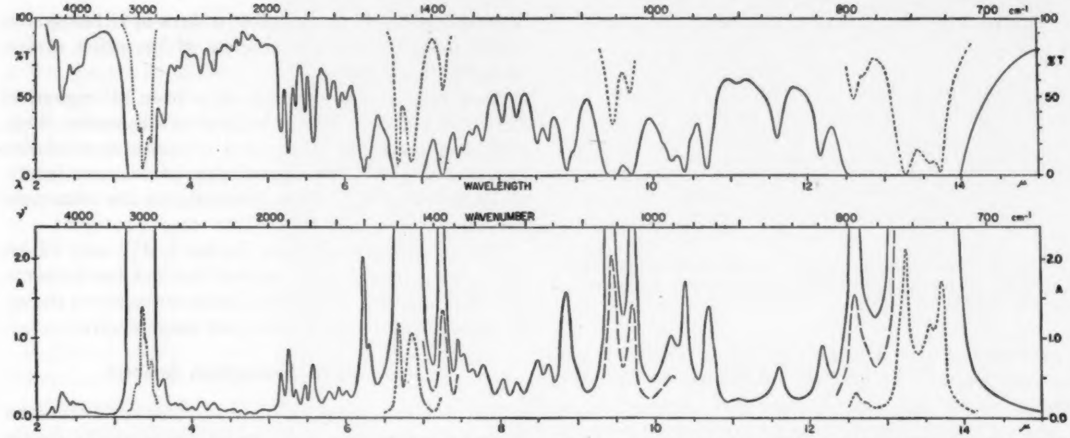

FIG. 7. Infra-red absorption spectra of 1-methyl-2-ethylbenzene. (Data recalculated from NBS—API Proj. No. 44—Serial 349—(Naval Res. Lab.) Cell thickness: ——— 0.250 cm; — — — 0.125 cm; - - - - - 0.025 cm. Upper curve in percent transmittance, lower curve in absorbance; both curves plotted linear in wave-length.

infra-red regions without a modifying prefix such as middle.

The *visible* region, like the above infra-red and ultraviolet regions is defined by the limits of the receiver, the human eye, and no sharp limiting value can be established. Individuals will vary with respect to their range of sensitivity and some individuals especially young blondes, can, when dark adapted see as far as 350 mμ in the ultraviolet and to 900 mμ in the infra-red, although the usually accepted limits of the visible spectrum are from 400 to 750 mμ. For color description it seems more desirable to use transmittance and wave-length for the spectral description, however, the apparent color of objects is influenced by the varied sensitivity of the eye, so that other systems of color description have been evolved which include this factor. These extended discussions and systems are beyond the scope of this paper.[9–11]

UNITS FOR RECORDING WAVE-LENGTH, WAVE NUMBER, OR FREQUENCY

The requirements of a system of notation for spectral distribution of radiant energy, in any of the regions mentioned in the previous section, are (1) it should not be unwieldy and preferably have significant figures concomitant with the accuracy of observation, the range of significant figures should be efficiently used, (2) the rate of dispersion should not radically differ from the effective accuracy or resolving power, (3) the dispersion should be linear with respect to properties of the observed data, and (4) the unit name should be simple so as to permit easy use in discussion and reference. It is obvious that to express the wave-length of sodium light as 0.0005895 mm provides an unwieldy number which is better represented by 589.5 mμ. A similar disadvantage is seen in the reference to the 3.5μ band in the infra-red as the 35,000 angstrom band, and for these same reasons we use a variety of units in our metric system so as to avoid values with a greater number of significant figures or decimal values than are essential for the proper indication of the number. In the use of wave-length notation it is suggested that the following units be used for the regions indicated.

TABLE VI. Frequency and wave number units for recording absorption spectra.

Unit frequency	Size	Range (from left to right)	Region
Fresnel	vib/sec.$\times 10^{-12}$	100 to 1500*f*	Near-infra-red, visual, and ultraviolet
Megacycle	vib/sec.$\times 10^{-6}$	30,000 to 30 Mc	Microwave
(cm^{-1})	cm^{-1}	400 to 5000 cm^{-1}	Infra-red
(cm$^{-1}\times 10^{-2}$)	cm$^{-1}\times 10^{-2}$	100 to 500 cm$^{-1}\times 10^{-2}$	Near infra-red, visual, and ultraviolet

The term *frequency*, ν, is often used to indicate both number of waves or cycles in a unit time and number of waves or cycles in a unit distance (wave number, ν'). The symbol for frequency is accepted as ν, however, many workers refer to wave number values as a form of frequency, although, strictly speaking, wave numbers should be designated by ν' or $\bar{\nu}$. Some data in wave number are indicated by $1/\lambda$ or λ^{-1}, the expression "λ^{-1} in cm$^{-1}\times 10^{-2}$" having actually appeared in the literature, which should certainly serve to emphasize the need for a unit and symbol for wave number values of this size. n, and σ have been used for wave numbers but without much support or justification. (Fig. 4.)

In the presentation of data in frequency or wave number the conversion from wave-length is made in accordance with the formula $\nu' = 1/\lambda = \nu/c$ where c the speed of light of 3×10^{10} cm per second and λ

---

[9] R. M. Evans, *An Introduction to Color* (John Wiley and Sons, Inc., New York, 1948).

[10a] D. B. Judd, *Colorimetry*, Nat. Bur. Stand. Circular No. 478 (1949) (in press).

[10b] D. B. Judd and K. L. Kelly, J. Research, Nat. Bur. Stand. 23, 355 (1939).

[11] Committee on Colorimetry, J. Opt. Soc. Am. 33, 534, 544 (1947); 34, 183, 245, 633 (1944); 35, 1 (1945).

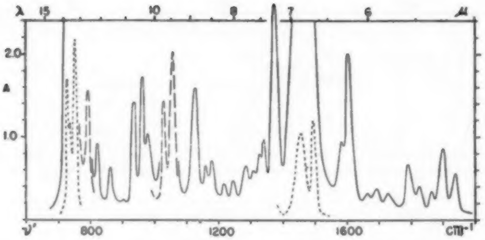

FIG. 8. Infra-red absorption spectra of 1-methyl-2-ethylbenzene (same as Fig. 7) recorded in absorbance and linear in wave number from 700 to 2000 cm^{-1} (15 to 5μ).

is expressed in cm. The unit for wave number, ν', is thus expressed in reciprocal centimeters or with the symbol, cm^{-1}. The unit "waves per centimeter" is somewhat cumbersome both as to name and size and it is apparent that a shorter name and a difference in size should be effected. One suggestion has been that the unit be called a *balmer*, with the symbol *B*, similar to other physical unit names such as *angstrom*, *farad*, *ohm*, *henry*, etc. Another suggestion has been to use the symbol *rc* for reciprocal centimeter, so as to avoid the necessity of negative power notation, cm^{-1} or 1/cm, and that the unit with the symbol *rc* could be called an "*arsee*." (Fig. 5.)

The *reciprocal centimeter* is of reasonable size in the usual infra-red region of observation, i.e., 500 to 5000 cm^{-1} being equivalent to the 2 to 20μ region, but in extension to the visible and ultraviolet without a change in unit size, the number of significant figures is out of proportion to the accuracy of observation. The visible range is 14,000 to 25,000 cm^{-1} (750 to 400 mμ), and the ultraviolet range is from 25,000 to 50,000 cm^{-1} (400 to 200 mμ). To avoid such large numbers, many workers have used the unit "cm$^{-1}\times10^{-2}$" so as to reduce the visual and ultraviolet region to 140 to 500 cm$^{-1}\times10^{-2}$. It is obvious that a simplified name for this unit is desirable. (Fig. 6.)

In the frequency notation (number of waves per centimeter×speed of light in centimeters per second ($\nu'\times c=\nu$)) a special name has been given a unit size which has been found to be quite useful in the description of visible and ultraviolet spectra. The unit is known as the *fresnel*, with the symbol *f*, and is defined as vibration per second×10^{12}. The visible region in this system extends from 400 to 750*f* (750 to 400 mμ) and the ultraviolet from 750 to 1500*f* (400 to 200 mμ). The identical numerical limits of the visible in wave-length and frequency notation are of interest. The expansion of the ultraviolet region on the frequency scale is comparable to the dispersion and for a quartz instrument the apparent slit width is nearly constant on the frequency scale.

In the present transition period between wave-length and frequency or wave number, where instrumental or accumulated data conditions may influence the method of presentation, no specific system can be insisted upon, however, it would be desirable if data in either system would include an upper abscissa of the other system on a non-linear basis.

As a means of presenting data from all regions of the spectrum on a nearly equivalent dispersion, Shurcliff[12] has suggested on octaval or constant resolution unit system (*CRU*) based on the log$_2$ of the wave-length, which gives an equivalent dispersion to the ultraviolet and infra-red regions.

The recommendations in Tables I, IV, and VI are made, not with an expectation of finality, but rather as an aid in uniform presentation, with an expected change in terminology as the science and usage evolve.

Descriptive Absorption Spectra

As a corollary to the ordinate and abscissa delineation of absorption spectra, it is desirable, especially for the applied deductions from the data, to present some of the terminology as may be useful in describing absorption spectra and the spectral changes which may result from variations in composition or conditions of observation. These descriptive terms have been classified as physical (optical) and chemical (structural) although a sharp separation is not possible and some of these effects belong in both classifications.

Physical—Descriptive of the Observed Data

Position change (λ or ν)

Bathochromic indicates a shift of the absorption band to longer wave-length values.

Hypsochromic indicates a shift of the absorption band to shorter wave-length values.

Color deepening is indicated by color changes resulting from a bathochromic effect, the order of color deepening being yellow-orange-red-purple-blue-green and results from an absorption band shift from the ultraviolet, across the visible and into the near infra-red.

Color lightening results from hypsochromic effects and is the reverse of color deepening.

Intensity change (*A*)

Hyperchromic indicates an increase in absorbance.

Hypochromic indicates a decrease in absorbance.

Fading is produced by destruction, removal or conversion of absorbing material and may be merely a hypochromic effect or a combination of several effects.

Darkening is produced by a hyperchromic effect resulting from conversion of absorbing material.

Curve shape and structure

Principal band generally refers to the first or strongest component in a series.

Symmetrical and *unsymmetrical* denote band shape. Narrow symmetrical bands generally indicate a single component, whereas unsymmetrical bands, especially with *inflexions* or separate maxima, indicate *component structure*. *Resolution* of bands into component structure may in some cases be effected by improved instrumental techniques. Other procedures to improve resolution include *solvent effects*, such as the improved resolution in the spectra of phenol in hexane as compared with the spectra in alcohol, and *temperature effects* in which improved resolution is often shown in spectra observed at low temperatures.

---

[12] W. A. Shurcliff, J. Opt. Soc. Am. 32, 229 (1942).

Absorption bands and component bands of a single compound which possess a simple numerical relationship on a frequency basis are said to belong to the same series. In infra-red spectra these bands are known as *overtones* and in the visible and ultraviolet they are known as *harmonic* or *multiple series*. In both series the multiple relations are generally in simple whole numbers.

Half-band width is used to indicate the width of an absorption band at half its height. Such a description is only applicable as a characteristic of the band, if the height of the band is expressed in absorbance units. In extremely narrow bands, this value is influenced by the effective slit width of the dispersing system.

Solution effects, where only minor shifts in band position or intensity are produced, are sometimes interpreted as physical rather than chemical effects and have been ascribed to changes in refractive indices, dielectric constant and other property variations of the solvent.

Isosbestic point is a point of equal extinction (absorbance) and is used to refer to the common crossing point of absorption spectra curves which results in the change of absorption spectra of a compound when the absorbing structure is changed, as in indicator changes and oxidation-reduction effects. The absorbance at such a point is characteristic of the amount of the compound present and is independent of the character or state of the equilibrium between the two absorbing substances.

Dichroism is used to describe color changes which result from unsymmetrical absorption bands or unsymmetrical visual stimulation resulting from changes in the relative visual stimulation compared with the concentration change in the absorbing solution.

The general problems of *color* description are beyond the scope of this paper and are extensively treated in other publications.[9, 10]

Chemical—Cause of Observed Absorption Bands

Resonance is a concept in chemical-physics which involves a summation effect of dynamic equilibria between electromeric modifications and the resulting effect of the surrounding electronic environment. Single atoms may show rotational effects with resulting selective energy absorption known as *rotational spectra* which is evident in the far infra-red. Bond effects between atoms results in selective absorption in the infra-red known as *vibrational spectra*, on which are superimposed rotational spectra effects. Combination of bond effects result in *electronic spectra* which are apparent in the visual and ultraviolet regions and which in turn may have superimposed vibrational and rotational spectra effects. Vibrational spectra are classified according to bond characteristics and vector motion. Electronic spectra, excepting in the extreme or far ultraviolet are the result of molecular configuration involving characteristic combinations of unsaturated bonding which are generally known as chromophores. (Fig. 7.)

Chromophores are radiant energy absorbing groups such as 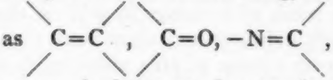 $>C=C<$, $>C=O$, $-N=C<$, $-N=N-$, etc.

A *chromogen* is that part of a complex molecule which contains a chromophore. An *auxochrome* is a substituent, such as the hydroxyl group, which is not a chromophore in itself but when attached to a chromophore in a certain position results in a marked bathochromic and hyperchromic effect. Simple chromophores do not as a rule show selective absorption in the visible spectra, but only in the ultraviolet region. Combination of simple chromophores together may result in a larger chromophore which shows visual absorption.

There are three recognized modes of combination of chromophores. (a) *Separated*, in which the two chromophores, although in the same molecule, are separated by an insulating linkage, such as methylene ($-CH_2-$) or oxygen ($-O-$), so that resonance effects are not transmitted between chromophores. The resulting absorption spectra being the addition of the absorption spectra of the separate chromophoric radicals. There may be slight influences of one resonance structure on the other even though they are "insulated" and there are different degrees of insulation. In addition increased molecular weight produces a small bathochromic effect.

(b) *Conjugated*, in which the separate chromophores are combined together so as to permit resonance transmission and to produce a single larger chromophore. The effect on the absorption band is almost multiplying, rather than additive, in that both bathochromic and hyperchromic shifts are produced. There is a limit to the number of unsaturated or resonance centers which may be conjugated together, so that unstable compounds or divided resonance may result from over conjugation. In addition to direct attachment together of chromophores it is possible to combine them together by transmitting linkages such as the ethenylene linkage ($-CH=CH-$). Covalent and coordinate linkages are capable of transmitting effects whereas ionic linkages produce insulating chromophoric effects. Combination of simple chromophores together by conjugated linkages may produce larger chromophores which possess unusual stability or color properties and to which distinctive names such as benzenoid, quinoid, indigoid, flavanoid, etc., are given to simplify nomenclature and discussion. (Fig. 8.)

(c) *Cumulated*, in which the two resonance centers share electrons in common so as to permit only one of the two forms to exist simultaneously, as in allene ($CH_2=C=CH_2$), and certain bisazo dyes. There is usually not a complete suppression of resonant forms and while a hypochromic effect is apparent there is usually some bathochromic effect as well as the apparent single chromophore.

Chemical or structural changes in absorption bands involve changes from one chromophoric form to another or the destruction or formation of a chromophoric form. *Indicators* generally imply change from one color form to another as a result of a change in acid or alkaline condition. A single indicator may show more than one change in color over a range of *pH* conditions. A study of the absorption spectra as the color changes shows that there is an equilibrium between the two structural forms and an isosbestic point of common absorbance can be determined. The absorption changes of indicators do not have to be visual and may involve changes in ultraviolet absorption. They may also be produced by oxidation-reduction, ionization, hydration and other reagent effects.

If the reaction results in a visual colorless form in one modification, this colorless form is known as the *leuco* form. Production of colored forms from the leuco form is often referred to as color development. A compound is considered to be *thermochromic* if a reversible absorption change is produced by heating or cooling. *Photo-* and *radio-chromic* compounds show reversible absorption effects resulting from radiant energy, x-ray or radioactive exposure.

Chemical *solvent effects* such as solvation are common and must be considered in the choice and purity of solvents. For example, iodine in chloroform gives a purple solution with a sharp absorption band at 540 mμ. The presence of a small amount of alcohol in the chloroform results in a brown color with an absorption maxima in the ultraviolet. A study of this effect[13] shows that the brown color is essentially the absorption spectra of iodine in alcohol, in which it forms a complex, and that the chloroform-alcohol solvent is actually an alcohol solution of the iodine which is merely diluted by the chloroform as an inert dilutant.

CONCLUSION

The study of the data in Table IV (λ and ν) with respect to current practices is perhaps more indicative of the trend than the consensus of opinion. One must accept this data as representing not only the research workers opinion but also that of the editorial control, the manufacturers notation and the hangover or lag effect of earlier notation or precedent. In an expression of opinion by spectroscopists at a recent conference there was almost unanimity for "wavelength" as one word, yet present day literature gives "wave length" a 2 to 1 preference. From the desires of spectroscopists it can be inferred that 2 to 1 lag is largely due to editorial or precedent influence. Similarly the preference for the use of wave number in lieu of wavelength for infra-red presentation shows a nearly equal division among spectroscopists although there is a predominance of the literature in wave-length. This again represents a trend in which the lag effects are not so much editorial as due to instrumental graduation and precedent. The increased use of wave number or frequency, however, does indicate the probable complete change in the future to this presentation, such as was made in the radio field from wave-length to frequency a few years ago.

Frequency is often used in a broad sense to include wave number, although strictly speaking, frequency involves a time factor and wave number a distance factor. However, since the speed of radiant energy is constant, the relation is a simple numerical factor and hence either system has the same dispersion rate.

Percent as one word is not widely accepted but is probably subject to "editorial" control more than purely technical words over which the editor may have no formed opinion.

For purposes of discussion of observed effects, it would seem desirable to have a unit of absorbance so as to indicate relative changes in that factor as one can in the wave-length or wave number direction. The wave number units of cm^{-1} and $\mathrm{cm}^{-1}\times10^{-2}$ could be improved upon.

The wide distribution and availability of spectrophotometric equipment (for example, over 3000 Beckman DU instruments are now in use in various types of laboratories throughout the world), has resulted in a marked increase in absorption spectra data and application as a part of the fundamental constants and measurements used to describe and characterize new compounds and reaction states. In the past two years about 10 percent of all of the technical papers in Chemistry have included some absorption spectra data. In the Journal of the American Chemical Society, of the approximately 2500 papers published in the past two years, over 300 papers included absorption spectra data.

With the improvement and development of rapid automatic and photoelectric instruments in the visual and ultraviolet regions (Cary, Beckman, General Electric, Brode, Harrison, Gibson, etc.) and double-beam automatic instruments in the infra-red (Baird, Perkin Elmer, Hilger, Beckman, etc.) it can be expected that the next decade will witness an even greater emphasis on the publication of absorption spectra data.

An inspection of the nomenclature and symbols used in some 1000 papers with absorption spectra data which were published in the past three years has provided the data for Tables III and V.

There are many reasons for the variations in nomenclature, some of which may account for more consistence than might actually exist in the minds of the individual authors, and might also indicate that certain terms which have wide adoption may not be those which are the most desirable or acceptable. Editors of journals may insist on "wave length" or "wave-length" when the author may have written "wavelength;" or "infra-red" may be required where the author has asked for "infrared." However, in other journals the editor allows a free reign in technical nomenclature and in most journals the editorial policy covers only a portion of the terms used and the balance of the nomenclature is left to the author.

---

[13] W. R. Brode, J. Am. Chem. Soc. 48, 1877 (1926).

The manufacturers of spectrophotometric equipment have exerted a definite influence on nomenclature by the terms and graduations applied to the instrument and the method of recording or presenting the data as influenced by the operation procedure of the instrument. This influence is particularly strong among research workers trained in other fields, such as biology or medicine, and who use the instrument for analytical or reaction rate measurements.

The authors of texts and compilations are less inhibited by editorial policy but generally tend to conform to what they feel is either a conservative or accepted practice. Examples of these systems are given in Table II.

The lack of uniformity of nomenclature as shown in Tables III and IV has been felt by many workers in their comparison of data published by different workers. The issuance of a collection of absorption spectra data on hydrocarbons by the National Bureau of Standards—American Petroleum Institute project, and the contemplated issuance of data on other types of compounds in the infra-red, visible and ultraviolet regions, by the National Bureau of Standards has stressed the importance of the establishment of a more uniform and acceptable system of absorption spectra nomenclature for the presentation of this data and for use in the published literature.

Suggestions have been made in Tables I, III, and V, as well as in the general discussion, for a system of nomenclature and presentation of absorption spectra data which embodies some of the past precedent with the technical evolution of absorption spectrophotometry as an applied determination for use in other fields of science.

The proposed system is not that which was proposed at the National Bureau of Standards[8] although it does include much of the same notation system. The suggested nomenclature in this article is also not in entire conformity with the present editorial practice of the American Institute of Physics; and hence, although the author recommends "wavelength," "wavenumber," and "infrared," these terms appear in this article, except where essential to compare systems, as "wave-length," "wave number," and "infra-red."

JOURNAL OF THE OPTICAL SOCIETY OF AMERICA VOLUME 39, NUMBER 12 DECEMBER, 1949

The Formation of Fringes in a Babinet Compensator

H. G. Jerrard
Department of Physics, The University College, Southampton, England

(Received July 21, 1949)

Details are given of the appearance of the field of view when two wedges of doubly refracting material are placed in arbitrary azimuths between crossed polarizing devices. In general the field of view presents a complex pattern but simple fringe systems appear for suitable orientation of the wedges, one of which is the well-known Babinet fringe system. Theoretical relationships are derived for the intensity distribution in the general case and for the simple cases. Photographs show how the simple fringe systems are formed out of the complex cases. A use of the patterns for detecting if the wedges of a Babinet compensator are correctly mounted is mentioned.

INTRODUCTION

WHEN a quartz wedge cut with its optic axis parallel both to its basal plane and to the edge of the wedge is placed in any azimuth between crossed polarizing devices, in general, the field of view is crossed by a system of equi-spaced fringes.* Complete darkness occurs if the optic axis of the wedge is parallel or perpendicular to the vibration direction of the polarizer. If, in addition, a second quartz wedge, having its optic axis parallel to its basal plane but perpendicular to the edge of the wedge be introduced in any azimuth between the polarizing devices so that the hypotenuse faces of the two wedges are opposed (see Fig. 1), then the field of view presents rather a complex pattern. As one wedge is rotated about an axis perpendicular to its basal plane the pattern undergoes an orderly but complicated change. In one position, namely when the two wedges form a plane parallel plate a set of equi-spaced fringes appears, the spacing of which is half that due to a single wedge. These fringes are the well-known Babinet fringes. If, however, the wedges are orientated at right angles to one another yet another set of fringes appear the spacing being intermediate between that due to the single wedge and the Babinet fringes, these fringes may conveniently

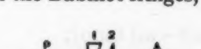

FIG. 1. Wedges mounted between polarizer *P* and analyzer *A*.

---

* The same holds whatever the azimuth of the optic axis with respect to the edge: for convenience, however, the axis is generally cut parallel or perpendicular to the edge of the wedge.

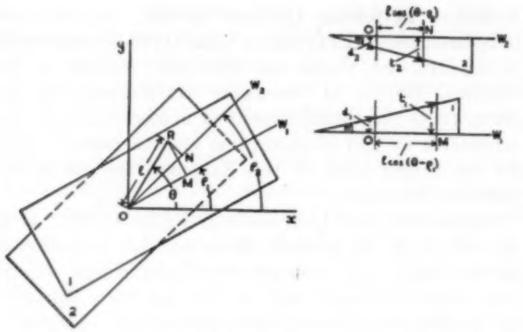

FIG. 2. The parameters. Ox, Oy are the coordinate axes. OW_1 and OW_2 are the directions of the lines of greatest slope of the wedges making azimuth angles ρ_1 and ρ_2 with Ox. R is any point having polar coordinates (l, θ). RM and RN are the perpendiculars to OW_1 and OW_2 respectively.

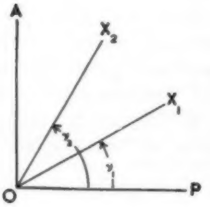

FIG. 3. OP and OA are the vibration directions of the polarizer and analyzer respectively; ν_1 and ν_2 are the angles measured from OP between the fast vibration directions OX_1 and OX_2 of the plate 1 and 2.

be called the pseudo-Babinet fringes. Since, to the writer's knowledge, no account of the patterns produced by two such wedges randomly orientated exists in the literature and as the process of the formation of the Babinet and pseudo-Babinet fringes are very instructive, it was decided to treat the problem in some detail.

THE GENERAL THEORY

Consider a two dimensional Cartesian system of coordinates Ox and Oy and suppose two wedges 1 and 2 of equal angle be placed as shown in Fig. 2 so that their lines of greatest slope make angles ρ_1 and ρ_2 respectively with Ox, and their thick ends are adjacent. In what follows these angles ρ_1 and ρ_2 will be called the azimuths of the wedges. At O, let the thicknesses of the wedges be d_1 and d_2 respectively. Then at any point R which has polar coordinates (l, θ) the thickness of wedge 1 is given by

$$t_1 = d_1 + l\cos(\theta-\rho_1)\tan\alpha$$

and that of wedge 2 by

$$t_2 = d_2 + l\cos(\theta-\rho_2)\tan\alpha,$$

where α is the angle of the wedge. If the material of the wedges be uniaxially doubly refracting and if δ_1 and δ_2 are the phase differences introduced by wedges 1 and 2, respectively, then

$$\delta_1 = (2\pi k/\lambda)(d_1 + l\cos(\theta-\rho_1)\tan\alpha)$$

and

$$\delta_2 = (2\pi k/\lambda)(d_2 + l\cos(\theta-\rho_2)\tan\alpha),$$

where k is the value of the birefringence and λ is the wave-length. In order to simplify the writing put

$$\Delta_1 = (2\pi k/\lambda)d_1; \quad \Delta_2 = (2\pi k/\lambda)d_2; \quad c = (2\pi k/\lambda)\tan\alpha$$

so that

$$\left.\begin{aligned}\delta_1 &= \Delta_1 + cl\cos(\theta-\rho_1)\\ \delta_2 &= \Delta_2 + cl\cos(\theta-\rho_2)\end{aligned}\right\}. \tag{1}$$

Now if two doubly refracting plates of phase differences δ_1 and δ_2 be placed between crossed linearly polarizing devices and if the intensity of the light emerging from the polarizer be taken as unity, then that emerging from the analyzer is given by[1]

$$\begin{aligned}I = &-\sin2\nu_1\cos2\nu_2\sin2(\nu_2-\nu_1)\sin^2\delta_1/2\\ &+\cos2\nu_1\sin2\nu_2\sin2(\nu_2-\nu_1)\sin^2\delta_2/2\\ &+\sin2\nu_1\sin2\nu_2\cos^2(\nu_2-\nu_1)\sin^2[(\delta_1+\delta_2)/2]\\ &-\sin2\nu_1\sin2\nu_2\sin^2(\nu_2-\nu_1)\sin^2[(\delta_1-\delta_2)/2],\end{aligned} \tag{2}$$

where ν_1 and ν_2 are as shown in Fig. 3 and defined in the legend.

If one imagines the two coordinate systems of Figs. 2 and 3 to be superimposed so that OP coincides with Ox and OA with Oy and OX_1 and OX_2 represent the optic axes of the wedges 1 and 2, and further if the values of δ_1 and δ_2 given by Eq. (1) be substituted in Eq. (2), then the resulting equation gives the intensity of the light emerging from the analyzer at the point R. The intensity is zero, when δ_1, δ_2, ν_1 and ν_2 are such as to satisfy the equation $I=0$ and so, in general, a complex intensity distribution pattern is obtained. If, as may be the case, ν_1 and ν_2 are zero or $\pi/2$, then the field of view is always completely dark: this case will not be considered in what follows.

APPLICATION TO SPECIAL CASES

1. Single Wedge between Crossed Polarizing Devices

Consider the case of a wedge in any arbitrary azimuth ρ_1 so that the optic axis makes an angle ν_1 with the vibration direction of the polarizer. If δ_1 be the phase difference at the point R, then the intensity is given by

$$I = \sin^2 2\nu_1 \sin^2\delta_1/2,$$

which is zero if $\sin\delta_1/2 = 0$ so that by substitution from Eq. (1), zero intensity occurs where

$$\Delta_1 + cl\cos(\theta-\rho_1) = \pm 2n\pi, \quad \text{where} \quad n = 0, 1, 2\cdots$$

or

$$\begin{aligned}l\cos(\theta-\rho_1) &= (\pm 2n\pi - \Delta_1)/c\\ &= p_n, \text{ say.}\end{aligned}$$

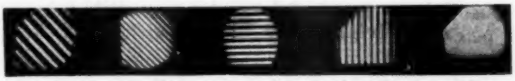
(a) (b) (c) (d) (e)

FIG. 4. Simple Fringe Systems (a) One wedge only (b) Babinet fringes (c) and (d) Pseudo-Babinet fringes, (e) uniform field of view. In each case $\rho_1 = \pi/4$.

---

[1] G. Szivessy, *Handbuch der Physik* 19, 924 (1928); H. G. Jerrard, J. Opt. Soc. Am. 38, 37 (1948).

For a given value of n this is the polar equation of a straight line where p_n and ρ_1 are the polar coordinates of the foot of the perpendicular from 0 to the line. Thus for values of $n=0, 1, 2\cdots$ the field of view is crossed by a set of equi-spaced fringes where the distance between two consecutive fringes is given by

$$a_1=p_{n+1}-p_n=2\pi/c.$$

Such a fringe system is shown in Fig. 4a, in which the wedge was so placed that $\rho_1=\nu_1=\pi/4$ and hence the fringes were most sharply defined.

2. Two Wedges between Crossed Polarizing Devices

(a) *Babinet fringes.* Suppose one wedge be placed in any azimuth ρ_1 and the second placed so that both wedges form a plane parallel plate. Then the intensity at the point R is found by making substitution

$$\nu_2=\nu_1+\pi/2 \text{ in Eq. (2).}$$

Thus

$$I=\sin^2 2\nu_1 \sin^2\tfrac{1}{2}(\delta_1-\delta_2),$$

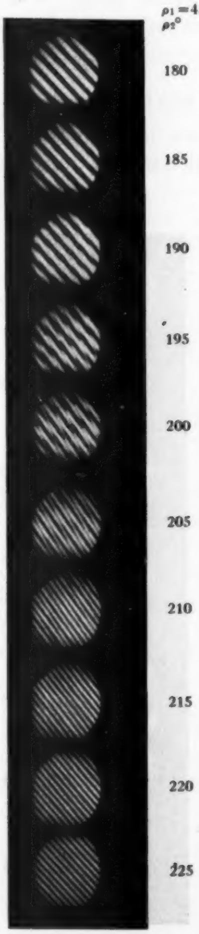

FIG. 5. The formation of the Babinet fringes. ρ_1 and ρ_2 are the azimuths of the wedges 1 and 2 with respect to the coordinate axis Ox.

so that the intensity is zero where

$$\sin\tfrac{1}{2}(\delta_1-\delta_2)=0.$$

Furthermore, $\rho_1=\nu_1$ and $\rho_2=\rho_1+\pi$, so that by Eq. (1) the loci of points of zero intensity are

$$\Delta_1+cl\cos(\theta-\rho_1)-\Delta_2-cl\cos(\theta-\rho_1-\pi)=\pm 2n\pi,$$

where $n=0, 1, 2\cdots$, which can be reduced to

$$l\cos(\theta-\rho_1)=\{\pm 2n\pi-(\Delta_1-\Delta_2)\}/2c$$
$$=q_n, \text{ say.}$$

In this case this equation represents a series of straight lines the spacing between which is given by

$$a_2=q_{n+1}-q_n=\pi/c$$

and where the polar coordinates of the foot of the perpendicular from 0 to the line are q_n, ρ_1.

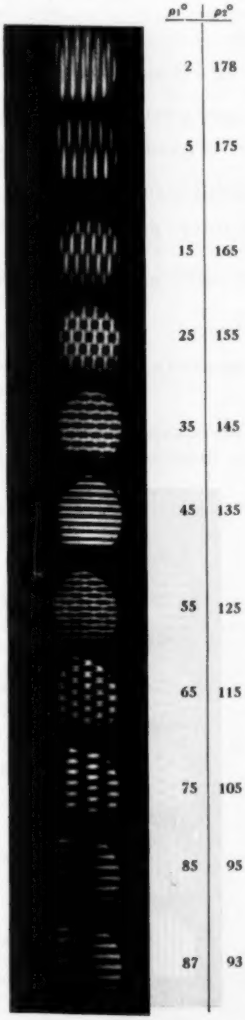

FIG. 6. The formation of the horizontal Pseudo-Babinet fringes. ρ_1 and ρ_2 are the azimuths of the wedges 1 and 2 with respect to the coordinate axis Ox.

This spacing is half that of the single wedge and the fringes which are shown in Fig. 4b for $\nu_1=\pi/4$ are the normal Babinet fringes.

(b) *Pseudo-Babinet fringes.* Suppose one wedge be placed in any azimuth ρ_1 and the second be arranged so that the lines of maximum slope are at right angles. The intensity at any point R can be obtained by making the substitutions

(1) $\rho_1=\nu_1, \quad \rho_2=\rho_1+\pi/2, \quad \nu_2=\nu_1+\pi$

or

(2) $\rho_2=\nu_1, \quad \rho_2=\rho_1-\pi/2, \quad \nu_2=\nu_1$ in Eqs. (1) and (2).

Thus for case (1)

$$I=\sin^2 2\nu_1 \sin^2 \tfrac{1}{2}(\delta_1+\delta_2)$$

so that the loci of points where the intensity is zero is given by

$$\sin\tfrac{1}{2}(\delta_1+\delta_2)=0$$

or

$$\Delta_1+cl\cos(\theta-\rho_1)+\Delta_2+cl\cos(\theta-\rho_1-\pi/2)=\pm 2n\pi$$

where $n=0, 1, 2\cdots$ i.e.,

$$cl\cos(\theta-\rho_1)+cl\sin(\theta-\rho_1)=\pm 2n\pi-(\Delta_1+\Delta_2).$$

Multiply throughout by $1/\sqrt{2}$

$$cl\{\cos(\theta-\rho_1)(1/\sqrt{2})+\sin(\theta-\rho_1)(1/\sqrt{2})$$
$$=(1/\sqrt{2})\{\pm 2n\pi-(\Delta_1+\Delta_2)\},$$
$$cl\{\cos(\theta-\rho_1)\cos\pi/4+\sin(\theta-\rho_1)\sin\pi/4\}$$
$$=(1/\sqrt{2})\{\pm 2n\pi-(\Delta_1+\Delta_2)\},$$

whence

$$l\cos\{\theta-(\rho_1+\pi/4)\}$$
$$=\{\pm 2n\pi-(\Delta_1+\Delta_2)\}/\sqrt{2}c=r_n, \text{ say.} \quad (3)$$

This equation represents a series of straight lines where the polar coordinates of the feet of the perpendicular from 0 to the lines are $(r_n, \rho_1+\pi/4)$. The spacing a_3 between the lines is given by

$$a_3=r_{n+1}-r_n=\sqrt{2}\pi/c.$$

This spacing is $\sqrt{2}$ times that of the normal Babinet fringes. If $\rho_1=\pi/4$, the fringes are horizontal and most sharply defined: these pseudo-Babinet fringes are shown in Fig. 4c.

For case (2) the loci of points of zero intensity are given by

$$l\cos\{\theta-(\rho_1-\pi/4)\}=\{\pm 2n\pi-(\Delta_1+\Delta_2)\}/\sqrt{2}c=s_n, \text{ say}$$

(cf. Eq. (3)), which again represents a series of straight lines of spacing $\sqrt{2}\pi/c$, but perpendicular to those of case (1). Figure 4d shows these pseudo-Babinet fringes when $\rho_1=\pi/4$, in which case they are vertical.

(c) *Uniform field of view.* As mentioned previously, if ν_1 and ν_2 are zero or $\pi/2$, then the field of view will be completely dark. However, it is possible to get uniform intensity for any value of ν_1 by suitable orientation of the wedges relative to each other. This obviously occurs when the wedges have their thick edges adjacent which may be expressed mathematically by the conditions

$$\rho_1=\nu_1; \quad \rho_2=\rho_1; \quad \nu_2=\nu_1+\pi/2$$

in which case

$$I=\sin^2 2\nu_1 \sin^2\tfrac{1}{2}(\delta_1-\delta_2),$$

which by substitution from Eq. (1) becomes

$$I=\sin^2 2\nu_1 \sin^2\tfrac{1}{2}(\Delta_1-\Delta_2).$$

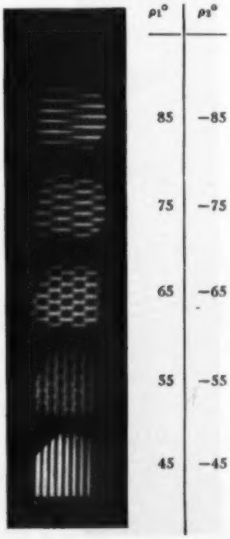

FIG. 7. The formation of the vertical Pseudo-Babinet fringes. ρ_1 and ρ_2 are the azimuths of the wedges 1 and 2 with respect to the coordinate axis Ox.

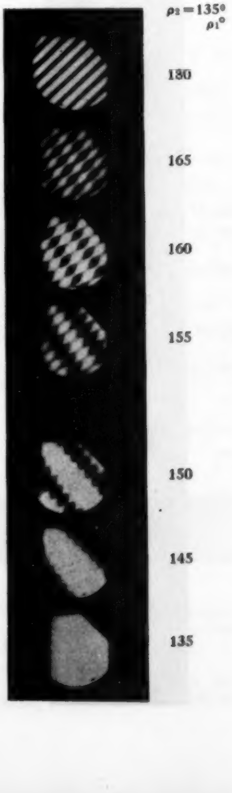

FIG. 8. The disappearance of the fringe system. ρ_1 and ρ_2 are the azimuths of the wedges 1 and 2 with respect to the coordinate axis Ox.

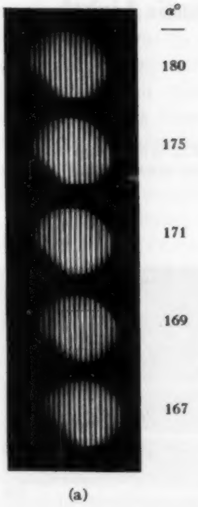

(a)

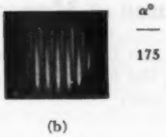

(b)

FIG. 9. Fringes when the wedges of a Babinet compensator are incorrectly set. Compensator mounted so that the line bisecting the obtuse angle between the azimuths of the wedges is (a) at 45° to the vibration direction of the polarizer, (b) at 90° to the vibration direction of the polarizer. α is the angle between the azimuth of each wedge.

Thus, for any given value of ν_1 the field of view is uniform. Such is the case shown in Fig. 4e. If $\Delta_1=\Delta_2$ i.e., the origin 0 is placed where the wedges have the same thickness then, of course, $\Delta_1=\Delta_2$ and complete darkness prevails.

(d) *Complex field of view.* The cases discussed in detail above are the only ones which give simple patterns. If the two wedges are randomly orientated, then apart from the particular solution $\sin\delta_1/2$ and $\sin\delta_2/2=0$ no simple mathematical solution of the equation $I=0$ exists. However, photographs have been taken which show the type of field presented and the manner in which the field assumes the fringe systems (a), (b), and (c) above.

Figure 5 shows how the Babinet fringes are built up. Starting with the wedges 1 and 2 in azimuths $\pi/4$ and π, respectively, wedge 1 is kept stationary and wedge 2 rotated through $\pi/4$ so that the Babinet fringes are formed.

Figure 6 shows how the field of view changes as the position of one wedge changes from 0 to $\pi/2$ while the position of the second wedge changes from π to $\pi/2$ in equal stages. In the process horizontal pseudo-Babinet fringes are formed. The formation of the vertical pseudo-Babinet fringes is shown in Fig. 7.

Figure 8 shows the disappearance of the fringes to form a uniform field of view.

CONCLUSION

From the above discussion a practical point of some importance arises. In constructing a compensator two facts must be observed. Firstly the wedges must be optically perfect—that is they must be so cut that when they are placed together their optic axes are at right angles and they form a perfect plane parallel plate and secondly the wedges must be mounted so as to be mechanically perfect—that is they must form a perfect plane parallel plate when assembled. If it is assumed that the wedges are free from the optical defect mentioned above[2] then any such mechanical defect in the completed compensator can be detected by placing it between crossed linearly polarizing devices and attempting to get complete extinction. If the latter is not possible and fringes of the type seen in Figs. 6 or 7 appear, the wedges are incorrectly mounted. As would be expected the effect of this maladjustment is less apparent when the compensator is placed in the position in which it is often used—namely in azimuth 45°. Figure 9a is a series of photographs taken with different angles between the wedges when the line bisecting the obtuse angle between the lines of greatest slope is at 45° to the vibration direction of the polarizer. From this it will be seen that for an angle between the wedges of about 5° no appreciable effect on the fringes is noticeable, whereas in the neighborhood of extinction it is very marked as can be observed in Fig. 9b.

In conclusion the author wishes to express his thanks to Professor A. M. Taylor for his interest and encouragement throughout this investigation.

APPENDIX

The experimental arrangement used in the above investigation is as shown in Fig. 10. *P* and *A* were Glan Thompson prisms mounted on graduated circles reading to 2 minutes of arc. The wedges were attached to two similar graduated circles and illuminated by parallel light. One particular difficulty was experienced in that due to the refraction produced by the wedges the final image did not always lie on the principal axis of the system but moved as the wedges moved. This at times caused a somewhat uneven intensity distribution over the field of view.

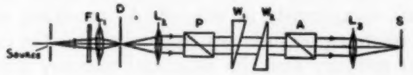

FIG. 10. The experimental arrangement. *F*, filter; *D*, diaphragm; *P*, polarizer; *A*, analyzer; W_1 and W_2 are the wedges; L_1, L_2, and L_3 are lenses; *S*, screen.

---

[2] For a detailed discussion of the optical defect see H. G. Jerrard, J. Sci. Inst. Phys. Ind. (November, 1949).

JOURNAL OF THE OPTICAL SOCIETY OF AMERICA VOLUME 39, NUMBER 12 DECEMBER, 1949

The Possibility of Enhanced Hg^{202} as a Source of Monochromatic Light*

J. RAND MCNALLY, JR., PAUL M. GRIFFIN, AND L. ELKIN BURKHART
Carbide and Carbon Chemicals Corporation, Oak Ridge, Tennessee

(Received September 12, 1949)

Electromagnetically enhanced Hg^{202}, as a source material for highly monochromatic radiation, is discussed briefly with relation to the effects of the isotopic impurities. A Fabry-Perot interferogram showing line purity in the 98.06 percent Hg^{202} is reproduced.

IN 1942, in discussing the possibility of a mercury isotope as a source of an improved wave-length standard, Meggers stated:[1]

> "If a single even isotope, say 202, which constitutes nearly 30 percent of ordinary mercury, could be isolated it would solve the problem of the primary standard to the satisfaction of all. This appears to be too difficult, but the same end may be attained in another way."

This other way, through neutron irradiation of gold to produce Hg^{198} with Hg^{199} as a small impurity, has been shown by Meggers[2] to fulfill satisfactorily the requirements of a primary standard. The first successful transmutation of gold to mercury in quantities sufficient for spectroscopic purposes was carried out by Alvarez and Wiens.[3] As late as 1946, Wiens remarked:[4]

> "Seven isotopes are present but since the isotope mass 202 is the most plentiful, one might be inclined to try to use the mass spectrograph for separating this isotope from ordinary mercury. This and all other methods for separating the mercury isotopes in quantities large enough to produce a strong light source have until now been unsuccessful."

Availability of the isotopes of mercury, enhanced in the 202 isotope to 98.06 percent, is concurrently reported[5] in a recent Letter to the Editor in *The Physical Review*. The expected relative intensities of the individual components in the 5461A transition of mercury (assuming no intensity anomalies) for the cases of natural mercury and the enhanced mercury are given in Table I, the notation being according to Schuler and Keyston,[6] the intensities being based on the natural abundances, the enhanced abundances, and the tables of White and Eliason,[7] and the relative positions being according to Burger and van Cittert.[8]

Although this figure of 98.06 percent is not the

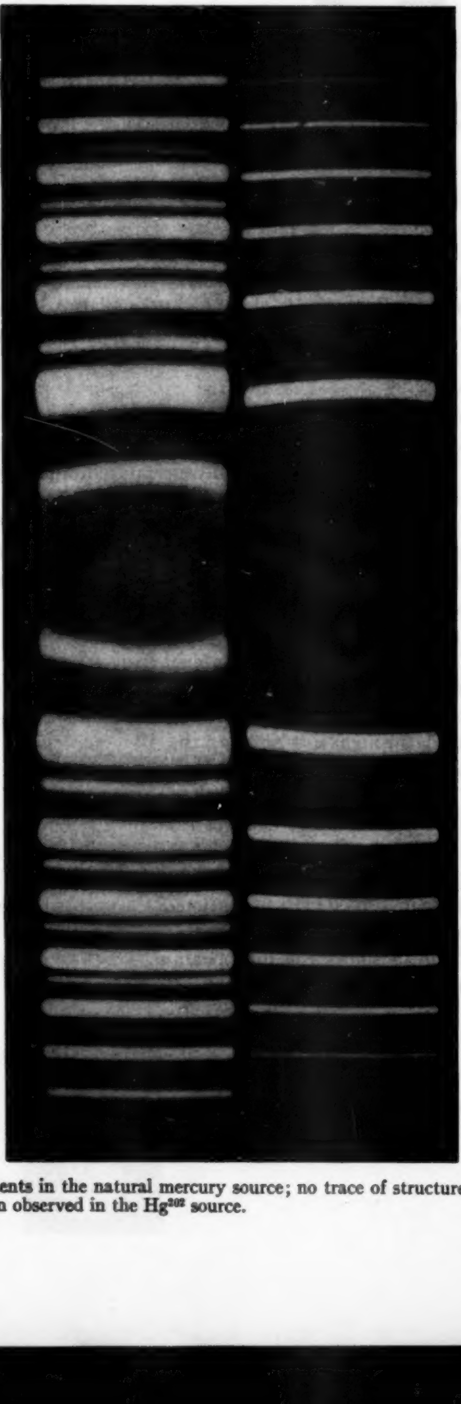

FIG. 1. Comparison of 5461A line structure in natural mercury and enhanced Hg^{202}. Electrodeless discharge sources and 10 mm etalon crossed with large Littrow-type prism spectrograph. The original plates show the presence of three 1.1 percent satellites as well as the 8.5 percent satellite due to two overlapping components in the natural mercury source; no trace of structure has been observed in the Hg^{202} source.

---

* This document is based on work performed for the AEC by Carbide and Carbon Chemicals Corporation, at Oak Ridge, Tennessee.

[1] W. F. Meggers, Rev. Mod. Phys. **14**, 59 (1942).
[2] W. F. Meggers, J. Opt. Soc. Am. **38**, 7 (1948).
[3] J. H. Wiens and L. W. Alvarez, Phys. Rev. **58**, 1005 (1940).
[4] J. H. Wiens, Phys. Rev. **70**, 910 (1946).
[5] C. P. Keim, Phys. Rev. **76**, 1270 (1949).
[6] H. Schuler and J. E. Keyston, Zeits. f. Physik. **72**, 430 (1931).
[7] H. E. White and A. Y. Eliason, Phys. Rev. **44**, 753 (1933).
[8] H. C. Burger and P. H. van Cittert, Physica **5**, 177 (1938).

ultimate purity attainable through the electromagnetic process it is natural to inquire into the possibility of utilizing isotopic mercury of this purity to produce a monochromatic and reproducible wave-length. Limitations on discerning these weak components will arise from Doppler broadening and from instrumental background. Preliminary studies[9] of these effects on a line having close-lying satellites, such as the 202 IV line in the enhanced material, indicate that under ordinary conditions of observation as much as 8.7 percent satellite intensity from either 200 III or 204 V could be tolerated without shifting the fringe maximum by more than one part in 50,000,000. It can be shown also that for a source at room temperature the contribution of Doppler broadening alone is simply to introduce very small wing effects due to the 0.78 percent 200 III and the 0.57 percent 204 V. Neither satellite maximum should be detectable in such a source.

The presence of extraneous weak maxima in an interference pattern may, however, be undesirable although they may have little or no effect on the intensity maximum of the main fringe. Thus, components other than the 200 III and the 204 V lines must be considered from another aspect since these can be separated more readily from the main line by appropriate choice of interferometer path length. The next strongest line is the triplet group, 201 c, 201 e, and 196 I, which has a total intensity less than 0.21 percent. If this intensity is to be greater than the minimum background intensity between orders in the Fabry-Perot pattern one requires reflecting coefficients in excess of 90 percent, a value in itself difficult to obtain. Consideration of the other components indicates that still more difficult experimental conditions must be met if the intensity contribution is to be equal or greater than background intensity (e.g., 198 II requires $r > 94$ percent).

TABLE I. Relative intensities of 5461 hyperfine structure components in natural and enhanced mercury.

Isotope	Position	Natural	Enhanced
196 I	−0.089 cm^{-1}	0.15	<0.02
198 II	−0.060	10.1	0.09
199 A	−0.320	5.7	0.04
199 B	0.000	10.2	0.07
199 C	0.756	1.1	0.01
200 III	−0.031	23.3	0.78
201 a	−0.751	0.1	0.00
201 b	−0.469	1.2	0.03
201 c	−0.089	5.3	0.15
201 d	−0.274	0.2	0.01
201 e	−0.089	1.4	0.04
201 f	0.194	2.8	0.08
201 g	0.124	1.1	0.03
201 h	0.304	1.1	0.03
202 IV	0.000	29.6	98.06
204 V	0.028	6.7	0.57

Figure 1 shows the 5461A Fabry-Perot interference pattern taken using an electrodeless discharge tube containing the 98.06 percent isotopic purity Hg^{202}. Preliminary over-exposed interferograms of this line at several etalon separations indicate no trace of satellite structure.

The present status of the mercury enhancement indicates that Hg^{202} may be separated from the natural species in sufficient quantity and in sufficient purity to produce lamps having a monochromatic and reproducible wave-length, namely, the 5461A line. Detailed investigation of this line and other lines of mercury based on present and future Hg^{202} purity is continuing.

Acknowledgment is made to those on isotope production whose cooperative efforts made this enriched isotope available, and to E. J. Greeley and E. L. Boorn of the glass-blowing laboratory.

---

[9] P. M. Griffin and J. R. McNally, Jr., Documents Y-345 and Y-438, Carbide and Carbon Chemicals Corporation, Oak Ridge, Tennessee; also, reported at Optical Society of America Meeting, March, 1949.

London Conference on Optical Instruments, July 1950

A conference on optical instruments will be held at the Imperial College of Science and Technology, London, England, on July 19–26, 1950, under the sponsorship of the Optics Sub-Committee of the British National Committee for Physics. This conference will cover recent advances in the construction and performance of optical instruments of all kinds. In addition to an exhibition of optical instruments, technical papers and invited lectures will be given. Visits to optical firms and laboratories will be arranged; receptions will be held by appropriate scientific societies. American scientists and technicians who may be visiting Great Britain next summer are invited to attend this conference, which will be partly concurrent with the official sessions of the International Commission of Optics. Further information, and membership application forms, may be obtained from Professor L. C. Martin, Department of Physics, Imperial College, Imperial Institute Road, London, S.W. 7, England.

JOURNAL OF THE OPTICAL SOCIETY OF AMERICA VOLUME 39, NUMBER 12 DECEMBER, 1949

Reflection from a Multilayer Filter

HARRY D. POLSTER
Institute of Optics, University of Rochester, Rochester, New York

(Received October 10, 1949)

The solution of the multilayer filter is obtained as a boundary value problem. A recursion formula is developed, which, applied once for each layer gives the reflected beam. A graphical means for determining the unknown quantity in the recursion formula has been shown to apply to dielectric layers.

The solution has been used to explain an irregular fringe shift in the reflected pattern from an interferometer, one of whose plates has a uniform wedge of dielectric deposited on it. It is shown that this irregular shifting of the fringes with thickness of the dielectric must be considered if interferometric determinations of index of refraction are to be made.

This method of determining the reflected beam has also been applied in finding the transmission characteristics of the frustrated total reflection filter. It is found that the width of the transmission band which, theoretically, could be arbitrarily small without loss of peak transmission, is limited by the uniformity in the thickness of the spacer layer.

SEVERAL papers have appeared recently[1–4] in which the problem of the reflection and transmission of a multilayer filter has been solved as a boundary value problem. The general solution can be given as the ratio of two determinants for the reflection, while for the transmission one of the determinants is immediately solved.

It has been found possible to reduce the problem of determining the reflection from such a filter by reducing the determinants to the form of continuants, and solving for an "effective refractive index" of the filter as a whole. This "effective index," $\bar{l}_1$, is a complex quantity that varies with the angle of incidence. It is defined from the relation for the reflected beam, analogously to the case for normal incidence on a single layer surface:

$$R=(1-\bar{l}_1)/(1+\bar{l}_1). \tag{1}$$

A recursion formula has been derived which yields $\bar{l}_1$ after being applied once for each layer in the filter.

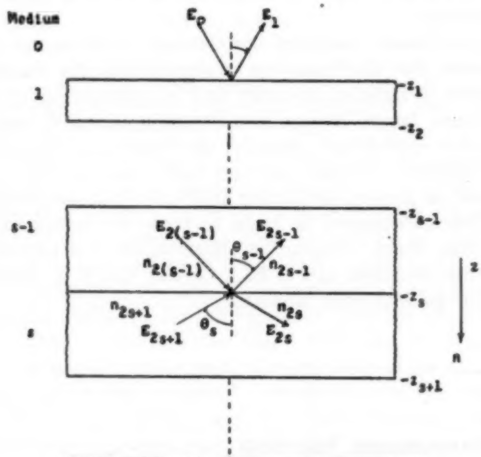

FIG. 1. The notation used in determining the reflected wave E_1, having an incident wave E_0. The unit vector, n, gives the z axis. The propagation vector, n_{2s}, is associated with the electric vector E_{2s}.

Consider the case of p layers of different homogeneous, isotropic substances whose surfaces of separation are infinite parallel planes, Fig. 1. Given a plane electromagnetic wave incident on the first surface, to determine the reflected wave. In the sth layer the electric and magnetic components of the wave are given by

$$\begin{aligned}\mathbf{E}(s)&=\mathbf{E}_{2s}\exp(ik_s\mathbf{n}_{2s}\cdot\mathbf{r})+\mathbf{E}_{2s+1}\exp(ik_s\mathbf{n}_{2s+1}\cdot\mathbf{r})\\ \mathbf{H}(s)&=(k_s/\omega)[(\mathbf{n}_{2s}\times\mathbf{E}_{2s}\exp(ik_s\mathbf{n}_{2s}\cdot\mathbf{r})+\mathbf{n}_{2s+1}\times\mathbf{E}_{2s+1}\\ &\qquad\times\exp(ik_s\mathbf{n}_{2s+1}\cdot\mathbf{r})]\end{aligned} \tag{2}$$

satisfying the boundary conditions

$$\left.\begin{aligned}\mathbf{n}\times\mathbf{E}(s-1)&=\mathbf{n}\times\mathbf{E}(s)\\ \mathbf{n}\times\mathbf{H}(s-1)&=\mathbf{n}\times\mathbf{H}(s)\end{aligned}\right\}\quad \text{at } z=z_s \tag{3}$$

and where $k_s=2\pi\mu_s/\lambda$, μ_s = refractive index of sth layer, λ = wave-length in air of incident radiation. Figure 1 indicates the meaning of the other terms in (2) and (3).

We consider separately the two cases of s and p polarization.

Case 1. *Electric vector normal to the plane of incidence (s-component)* · · · ·

For this case

$$\mathbf{n}\cdot\mathbf{E}_0=\mathbf{n}\cdot\mathbf{E}_1=\cdots=\mathbf{n}\cdot\mathbf{E}_{2p+2}=0 \tag{5}$$

and the boundary conditions give

$$\begin{aligned}\alpha_{s-1,s}\mathbf{E}_{2(s-1)}+\alpha_{s-1,s}'\mathbf{E}_{2s-1}-\alpha_{s,s}\mathbf{E}_{2s}-\alpha_{s,s}'\mathbf{E}_{2s+1}&=0\\ \alpha_{s-1,s}\mathbf{E}_{2(s-1)}-\alpha_{s-1,s}'\mathbf{E}_{2s-1}-l_s\alpha_{s,s}\mathbf{E}_{2s}+l_s\alpha_{s,s}'\mathbf{E}_{2s+1}&=0\end{aligned} \tag{6}$$

---

[1] A. Herpin, Comptes Rendus **225**, 182–183 (1947).
[2] W. Weinstein, J. Opt. Soc. Am. **37**, 576–581 (1947).
[3] L. N. Hadley and D. M. Dennison, J. Opt. Soc. Am. **37**, 451–465 (1948).
[4] R. L. Mooney, J. Opt. Soc. Am. **35**, 574–583 (1945).

for $s=1, 2, \cdots, p+1$, where

$$\begin{array}{ll}\alpha_{s,s}=\exp(ik_s\mathbf{n}_{2s}\cdot\mathbf{r}_s) & \alpha_{s,s+1}=\exp(ik_s\mathbf{n}_{2s}\cdot\mathbf{r}_{s+1}) \\ \alpha_{s,s}'=\exp(ik_s\mathbf{n}_{2s+1}\cdot\mathbf{r}_s) & \alpha_{s,s+1}'=\exp(ik_s\mathbf{n}_{2s+1}\cdot\mathbf{r}_{s+1})\end{array} \tag{7}$$

and

$$t_s=\frac{k_s\cos\theta_s}{k_{s-1}\cos\theta_{s-1}}, \tag{8}$$

while from Snell's law

$$k_s\sin\theta_s=k_{s-1}\sin\theta_{s-1} \quad s=1, 2, \cdots, p+1. \tag{9}$$

Also $\mathbf{E}_{2p+3}=0$ since there is no reflected beam in the $(p+1)^{st}$ medium.

This set of $2p+2$ equations can be solved to give $\mathbf{E}_1=R\mathbf{E}_0$, where R is the ratio of two determinants whose corresponding elements are identical except for the first column. The two determinants are written as one, with a double first column. The first half of the first column gives the numerator, the second half the denominator. Only the non-zero elements are given.

$$R=-\left|\begin{array}{ccccccccccc}
N & D & & & & & & & & & \\
\alpha_{0,1} & \alpha_{0,1}' & -\alpha_{1,1} & -\alpha_{1,1}' & & & & & & & \\
\alpha_{0,1} & -\alpha_{0,1}' & -t_1\alpha_{1,1} & t_1\alpha_{1,1}' & & & & & & & \\
 & & \alpha_{1,2} & \alpha_{1,2}' & -\alpha_{2,2} & -\alpha_{2,2}' & & & & & \\
 & & \alpha_{1,2} & -\alpha_{1,2}' & -t_2\alpha_{2,2} & t_2\alpha_{2,2}' & & & & & \\
 & & & & \alpha_{2,3} & \alpha_{2,3}' & -\alpha_{3,3} & -\alpha_{3,3}' & & & \\
 & & & & \alpha_{2,3} & -\alpha_{2,3}' & -t_3\alpha_{3,3} & t_3\alpha_{3,3}' & & & \\
 & & & & & & \ddots & \vdots & \ddots & & \\
 & & & & & & & & \alpha_{p,p+1} & \alpha_{p,p+1}' & -\alpha_{p+1,p+1} \\
 & & & & & & & & \alpha_{p,p+1} & -\alpha_{p,p+1}' & -t_{p+1}\alpha_{p+1,p+1}
\end{array}\right|. \tag{10}$$

By factoring out the uppermost non-zero element in each column, subtracting column $2s$ from column $2s+1$, and then subtracting row $2s-1$ from row $2s$ (except in the first two rows which must be handled differently in each case to make all the elements in the first column vanish except the first), the order of the determinants is reduced by unity. They are now in the form of continuants, the only non-zero elements appearing in the principal and two adjacent diagonals.

$$R=-\left|\begin{array}{ccccccc}
(\pm1-t_1) & -t_1 & & & & & \\
\exp i\delta_1 & i\sin\delta_1 & -1/b_1 & & & & \\
 & b_1\exp-i\delta_1 & (1-t_2) & & & & \\
 & \exp i\delta_2 & i\sin\delta_2 & -1/b_2 & & & \\
 & & b_2\exp-i\delta_2 & (1-t_3) & & & \\
 & & & \ddots & \ddots & & \\
 & & & & (1-t_p) & -t_p & \\
 & & & & \exp i\delta_p & i\sin\delta_p & -1/b_p \\
 & & & & & b_p\exp-i\delta_p & (1-t_{p+1})
\end{array}\right|. \tag{11}$$

Here the $+$ sign in the first element refers to the numerator, the $-$ sign to the denominator.

$$\delta_s=k_s(z_{s+1}-z_s)\cos\theta_s=(2\pi\mu_sd_s\cos\theta_s)/\lambda, \tag{12}$$

the advance in phase on a single passage through the sth layer.

$$b_s=\exp-ik_s\{\mathbf{n}_{2s}\times\mathbf{n}\}\cdot\{\mathbf{n}\times(\mathbf{r}_{s+1}-\mathbf{r}_s)\},$$

a quantity that has significance for the transmitted beam only.

From (11) we obtain (1) immediately by expanding each determinant to give

$$R=-\frac{(1-t_1)D_2+t_1D_3\exp i\delta_1}{(-1-t_1)D_2+t_1D_3\exp i\delta_1}=\frac{1-\bar{t}_1}{1+\bar{t}_1} \tag{13}$$

where D_s is the minor determinant whose principal diagonal includes the elements $s, s; s+1, s+1; \cdots 2p+1, 2p+1$, and

$$\bar{t}_1=t_1\left(1-\frac{\exp i\delta_1}{D_2/D_3}\right). \tag{14}$$

The D's are related in the following way:

$$D_{2s-1}/D_{2s}=1-\bar{t}_s=1$$
$$-t_s\left(1-\frac{\exp i\delta_s}{i\sin\delta_s+[\exp -i\delta_s/(D_{2s+1}/D_{2s+2})]}\right) \tag{15}$$

where

$$\bar{t}_s=t_s\frac{\bar{t}_{s+1}-i\tan\delta_s}{1-i\bar{t}_{s+1}\tan\delta_s}. \tag{16}$$

To determine the reflection from a multilayer filter, one starts by determining

$$\bar{t}_p=t_p\frac{t_{p+1}-i\tan\delta_p}{1-it_{p+1}\tan\delta_p}$$

from the known values of t_{p+1} and δ_p. Then the $\bar{t}$'s with successively decreasing subscripts are derived until $\bar{t}_1$ is determined. There will be as many operations as there are layers in the filter.

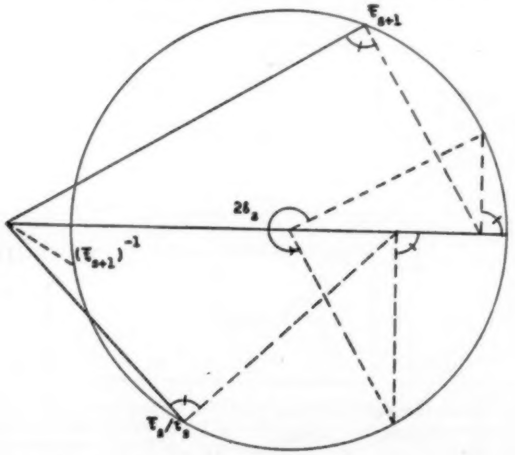

FIG. 2. Construction for determining $\bar{t}_s/t_s$ from the known values of $\bar{t}_{s+1}$ and δ_s. Drop a perpendicular from $\bar{t}_{s+1}$ to the axis and then up to the circle, as shown. Lay off the angle $2\delta_s$ around the circle, drop a perpendicular to the axis, and locate the point on the circle that makes the radius vector perpendicular to the line from the axis point. The radius vector is $\bar{t}_s/t_s$, and if multiplied by t_s will give $\bar{t}_s$.

Case 2. *Electric vector parallel to the plane of incidence (p-component)*$\cdots$

In this case we have, analogously to (5)

$$\mathbf{n}\cdot\mathbf{H}_0=\mathbf{n}\cdot\mathbf{H}_1=\cdots=\mathbf{n}\cdot\mathbf{H}_{2p+2}=0. \tag{17}$$

In the sth layer we take

$$\begin{aligned}\mathbf{H}(s)&=\mathbf{H}_{2s}\exp(ik_s\mathbf{n}_{2s}\cdot\mathbf{r})+\mathbf{H}_{2s+1}\exp(ik_s\mathbf{n}_{2s+1}\cdot\mathbf{r})\\ \mathbf{E}(s)&=(\omega/k_s)[\mathbf{n}_{2s}\times\mathbf{H}_{2s}\exp(ik_s\mathbf{n}_{2s}\cdot\mathbf{r})\\ &\qquad+\mathbf{n}_{2s+1}\times\mathbf{H}_{2s+1}\exp(ik_s\mathbf{n}_{2s+1}\cdot\mathbf{r})].\end{aligned} \tag{18}$$

When we solve for $\mathbf{H}_1=R\mathbf{H}_0$ we find a solution identical to that found for $\mathbf{E}_1=R\mathbf{E}_0$ in Case 1, except that now the t's are defined by

$$t_s=\frac{k_{s-1}\cos\theta_s}{k_s\cos\theta_{s-1}}. \tag{19}$$

Hence either case can be solved by the same recursion formula (16).

Immediately obvious are the values of $\bar{t}_s$ for $\delta_s=n\pi$ or $(2n-1)\pi/2$, n an integer. For $\delta_s=n\pi$, $\mu_sd_s\cos\theta_s=n\lambda/2$, and

$$\bar{t}_s=t_s\bar{t}_{s+1} \tag{20}$$

while for $\delta_s=(2n-1)\pi/2$, $\mu_sd_s\cos\theta_s=(2n-1)\lambda/4$, and

$$\bar{t}_s=t_s/\bar{t}_{s+1}. \tag{21}$$

For these cases the reflection can be quickly calculated.

A simple graphical means for computing the $\bar{t}$'s exists for dielectrics because $\bar{t}_s/t_s$, being a bilinear function of $\tan\delta_s$, has its locus for a variation of δ_s on a circle in the complex plane.[5] To determine $\bar{t}_s$ from the known values of $\bar{t}_{s+1}$ and δ_s, first mark off $\bar{t}_{s+1}$ and $(\bar{t}_{s+1})^{-1}$ and draw the circle through these points whose center lies on the real axis. Figure 2 indicates the rest of the construction.

This construction is valid for all values of $\bar{t}_{s+1}$, however the accuracy decreases as $\bar{t}_{s+1}$ becomes very large, as in the case of a high reflection. In this case the circle has a large radius and a change in δ_s of several degrees may correspond to a change in $\bar{t}_s/t_s$ of only a few minutes. Hence it is better to compute directly from (16).

ABSORBING MEDIA

In case the sth layer is absorbing

$$k_s=2\pi(\mu_s+i\eta_s)/\lambda \tag{22}$$

and the corresponding t's and θ_s become complex according to Eqs. (8), (19), and (9). If only the $p+1^{st}$ medium, the substrate for the filter, is absorbing, then all the δ's are real and the reflection can be computed graphically as above.

---

[5] S. A. Schelkunoff, *Electromagnetic Waves* (D. Van Nostrand and Company, Inc., New York, 1943), p. 199.

AN APPARENT ANOMALOUS FRINGE SHIFT IN A REFLECTION INTERFEROMETER*

This method of determining the reflected beam from an interference filter has been used to explain an apparent anomalous effect in the fringe shift across the aperture of an interferometer. Figure 3 indicates the coating of the interferometer plate. First an opaque layer of aluminum was deposited, then a wedge of dielectric, and finally, over half of the plate, another opaque layer of aluminum. The other interferometer plate was coated with a semi-transparent aluminum film having a density of approximately 0.9. The two plates were separated by 5 micron tin foil spacers, and their inclination adjusted to make the fringes run up the wedge. A photograph of the reflected fringe pattern is shown in Fig. 4. The uniform shift along the upper half of the picture indicates that the thickness of the wedge increased uniformly, while the non-uniform shift in the lower half shows the anomalous effect.**

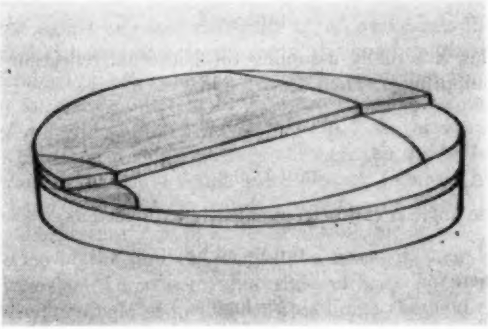

FIG. 3. The coating of the interferometer plate to produce the anomalous fringe shift. First, an opaque layer of aluminum; then, a wedge of high index dielectric; and, finally, over half the plate another opaque aluminum layer.

A calculation of the phase shift on reflection from an opaque aluminum surface covered by a layer of dielectric showed the reason for the effect. The solution was obtained by the graphical method by drawing the characteristic circle for opaque aluminum*** covered with ZnS. Values of $\bar{t}_1$ for different thicknesses of ZnS were read off the circle directly, and the amplitude and phase shift of the reflected beam were determined from (1). Figure 5 is a plot of the results. It is seen that at the position of minimum reflection the rate of increase of phase shift is greatest. Hence, in the fringe pattern, at those points, the shift toward smaller separation of the interferometer plates will be most rapid.

FIG. 4. The reflected fringe pattern. The upper, uniform shift indicated the regularity of the wedge, while the lower irregular shift shows the anomalous effect.

This non-uniform shifting of the fringes with increasing thickness of the dielectric will lead to erroneous results if one attempts to interpret the fringe shift as a measure of the optical thickness of the dielectric. Such an interpretation is valid only at positions where the optical thickness is an integral number of half-waves. (There is another position at which this is true as indicated by the intersection of the phase curve with the straight line, but the optical thickness at this point is a function of the index of the aluminum as well as the index of the dielectric.) This must be considered if this method is used to determine the refractive index of a dielectric.

FRUSTRATED TOTAL REFLECTION FILTERS

An interesting application of this method is to the problem of the frustrated total reflection (FTR) filter.[6] This filter is essentially a Fabry-Perot interferometer in which the reflecting plates are two frustrated total reflection surfaces. These are surfaces that would produce total internal reflection, except that a thin layer of low index dielectric deposited on them allows a small amount of energy to penetrate, provided that the index of the medium into which it is transmitted is sufficiently high. The amount of energy that is transmitted depends inversely on the thickness of the low index frustrating layer. Because the reflecting power of such surfaces can be made arbitrarily close to 100 percent, they produce interferometers with extremely high resolving power, or filters with extremely narrow pass bands.

Since the absorption at the surfaces is negligible, transmission peaks of 100 percent should theoretically be obtained. Actually the pass bands of the polarized s and p components are not at the same spectral position so that only 50 percent of the unpolarized light should be transmitted at a particular wave-length.

Such a filter is made by depositing three dielectric layers on a face of a high index equilateral prism. The

---

* The following work was supported by the Engineer Research and Development Laboratories through contract No. W-44-009 eng-470.

** A lead to the solution of the anomalous shift was due to R. G. Scott, who observed that the most rapid shift occurred at points of minimum reflection from the lower interferometer plate.

*** The constants for aluminum were obtained from G. Hass (Optik **1**, 2–8 (1946)).

[6] P. Leurgans and A. F. Turner, J. Opt. Soc. Am. **37**, 983A (1947).

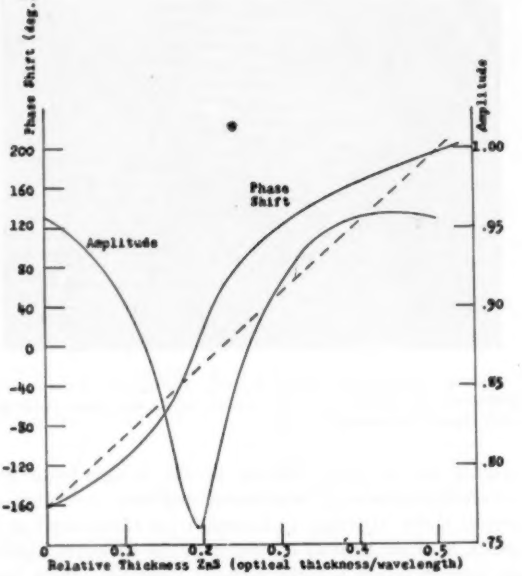

FIG. 5. The amplitude and phase shift of the reflected beam from an aluminum surface covered with ZnS, as a function of the thickness of the ZnS. The dotted line indicates the phase shift due to a double passage through the ZnS layer.

first is a low index frustrating layer whose thickness determines the half-width of the filter; next, is a high index spacer layer whose thickness determines the position of the transmission band; and, finally, a low index layer identical to the first. To this surface is cemented an uncoated prism identical to the first, using a cement whose index is comparable to that of the glass.

To predict the characteristics of such a filter one can use the simple equation for the transmission of a Fabry-Perot interferometer in which the absorption is negligible,

$$T=\left[1+\frac{4|R|^2\sin^2(\delta_0+\Delta)}{(1-|R|^2)^2}\right]^{-1}, \tag{23}$$

where

$|R|^2$ = reflecting power of the interferometer plates
δ_0 = phase advance on a single passage through the spacer layer
$=(2\pi\mu_0 d_0\cos\theta_0)/\lambda$
Δ = phase shift of light incident in the spacer layer on reflection from one of the interferometer plates.

To determine $|R|$, δ_0, and Δ we need consider only half of the FTR filter. The incident medium, then, is the high index spacer layer, and the medium into which the energy is transmitted is the glass prism. Thus the problem is reduced to that of a single layer filter, Fig. 6. From (16) we get

$$\bar{l}_1=l_1(l_2-i\tan\delta_1)/(1-il_2\tan\delta_1). \tag{24}$$

Now μ_0, μ_1, μ_2, and θ_2 are known, while θ_0 and θ_1 are determined from (9). If μ_1 is small enough to allow FTR, then $\sin\theta_1>1$ and $\cos\theta_1$ is a pure imaginary,

$$\cos\theta_1=i\,(\sin^2\theta_1-1)^{\frac{1}{2}}. \tag{25}$$

Hence the l's (8, 19) and δ_1 (12) become pure imaginary quantities, and they can be written

$$\begin{aligned} l_2&=-il_2' \\ l_1&=il_1' \\ \delta_1&=i\gamma. \end{aligned} \tag{26}$$

Then,

$$\bar{l}_1=il_1'(-il_2'+\tanh\gamma)/(1-il_2'\tanh\gamma). \tag{27}$$

From this formula we can determine $|R|$ using Eq. (1).

To get an analytical expression for Δ we make an approximation that results in a negligible error for filters of narrow pass bands. For these, $\tanh\gamma$ is very close to unity, and we approximate

$$\tanh\gamma=1. \tag{28}$$

This is actually assuming total internal reflection for computing Δ. Then, $\bar{l}_1=il_1'$ and

$$R=(1-il_1')/(1+il_1') \tag{29}$$

so that

$$\tan(\Delta/2)=-l_1'. \tag{30}$$

The angle Δ can be conveniently expressed as

$$\tan\Delta=\operatorname{csch}\beta, \tag{31}$$

where

$$\beta=\log l_1'. \tag{32}$$

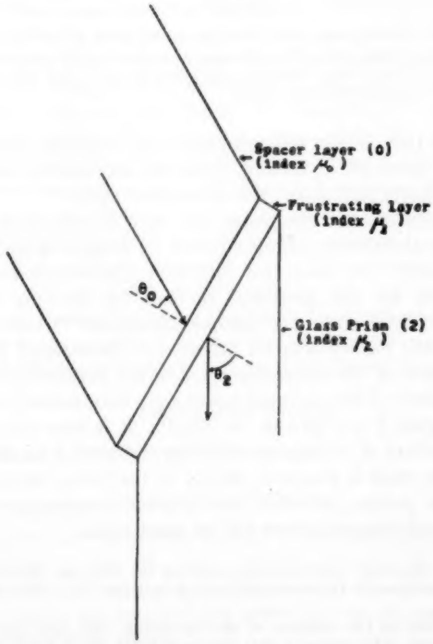

FIG. 6. The problem of determining the transmission of an FTR filter is reduced to finding the reflected amplitude and phase of light incident in the spacer layer.

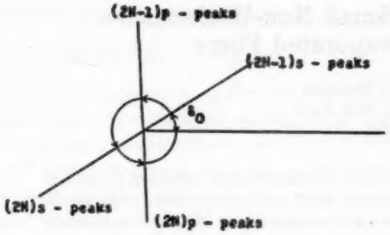

FIG. 7. Values of δ_0 for s and p peaks for an *FTR* filter using a high index glass prism (1.72), cryolite (1.34) frustrating layer, and ZnS (2.38) spacer layer. N is the order number.

From the value of Δ, the required value for the thickness of the spacer layer, δ_0, is determined from the condition for maximum transmission in Eq. (23),

$$\delta_0+\Delta=n\pi,\quad n \text{ an integer.} \tag{33}$$

It should be noted that since t_1', t_2', and Δ are different for the s and p components, the band widths (determined by $|R|$) and the spectral location (determined by δ_0) will be different in the two cases. The values of δ_0 for a typical filter are shown in Fig. 7. As the advance in phase on a single passage through the spacer layer increases, the first band is an s-band, followed by a p band. Higher order bands are separated from these by an increase in δ_0 of an integral multiple of π.

One of the limitations of these filters is their high dispersion, i.e., their rapid shift of pass band with changing angle of incidence. This limits the field they can cover without excessively increasing the band width. The dispersion can be calculated from the condition (33). Differentiating, we get,

$$d\delta_0+d\Delta=0. \tag{34}$$

Neglecting the dispersion in the dielectric layers,

$$d\delta_0/\delta_0=-(d\lambda/\lambda)-\tan\theta_0 d\theta_0+dd_0/d_0 \tag{35}$$

$$d\Delta=-\operatorname{sech}\beta d\beta=\operatorname{sech}\beta(-\tan\theta_1 d\theta_1+\tan\theta_0 d\theta_0) \tag{36}$$

These relations can be expressed in terms of $d\theta_2$, the change in angle of incidence in the prism. From (9) we get,

$$\tan\theta_s d\theta_s=\tan^2\theta_s \cot\theta_2 d\theta_2 \quad s=0,1 \tag{37}$$

where

$$\tan^2\theta_1=-\sin^2\theta_1/(\sin^2\theta_1-1). \tag{38}$$

Hence,

$$\begin{aligned} d\delta_0+d\Delta&=0\\ &=-(d\lambda/\lambda)+(dd_0/d_0)-\left[\left(1+\frac{\operatorname{sech}\beta}{\delta_0}\right)\tan^2\theta_0\right.\\ &\qquad\left.-\tan^2\theta_1(\operatorname{sech}\beta)/\delta_0\right]\cot\theta_2 d\theta_2. \end{aligned} \tag{39}$$

The dispersion of the filter is given by

$$\begin{aligned} d\lambda/d\theta_2=-\lambda&\left[\left(1+\frac{\operatorname{sech}\beta}{\delta_0}\right)\tan^2\theta_0\right.\\ &\left.-\tan^2\theta_1(\operatorname{sech}\beta)/\delta_0\right]\cot\theta_2. \end{aligned} \tag{40}$$

Using this formula, values for the dispersion were computed for second-order s and p peaks at λ6500, and for a second-order p peak at λ5500. These are compared with observed values in Table I. The filters were made using cryolite for the frustrating layers and ZnS for the spacer layer. Also included are the values obtained when the dispersion of the dielectric layers is not neglected.

TABLE I. Dispersion of *FTR* filter (normal incidence in air, 60° incidence on *FTR* surface).

Wave-length (A)	Band	Computed dispersion (A/deg.) Neglecting dispersion of dielectric	Including dispersion of dielectric	Observed dispersion (A/deg.)
5500 ($\mu_0=2.38$)	$2p$	59.0	50.5	45.4
6500 ($\mu_0=2.30$)	$2p$	74.0	60.7	70.1
	$2s$	65.5	52.0	58.8

Another useful relationship obtained from (39) is the shift in the transmission band with changing thickness of the spacer layer. We find,

$$d\lambda/dd_0=\lambda/d_0. \tag{41}$$

This indicates that for low order filters, those for which $d_0<\lambda$, very small changes in d_0 will shift the pass band appreciably. Because of this, slight non-uniformities in the thickness of the spacer layer will result in an appreciable broadening of the transmission band. Thus, if the frustrating layers are deposited to give a 10A pass band, while the non-uniformity in the thickness of the spacer layer is as great as, say, 5A over the area of the filter, the total band width may be increased to the order of 30A.

This is one of the problems associated with the production of any low order narrow pass band filter of the interferometer type. The non-uniformity in the thickness of the spacer layer and not the reflecting power of the plates may limit the narrowness of the transmission band.

JOURNAL OF THE OPTICAL SOCIETY OF AMERICA VOLUME 39, NUMBER 12 DECEMBER, 1949

A Method for Measuring Extremely Small Non-Uniformities in the Optical Thickness of Evaporated Films

ALAN E. GEE* AND HARRY D. POLSTER
University of Rochester, Rochester, New York

(Received August 8, 1949)

Methods are described for measuring accurately the half-widths of frustrated total reflection filters (see reference 1) of very narrow pass bands, and for detecting extremely small non-uniformities in the spacer layers of these filters. The latter method, permitting observation and measurement of thin film non-uniformities appreciably less than one unit cell provides a very sensitive means of studying thin film structures and the mechanism of formation.

IN the course of an investigation to determine the characteristics of frustrated total reflection (FTR) filters,[1] a simple method for measuring the half-widths of the filters was developed. This led directly to an optical method for detecting and measuring non-uniformities of less than 1A in the thickness of a thin film. This small value, less than 1/5000 of the wave-length of the measuring light, is possible because of the great number of multiple reflections of the light in the spacer layer of the filter.

The FTR filter can be made with transmission band half-widths as narrow as 5A. It is difficult to measure accurately pass bands this narrow unless a spectrometer of very high dispersion is available. In the absence of such an instrument, a simple scheme was devised to measure accurately the half-width, using the dispersion of the filter itself with varying angle of incidence.

The pass band of the FTR filter shifts rapidly in wave-length with varying angle of incidence. Thus, if the filter is placed in a beam of collimated monochromatic light and provision made for the controlled rotation of the filter, the energy passed by the filter with varying angle of incidence will depend upon the width of the pass band. This procedure amounts to sweeping the pass band across a monochromatic source rather than the more conventional method of sweeping a source of varying wave-length across the fixed pass band. The band width of the filter varies with changing angle of incidence, so that the method is accurate only for filters of narrow pass band. However, these are the only filters requiring a special method of measurement.

In practice, the filters were all constructed so that they had a pass band centered at the H_α spectrum line, 6563A. A hydrogen Geisler tube was used as the source, and a standard laboratory spectroscope provided collimator, rotating table, and viewing telescope. A photo-multiplier tube and amplifier were used as the receiver. Half-widths of the filters were measured by noting the angular positions of the table for half-peak transmission on each side of the position for peak transmission. The angular values were converted to half-width by measuring, with a spectrometer, the shift in wave-length of the pass band for small changes in the angle of incidence. A wave-length interval centered about the peak wave-length was used for this measurement to render insignificant the variation of this angular value with wave-length.

An alternate method for roughly approximating the half-width of the FTR filter is to place it in front of the entrance slit of a spectrometer, illuminated by a pinhole white light source at a distance of about eight inches. Thus the filter is illuminated with approximately collimated white light, and the pass band is viewed visually through the spectrometer telescope.

It was immediately noted that filters whose pass bands appeared less than 5A wide when viewed visually with a spectrometer, actually had pass bands very much wider than this when measured with the hydrogen source. Further, it was noted that the measured peak transmissions of such filters were much lower than would be expected either from theoretical considerations or the appearance of the pass band in the spectrometer.

The only basic difference in employment of the filters for the two tests was in the aperture of the filter being utilized. For visual testing with the spectrometer, an area equal to the area of the entrance slit was utilized; for testing with the H_α source, the full filter aperture was effective. To investigate the cause of the widely different results, the photo-multiplier was removed from the telescope of the spectroscope, and the eye placed at the slit image. This resulted in a Maxwellian view of the filter aperture. The reason for the different half-width values with the two methods was immediately apparent. Rather than uniformly brightening and darkening, with rotation of the filters, the illumination of the aperture was seen to be very irregular. In most instances an irregularly curved illuminated line was seen to cross the filter aperture as the angle of incidence was varied. The wave-length of peak transmission of the filters obviously varied with different areas of the filter, so the measured pass band at full aperture actually consisted of a whole series of overlapping narrower pass bands. This accounted for both the increased width of the pass band and the decreased peak transmission as measured with the H_α source.

The peak transmission of the filter from simple interferometer theory, occurs when

---

* Now at Frankford Arsenal, Philadelphia, Pennsylvania.

[1] P. Leurgans, and A. F. Turner, "Frustrated total reflection interference filters," J. Opt. Soc. Am. 37, 983A (1947).

$$\delta_0+\Delta=N\pi;\quad N=0,1,2,\cdots,\tag{1}$$

where $\delta_0=(2\pi/\lambda)\mu_0d_0\cos\theta_0$, μ_0d_0 = optical thickness of the spacer layer, θ_0 = angle of incidence in the spacer layer, Δ = phase retardation on reflection in the spacer layer, and λ = wave-length of peak transmission in air.

From this it was apparent that the variation in pass band location observed must have been due to a variation in μ_0d_0. Further consideration indicated that an extremely small variation in μ_0d_0 would produce a shift in the pass band that could be observed and measured as a displacement of the illuminated area of the filter as observed in the Maxwellian view.

Two methods are available for determining quantitatively this change in μ_0d_0. These consist of measuring directly the shift of the pass band of the filter with change in angle of incidence, and correlating this $d\lambda/d\theta_a$ with the desired $(d\mu_0d_0)/(d\theta_a)$; or, of computing directly the $(d\mu_0d_0)/(d\theta_a)$ for the particular filter being measured. θ_a refers to the angle of incidence in air.

To determine the various relationships involved, Eq. (1) is differentiated.

$$d\delta_0+d\Delta=0.\tag{2}$$

Now Δ, the phase shift of light in the spacer layer on reflection from a frustrating layer, has different values for the two polarized components of the radiation.

It is given by[2]

$$\tan(\Delta/2)=-t_1',\tag{3}$$

where, for the s component,

$$t_1'=\frac{\mu_1\cos\theta_1}{i\mu_0\cos\theta_0},\tag{4}$$

and for the p component

$$t_1'=\frac{\mu_0\cos\theta_1}{i\mu_1\cos\theta_0};\tag{5}$$

also

$$\mu_2\sin\theta_2=\mu_1\sin\theta_1=\mu_0\sin\theta_0,\tag{6}$$

where μ_0 = index of spacer layer, μ_1 = index of frustrating layer, μ_2 = index of glass prism, θ_0 = angle of incidence in the spacer layer, θ_1 = angle of incidence in the frustrating layer, θ_2 = angle of incidence in the glass prism, and

$$\cos\theta_1=i(\sin^2\theta_1-1)^{\frac{1}{2}}.\tag{7}$$

Since $\sin\theta_1>1$, $\cos\theta_1$ is a pure imaginary, and t_1' is real. (The expression for Δ is actually an approximation valid only for total internal reflection. However, for narrow pass band filters, the error introduced by this approximation is negligible.)

A more convenient relation for determining Δ is

$$\tan\Delta=\operatorname{csch}\beta,\tag{8}$$

where

$$\beta=\log t_1'=\pm\log(\mu_1/\mu_0)+\log(\cos\theta_1/i\cos\theta_0).\tag{9}$$

The upper sign refers to the s, the lower sign to the p component. Now from (1) we have

$$\frac{d\delta_0}{\delta_0}=\left(\frac{1}{\mu_0}\frac{d\mu_0}{d\lambda}-\frac{1}{\lambda}\right)d\lambda+\frac{d(d_0)}{d_0}-\tan\theta_0d\theta_0,\tag{10}$$

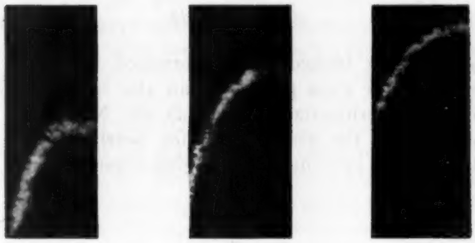

FIG. 1. Maxwellian field photograph of the transmission of collimated, monochromatic radiation through an FTR filter. Angle of incidence changed ten minutes between exposures, corresponding to a thickness change of approximately 5A.

while from (8) we obtain

$$\begin{aligned}d\Delta&=-\operatorname{sech}\beta d\beta\\&=-\operatorname{sech}\beta\left(\pm\frac{d\log(\mu_1/\mu_0)}{d\lambda}d\lambda-\tan\theta_1d\theta_1\right.\\&\qquad\left.+\tan\theta_0d\theta_0\right).\end{aligned}\tag{11}$$

We can express $d\theta_0$ and $d\theta_1$ in terms of $d\theta_2$ using the relations (6) and (7)

$$\begin{gathered}\cot\theta_rd\theta_r=\frac{d\log(\mu_2/\mu_r)}{d\lambda}d\lambda+\cot\theta_2d\theta_2,\quad r=0,1\\ \tan^2\theta_1=-\sin^2\theta_1/(\sin^2\theta_1-1).\end{gathered}\tag{12}$$

Hence Eq. (2) becomes

$$\begin{aligned}\left(A\frac{1}{\mu_0}\frac{d\mu_0}{d\lambda}-B\frac{1}{\mu_1}\frac{d\mu_1}{d\lambda}-C\frac{1}{\mu_2}\frac{d\mu_2}{d\lambda}-\frac{1}{\lambda}\right)d\lambda&\\ -C\cot\theta_2d\theta_2+d(d_0)/d_0=0,&\end{aligned}\tag{13}$$

where

$$\begin{aligned}A&=(1\pm(\operatorname{sech}\beta)/\delta_0)+(1+(\operatorname{sech}\beta)/\delta_0)\tan^2\theta_0,\\ B&=\tan^2\theta_1\,(\operatorname{sech}\beta)/\delta_0\pm(\operatorname{sech}\beta)/\delta_0,\\ C&=(1+(\operatorname{sech}\beta)/\delta_0)\tan^2\theta_0-\tan^2\theta_1\,(\operatorname{sech}\beta)/\delta_0.\end{aligned}$$

Again the upper sign is for the s, the lower the p component.

In this expression β, Δ, and δ_0 are given by (9), (8), and (1), respectively, and have different values for the s and p components. From this we can determine either

$$(d\lambda/d\theta_2)_{d_0},\quad(dd_0/d\theta_2)_\lambda,\quad\text{or}\quad(dd_0/d\lambda)_{\theta_2}.$$

---

[2] Harry D. Polster, J. Opt. Soc. Am. 39, 1038 (1949).

Experimentally, we can determine the shift of a contour line as we change the angle of incidence in air, (θ_a), using monochromatic radiation. It is improbable that the gross non-uniformity observed is due to variation in μ_0 across the filter aperture. Thus, the change in thickness corresponding to the shift could be computed directly as

$$\frac{d(d_0)}{d\theta_a}=\frac{d(d_0)}{d\theta_2}\frac{d\theta_2}{d\theta_a},$$

$d\theta_2/d\theta_a$ being immediately determined from the geometry of the glass prism. It can also be determined from the experimental value for $d\lambda/d\theta_a$. Neglecting the dispersion in the glass, which for nearly normal incidence in air introduces a negligible error

$$\frac{d\lambda}{d\theta_a}=\frac{d\lambda}{d\theta_2}\frac{d\theta_2}{d\theta_a}.$$

Hence

$$\frac{d(d_0)}{d\theta_a}=\frac{[d(d_0)]/[d\theta_2]}{(d\lambda)/(d\theta_2)}\frac{d\lambda}{d\theta_a}$$

$$=\frac{d(d_0)}{d\lambda}\frac{d\lambda}{d\theta_a}. \qquad (14)$$

From Eq. (13)

$$\frac{d(d_0)}{d\lambda}=\frac{d_0}{\lambda}\left[1-\left(\frac{A\,d\mu_0}{\mu_0\,d\lambda}-\frac{B\,d\mu_1}{\mu_1\,d\lambda}-\frac{C\,d\mu_2}{\mu_2\,d\lambda}\right)\lambda\right]. \qquad (15)$$

A calculation based on ZnS for the spacer layer, cryolite for the frustrating layer, and Bausch and Lomb extra dense flint (EDF−3) for the glass gives

$$\left(\frac{A\,d\mu_0}{\mu_0\,d\lambda}-\frac{B\,d\mu_1}{\mu_1\,d\lambda}-\frac{C\,d\mu_2}{\mu_2\,d\lambda}\right)\lambda=-.26 \text{ at } 6500\text{A}.$$

Hence within an error of about 25 percent we can write

$$\frac{d(d_0)}{d\theta_a}=\frac{d_0}{\lambda}\frac{d\lambda}{d\theta_a}. \qquad (16)$$

Thus, experimental determination of $d\lambda/d\theta_a$ provides us with a simple means of determining $d(d_0)$ approximately, or we may compute a more exact value for the particular filter tested.

Figure 1 is a Maxwellian view photograph of an FTR filter for three angular positions differing by ten minutes of arc. Measurement of $d\lambda/d\theta_a$ for the filter gives a value of 60A per degree or 1A per minute of arc for the second-order s peak at 6563A. The thickness, d_0, of the spacer film was 2270A. Thus, using the approximate relationship (16)

$$d(d_0)=\frac{d_0}{\lambda}\left(\frac{d\lambda}{d\theta_a}\right)d\theta_a$$

$$=\frac{2270\times1\times10}{6563}$$

$$=3.46\text{A},$$

or correcting for the dispersion

$$d(d_0)=1.26\times3.46=4.35\text{A}.$$

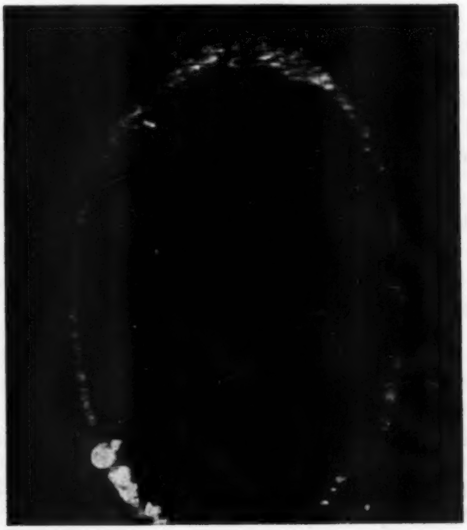

FIG. 2. Contour line for rapid evaporation of spacer layer (100A/sec.).

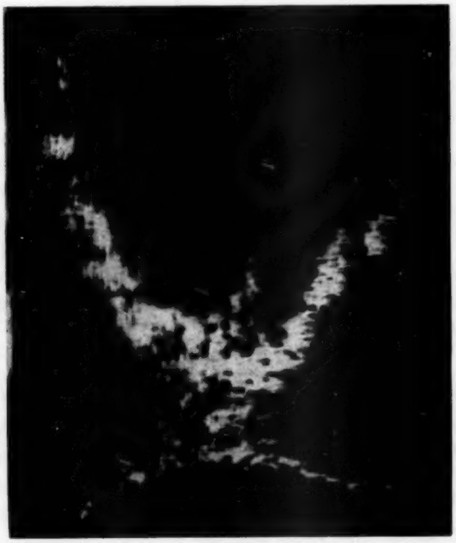

FIG. 3. Contour line for slow evaporation of spacer layer (10A/sec.).

This, then, is the contour interval between successive photographs in Fig. 1, and we are measuring thickness variations of the order of one unit cell of the material of the film.

Actually, displacement of the contours in Fig. 1 could be detected for angular movements as small as one minute. Such a movement corresponds to a thickness differential of less than ½A. The ability to detect such small displacements depends primarily upon the theoretical narrowness of the pass band of the filter. Increasing the thickness of the frustrating layers of the filter narrows the theoretical pass band and sharpens the contour line observed, thus increasing the ability to resolve small displacements.

In practice, it was found that filters utilizing 60° EDF−3 prisms and having cryolite frustrating and zinc sulfide spacer layers of 7/4 and 5/4 waves, respectively, at 4358A were ideal. Such a filter has for normal incidence a 2*s* peak very near 6563A and a 2*p* peak very near 5461A, both very convenient line source wavelengths. Also, the filter is convenient to make, having all film thicknesses even multiples of ¼ wave increments of the monitoring source, and has a very narrow theoretical pass band.

To date the extreme sensitivity of the FTR filter to uniformity in the spacer layer has defeated attempts to make the filters having very narrow pass bands and appreciable area. Two types of non-uniformity are involved: a general non-uniformity such as is evidenced in Fig. 1 and a localized non-uniformity or roughness in the spacer layer. An attempt was made to improve the former condition by rotating the prisms during deposition of the films. Preliminary results are presented here as an example of application of the test.

The prisms were rotated about an axis perpendicular to their center at a speed of approximately 120 r.p.m. during evaporation of the films. Figure 2 presents the Maxwellian view of a filter in which the evaporation was allowed to proceed at the rapid rate of approximately 100A of optical thickness per second. Note the axial symmetry of the contour. The foreshortening is due to the 60° viewing angle. Slight rotation of the filter indicated that the spacer film was generally concave in cross section, being thinnest at the center of rotation, and thickest at the edges. Intensity of the contour was very low, indicating low transmission. Figure 3 shows a filter in which the speed of evaporation was only 10A per second. Note that axial symmetry is lacking and approximate line symmetry substituted. The contours were very bright, indicating high transmission. It is interesting to note the great amount of fine structure evident in Fig. 3. This represents the second type of non-uniformity, or roughness in the film. It was pointed out that gross non-uniformities observed were probably not due to variations in the index of the spacer film. No such assurance is felt for the fine structure observed. The method detects non-uniformities in the *optical* thickness, and part or all of the fine structure observed could be caused by index variations in the spacer layer.

This method, permitting as it does observation of the film non-uniformities considerably less than one unit cell, presents a very sensitive method for studying thin film structures and the mechanics of their formation.

It is felt that profitable investigation into the characteristics of evaporated films under varying conditions of evaporation could be made using this method. Effects of plate temperature, evaporation speed, pressures, boat and filament design, and shadowing are a few problems that come immediately to mind. Different materials can be used subject to the limitation that a FTR-type filter can be made from them.

In conclusion, the authors wish to express their thanks to Drs. A. F. Turner and P. Leurgans of the Bausch and Lomb Optical Company who supplied special high index cement and made many helpful comments.

Letters to the Editor

Multi-Slit Double Monochromator Using No Moving Parts

W. A. Shurcliff
Research Laboratory, Polaroid Corporation, Cambridge, Massachusetts

September 15, 1949

GOLAY[1] has described a new and important means of obtaining a greatly increased radiant flux from a monochromator without increasing the effective band width. Special diaphragms are rotated in synchronism in front of the (considerably widened) entrance and exit slits; the emerging, impure radiation produces in a tuned detector an electrical response which is proportional to the power in the desired band, and which is independent of the undesired radiation passed by the wide slits. Unfortunately the method is inapplicable when rapidly fluctuating sources or slow-response detectors are involved; it cannot be used with photographic or visual detection, or in photo-chemical studies requiring monochromatic radiation.

Figure 1 illustrates an alternative, *deviation*-coding scheme which doubles the output and (a) provides essentially double-monochromator purity, (b) requires no moving parts, (c) is suited even to rapidly-varying sources, (d) can be used with fast- or slow-response detectors, and (e) can be used in photo-chemical studies requiring monochromatic radiation. The two prisms are oppositely oriented and are imaged on each other by lens L. There are three sets of slits: A_1, A_2 are curved entrance slits; B_1, B_2 are the respective, conjugate, straight intermediate slits; C_1, C_2 are the respective, conjugate, curved exit slits. Each slit and opaque separator strip is of the same width. Radiation of desired wave-length traverses the slit train A_1, B_1, C_1 and likewise the train A_2, B_2, C_2; decentered lenses could be used to bring the two emerging beams together, as at a specimen or detector of small area. Radiation of undesired wave-length is denied passage; for example, radiation of too long wave-length which passes through A_1 and then B_2 reaches neither C_1 nor C_2 and is thus eliminated.[2]

Instead of two slit trains, four might be used, quadrupling the output. Here, to avoid spectral contamination, the relative widths of the separator strips would have to be in suitable proportion[3] such as 1, 3, 1.

Using 16 trains, the gain would be sixteen-fold, and a suitable proportion might be 1, 3, 1, 9, 1, 3, 1, 27, 1, 3, 1, 9, 1, 3, 1. To reduce the entrance slit area wastage implied in this proportion ($65/81 \cong 80$ percent blocked off by separator strips), four prisms, successively oppositely-oriented, could be used instead of two, with conjugate sets of slits between successive prisms. Here the proportion 1, 1, 1, 3, 1, 1, 1, 3, 1, 1, 1, 3, 1, 1, 1 is suitable, and the aggregate area of the separator strips only slightly exceeds that of the slit openings.

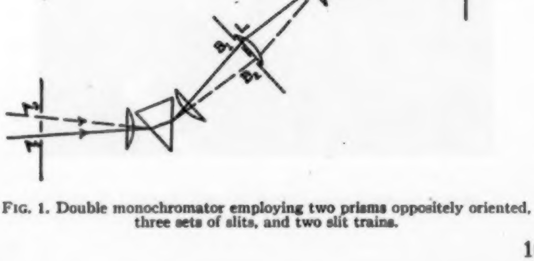

FIG. 1. Double monochromator employing two prisms oppositely oriented, three sets of slits, and two slit trains.

Although the deviation-coding approach avoids the (Golay system) drawbacks stated in the first paragraph, new problems are introduced, e.g., constructing the slit systems, or varying the wave-length and band width. (These variations might be unnecessary in certain applications.)

[1] M. J. E. Golay, J. Opt. Soc. Am. **39**, 437 (1949).

[2] An interesting situation arises if the two slits of width w are made contiguous, forming an aggregate slit of width $2w$. The effect of the two oppositely-oriented prisms can easily be shown to be such that, compared to a single monochromator using one of the identical prisms and having a slit width w, the bandwidth is the same and the quantity of radiation transmitted is doubled. This gain disappears if the prisms are given like orientation. In the General Electric Company commercial spectrophotometer, the two prisms are virtually oppositely oriented.

[3] I am indebted to Dr. R. Clark Jones for suggesting the proportions here proposed.

International Colloquium on Solid Thin Films*

P. Jacquinot
Laboratoire de l'Electro Aimant, Bellevue (S. et O.), France
AND
P. Rouard
Faculté des Sciences, Marseille, France

October 4, 1949

UNDER the auspices of the Centre National Français de la Recherche Scientifique and the Rockefeller Foundation, an international colloquium on the study of solid thin films was held in Marseille April 19–23, 1949. About 30 physicists took part: American, British, French, Dutch, Czech, Swiss, and Italian. Marseille was chosen for the meeting place because of the very prominent position the study of thin films has always held in the physics laboratory of its university which, at the beginning of this century, witnessed the remarkable contributions of Perot, Fabry, Buisson, and others. At the present time P. Rouard, M. Perrot, P. Cotton, D. Male, and others are working there on similar problems. About 40 papers were presented. They will be published soon in a special issue of the Journal de Physique. We shall give here a brief summary of the problems which were discussed.

The first papers dealt with the theory of single and multiple thin films. This problem can be approached in different ways, but at present it is always the electromagnetic theory of light (Drude, Goldschmidt, Rouard, etc.), which serves as the starting point. The calculations involved are long and laborious. To M. Perrot should go the credit for showing that the problem can be solved by an approximate graphical method which is sufficiently accurate in practice. P. Cotton and D. Male pointed out in their papers the advantages of this method which permits an over-all survey and an understanding of the phenomena that would not be obtained by the exclusive use of computing machines.

Other participants, such as F. Abelès of Paris, and F. Scandone and L. Ballerini of Florence used the methods of matrix calculus. The latter authors were able to prove the existence of a "resonance thickness," for any given angle of incidence, for which the fraction of light absorbed by a thin film goes through a maximum. For any given thickness, there is, similarly, a "resonance angle of incidence" at which the absorption is a maximum, a result which had been observed previously by P. Cotton in the special case of thin films of silicon.

Finally, B. Blaisse and B. H. Billings introduced in their papers the concept of optical impedance, which enabled them to study the optical properties of thin films utilizing methods which have long been known in the theory of electricity and profiting by established results in that field. For instance, they proved that a thin film can be treated like an optical quadrupole.

Matters of cleaning glass, of preparation of the films, and of accessory techniques were the subjects of thorough discussions. O. S. Heavens discussed in detail the mechanism of deposition of thin films by thermal evaporation and pointed out the relative influence of different factors which enter in this operation. Different set-ups used for carrying out the deposition of thin films were described by A. Adant, J. Roig, C. Dufour, and P. Jacquinot. The apparatus of the latter authors enables one to measure the optical properties of the films during evaporation and in a single evacuation to deposit several different films independently controlled. Another set-up, described by P. Jacquinot, produces films of variable thickness in one direction. according to any given law. One can make different kinds of photometric wedges as well as filters for the control of diffraction in spectrographs (apodizers).

Measurements of the thickness of films may be made in different ways. According to F. Abelès, one may combine photometric and polarimetric methods to obtain both the index and the thickness. Or again, if the thickness is greater than 50A, one may use a method due to Tolansky, following the method of Wiener which makes use of interference phenomena. F. Suhner has determined the thickness and indices of thin films by immersing them in liquids of different indices and studying the ellipticity produced when a beam of monochromatic light is reflected from them. Vasicek used a polarimetric method to study inhomogeneous thin films deposited on glass.

Once a film has been deposited it undergoes gradual changes and M. Perrot reported on his systematic investigations of them. He was able to detect a spontaneous aging even in the vacuum in which the film was produced. When this process of aging comes to an end, reversible changes are observed in the optical properties if the film is placed alternately in vacuum and in air.

The protection of thin films against external influences formed the subject of very interesting papers by Miss F. Flamant and N. W. Scott. For this purpose the latter used a film of an oxide of silicon with thickness about 1500A. Miss Flamant studied primarily the resistance of the films to the action of ocean air. Her results agree with those of N. W. Scott insofar as the beneficial protective effect of silicon monoxide is concerned.

The study of the optical properties of single thin films formed the subject of papers by P. Cotton on silicon, by H. Kuhn on silver, and by P. Rouard on platinum. In the study of silicon P. Cotton developed an ingenious method of stepped deposits for determining the complex refractive index and film thickness as a function of the values of the reflection factors R and R' and of the transmission factor T. He found in these films of silicon that the transmission factor undergoes oscillations as the thickness increases, thus definitely proving the existence of "resonance thicknesses." H. Kuhn was interested in thin films of silver, particularly in their application to the Fabry-Perot interferometer. For silver films of different thicknesses, produced by thermal evaporation, he determined the factors of reflection R and of transmission T. It is thus possible to choose the thickness of silver which, for a given wave-length, will give a satisfactory interference etalon despite the contradictory requirements for high resolving power and for sufficiently bright fringes. The platinum films studied by P. Rouard are less than 20 millimicrons thick. The curve of the second surface reflection factor R' goes through a very low minimum for film thicknesses in the neighborhood of 25A. The position of this minimum does not change with wave-length, unlike films of gold and silver deposited by cathode sputtering. Also for aluminum, beryllium, zinc, and magnesium the position of this minimum does not vary. Internal reflections in a plate of glass can therefore be eliminated with the aid of one of the non-selective metals. Films of suitable thickness for this purpose have excellent adherence, especially aluminum.

Another series of papers was devoted to the numerous applications of thin films in optics. J. Strong, illustrating his paper with numerous lantern slides, reviewed the history of aluminizing large telescope mirrors. This culminated in the making of the 200-in. mirror for Mount Palomar. F. Dourneau gave a paper on the preparation of iron oxide (evaporation of iron, which is subsequently oxidized) which can be used for making a beam divider (reflection 45 percent, transmission 45 percent) with small light losses. It is slightly colored, but extremely durable.

The very important problem of anti-reflection coatings was, of course, brought up. Two papers were presented supplementing conventional procedures and the very thin metallic anti-reflection coatings mentioned above. J. Strong described a system using a film with index increasing normally to the surface, starting with a value n near that of the glass and grading up to a value of n^2. This was coated with a quarter-wave film of index n. The result is the same as if a glass of index n^2 had been treated with a film of index n, which can be realized with a very hard and well adhering material. A. F. Turner described "achromatic" anti-reflection coatings, i.e., films whose reflection vanishes for more than one wave-length. Use is made of several films, each thicker than the one below, and of suitably chosen indices.

Applications of films to interferometry were studied in detail by Kuhn (silver, see above) and furthermore by P. Jacquinot, who reported on the work done at Bellevue, largely by C. Dufour. The brightness of the Fabry-Perot interferometer can be doubled if, instead of the silver films, one uses multiple films made of alternating layers of high index and low index dielectrics. In this manner one can obtain a reflection factor as high as 0.90 with very little absorption. This reflection factor is still too low if very narrow fringes are desired, but if a film of silver is covered in succession with a low index film and a high index film, a reflection factor of as much as 94 percent can be reached, while retaining a transmission factor as high as 4 percent. Dufour has shown that an interferometer treated in this manner gives fringes of the same brightness (which depends solely on $T/(1-R)$) as the film of silver alone would have given, although the fringes are much finer. This procedure enables one to obtain particularly fine localized fringes (Fizeau-Tolansky fringes for the study of surfaces).

S. Tolansky gave a paper on measurements of phase change at metallic reflection for large angles of incidence, using fringes of equal chromatic order in white light. In another paper Tolansky discussed the errors introduced in the measurement of thicknesses of thin films by Wiener's method. These arise from the fact that a film deposited on another film, whose thickness increases by regular steps, does not follow the form of the steps exactly. He discussed further a new set-up for localized fringes using multiple beams formed in a thin plate (for instance of mica) rendered partly reflecting on both surfaces and strongly curved, and also a method for examining surfaces using superposition fringes in white light, produced with the aid of pieces of mica silvered on both sides and obtained from a single sheet cut in two.

By using two Fabry-Perot etalons in series H. Kuhn was able to increase the contrast between the fringes and the background, as is necessary for detecting faint spectral lines. Taking suitable precautions to reduce the effect of reflections between the two etalons, he was able to obtain a contrast of 3000 for the green cadmium line and to detect very clearly the lines of He 3 in a sample of helium which contained this isotope in the proportion of 1:700.

Interference filters, which are nothing but interferometers having a very small difference in optical path, formed the subject of many papers. Simple filters of the classical Fabry-Perot type were handled by several participants, and many novelties were presented. The method of K. M. Greenland enables one to produce filters whose transmission band is located at a prescribed wave-length to the nearest 10A. It is based on second-surface observations of the films in reflected light during evaporation. A minimum of reflection is obtained as a narrow band whose spectral position can easily be located. The transmission band of the classical Fabry-Perot filter can be made narrower with the aid of metallic films enhanced with quarter-wave films of transparent materials of high and low index. Such filters have been made by A. F. Turner and C. Dufour. Their band width can be reduced to as little as 20A (Turner) with the aid of several pairs of alternately high and low index films. At the same time the transmission remains the same, as pointed out by Dufour. C. Dufour presented a theoretical study of the "double" Fabry-Perot filter which results from the combination of two filters into one by bringing them together with a common silver film between. Such filters give high contrast between the transmitted peaks and the background. They have interesting properties depending on the relationship between the reflection factors of the intermediate reflecting film and of the two outer films. Thus for some conditions the transmission bands are less bright, or they may be double, as has been observed by A. F. Turner. P. Jacquinot has shown that this doubling of the bands is a very simple consequence of the continuity between the double etalon and the simple etalon of double thickness.

A new kind of filter presented by A. F. Turner, and called by him a "frustrated total reflection filter," utilizes, in place of metallic reflection, the degenerate total reflection which takes place when the medium containing the evanescent wave of total reflection is extremely thin. By varying the thickness of this medium one can completely control the reflection factor and the transmission factor, whose sum is always equal to unity. The reflection factor can be increased in this manner without the introduction of absorption, which enables one to make filters passing a very narrow band (as little as 10A), and whose transmission at the maximum is equal to 1 for polarized light. After the description of these filters by A. F. Turner, C. Dufour pointed out that, although the transmission at the maximum is much greater than for the Fabry-Perot filter at normal incidence, they must transmit less energy since their angular aperture is smaller as a result of the inclination of the films. However, their superiority remains considerable for those regions of the spectrum where no highly reflecting metallic films of low absorption are known.

Turner's filter was used in the infra-red and with ultra-short waves of one centimeter wave-length by B. H. Billings, who showed a filter which passes a band 1/10 of a micron wide in the vicinity of 5 microns.

Reflection filters were studied in papers by B. H. Billings and A. F. Turner. Billings concerned himself with Dennison-Hadley filters. These make use of the fact that a thin metallic film whose electrical resistance is equal to the intrinsic impedance of free space (377 ohms) absorbs completely all of the energy of a given wave-length falling on it if it is mounted a quarter-wave in front of a perfect mirror. Turner used several semitransparent aluminum films spaced a half-wave from each other in front of an opaque aluminum mirror to obtain narrower reflection peaks.

The "cold light reflectors" of A. F. Turner enable one to reflect a high percentage of visible light and at the same time transmit large amounts of infra-red. This result is obtained with the aid of a film of germanium or similar substance having a high transmission in the infra-red, and covering it with pairs of transparent quarter-wave films of alternately low and high index in such a manner that its reflection factor in the visible is raised as high as 90 percent.

* Translation by J. Camus, University of Arkansas and I. Epstein and A. F. Turner, Bausch and Lomb Optical Company.

Nomograph of Hg 5461 Structure as a Function of Etalon Separation*

J. Rand McNally, Jr.
Carbide and Carbon Chemicals Corporation, Oak Ridge, Tennessee
October 9, 1949

THE structure of the 5461A line of natural mercury has been studied by numerous investigators.[1] Correlation of their published data with observed line structure in Fabry-Perot patterns, a useful criterion of etalon adjustment, is a tedious task unless a simplified nomograph of the structure and the expected relative intensities is available. The author is not aware of any such nomograph in the literature and believes that the nomograph suggested in this letter may prove as useful to others as to himself.

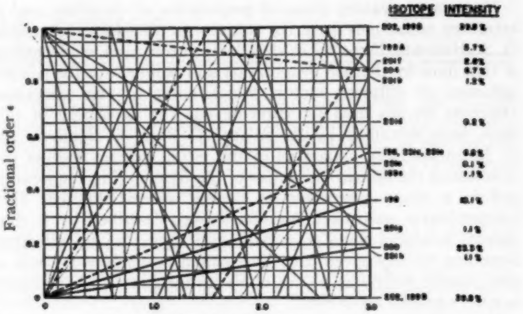

FIG. 1. Structure of mercury 5461 interference fringe system as a function of the separation of the plates of a Fabry-Perot interferometer.

The fractional order of interference of a satellite from a main line may be expressed as $\epsilon = 2t\Delta\sigma$, where t is the etalon separation, $\Delta\sigma$ is the wave-number separation between satellite and main fringe, and ϵ is the fractional order as measured positively from the reference fringe *toward the center* of the fringe system. If ϵ is plotted for all satellites as a function of t, straight lines of slope $2\Delta\sigma$ result. The total number of satellites between two successive main fringes will be identical with the number of satellites, of which some correspond to ϵ greater than unity, some to ϵ less than zero.

The components of the 5461A line of natural mercury are so plotted in Fig. 1, the unresolved 202 and 199 B components being chosen as the reference fringe system. Here, the notation of components is according to Schuler and Keyston; the intensities are based on the natural abundances of the isotopes and the intensity tables of White and Eliason,[2] and the wave-number separation data are taken from Burger and van Cittert. Intensity anomalies caused by unusual source conditions have been reported[1] and hence caution should be exercised in the use of these expected intensity values.

The structure of a given Fabry-Perot pattern of the 5461A line may be predicted immediately by sighting along a straight line perpendicular to the base at the appropriate value of the etalon thickness.

Acknowledgment is made to P. M. Griffin for discussions leading up to the construction of this nomograph, and to Miss L. M. Howard for the finished graph.

* This document is based on work performed for the AEC by Carbide and Carbon Chemicals Corporation at Oak Ridge, Tennessee.

[1] E. H. Collins, Phys. Rev. **43**, 753 (1928); H. Schuler and J. E. Keyston, Zeits. f. Physik. **72**, 430 (1931); S. Mrozowski, Zeits. f. Physik. **78**, 826 (1932); M. L. Pool and S. J. Simmons, Phys. Rev. **44**, 744 (1933); H. C. Burger and P. H. van Cittert, Physica **5**, 177 (1938).

[2] H. E. White and A. Y. Eliason, Phys. Rev. **44**, 753 (1933).

A Mount for a Perot-Fabry Interferometer without Etalon Ring

Heinz Haber
U.S.A.F. School of Aviation Medicine, Randolph Air Force Base, Texas
October 20, 1949

THE necessity to develop a mount including a fine adjustment device for a Perot-Fabry interferometer without etalon ring arose in conjunction with the design of an interferometrically controlled ruling engine for diffraction gratings. This engine was partially constructed in the Kaiser Wilhelm Institut für physikalische Chemie at Berlin-Dahlem in collaboration with Dr. Hans

Kienle, Astrophysikalisches Observatorium, Potsdam, during the years 1942–1945. This interferometer mount and its adjustment principle worked satisfactorily; it will be reported briefly, since its principle may be useful in connection with other optical designs.

According to Fig. 1, the interferometer consists of two independent units I and II, each bearing one Perot-Fabry interferometer plate P_1 and P_2. The first unit permits coarse adjustment of the interferometer, whereas the second unit serves to accomplish the fine adjustment. The plates, in order to achieve smallest thicknesses of the air disk of the interferometer, are shaped so as to offset the actual interferometrical surfaces from the main bodies of the plates. The plates are mounted within cylindrical troughs T_1 and T_2, and rest against three ball-bearing balls arranged at the corners of an isosceles triangle. The plates are held in position by three equally arranged levers, L, bearing steel balls which rest against the ground-off surfaces of the plates. The levers L, which are operated by the screws X, hold the plates firmly in position without exerting any stresses upon the actual interferometrical surfaces. The troughs, T, are suspended to L-shaped, reenforced frames F_1 and F_2 by means of three strong flat springs A and B consisting of hardened steel. These springs are also arranged in an isosceles triangle.

The coarse adjustment unit I works as follows: Opposite the lower ends of the springs A, three screws Y mounted into the frame F_1, rest with their steel ball ends against three cylinders of hardened steel which are sunk into the back face of the trough T_1. By manipulating alternately the screws Y, the plate P_1 can be swung to achieve a parallelism accurate to about one wave-length over any diameter of the plates. An optimum compromise between maneuverability and stability of the plate P_1 could be reached by springs A about 1-mm thick.

The second trough T_2 is suspended to its frame in the same manner as the first one, yet by means of much stronger springs B which are about 2-mm thick. At the lower ends of these springs round bolts K consisting of hardened steel, are mounted so as to stick freely through holes drilled through the body of the frame F_2. With their rounded rear ends these bolts lean against thin steel springs C about 0.2-mm thick. The springs C are mounted in such a manner that, by means of the micrometer screws Z, minute changes in the pressure of the springs C against the bolts can be applied. The screws Z have a pitch of 0.35 mm. The adjustable pressure against the bolts results in slightest deformations of the springs B, thus altering the position of the plate P_2. By operating alternately the screws Z, the plate P_2 can be swung around until an accurate adjustment of the interferometer is accomplished. The advance ratio between the screws Z and the corresponding outermost point of the interferometrical surface is determined by the lever ratio of the springs C and the thicknesses of the springs B and C. In the present design this advance ratio is equal to 30,000:1. This ratio secures a good compromise between maneuverability and stability of the fine adjustment unit.

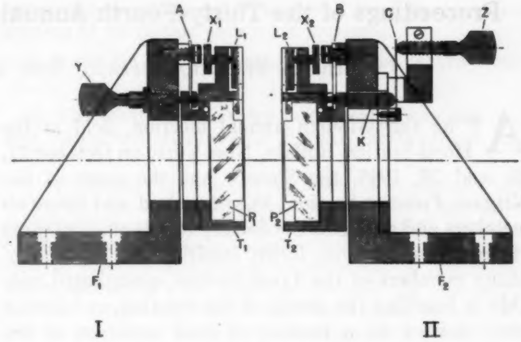

FIG. 1.

The total procedure of adjusting the instrument lasts about three to five minutes. If kept at a constant temperature [$\Delta T \sim \pm 0.025°C$], the instrument maintains its adjustment for several hours. Occasionally a readjustment is necessary after about thirty minutes. After this period of time the various components of stresses have achieved an equilibrium and the major creeping effects have ceased.

JOURNAL OF THE OPTICAL SOCIETY OF AMERICA VOLUME 39, NUMBER 12 DECEMBER, 1949

Proceedings of the Thirty-Fourth Annual Meeting of the Optical Society of America

HOTEL STATLER, BUFFALO, NEW YORK, OCTOBER 27, 28, AND 29, 1949

AT its thirty-fourth annual meeting, held in the Hotel Statler, Buffalo, New York, on October 27, 28, and 29, 1949, the Society was the guest of the Niagara Frontier Section. Four hundred and fifty-two members and guests of the Society registered, including visitors from London, Delft, Madrid, and Stockholm. Many members of the Local Section contributed notably in handling the details of the meeting, and in this were assisted by a number of staff members of the University of Buffalo. These activities were correlated by Mr. Glenn Smith, Chairman of the Niagara Frontier Section. The appreciation of the Society is due these people for arranging a smooth-running meeting.

One interesting feature of the convention was a trip through the manufacturing plant of the American Optical Company, which was taken by one hundred and seventy members and guests of the Society. In addition to the tour of the plant, exhibitions of specialized equipment had been arranged through the efforts of members of the American Optical staff.

The technical sessions of the meeting began with an invited Symposium on Microscopy which was particularly notable for the variety of topics and the widely diversified approaches of the speakers. Other invited papers during the three-day sessions covered a wide scope of interests including remarkably accurate measurements made with simple equipment, a comparison of the mechanisms of the eye and the camera, the extension of infra-red and Raman methods, and discussions of excitation and sampling problems of special interest to analytical spectroscopists.

It is worthy of note that the contributed papers whose abstracts appear in this issue covered so many branches of optics that it was impossible to classify the sessions at which they were presented under any general descriptive heading. Consequently, these designations, which had traditionally been included in the program, were omitted on this occasion.

The feature of the annual dinner, attended by two hundred and seventy-five members and guests, was the presentation of the Frederic Ives Medal to Dean George Russell Harrison for distinguished work in optics, followed by an address by Dean Harrison entitled "Retrogression in Spectroscopy."

A meeting of representatives of the Society's Local Sections was held on Thursday evening.

ANNUAL BUSINESS MEETING

A business session was called on Friday morning, President Kingslake presiding. The reports of the Secretary, Treasurer, and Editor of Publications for the fiscal year 1948 were presented and accepted. Announcement was made of future meetings to be held in New York City on March 9, 10, and 11, 1950, and in Cleveland, Ohio, on October 26, 27, and 28, 1950. The meeting recessed to reconvene at the annual dinner, at the close of which the newly elected officers assumed their duties.

MEETING OF THE BOARD OF DIRECTORS

A meeting of the Board of Directors was held on Wednesday, October 26. The minutes of this meeting appear on page 1063 of this issue.

BRIAN O'BRIEN, *Chairman*
R. H. GILLETTE, *Vice Chairman*
Program Committee

Program of Sessions

Titles and Abstracts of Papers

1. Invited paper, entitled "Microscope Optics," BY L. V. FOSTER, *Bausch & Lomb Optical Company.*

2. Invited paper, entitled "The Optical Microscope as Seen by a User," BY PETER GRAY, *University of Pittsburgh.*

3. Invited paper, entitled "Microscope Imagery and Interpretations," BY H. OSTERBERG, *American Optical Company.*

4. Invited paper, entitled "Microspectroscopy," BY JOHN LOOFBOUROW, *Massachusetts Institute of Technology.*

5. Invited paper, entitled "Electrons *Vs.* Protons—A Comparison of Microscopes," BY L. MARTON, *National Bureau of Standards.*

6. Infra-Red Microspectroscopy. ELKAN R. BLOUT, GEORGE R. BIRD, AND DAVID S. GREY, *Research Laboratory, Polaroid Corporation, Cambridge, Massachusetts.*

The determination of the infra-red spectra of much smaller amounts of materials than have been used hitherto has been made possible by the design and construction of microscope objectives achromatized over large portions of the spectrum.[1] We shall describe a simple infra-red microspectrometer now in use in our laboratory which makes use of spherical reflecting microscope objectives[2] and a Perkin-Elmer infra-red spectrometer. The objectives have a numerical aperture of 0.40 and, since they contain no refractive elements, they may be used to wave-lengths well beyond those possible of attainment with prism spectrometers. The magnification to the entrance slit of the spectrometer is approximately 22 times. With this instrument we have been able to determine the spectra of some fibers, certain crystals, and tissue areas. Data will be presented which will indicate the resolution obtainable, the minimum sample dimensions required, and other prerequisites for satisfactory results. Comparison data will be presented on materials of biological interest, such as thymine (a single crystal *vs.* an evaporated film), phenyl alanine (single crystal *vs.* mineral oil mull), nucleohistone (bundle of fibers *vs.* cast film), and tissue sections. We shall also show the spectra and some preliminary polarization measurements of some natural and synthetic fibrous materials, such as ramie, cellulose acetate, and polyvinyl alcohol.

---

[1] Barer, Cole, and Thompson, Nature **163**, 198 (1949).

[2] Land, Blout, Grey, Flower, Husek, Jones, Matz, and Merrill, Science **109**, 371 (1949).

7. Color Phase Contrast: Requirements and Applications.

CHARLES PROFFER SAYLOR, *National Bureau of Standards,* ARTHUR T. BRICE, *Phase Films, Ross, California,* AND F. ZERNIKE, *University of Groningen, Netherlands.*

In color phase contrast, which was first discussed by Zernike (National Academy of Sciences, Spring Meeting, 1948),[1] several difficult requirements must be met for the attainment of maximum brilliance and usefulness. The system itself is one in which a controlled chromatism of the phase plate is sought instead of the customary attempt at equality of phase difference at all wave-lengths. The thickness and dispersion of the phase ring in relation to the general aperture can be such that zero phase contrast will occur at one or more wave-lengths of transition in color sensation. If the phase contrast is made high but opposite in spectral zones of relatively pure color sensation, striking and beautiful microscopical images can be formed with objects of low inherent contrast. The greatest advantage of this system lies not in the beauty of the images but in the clear distinction which is afforded between effects caused by scattering or general absorption and those caused by small differences of refractive index or thickness.

---

[1] F. Zernike, Physica **9**, 686, 974 (1942).

8. An Extension of Toraldo's Theory of Phase Contrast.

L. IVAN EPSTEIN, *Bausch & Lomb Optical Company.*

G. Toraldo di Francia[1] has calculated the light intensity distribution in the phase contrast image of a transparent, uniformly phase-shifting semi-infinite plane on a transparent background. He supposes Köhler illumination parallel to the axis of the microscope, so that the illuminating light comes to a focus in a point at the center of the back focal plane of the objective. The phase pattern is a circular spot in the middle of the aperture. The author has extended this theory to the case of an annular phase pattern filled with light. The theory of this form of image formation is merely a special case of a more general theory due to Duffieux[2] and his students.

---

[1] G. Toraldo di Francia, Nuovo Cimento, Series 9, VI, **1**, 30 (1949).

[2] Duffieux, Tirouflet, Guenoche, and Lansraux, Ann. de Physique **19**, 355 (1944).

9. Motion Pictures of Some Optical and Electrical Effects in Barium Titanate Crystals.

NORMAN J. FIELD AND A. P. DEBRETTEVILLE, JR., *Signal Corps Engineering Laboratories, Fort Monmouth, New Jersey.*

In the course of studying the properties of single crystals of barium titanate,[1] certain interesting optical phenomena were observed. Some of these include variation of crystal domains with applied electric fields, and phase transitions resulting from absorption of infra-red radiation by the crystal. These effects have been recorded by cine photo-micrographic methods, using the optical microscope to observe a crystal approximately 1 mm. square. A brief discussion and showing of the motion picture are presented.

---

[1] N. J. Field and A. P. DeBretteville, Jr., Phys. Rev. **72**, 1119 (1947).

10. The Photo-conductivity in Crystal Phosphors.

RUDOLF FRERICHS, *Department of Physics, Northwestern University.*

By combining the theory of secondary photo-currents with the model of a crystal phosphor, a theory of the photo-conductivity in crystal phosphors—especially in CdS crystals—can be given. This theory agrees qualitatively with the results of previous and present experiments.[1] A quantitative energy scheme of CdS, which is the basis for this theory, has been determined from measurements of the emission and absorption spectra of CdS crystals. In accordance with the theory the final current reached after prolonged irradiation is proportional to the square root of irradiation. The initial slope of the decay curve is proportional to the intensity of irradiation. Under periodical irradiation with gamma-rays the amplitude of the current slowly increases to a final value. When a CdS crystal is heated and then cooled to liquid air temperature, irradiation produces a small primary current of less than 10^{-13} amp. at first. With continuous irradiation and after a slight delay this current suddenly increases until it reaches a constant value of 10^{-8} amp. It is shown that many crystals that are useful for crystal counters behave like crystal phosphors in the temperature range used. A list of "counting crystals" is given and discussed according to these ideas.

---

[1] R. Frerichs, Phys. Rev. **72**, 594 (1947). The complete literature on "crystal counters" is given by R. Hofstadter, Nucleonics **4**, 2, 29 (1949).

11. The Fluorophotometric Determination of Uranium.

GEORGE R. PRICE,* RENATO J. FERRETTI,† AND SAMUEL SCHWARTZ,‡ *Argonne National Laboratory.*

A fluorophotometric method for uranium determination has been developed that covers a range from 10^{-10} g to 10^{-4} g, with a standard error of about 2×10^{-11} g at the lower limit, and which is so remarkably free from interferences that purification of unknowns is almost never required even when impurity concentrations are thousands or tens of thousands of times greater than the uranium concentration. This method is a refinement of the well-known sodium fluoride bead test for uranium. The extreme sensitivity results principally from use of special photoelectric fluorophotometers to be described in the following paper. The ability to tolerate enormous excesses of impurities depends on the findings that no substance investigated gives interfering fluorescence in the procedure employed, and that percent quenching of uranium fluorescence is independent of uranium concentration (except at concentrations so high that uranium quenches itself), which means that quenching can be reduced by reducing sample size and can be measured and corrected for by adding known amounts of uranium to portions of the unknowns.

---

* Now at Bell Telephone Laboratories, Murray Hill, New Jersey.

† Now at Georgetown University, Washington, D. C.

‡ Now at Department of Medicine, University of Minnesota, Minneapolis, Minnesota.

12. Sensitive Fluorophotometers.

GEORGE R. PRICE,* RENATO J. FERRETTI,† AND SAMUEL SCHWARTZ,‡ *Argonne National Laboratory.*

A series of special fluorophotometers were developed for the uranium determination method described in the preceding paper. Most of these employed the H4 mercury arc and the 1P21 multiplier photo-tube plus a d.c. galvanometer. The best ones gave linear response within three percent over a hundred thousand-fold range of light intensity, and were sufficiently sensitive to detect fluorescence in every liquid and solid tested except powdered graphite.

* Now at Bell Telephone Laboratories, Murray Hill, New Jersey.
† Now at Georgetown University, Washington, D. C.
‡ Now at Department of Medicine, University of Minnesota, Minneapolis, Minnesota.

13. Fluorescence Studies of Plutonium and Neptunium.

GEORGE R. PRICE,* *Argonne National Laboratory.*

A number of compounds of plutonium and neptunium were tested for fluorescence under a variety of optical conditions at different temperatures and both in the pure state and in liquid and solid solution. Special search was made for resonance fluorescence of the plutonyl ion corresponding to a particularly sharp absorption band in the infra-red. No fluorescence was found that appeared to be characteristic of the metal ions themselves.

* Now at Bell Telephone Laboratories, Murray Hill, New Jersey.

14. Invited paper, entitled "High Precision Measurements with Simple Equipment,"

BY A. C. S. VAN HEEL, *Technical University, Delft, Holland.*

15. A Dielectric Interferometer Filter.*

HARRY D. POLSTER, *Institute of Optics, University of Rochester.*

Interferometer filters using semitransparent metal films as the reflecting surfaces[1] are effective in isolating a narrow spectral region. One of their limitations is the drop in peak transmission with decreasing band width, caused by the absorption in the metal films. It is known[2,3] that multilayer dielectric filters can provide a high reflectivity over an appreciable spectral range. Hence, it should be possible to form an interferometer filter using all dielectric materials, having little absorption and scattering, which will have much greater peak transmission for comparable band widths. A filter has been made on this principle by evaporating ZnS and cryolite alternately to form a 15-layer filter. Layers 1–7 and 9–15, all of quarter-wave optical thickness, provide the two reflecting surfaces. The eighth layer, deposited to a half-wave optical thickness, is the spacer element in the filfer for a first-order pass band. This filter has a peak transmission of 80 percent and a half-width of 60A. Its limitation lies in the side bands that are transmitted. For a filter isolating a region around 5200A the side bands rise to five percent transmission at 4400A and 6200A.

* This research was supported by the Engineer Research and Development Laboratories through Contract No. W-44-009 eng-470.

[1] L. N. Hadley and D. M. Dennison, J. Opt. Soc. Am. **37**, 451–65 (1947).

[2] M. Banning, J. Opt. Soc. Am. **37**, 792 (1947).

[3] G. N. Ramachandran, Proc. Ind. Acad. Sci. **A16**, 336–48 (1942).

16. Thickness Non-uniformities in Evaporated Films.

A. E. GEE* AND H. D. POLSTER, *Institute of Optics, University of Rochester.*

A method has been devised for observing non-uniformities of the order of 1A in the optical thickness of evaporated films. This is made possible through the use of the frustrated total reflection filter.[1] A Maxwellian view of such a filter illuminated by a monochromatic, collimated slit of light will depend on the angle of incidence of the light. If the spacer layer of the filter has constant optical thickness over the entire aperture, the field will brighten and darken uniformly as the angle of incidence is altered. If, however, the optical thickness is not constant, a contour line will be observed that will sweep across the field with changing angle of incidence. The half-width of this contour line depends directly on the theoretical half-width of the filter's transmission band. It is possible to compute from simple interferometer theory the shift in spacer layer thickness corresponding to a given change in the angle of incidence. Hence, a photograph of the Maxwellian view provides a contour line to a high order of accuracy. A complete contour map is provided by successive photographs.

* Now at Frankford Arsenal.

[1] P. Leurgans and A. F. Turner, J. Opt. Soc. Am. **37**, 983A (1947).

17. Molecular-Type Dichroic Film Polarizers for 0.75 to 2.8 μ-Radiations.

R. P. BLAKE,* A. S. MAKAS, AND C. D. WEST, *Polaroid Corporation.*

To meet military demands for near infra-red polarizers, our laboratory, starting from its experience with visual dichroic polarizers,[1] during the late war developed a practical film polarizer (Type H_D) for the narrow band 0.75 to 1.0 μ This product is related to the visual polarizer Type *H* but comprises a much higher volume and area concentration of linear polyiodine[2] on oriented polyvinyl alcohol (PVA) film. One of us (R.P.B.) soon thereafter found that suitable heat treatment of Type H_D film brings forth, without substantial change in iodine content or in x-ray diffraction, a new absorption region beyond the known absorptions of either the diatomic and polyatomic iodine molecules, or of PVA. Since the new absorption region can be rendered highly dichroic it allows the preparation of a practical polarizer (Type H_R) for the range 0.75 to 2.8 μ. The newer polarizers thus take over in the far red where the older Type *H* polarizer begins to fail; and the type H_R polarizer itself fails where the strong O-H and C-H absorption of PVA sets in unfavorably. We shall present spectrophotometric curves representative of both the newer infra-red and the older related visual polarizers along with some evidence bearing on their structure, and point out some possible applications—for example, the useful range of Type H_R polarizer approximately covers the useful response range of present commercial lead sulfide photo-cells, and more than covers the present range of image formation by infra-red photography, phosphors, or electron tubes.

* Now with Carter's Ink Company, Cambridge, Massachusetts.

[1] J. Alexander, *Colloid Chemistry* (Reinhold Publishing Corporation, New York, 1946). See Land and West, Volume 6, Chapter 6.

[2] C. D. West, J. Chem. Phys. **15**, 689 (1947); **17**, 219 (1949).

18. Ultrafrequency Excitation of Hg 198 Lamps for Interferometer Illumination.

EDWARD JACOBSEN AND GEORGE R. HARRISON, *Massachusetts Institute of Technology.*

Meggers[1] has developed an electrodeless Hg 198 lamp for interferometric purposes, and has reported preliminary wavelength determinations of high precision. He has reported[2] that the life and brightness of the lamps increases with frequency of excitation between 10 and 100 Mc, the lamps burning indefinitely with high intensity at the upper frequency. In the present experiments, characteristics of a lamp furnished by Meggers have been compared at 150- and 3000-megacycle-excitation (200- and 10-cm waves) and great improvements in intensity, efficiency, and convenience are found at the higher frequency. Intensity of the Hg 5461 line increased more than 16-fold at 3000 over 150 Mc, 40-watt excitation being used in each case. Continuous magnetron excitation was used at the higher frequency, with a 10-cm resonant cavity and a very thin layer of cooling water over the lamp. No decrease in light intensity was observed over extended operation, and Fabry-Perot patterns showed little increase in broadening of fringes at the high intensity over the low. Motion of one of a pair of Michelson interferometer back-mirrors over more than 150 mm without undue sacrifice of fringe contrast was possible using this source, whereas with an ordinary cold mercury arc about 15 mm was the maximum.

[1] W. F. Meggers, J. Opt. Soc. Am. **38**, 7 (1948).
[2] Verbal communication.

19. Ultraviolet Characteristics of the High Pressure Xenon Arc. William A. Baum and Lawrence Dunkelman, *Naval Research Laboratory, Washington, D. C.*

The ultraviolet characteristics of a 0.5-kw d.c. arc through xenon gas were investigated. The lamp used for this study has a quartz envelope and contains pure xenon under a pressure of roughly 20 atmos. when operating; its general characteristics have been described by Schulz.[1] The spectral radiance in milliwatts per 100A per steradian per square centimeter between 2000 and 5000A was measured photographically by comparison with the positive crater of a spectroscopically pure carbon arc. An ultraviolet radiance contour map of the arc stream was also obtained photographically. It was found that the lamp radiates a smooth ultraviolet continuum, which extends to the air cut-off and is interrupted by only a few weak lines. The radiance of the most intense part of the arc exceeds that of the carbon crater by a factor of 23 of 2500A, 12 at 3000A, and six at 3500A. Comparison with other ultraviolet-continuum sources shows the xenon arc to be unusually intense.

[1] P. Schulz, Zeits. f. Naturforschung **2a**, 583 (1947); Ann. d. Physik **6**, 95 (1947); Ann. d. Physik **6**, 107 (1947).

20. The Torus Grating. Heinz Haber, *USAF School of Aviation Medicine, Randolph Air Force Base, Texas.*

The torus grating is defined as a calotte of a circular torus bearing a grating ruling on its concave side. In contrast to the spherical grating, the torus grating is capable of eliminating astigmatism, in general, for two points in the spectrum. These two stigmatic points can be adjusted to any desired wave-length within a wide range of the spectrum by choosing suitable values for the angles of incidence and diffraction. In the rest of the spectrum astigmatism is considerably smaller than that prevailing in spectra of spherical gratings. Moreover, astigmatism is negligible in the proximity of the two stigmatic points, giving rise to "quasi-stigmatic" ranges in the torus grating spectrum. The extension of these quasi-stigmatic ranges depends on the size of tolerable astigmatism. If based upon an astigmatism equal to the diffraction width of the spectral images, a quasi-stigmatic range can be as wide as 1000A. With light sources of small size a considerable gain in spectral intensity results from the lack of astigmatism. The theory of the torus grating further demonstrates that coma, aberration, and curvature of spectral lines in the torus grating spectrum are generally smaller than the same image imperfections in spectra of spherical gratings.

21. The Permanence of Glass Standards Issued to Check the Photometric Scale of Spectrophotometers. Kasson S. Gibson and Marion A. Belknap, *National Bureau of Standards.*

Shortly after the introduction of commercially available photoelectric spectrophotometers, the National Bureau of Standards began issuing calibrated glass disks for assistance in checking the photometric scale of spectrophotometers.[1] Although no complete account of this work has been published, reference has been made to these standards in various publications.[2-4] Certain of these glasses—a carbon yellow, a cobalt blue, and a copper green—were carefully measured and values of spectral transmittance adopted in 1933. Since then they have been mostly kept in the dark in filing envelopes, with only occasional use. Remeasurement of these glasses after 16 years shows no certain change in their spectral transmittances. In addition, exposure tests have been made on similar glasses over the last three years by exposing them to south skylight (including sunlight) under a clear plate glass cover. Small but definite changes of spectral transmittance have been found for the carbon yellow and copper green glasses during this exposure, but the changes for the cobalt blue glass border on the uncertainties of measurement. These results indicate that, except with the most careless usage and exposure, the glass standards of spectral transmittance issued by the Bureau should remain unchanged for a long time.

[1] Gibson, Walker, and Brown, J. Opt. Soc. Am. **24**, 58 (1934).
[2] K. S. Gibson and M. M. Balcom, J. Opt. Soc. Am. **37**, 593 (1947); J. Research Nat. Bur. Stand. **38**, 601 (1947).
[3] Nat. Bur. Stand. Letter Circular LC 929 (1948).
[4] K. S. Gibson, Nat. Bur. Stand. Letter Circular C 484 (1949).

22. An Electrical Tristimulus Integrator. E. W. Peterson, H. H. Grossman, J. L. Saunderson, V. J. Caldecourt, *The Dow Chemical Company, Midland, Michigan.*

An automatic integrator has been attached to a General Electric recording spectrophotometer to give the tristimulus values X, Y, and Z of the spectrophotometric curve being recorded. The instrument uses the weighted ordinate method of integration, with the ordinates spaced every ten millimicrons from 400 to 700 mμ. At each ordinate, a condenser for each of the three tristimulus functions is given a charge which is proportional to the product of the transmission or reflection reading times the values of the quantities $(E_c\bar{x})$, $(E_c\bar{y})$, and $(E_c\bar{z})$ at that ordinate. After completion of the spectrophotometric curve, the 31 condensers of each function are paralleled and the sum of charges determined by measurement of the three voltages on the three gangs of condensers. The voltage measurements are made automatically during the time the spectrophotometer is returning from 700 mμ to 400 mμ, and the results are read from calibrated clocks. Preliminary tests indicate that an absolute accuracy of ± 0.1 percent in the tristimulus values X, Y, and Z has been achieved.

23. Calculation of Subtractive Color Mixtures. H. R. Davidson, *General Aniline and Film Corporation.*

A set of simple equations for the calculation of tristimulus values of subtractive color mixtures in solution has been developed for the specialized case in which the ratios of transmittances of the component colorants are constant over all wave-lengths in the visible spectrum. The values calculated are shown to represent the maximum values for mixtures of components with ratios of transmittance which differ from the specialized case, and it may also be demonstrated that no points of inflection may exist in the plots of tristimulus values *vs.* concentration of components. In practical mixtures, departures from these theoretically derived relationships are due to interaction of the components. In use, the equations prove to be sufficiently accurate for most mixtures in which the color gamut is small, and for larger color gamuts, a method of successive approximations can be used.

24. Munsell Renotations Used to Study Color Space of Hunter and of Adams. Dorothy Nickerson, *Cotton Branch, PMA, U. S. Department of Agriculture, Washington, D. C.*

The colorimetric scales of recent Hunter[1] and Adams[2] proposals have been studied in terms of the smoothed curves of the Munsell renotation space. Three conversion tables have been prepared, each to correspond with Table I, pp. 397–405 of reference 3.[3] One of the new tables provides the I.C.I. tristimulus data (X, Y, Z) needed to calculate tables for Adams' "chromatic value," and for Hunter's a and b. Each of the three series extends to the hue, value, and chroma limits of the original table, except that the Hunter data are given for 20 instead of 40 hues on values other than 5/. Results will be shown in the form of diagrams.

A knowledge of the visual color spacing of the coordinates used to express the results of any color measuring instrument makes it possible to understand the instrument results in terms of color experience, and to assess the accuracy and precision of the instrument in terms of standard colorimetric practice and known color tolerances. Use of the Munsell renotation data makes it possible to obtain this knowledge for any instrument or system that is in any way based upon or related to the I.C.I. system of colorimetry. A specific example will be given regarding a study of the new Hunter color difference meter and its applicability for use in the colorimetry of the limited color range of raw cottons.[4]

[1] R. S. Hunter, J. Opt. Soc. Am. **38**, 661A (1948).
[2] E. Q. Adams, J. Opt. Soc. Am. **36**, 717A (1946).
[3] Newhall, Nickerson, and Judd, "Final Report of the OSA Subcommittee on the Spacing of the Munsell Colors," J. Opt. Soc. Am. **33**, 385–418 (1943).
[4] Dorothy Nickerson, "Color measurements of standards for grades of cotton," Textile Research J. **16**, No. 9 (1946).

25. An Improved Gloss Recorder. RICHARD S. HUNTER, *Henry A. Gardner Laboratory, Inc.*

The design and improvement of a continuous gloss recorder is described. This type of recorder is used in paper mills to indicate the uniformity of surface polish imparted to coated paper. Paper of the type used in the *Journal of the Optical Society of America* until recently and many other magazines is coated on both sides with a clay-adhesive mixture and then polished to give surfaces on which halftone prints will be clearly rendered. Experience with existing gloss recorders in paper mills has shown that some of the paper dust which is always present tends to accumulate on optical elements of the exposure head and causes the glossmeter to change calibration with time, even though blasts of compressed air and other measures to prevent this dust accumulation are taken. In a new gloss exposure head, there are test and reference beams which pass together through the only optical elements exposed to paper dust. Any accumulation of dust on these glass windows therefore diminishes the two beams equally but does not alter the ratio of one to the other, which is measured as gloss. It is shown that use of the stable measuring method developed by Brice[1] and photo-cells paired for temperature response produces a gloss recorder that is stable in calibration over periods as long as a week.

[1] B. A. Brice, "A compensating circuit for blocking-layer photoelectric cells," Rev. Sci. Inst. **8**, 279 (1939).

26. Spectral Reflectance Measurements in the Ultraviolet. NISSON A. FINKELSTEIN, *Massachusetts Institute of Technology.*

The high speed automatic recording spectrophotometer described by Harrison[1, 2] has been modified by addition of an integrating sphere and a hydrogen discharge source yielding a continuous ultraviolet and visible spectrum of high intensity. This source, developed with the assistance of Wyckoff[*] from the design described by Allen,[3] has twice the intensity and emits radiation throughout 64 times as great a solid angle as do commercially available sources of this type. With this instrument, spectrophotometric reflectance curves are obtained from 2400A to 6000A in four minutes, using a slit-width corresponding to a wave-length interval of 20A. This equipment has been used to measure the spectral reflectance of living human skin.

[1] G. R. Harrison, J. Opt. Soc. Am. **28**, 49 (1938).
[2] G. R. Harrison and E. P. Bentley, J. Opt. Soc. Am. **30**, 290 (1940).
[*] M.I.T. Biology Department.
[3] A. J. Allen, J. Opt. Soc. Am. **31**, 268 (1941).

27. Spectrophotometric Studies of Living Human Skin in the Ultraviolet. SEIBERT Q. DUNTLEY, *Massachusetts Institute of Technology,* EDWARD A. EDWARDS, *Harvard Medical School and Tufts Medical School,* AND NISSON A. FINKELSTEIN, *Massachusetts Institute of Technology.*

The spectral reflectance of living human skin from 2400A to 6000A has been measured (see the preceding abstract), for nine individuals. The effects in the ultraviolet of five pigments (oxyhemoglobin, reduced hemoglobin, carotene, melanin, and melanoid) identified previously in the visible[1, 2] have been determined. Vitamin A has been observed to be a sixth pigment which influences the shape of the reflectance curve of skin in the ultraviolet. An extract of melanin has been treated to produce a substance having the spectrophotometric characteristics of melanoid. The absorption of melanin has been found to increase uniformly from 6000A to 2400A and to mask the absorption characteristics of the other pigments in skins having a high melanin content. The presence of carotene in human blood has been observed in the ultraviolet. Racial comparison curves show no pigments in the colored races additional to those found in the caucasian race.

[1] E. A. Edwards and S. Q. Duntley, "The pigments and color of living human skin," Am. J. Anat. **65**, 1 (1939).
[2] E. A. Edwards and S. Q. Duntley, J. Opt. Soc. Am. **38**, 660A (1948).

28. Chromaticity Confusions of Color Defectives. DEAN FARNSWORTH, *Medical Research Laboratory, U. S. Submarine Base, New London, Connecticut.*

Chromaticity confusions are given for 12 deutans, six protans, and one tritan, using a method by which data can be secured from partial as well as complete dichromats and which includes the effect of macular and ocular pigmentation. The differences between observers are real, and the attributive causes are discussed. Results provide additional material for theoretical studies and data which can be applied directly to the construction of all tests for color blindness. The terms protan, deutan, and tritan are proposed as names for the three types of color deficiency, in which each type includes all degrees of defect. Conclusions are that (1) there is a complete trichotomy of the three known types of color deficiency, (2) wide variations exist between defectives of the same type, but (3) this experimental method indicates a continuum between anomalous trichromacy and dichromacy within each type, and (4) discrimination by protanopes and deutanopes is not substantially less than by normals in the yellow-blue direction.

29. Tritanopia with Abnormally Heavy Ocular Pigmentation. DEANE B. JUDD, *National Bureau of Standards,* AND LORENZO PLAZA, *Institute of Optics, Madrid.*

The chromaticity confusions characteristic of tritanopia may be represented on the (x,y)-chromaticity diagram of the standard I.C.I. coördinate system by a family of straight lines intersecting at a copunctal point somewhere in the region between $x=0.18$, $y=0.00$ (König theory)[1] and $x=0.165$, $y=0.000$ (Müller theory).[2] A case of a typical congenital tritanopia reported by Farnsworth[3] departed from typical tritanopia,[4] first by having a luminosity function abnormally curtailed on the short-wave end (no vision up to about 460 mμ), second by having chromaticity confusions among object colors describable by straight lines on the (x,y)-plot intersecting in an area surrounding $x=0.15$, $y=0.05$, and third by confusing incandescent lamp light at a color temperature of 2900°K with the spectrum at 586 mμ instead of the typical tritanopic value of 578 mμ. It has been found that all three of these disagreements with typical tritanopia are to be expected from a tritanope possessing normal macular pigmentation[5] combined with a lens pigment[6] five times normal. We believe that the Farnsworth case of a typical tritanopia is actually a case of congenital tritanopia combined with abnormally heavy ocular pigmentation.

[1] D. B. Judd, "Standard response functions for protanopic and deuteranopic vision," J. Opt. Soc. Am. **35**, 199 (1945); J. Research Nat. Bur. Stand. **33**, 407 (1944); RP1618.

[2] D. B. Judd, "Response functions for types of vision according to the Müller theory," J. Research Nat. Bur. Stand. **42**, 1 (1949).

[3] D. Farnsworth, "Description of a subject congenitally deficient in violet-yellow vision," J. Opt. Soc. Am. **33**, 350 (1943).

[4] Letter of May 26, 1945, from Farnsworth to Judd.

[5] G. Wald, "Human vision and the spectrum," Science **101**, 653 (1945).

[6] E. Ludvigh and E. F. McCarthy, "Absorption of visible light by the refractive media of the human eye," Arch. Opth. **20**, 37 (1938).

30. Invited paper, entitled "The Eye and the Camera," by George Wald, *Harvard University.*

31. Photopic Thresholds for Red Light in an Unselected Sample of Color Deficient Individuals.* Alphonse Chapanis and R. M. Halsey, *The Johns Hopkins University.*

It is generally assumed that "darkening" of the red end of the spectrum can be used as a criterion of protanopia or protanomaly. If this is correct, absolute photopic thresholds for red light, in a random sample of color-deficient individuals, should form two distinct distributions. To test this hypothesis, we studied 47 color deficient men, selected solely on the basis of being "color blind." Sixteen normal persons were also examined. The subject viewed a flashing light of 640 mμ monocularly, using central fixation, and adjusted an optical wedge to locate his threshold. The results show that the average amount of energy required for threshold vision, as well as the variability of the measures, is less for normals than for the color deficient. For the color deficient alone, the thresholds form a continuous distribution rather than two distinct groups. There is, however, some slight evidence of bimodality in the distribution. This supports the hypothesis that "darkening of the red" is not uniquely characteristic of a particular group of color deficient individuals.

* Research performed under Contract N5-ori-166, Task Order I, between the Special Devices Center, ONR, and The Johns Hopkins University.

32. Microwave Test of a Theory of the Stiles and Crawford Effect. J. N. Jean and Brian O'Brien, *Institute of Optics, University of Rochester.*

The quantitative theory of the Stiles and Crawford effect proposed by one of us[1] is limited by the assumption that ray optics are sufficient to describe the multiple reflection of light within a retinal cone. Since a human retinal cone is only a few wave-lengths in diameter, diffraction must modify the geometrical theory. A test has been made using radiation of 3-cm wave-length and a scale model bearing the same relation to this wave-length as does a human foveal cone to visible light. Radiation was produced with a klystron oscillator and detected with a receiver calibrated directly in signal strength. Models of a foveal cone ellipsoid were made of rigid polystyrene foam of refractive index 1.0185 at 9377 Mc. The cone models were 16.4 cm diameter at the base with included angle 7°18″. Signal strength, measured as a function of angle from the axis of the cone, was plotted according to relation that 1-mm lateral displacement in the adult human pupil corresponds to 2.5 degree obliquity of the ray within the vitreous humor.[1] The resultant plot matches very closely the curves published by Stiles and others for the light adapted eye.[2] The effect of diffraction thus improves the quantitative agreement, lending additional support to the theory.

[1] B. O'Brien, J. Opt. Soc. Am. **36**, 506 (1946); **37**, 275 (1947).

[2] W. S. Stiles and B. H. Crawford, Proc. Roy. Soc. **B112**, 428 (1933); **116**, 55 (1934); W. S. Stiles, Proc. Roy. Soc. **B127**, 64 (1939).

33. Eye Movements and the Variation of Visual Acuity with Test Object Orientation. W. R. J. Brown, *Research Laboratories, Eastman Kodak Company.*

A possible explanation is given for the phenomenon of higher visual acuity as measured with a parallel line test object when the lines are vertical or horizontal than when the lines are at forty-five degrees.[1] This explanation is based on a dynamic theory of visual acuity.[2] The difficulties in explaining the effect by astigmatism of the observers, the structure of the retina, or by continuously driven small oscillations of the eye are discussed. An explanation of the effect is provided by assuming that the eye acts as a sphere held in orientation by two pairs of elastic muscles and that its movements are damped by viscous friction. This hypothesis explains the phenomenon if the average time between the involuntary "jumps" of the eye, which initiate the vibrations, is greater than the time required for the oscillations to decay to forty percent of their initial value. Since the average time between jumps is relatively long (0.5–0.6 sec.)[3] the hypothesis seems reasonable. Therefore, the observed variation of visual acuity with angle appears to substantiate the dynamic theory of visual acuity.

[1] G. C. Higgins and K. Stultz, J. Opt. Soc. Am. **38**, 756 (1948).

[2] L. A. Jones and G. C. Higgins, J. Opt. Soc. Am. **38**, 398 (1948).

[3] Lord and Wright, Nature **162**, 25 (1948).

34. Visual Acuity through Various Types and Grades of Sun Glass Lenses. R. H. Peckham, *Temple University School of Medicine.*

Using a psychometric technique, and logarithmically varying checkered targets, the monocular visual acuity of 27 subjects was measured with and without sun glass lenses prepared by (a) grinding and polishing to finished curve, (b) bending polished plate glass, and (c) bending naturally fire-polished drawn sheet glass. The binocular acuity of 43 additional subjects was measured with and without glasses of Type (c) selected to resolve (d) 40, (e) 20, and (f) 14 lines per inch at 35 feet through a telescope. The average monocular acuity was 1.117′. With the lens (a) this was 1.209′, with (b) 1.193′, and with (c) 1.212′. The average binocular acuity was 1.037′. Through the glasses (d) this was 1.105′, through (e) 1.086′, and through (f) 1.097′. Statistically significant differences due to brightness exist between no sun glass and any of the sun glass lenses, as expected. No such differences exist between types (a), (b), and (c), nor between grades (d), (e), and (f). It is concluded that the grading of sun glass lenses by optical resolving power is not valid, and that no method of preparing sun glass lenses has, in itself, any superiority with regard to sharpness of seeing.

35. Theory of the Induced Effect in Binocular Vision.* Kenneth N. Ogle, *Mayo Foundation and Mayo Clinic.*

This paper deals with the apparent distortion of stereoscopic perception of space caused by magnifying the image of one eye in the vertical meridian. This distortion is shown to be consistent with that reorientation in the frame of reference of binocular spatial localization when the eyes are turned to asymmetrical convergence, which is necessary if that localization is to remain egocentric. The theory of the effect is correspondingly postulated and the results are shown to be in quantitative agreement.

---

[*] K. N. Ogle, J. Opt. Soc. Am. **30**, 145–161 (1940). A. S. Householder, Bull. Math. Phys. **5**, 155–160 (1943).

36. A Study of Low Intensity Reciprocity Law Failure in Photographic Exposure. JULIAN H. WEBB, *Research Laboratories, Eastman Kodak Company, Rochester, New York.*

Theory and experimental results are given to show that the energy depth ϵ of the traps for the initially trapped electrons in latent image formation can be determined from measurements of reciprocity law failure at different temperatures.* The average value of ϵ(0.7 ev) found is in close agreement with the spectral sensitivity of the Herschel effect which occurs by optical instead of thermal ejection of electrons. The present paper is concerned principally with the mechanism of low intensity reciprocity law failure as it is related to the exposure required to establish the sublatent image speck, which is just stable but not developable. To establish the stable sub-speck two or more effective quanta must be absorbed by a grain within a critical time element τ. Using probability formulas, theoretical reciprocity curves are calculated based on the requirement that 1, 2, 3 or, in general, a multiplet s of quanta must be absorbed in a critical time τ to form the stable sub-speck. It is shown that the reciprocity failure curves under these conditions (log It *vs.* log I) must approach at low intensities the limiting slopes of 0, 1, 2 or, in general, $(s-1)$, respectively. This affords a sharp experimental criterion for determining the value of s, which, according to experimental measurements, is two. The theory shows clearly why the reciprocity failure curves at two temperatures are parallel in the horizontal (log I) direction. A reciprocity failure curve derived on the basis of two quanta to establish the stable sub-speck, and six additional quanta to complete the latent-image agrees closely with experiment.

---

[*] A similar analysis of the electron trap depth soon to be published has been worked out by E. Katz (private communication).

37. Objectives and Methods of Density Measurement in Color Film Sensitometry. FRANKLIN C. WILLIAMS, *Kodak Research Laboratories.*

Density measurements used in color film sensitometry can be divided into two broad classes; integral densitometry, which provides description of the multilayer image as a whole, in terms of its absorptions; and analytical densitometry, which gives a description of the image in terms of its components, by determining their individual density values. Each class contains sub-classes formed by special definitions of density. Terms and units are defined for each class and sub-class; for each the field of usefulness and methods of measurement are briefly discussed.

38. The Analytical Equation of the Emulsion Calibration Curve of Photographic Photometry. MILTON GREEN AND T. SCHREIBER, *Signal Corps Engineering Laboratories.*

By a careful study of its preliminary curve, an accurate expression for the emulsion calibration curve has been arrived at. It involves five constants which are characteristic of the emulsion. A power series expansion of gamma-log intensity in terms of density will, for three terms (this corresponds to five constants), give a very close fit also. Two constants of the above equations are translational and only affect the location of the curve relative to the coordinate axes. A third constant can be used as a scaling factor which sets the units of measure of one coordinate axis relative to the other. Thus, there are two constants remaining which determine the shape of the curve. If these two constants were identical for all emulsions, then a single appropriate transmittance scale would suffice to linearize all emulsion calibration curves.[1] Experiment shows them to vary somewhat. Hence, a single transmittance scale that will linearize some emulsion curves fairly accurately will linearize others only approximately.

---

[1] H. K. Hughes and R. W. Murphy, "Emulsion calibration scale for quantitative spectroscopic analysis," J. Opt. Soc. Am. **39**, 501 (1949).

39. Color Correction in Optical Systems and Types of Glass. M. HERZBERGER AND H. JENKINS, *Eastman Kodak Company, Research Laboratories.*

The authors suggest that the optical qualities of a transparent material are given with the help of three graphs, one a plot of the reciprocal dispersion $1/(n_F-n_C)$ against the ν-value, the other two giving two data ρ_A and ρ_h signifying the deviation of the dispersion of the glass towards the red and violet end of the spectrum from the regular standard. A universal dispersion formula is given which permits one (a) to calculate the refractive index for any given wave-length if the above data are given; (b) to compute the above data if the refractive index is given for four or more values. The dispersion formula is linear with respect to the given data. The graphs so designed permit one to estimate immediately the powers of a doublet corrected for two wave-lengths and the amount of the secondary spectrum in the red and violet end for any two given glasses. Testing these formulas for different types of glass and other optically important materials (fluorite, quartz, lithium fluorite, salt etc.) shows an agreement with the measurements throughout the spectrum which is sufficient for optical calculation ($\pm 2\times 10^{-5}$).

40. On the Possibility of a Spathic Polarizer which Transmits More than One-half of the Incident Unpolarized Light.* R. CLARK JONES, *Polaroid Corporation, Cambridge, Massachusetts.*

A spathic polarizer is here defined as a polarizer which preserves the cross section, solid angle, and frequency band width of the beam of light which passes through it. Examples of spathic polarizers are Nicol prisms and Polaroid light-polarizing sheeting. It is easy to make a non-spathic polarizer which, except for reflection losses, transmits all of the incident unpolarized light as polarized light. A thick slab of calcite and a half-wave plate suffices. But no spathic polarizer known to the writer has a transmission of more than 50 percent. Arguments will be presented to show that a spathic polarizer which transmits all of the incident unpolarized light is impossible because it would violate the second law of thermodynamics. For green light emitted by a blackbody at 3000° K, it will be shown that a spathic polarizer at room temperature with a transmission of 99.1 percent is thermodynamically possible, and the operating principles of a type of spathic polarizer will be described which has in principle a transmission of 89 percent. It will further be shown that any spathic polarizer which has a transmission greater than 50 percent cannot be a purely thermal device: it must contain a non-thermal pump which is capable of raising the temperature of part of the system above the highest initial temperature. Spathic polarizers with transmission factors greater than 50 percent may be used to increase without limit the brightness of a source of light; this cannot be done by a purely thermal pump.

---

[*] Max Planck, *Theory of Heat Radiation* (P. Blakiston's Son and Company, Philadelphia, 1914).

41. Secondary Color in Optical Relay Systems. Robert E. Hopkins, *Institute of Optics, University of Rochester.*

A submarine periscope is a well known example of an optical relay system. Under certain conditions secondary color and field curvature become excessive in such systems. This paper will include an analysis of secondary color and field curvature in optical relay systems. It will be shown that secondary color can always be reduced to the tolerance, but usually at the expense of field curvature.

42. Ray Tracing with the Selective Sequence Electronic Calculator. H. R. J. Grosch, *International Business Machines Corporation and Watson Scientific Computing Laboratory, Columbia University.*

The SSEC has been used to trace skew rays through a large-aperture photographic objective.* One ray is carried through the entire system and its intersection with the focal plane is determined; if sin I or sin I′ exceeds unity, or if vignetting occurs, the sequence is interrupted and the next ray is started. All calculations are checked by duplication, and an over-all check is applied to the direction cosines of the ray after each refraction. All work is carried to twelve decimal places. The pertinent results for each surface and the focal plane are printed, and are punched in standard cards,* in duplicate. Total time required for one ray, through eleven surfaces, is 115 seconds. A brief description of the SSEC will be given.

* H. R. J. Grosch, "Ray tracing with punched card equipment," J. Opt. Soc. Am. **35**, 803A (1945).

43. Fresnel Diffraction Near a Narrow Slit.* Robert A. Woodson, *Northwestern University.*

Fresnel's integrals and the Cornu spiral are adequate for solving certain diffraction problems when the field point is many wave-lengths from the diffracting aperture and when the diffraction angle is small. However, the errors in phase and amplitude become appreciable for field points near a narrow slit. A new vibration spiral has been developed to replace the Cornu spiral for field points near a slit. This spiral takes account of both the radiation field and the induction field with their respective obliquity factors and amplitude dependence upon distance. The phase errors in the Cornu spiral (arising from neglecting higher order terms) have been reduced greatly in the new spiral. A different vibration spiral must be used for each field plane (parallel to the slit plane) because of the unique amplitude dependence upon the position of the field plane. Using microwaves of 3.2-cm wavelength, diffraction experiments have been performed to test the new vibration spiral. Results indicate that within experimental error, the vibration spiral is confirmed, whereas the Cornu spiral leads to gross errors.

* Slater and Frank, "Mathematical formulation of Huygens' principle," in *Electromagnetism* (McGraw Hill Book Company, Inc., New York, 1947), pp. 170–173.

44. A New Method for the Accurate Measurement of Phase Differences.* Frits Zernike, *University of Groningen, Netherlands.*

The well-known diffraction figure of three equidistant slits may be considered as formed by the fringes of equal intensity caused by the outer slits, together with the coherent background from the middle slit, which alternately reinforces and suppresses these fringes. This effect disappears when the focus of the observing telescope is changed so as to cause a geometric path difference of a quarter wave between the middle and outer beams, resulting in two accurate settings of the drawtube inside and outside focus for which the fringes are all of equal brightness. A phase strip in front of the middle slit gives an outward or inward shift of these settings, which measures its path difference with an accuracy of a few thousandths of a wave. To compensate for the absorption of the strip the middle slit is made much wider than the outer slits. The effect is reversed if two phase strips are placed in front of the outer slits. By an arrangement with five slits, both possibilities may be alternately switched in, thus doubling the precision. The method is especially valuable for testing larger samples of the material prepared for cutting out the small phase rings to be inserted in microscope objectives. Applications of the same photometric setting to other interference measurements are indicated.

* *Note.*—To be read by Arthur T. Brice.

45. Establishment of Lens Centering Tolerances. Glenn Wooters, *Bausch & Lomb Optical Company.*

Before lens-centering tolerances can be established, it is necessary to be able to compute the effect of eccentric lenses. The transfer coefficients developed by M'Aulay and Cruickshank can be adapted to computing the effect of decentered elements. This is especially useful for wide aperture systems, such as microscope objectives. This has the advantage over other computational systems in that other tolerances, such as thickness, surface quality, index and spacing, can be established at the same time. The work with microscope objectives has resulted in some centering tolerances of only a few microns. The computations have been verified by experimental results.

46. Invited paper, entitled "The Effect of Gaseous Atmospheres on Excitation in Emission Spectroscopy," by B. F. Scribner, *National Bureau of Standards.*

47. Emission Spectra of Technetium. William F. Meggers and Bourdon F. Scribner, *National Bureau of Standards.*

Three milligrams of highly purified ^{43}Tc^{99} were loaned by the United States Atomic Energy Commission. Solutions containing 50 to 100 micrograms of Tc were dried on copper electrodes and excited with low and high energy discharges from an ARL multisource unit. A stigmatic concave grating was employed to photograph the spectra from 2100A to 9000A within which limits more than 2000 lines characteristic of Tc were recorded. Wave-lengths were measured relative to iron standards, relative intensities were estimated on a scale of 1 to 1000, and almost every line was definitely assigned either to neutral Tc atoms or to singly charged Tc$^+$ ions. The ground state of Tc atoms is established as $(4d^5\,5s^2)$ $^6S_{2\frac{1}{2}}$. The lowest level of the $(4d^6\,5s)$ ^6D term is at 2572.9 cm^{-1} whereas the associated ^4D term begins at 10516.5 cm^{-1}. Almost all the stronger Tc I lines are explained as combinations of these even terms with odd terms identified as $(4d^5\,5s\,4p)$ $^8P^\circ$ and $(4d^6\,4p)$ $^4(PDF)^\circ$ or $(4d^6\,4p)$ $^6(PDF)^\circ$. Tested by the combination principle the average error in measured wave-lengths of Tc lines appears to be less than ±0.02A. Prominent lines of the Tc I spectrum have wave-lengths 4297.05, 4262.27, 4238.19, and 3636.10A; outstanding lines of the Tc II spectrum have wave-lengths 2543.24, 2610.00, and 2647.02A.

48. Extensions to the Analysis of the Infra-red Spectra of the Noble Gases. Curtis J. Humphreys, *National Bureau of Standards, Washington, D. C.*

Although the first spectra of neon, argon, krypton, and xenon are among the most completely analyzed atomic spectra, there have long been a small number of missing levels particularly among those arising from the s^2p^5f configuration. The most intense combinations of such levels are in the infrared region making observations between one and two microns necessary to establish all of them. New observations have been made with the recently completed high resolution grating spectrometer. These observations cover the same range as those of Sittner and Peck,[1] but include neon, and yield wave-lengths of 13 krypton lines not previously reported. All new lines and all intense lines not classified by Sittner and Peck are accounted for as combinations of new or known levels. In accordance with the *jl*-coupling scheme discussed by Racah,[2] the levels of the noble gases are arranged in pairs. These are extremely close for the *f*-levels, and in some instances have never been resolved. The location of all pairs has now been established or confirmed by infra-red combinations. On the basis of the predictions of Edlén[3] the separation of several of the close pairs has been undertaken, and the necessary conditions for resolution will be discussed.

[1] W. R. Sittner and E. R. Peck, J. Opt. Soc. Am. **39**, 474 (1949).
[2] G. Racah, Phys. Rev. **61**, 537 (1942).
[3] Unpublished material.

49. The Use of Briquetted Samples in the Spectrochemical Analysis of Carbon and Alloy Steels and Other Metals. J. F. Woodruff, *Armco Steel Corporation.*

At the Armco Steel Corporation, over a period of several years, a number of spectrochemical methods have been developed which utilize briquetted powders, drillings, millings, nibblings, and grindings. The paper describes briquetted sample techniques for the routine analysis of steel, zinc, and zinc base alloys. Low and plain carbon steels are analyzed quantitatively for such elements as tin, lead, manganese, nickel, chromium, molybdenum, cobalt, titanium, aluminum, zinc, and boron. Zinc and zinc base alloys are analyzed quantitatively for cadmium, iron, lead, tin, antimony, and aluminum. Operational details, such as sample holders, spectrum lines utilized, source-units and source-unit constants employed, and precision and accuracy data over a five-year period are discussed.

50. An Introductory Study of the Spectral Characteristics of Ferrous Alloys. J. Convey and J. K. Hurwitz, *Canadian Bureau of Mines.*

The wave-lengths of the spectral lines of the low alloy steel spectrum have been measured for purposes of identification in the region 2327–4384A. The description of the observed lines included the following information:[1, 2] wave-length, atomic origin, designation of the transition, excitation potential, visual intensity, and possible interferences. For the spectrochemistry of Ni, Cr, Mn, Si, and V in low alloy and stainless steels, homologous line pairs were selected primarily on the basis of similar excitation potentials and freedom from interference. To test the homologous nature of these line pairs, the spectra of low alloy and stainless steels were recorded photographically using a wide range of source conditions. An A. R. L. multisource unit and a Baird Associates 3-meter grating spectrograph were used. Results indicate small lateral shifts in the working curves for large changes in the spark discharge. The high nickel and chromium content in stainless steel enhances the spectral lines of iron relative to those lines of the alloying elements with the exception of nickel. This phenomenon is being investigated more fully at the present time.

[1] W. F. Meggers, J. Opt. Soc. Am. **36**, 431 (1946).
[2] G. R. Harrison, *M. I. T. Wavelength Tables* (John Wiley and Sons, Inc., 1939).

51. Anomalous Rotational Isotope Effect in Mercury Hydride. S. Mrozowski, *University of Buffalo.*

All lines of mercury hydride bands show a structure which is due to the isotopic constitution of mercury. Its complexity is caused by an overlapping of three effects of different nature: (1) The normal vibrational and rotational isotope effect due to a difference in masses. (2) The nuclear isotope shift effect caused by the differences in nuclear volumes. The effect is evidenced by large vibrational shifts and by deviations from the normal rotational effect at high rotational quantum numbers. (3) The hyperfine structure splitting of levels belonging to the two odd isotopes of mercury with nuclear moments 1/2 and 3/2. In continuation of this work the deviations in the rotational shifts where studied under improved conditions and it has been shown that they occur not only for high but extend in branches all the way down to the zero lines. All the rotational shifts in the band system $^2\pi \rightarrow {}^2\Sigma$ are about 25 percent larger than calculated for normal rotational isotope effect in the mercury hydride, and only 10 percent larger than theoretical in the mercury deuteride. On the other hand in the band system $^2\Sigma \rightarrow {}^2\Sigma$ the observed shifts in the mercury hydride are about 20 percent smaller than the calculated ones and on top of that at large quantum numbers show some additional perturbations.

52. Invited paper, entitled "Infra-Red and Raman Spectra of Crystals," by Donald F. Hornig, *Brown University.*

53. New Raman Spectrograph and Source. A. C. Menzies, *Hilger and Watts Ltd., London, N.W. 1.*

A two prism spectrograph with novel features has been designed specially for the Raman effect, having two cameras, F/5.7 and F/1.5, mounted on the same arm, pivoted so that one takes the place of the other smoothly. Either rapid spectrograms or ones with greater dispersion are taken at will, and for research purposes the fast camera aids in selection of material or arrangement of illumination. Dispersions are 1 mm for 18.8 and 63A, respectively, at 4358A. Alternatively, one position can be used for the camera chosen, and the other for a scanning device, so that change from photography to direct reading is simple. The source is a new arrangement in which no mirrors are incorporated, but consists of a light furnace depending upon the high reflectivity of materials such as magnesium oxide, so that lack of specular reflection is more than compensated by using some of the light more than once. With the combination, the complete Stokes spectrum of CCl_4 can be seen with the naked eye, and all but the doublet in the anti-Stokes spectrum. Using 6 ml, the 991 cm^{-1} line of benzene is photographed in $\frac{1}{2}$ sec. with the slow camera.

54. Infra-Red Spectrophotometer with Cathode-Ray Display. A. C. Menzies, *Hilger and Watts, Ltd., London, N.W. 1.*

An infra-red spectrophotometer with cathode-ray presentation has been developed following the general principles of those made by Sutherland[1] and by Thompson,[2] but differing from theirs in details, particularly of electronic circuits. The detector is a thermocouple, having a time-constant of fifteen milliseconds. The wave-length range covered is 1.5 to 25.7 μ. with 8 cams. Scanning time of the trace on the long-delay glow tube is variable, from 15 to 50 seconds in four steps. A small fast electrolytic recorder is incorporated, so that a note of the trace can be taken at will. Push-pull amplifiers are used: the preamplifier is compact and housed in the infra-red spectrometer, and the valves used for it are of one type and not specially selected. The main amplifier is conventional, and output from it is d.c. restored to ground and the chopper component is filtered out. The remaining signal is d.c. amplified and applied to the vertical plates of the C.R.T. The instrument is suited for observations of transient phenomena, and for rapid analyses, selection and control. Photographs of traces on the tube are shown, up to 23 μ.

[1] Daly and Sutherland, Proc. Phys. Soc. LIX, **77** (1947).
[2] King, Temple, and Thompson, Nature **158** (August, 1946).

55. The Carbon Arc as an Infra-Red Source.[†] C. S. Rupert and John Strong, *Johns Hopkins University.*

The positive crater of the carbon arc is a highly satisfactory source for infra-red spectroscopy. The brightness increase over the globar (approximately 7 × at 6.5 μ and 5 × at 15 μ) permits a gain of between 2 and 3 in resolving power. Under correct operating conditions small changes in the arc current alter the size but not the temperature of the crater. The detector output is constant to 2% when the edges of the crater image are diaphragmed off at the entrance slit. Scattered light is intolerable in a single-prism monochromator, but negligible when a suitable double monochromator, such as a prism-grating combination, is used. The circular shape of the arc crater suggests the use of the image slicer[*] designed to cut up a circular stellar image and put the light through a slit. We have constructed a three division slicer. Second-hand low intensity motion picture projection arcs, generally available, are adaptable to spectroscopic use. Our arc burns unattended for 40 to 50 minutes in an entirely satisfactory manner. This source should have particular value in increasing the signal to noise ratio for high resolution spectroscopy, infra-red microscopy, and high speed scanning of the spectrum.

[†] Supported in part by Contract Nori—166-5.

[*] Bowen, Astrophys. J. **88**, 113 (1938).

56. Refractive Index of Silver Chloride for Visible and Infra-Red Radiant Energy.[*] Leroy W. Tilton, Earl K. Plyler, and Robert E. Stephens, *National Bureau of Standards.*

The refractive indexes of a 31° prism of silver chloride were measured at 30 wave-lengths at a constant room temperature of 23.9°C, from 0.578 to 20.6 μ by use of a minimum-deviation spectrometer and a Perkin-Elmer infra-red spectrometer equipped with a calibrated screw for operation of the Littrow mirror. A cadmium-mercury lamp was the source from 1 to 2 μ. From 2 to 20 μ various Baird's reflection interference filters and the absorption bands of carbon dioxide, carbon disulphide, water, methylcyclohexane, polystyrene, trichlorobenzene, and chlorobenzotrifluoride were used, with a Globar as source, for the identification of wave-lengths. In the visible region two prisms, one pressed and polished, the other sawed and lapped, were used and the results compared. The sensitivity of index to temperature is approximately -6.1×10^{-5} per centigrade degree for wavelength 610 mμ.

[*] The work described in this paper was carried out in part under Contract S and A 28658 between the Bureau of Ships and the National Bureau of Standards in order to extend our knowledge of the optical properties of this medium.

57. Artificial Sapphire for Optical Elements. Robert E. Hopkins and Brian O'Brien, *Institute of Optics, University of Rochester.*

Artificial sapphire of acceptable optical quality is now readily available in sizes up to 20 mm in diameter and 10 mm thick. Interferometer studies show that the samples are sufficiently uniform in index for most optical requirements. Practical methods for polishing optical surfaces have been worked out. Calculations have been made which show that the birefringence of the sapphire is not objectionable in lenses of moderate field of view if the optical axis of the crystal coincides with the lens axis. Methods have been devised to compensate the effects of double refraction if it becomes excessive. A 1-in. focal length f/1.5 Petzval lens has been designed and constructed with two sapphire elements. The design characteristics and results from testing the lens will be discussed.

58. Invited paper, entitled "Spectroscopic Analysis of Segregates in Alloys," by J. Convey, *Canadian Bureau of Mines, Ottawa.*

59. Comparative Results of Photographic and Direct Reading Methods of Analysis of High Alloy Steels. W. Magrun,[*] M. Windle,[*] and J. H. Jurmain, *Baird Associates, Inc.*

An evaluation is made of the three types of spectrographic equipment now commercially available—grating, prism, and direct reading, in their applicability to the analysis of a wide range of high alloy steels. The necessity and effectiveness of a method of compensation for the large variation of iron, the dilution method, is demonstrated. A comparison is made between results obtained both chemically and spectrographically.

[*] With Simonds Saw and Steel Company, Consultants for Baird Associates, Inc.

Bibliography:
Harrison, Lord and Loofbourow, *Practical Spectroscopy*, Prentice Hall, Inc., New York, 1948; J. H. Coulliette, "Nickel and chromium in stainless steel," Ind. Eng. Chem. **15**, No. 12 (1943); Post, Schoffstall, and Hurley, "Dilution factor in spectrochemical analysis," Ind. Eng. Chem. **17**, 412 (1945); Carpenter, DuBois, and Sterner, "Direct reading spectrometer for ferrous analysis." J. Opt. Soc. Am. **37**, No. 9, 707–713 (1947).

60. A D.C. Arc Source and Automatic Controller. G. H. Fetterley and W. M. Hazel, *Norton Company Research Laboratory.*

An effective source of direct current having any desired output up to 45 amperes at 150 volts is described, being characterized by small size, light weight, low cost, and negligible maintenance. While it has superseded all other d.c. sources, regardless of cost, in the Norton Company laboratories, it is particularly recommended where cost is an important consideration. It is also a useful auxiliary unit where highly refractory materials are analyzed regularly, since these materials are sometimes difficult to volatilize completely with the familiar multi-purpose type of source. An automatic current controller is also described as a separate unit, and can be used to hold the current within ± 0.5 ampere at any selected value between 5 and 15 amperes.

Bibliography:
Green and Kuper, "Constant current sources," Rev. Sci. Inst. **11**, 250–256 (1940); E. V. Potter and A. Scott, "An automatic arc-current regulator," Rev. Sci. Inst. **18**, 722–726 (1947).

61. New Spectrometer for Production Control Quantometer. M. F. Hasler, R. W. Lindhurst, J. W. Kemp, and M. C. Kraushaar, *Applied Research Laboratories, Glendale, California.*

A new vertical spectrometer has been developed which is particularly suited for routine direct-reading applications such as are encountered in production control work. Primary thermal and mechanical stability are achieved by using a heavy, aluminum-plate, box weldment as the basic mount for the various optical elements. All such elements, including the arc-spark stand, the fixed primary slit, the original diffraction grating, the receiver slits, the receiver condensing mirrors, and the multiplier photo-tubes are rigidly mounted to this weldment. This, in turn, is mounted on rubber shock absorbers inside a constant temperature sheet metal case. Constant temperature is achieved by running tap water through a system of tubing mounted in the walls of the case. Long term variations in temperature are compensated by a monitor system which allows the operator to very rapidly and accurately position small four-inch sections of the receiver slit system with respect to the spectrum. The net result is a very stable spectrometer which is quite independent of its surroundings both as to vibration and temperature. Details of design and construction are discussed.

62. Recent Advances in the Direct-Reading Analysis of High Percentage Alloys. M. F. Hasler, *Applied Research Laboratories, Glendale, California.*

Three significant advances have been made in the last year in connection with the spectrochemical analysis of high percentage alloys. The first is the development of source conditions which, in combination with the latest direct-reading apparatus, allow a precision of analysis for high percentage constituents of from 0.3–0.4 percent of the quantity being measured, and this by means of a single determination. The second is the accomplishment of this high precision under excitation conditions which provide complete independence in the determination of one element from changes in the concentrations of the other elements. The third is the development of rigorous calculating methods which make possible the rapid analysis of all constituents, including those of high percentage, in any alloy system. The application of these advances to the analysis of stainless steels and tool steels is discussed in detail. The net result is the availability of high speed, direct-reading methods of analysis which can compete in accuracy, for all metallic constituents, with routine chemical methods.

Author Index of Papers

Baum, William A. and Lawrence Dunkelman—No. 19
Belknap, Marion A.—see Gibson, Kasson S.
Bird, George R.—see Blout, Elkan R. and David S. Grey
Blake, R. P., A. S. Makas, and C. D. West—No. 17
Blout, Elkan R., George R. Bird, and David S. Grey—No. 6
Brice, Arthur T.—see Saylor, Charles Proffer and F. Zernike
Brown, W. R. J.—No. 33
Caldecourt, V. J.—see Peterson, E. W., H. H. Grossman, and J. L. Saunderson
Chapanis, Alphonse and R. M. Halsey—No. 31
Convey, J.—No. 58
——**and J. K. Hurwitz**—No. 50
Davidson, H. R.—No. 23
deBretteville, A. P., Jr.—see Field, Norman J.
Dunkelman, Lawrence—see Baum, William A.
Duntley, Seibert Q., Edward A. Edwards, and Nisson A. Finkelstein—No. 27
Edwards, Edward A.—see Duntley, Seibert Q. and Nisson A. Finkelstein
Epstein, L. Ivan—No. 8
Farnsworth, Dean—No. 28
Ferretti, Renato J.—see Price, George R. and Samuel Schwartz
Fetterley, G. H. and W. M. Hazel—No. 60
Field, Norman J. and A. P. deBretteville, Jr.—No. 9
Finkelstein, Nisson A.—No. 26
——see Duntley, Seibert Q. and Edward A. Edwards
Foster, L. V.—No. 1
Frerichs, Rudolf—No. 10
Gee, A. E. and H. D. Polster—No. 16
Gibson, Kasson S. and Marion A. Belknap—No. 21
Gray, Peter—No. 2
Green, Milton and T. Schreiber—No. 38
Grey, David S.—see Blout, Elkan R. and George R. Bird
Grosch, H. R. J.—No. 42
Grossman, H. H.—see Peterson, E. W., J. L. Saunderson, and V. J. Caldecourt
Haber, Heinz—No. 20
Halsey, R. M.—see Chapanis, Alphonse
Harrison, George R.—see Jacobsen, Edward
Hasler, M. F.—No. 62
——**R. W. Lindhurst, J. W. Kemp, and M. C. Kraushaar**—No. 61
Hazel, W. M.—see Fetterley, G. H.
Herzberger, M. and H. Jenkins—No. 39
Hopkins, Robert E.—No. 41
——**and Brian O'Brien**—No. 57
Hornig, Donald F.—No. 52
Humphreys, Curtis J.—No. 48
Hunter, Richard S.—No. 25
Hurwitz, J. K.—see Convey, J.
Jacobsen, Edward and G. R. Harrison—No. 18
Jean, J. N. and Brian O'Brien—No. 32
Jenkins, H.—see Herzberger, M.
Jones, R. Clark—No. 40
Judd, Deane B. and Lorenzo Plaza—No. 29
Jurmain, J. H.—see Magrun, W. and M. Windle
Kemp, J. W.—see Hasler, M. F., R. W. Lindhurst, and M. C. Kraushaar
Kraushaar, M. C.—see Hasler, M. R., R. W. Lindhurst, and J. W. Kemp
Lindhurst, R. W.—see Hasler, M. F., J. W. Kemp, and M. C. Kraushaar
Loofbourow, John—No. 4
Magrun, W., M. Windle, and J. H. Jurmain—No. 59
Makas, A. S.—see Blake, R. P. and C. D. West
Marton, L.—No. 5
Meggers, William F. and Bourdon F. Scribner—No. 47
Menzies, A. C.—Nos. 53 and 54
Mrozowski, S.—No. 51
Nickerson, Dorothy—No. 24
O'Brien, Brian—see Hopkins, Robert E.
——see Jean, J. N.
Ogle, Kenneth N.—No. 35
Osterberg, H.—No. 3
Peckham, R. H.—No. 34
Peterson, E. W., H. H. Grossman, J. L. Saunderson, and V. J. Caldecourt—No. 22
Plaza, Lorenzo—see Judd, Deane B.
Plyler, Earl K.—see Tilton, Leroy W. and Robert E. Stephens
Polster, Harry D.—No. 15
——see Gee, A. E.
Price, George R.—No. 13
——**Renato J. Ferratti, and Samuel Schwartz**—Nos. 11 and 12
Rupert, C. S. and John Strong—No. 55
Saunderson, J. L.—see Peterson, E. W., H. H. Grossman, and V. J. Caldecourt
Saylor, Charles Proffer, Arthur T. Brice, and F. Zernike—No. 7
Schreiber, T.—see Green, Milton
Schwartz, Samuel—see Price, George R. and Renato J. Ferretti
Scribner, Bourdon F.—No. 46
——see Meggers, William F.
Stephens, Robert E.—see Tilson, Leroy W. and Earl K. Plyler
Strong, John—see Rupert, C. S.
Tilton, Leroy W., Earl K. Plyler, and Robert E. Stephens—No. 56
van Heel, A. C. S.—No. 14

Wald, George—No. 30
Webb, Julian H.—No. 36
West, C. D.—see Blake, R. P. and A. S. Makas
Williams, Franklin C.—No. 37
Windle, M.—see Magrun, W. and J. H. Jurmain
Woodruff, J. F.—No. 49
Woodson, Robert A.—No. 43
Wooters, Glenn—No. 45
Zernike, Frits—No. 44
——see Saylor, Charles Proffer and Arthur T. Brice

Minutes of the Thirty-Fourth Meeting of the Board of Directors of the Optical Society of America, Incorporated

Hotel Statler, Buffalo, New York, October 26, 1949

In addition to the transaction of routine business, the following items of general interest to members of the Society were considered.

Announcements by Secretary

Results of letter ballots:

1. Approval of resolution to appoint R. C. Gibbs to succeed A. H. Pfund as a member of the Nominating Committee and as a member of the Committee on Honorary Membership.
2. Approval of award of Frederic Ives Medal to George R. Harrison.
3. Approval of resolution to hold the annual meeting in 1950 in Cleveland, Ohio, on October 26, 27, and 28.
4. Approval of resolution to appoint Wallace R. Brode Editor of Publications to fill the unexpired term of George R. Harrison (resigned as of December 31, 1949).

Announcement by President

Appointment of Tellers for 1949 election:

Duncan Macdonald	John Sterner
Dwight P. Merrill	William A. Shurcliff, *alternate*

Report of Tellers

The report indicated the election of the following officers:

For a term of two years	
President	William F. Meggers
Vice President	Brian O'Brien
For a term of four years	
Secretary	Arthur C. Hardy
Treasurer	W. W. Graeper
For a term of two years	
Secretary for Local Sections	Stanley S. Ballard
For a term of four years	
Directors-at-large of the Board of Directors	John Strong Mary Warga

Actions by Board of Directors

Appointment of Chairman of Program Committee for March 9, 10, and 11, 1950 meeting:

Herbert R. J. Grosch

Appointment of Program Committee for October 26, 27, and 28, 1950 meeting:

W. E. Forsythe, *Chairman*
Stanley S. Ballard
B. T. Barnes
R. A. Beth
Hans Jaffe
Leonard Olsen
C. D. Spencer
A. H. Taylor

Appointment of Arthur C. Hardy to represent the Optical Society of America on the general committee of the American Institute of Physics to consider plans for an anniversary meeting of the A.I.P., tentatively scheduled for the week of October 22, 1951, in Chicago.

Nomination of Rudolf Kingslake as O.S.A. Representative on the Governing Board of the American Institute of Physics to fill the unexpired term of A. G. Worthing, deceased.

Nomination of Rudolf Kingslake as O. S. A. Representative on the Governing Board of the American Institute of Physics for a term of three years to expire in February, 1953.

Membership

The Secretary reported informally a net gain in membership of one hundred and twenty-four between January 1 and October 1, 1949.

Arthur C. Hardy, *Secretary*

Author Index to Volume 39

Reference with (A) are abstracts of papers presented at meetings of the Optical Society of America; (T) designates title only; (L) designates Letters to the Editor.

Agnew, J. T., R. G. Franklin, R. E. Benn, and A. Bazarian. Combustion studies with the orthicon spectrograph —409(L)
Anderson, Scott. Orientation of methylene blue molecules adsorbed on solids—49
Arnold, George W., Jr. (see Coleman, Howard S.)—864
Aughey, Henry. Rapid mobile analyzer for minute amounts of lead in air—292

Baker, Howard DeHaven. Course of foveal light adaptation measured by the threshold intensity increment—172; Erratum—367
Baker, Katherine Eleanor. Some variables influencing vernier acuity. I. Illumination and exposure time. II. Wavelength of illumination—567
Barnett, C. E. and L. D. Grady. Emission characteristics of fluorescent pigments—663
Bartlett, N. R. and A. L. Sweet. Visibility on cathode-ray tube screens: signals on a P-7 screen exposed for different intervals—470
——**, S. B. Williams, and R. M. Hanes.** Visibility on cathode-ray tube screens. Effect of size and shape of pip —463
Baum, William A. and Lawrence Dunkelman. Ultraviolet characteristics of the high pressure xenon arc—1055(A)
Baumgartner, R. R. (see Sihvonen, Y. T.)—257
Bazarian, A. (see Agnew, J. T.)—409(L)
Beckman, A. O. (see Miller, W. C.)—377
Belknap, Marion A. (see Gibson, Kasson S.)—1055(A)
Benn, R. E., W. S. Foote, and C. T. Chase. Image orthicon in spectroscopy—529
—— (see Agnew, J. T.)—409(L)
Benson, Nels C. (see Goldberg, Benjamin)—497, 631(A)
Berry, Richard N. (see Riggs, Lorrin A.)—427
Best, George H. Emissivities of copper and aluminum—1009
Billings, Bruce H. Haidinger fringes in a basal section of calcite—39
—— Electro-optic effect in uniaxial crystals of the type XH_2PO_4. I. Theoretical—797
—— Electro-optic effect in uniaxial crystals of the type XH_2PO_4. II. Experimental—802
—— **and M. A. Pittman.** Frustrated total reflection filter for the infra-red—978
Biltz, Martin. Dependence of the sensitivity of unsensitized photographic emulsions upon temperature—994
Bird, George R. (see Blout, Elkan R.)—1052(A)
Blake, R. P., A. S. Makas, and C. D. West. Molecular-type dichroic film polarizers for 0.75 to 2.8 mμ-radiations —1054(A)
Blout, Elkan R., George R. Bird, and David S. Grey. Infra-red microspectroscopy—1052(A)
Brewer, W. L., W. T. Hanson, Jr., and C. A. Horton. Subtractive color reproduction. The approximate reproduction of selected colors—924
Brice, Arthur T. (see Keck, Paul H.)—507
—— (see Saylor, Charles Proffer)—1053(A)
Brode, Wallace R. Presentation of absorption spectra data —1022
—— Book review—528
—— **and Donald L. Timma.** Influence of extraneous elements on line intensity. IV. Etxraneous element effects in the direct-current arc—478
Brown, W. R. J. Eye movements and the variation of visual acuity with test object orientation—1057(A)
—— **and D. L. MacAdam.** Visual sensitivities to combined chromaticity and luminance differences—808
Bube, Richard H. Correlation between cathodoluminescence efficiency and decay as a function of temperature—681, 628(A)
Bullock, B. W. and S. Silverman. Rapid scanning spectrometer for oscillographic recording—200(L)
Bundy, F. P. and H. M. Strong. Transmission of light from diffuse sources by periscope tubes—393; Addendum—698
Burkhart, L. E. (see McNally, J. R., Jr.)—1036
Burnham, Robert W. Comparison of color systems with respect to uniform visual spacing—387
Burton, Ralph A. Modified Schlieren apparatus for large areas of field—907
Byler, W. H. Multibanded emission spectra of zinc-cadmium sulfide phosphors—91(L)

Cady, Willoughby M. and Gary Gordon. Photographic spectral sensitometry with a biprism—368
Carman, P. D. Photogrammetric errors from camera lens decentering—951, 632(A)
Caldecourt, V. J. (see Grossman, H. H.)—261
—— (see Peterson, E. W.)—1055(A)
Chalker, W. R. (see Houghton, H. G.)—955
Chamberlain, Katherine (see Kaczor, Emil)—637(A), 917
Chapanis, Alphonse. Diagnosing types of color deficiency by means of pseudo-isochromatic tests—242
—— **and R. M. Halsey.** Photopic thresholds for red light in an unselected sample of color deficient individuals—1057(A)
Chase, C. T. (see Benn, R. E.)—529
Coleman, Howard S. and Harold E. Rosenberger. Comparison of photographic and photoelectric measurements of atmospheric attenuation of brightness contrast—990
——**, George W. Arnold, Jr., and Walter D. Luedecke.** Method of measuring the contrast rendition of telescopic systems—864
——**, Madeline F. Coleman, and Samuel W. Harding.** Influence of magnification on resolving power of telescopic systems for Foucault test objects of different inherent contrast—771
——**, Madeline F. Coleman, David L. Fridge, and Samuel W. Harding.** Coefficient of specific resolution of the human eye for Foucault test objects viewed through circular apertures—766
——**, Fred J. Morris, Harold E. Rosenberger, and Marshall J. Walker.** Photoelectric method of measuring the atmospheric attenuation of brightness contrast along a horizontal path for the visible region of the spectrum—515
Coleman, Madeline F. (see Coleman, Howard S.)—766, 771
Condit, H. R. (see Jones, Loyd A.)—94, 135, 790
Convey, J. Spectroscopic analysis of segregates in alloys—1060(T)
—— **and J. K. Hurwitz.** Introductory study of the spectral characteristics of ferrous alloys—1061(A)
Cornu, A. F. and P. A. Tardy. Improvement in routine analysis with the Beckman I. R. 2 infra-red spectrophotometer by a slight mechanical modification—613(L)
Coulman, C. E. and G. R. Petrie. Some notes on the designing of aspherical magnifiers for binocular vision—612(L)

Cramer, A. I. (see Weyl, W. A.)—889(L)
Crawford, M. F., W. M. Gray, A. L. Schawlow, and F. M. Kelly. Transmission and reflection coefficients of aluminum films for interferometry—888(L)

Davidson, H. R. Calculation of subtractive color mixtures —1055(A)
—— **and L. W. Imm.** Continuous, automatic tristimulus integrator for use with the recording spectrophotometer—633(A), 942
Davis, George E. Method of measuring high intensities at the focus of a parabolic reflector with large relative aperture—541
Dawson, L. H. (see Plymale, W. S., Jr.)—626(A), 712
deBretteville, A. P., Jr. (see Field, Norman J.)—1053(A)
de Launay, Jules. Note on the photo-pupil reflex—364
de Vries, Hl. Light quanta and vision—201(L)
di Francia, G. Toraldo. Retina cones as dielectric antennas —324(L)
Di Jorio, Mario. General theory of isoplanatism for finite aperture and field—305
Dunkelman, Lawrence (see Baum, William A.)—1055(A)
Duntley, Seibert Q., Edward A. Edwards, and Nisson A. Finkelstein. Spectrophotometric studies of living human skin in the ultraviolet—1056(A)
Dyer, C. A. (see Mouzon, J. C.)—203

Edwards, Edward A. (see Duntley, Seibert Q.)—1056(A)
Ehrenberg, W. X-ray optics: the production of converging beams by total reflection—741
—— X-ray optics: imperfections of optical flats and their effect on the reflection of x-rays—746
Ellickson, R. T. (see Scott, F. R.)—64
Enns, J. H. and R. A. Wolfe. Air interrupter type spectrographic light source—298
Enright, D. P. (see Weyl, W. A.)—889(L)
Epstein, L. Ivan. Out of focus diffraction patterns—226
—— Aberrations of slightly decentered optical systems—847
—— An extension of Toraldo's theory of phase contrast—1053(A)
Evans, John W. Birefringent filter—229; Correction—412
Evans, Ralph M. On some aspects of white, gray, and black—774

Fano, U. Remarks on the classical and quantum-mechanical treatment of partial polarization—859
Farnsworth, Dean. Chromaticity confusions of color defectives—1056(A)
Fassel, Velmer A. Quantitative spectrographic analysis of the rare earth elements. III. Determination of major constituents in complex mixtures—187
Fellgett, P. B. On the ultimate sensitivity and practical performance of radiation detectors—970
Ferretti, Renato J. (see Price, George R.)—1053(A), 1053(A)
Fetterley, G. H. and W. M. Hazel. D.c. arc source and automatic controller—1060(A)
Field, Norman J. and A. P. deBretteville, Jr. Motion pictures of some optical and electrical effects in barium titanate crystals—1053(A)
Finkelnburg, Wolfgang. Conditions for blackbody radiation of gases—185
Finkelstein, Nisson A. Spectral reflectance measurements in the ultraviolet—1056(A)
—— (see Duntley, Seibert Q.)—1056(A)
Fonda, Gorton R. (see Studer, Frank J.)—655
Foote, W. S. (see Benn, R. E.)—529
Foster, L. V. Microscope optics—1052(T)
Frank, Sylvia (see Hecht, Selig)—922
Franklin, R. G. (see Agnew, J. T.)—409(L)
Fred, Mark (see Tomkins, Frank S.)—357, 637(A)
Frerichs, Rudolf. Photo-conductivity in crystal phosphors —1053(A)
Fridge, David L. (see Coleman, Howard S.)—766
Friedman, H. and C. P. Glover. Optical transmission of additively colored alkali halide crystals in the visible and near infra-red—795(L)
Fry, D. L. Infra-red absorption analyses used in control of a pilot-plant process—402
—— (see Sihvonen, Y. T.)—257

Gabel, Joseph W. and E. I. Stearns. Auxiliary working standard equivalent to magnesium oxide on a General Electric spectrophotometer—481
Garlick, G. F. J. and A. F. Gibson. Luminescence of photoconducting phosphors—935
Gayhart, E. L. and Rochelle Prescott. Interference phenomenon in the schlieren system—546
Gee, Alan E. and Harry D. Polster. Method for measuring extremely small non-uniformities in the optical thickness of evaporated films—1044
—— **and H. D. Polster.** Thickness non-uniformities in evaporated films—1054(A)
Geiger, Ernesto E. Direct calculation of achromatized and corrected optical systems—193
Geiger, Felix E., Jr. Effect of finite aperture on the fringe intensity distribution of Fabry Perot interferometers—249
George, K. P. (see Miller, W. C.)—377
Gibson, A. F. (see Garlick, G. F. J.)—935
Gibson, Kasson S. and Marion A. Belknap. Permanence of glass standards issued to check the photometric scale of spectrophotometers—1055(A)
Gilstein, J. B. (see Hett, J. H.)—909
Glover, C. P. (see Friedman, H.)—795(L)
Goddard, P. E. (see Pearlman, D.)—628(A), 695
Golay, Marcel J. E. Multi-slit spectrometry—437
Goldberg, Benjamin and Nels C. Benson. Analysis of para-elliptic reflector—497, 631(A)
Gordon, Gary (see Cady, Willoughby M.)—368
Grady, L. D. (see Barnett, C. E.)—663
Graham, Robert (see Safonov, George)—406
Gray, Peter. Optical microscope as seen by a user—1052(T)
Gray, W. M. (see Crawford, M. F.)—888(L)
Green, Milton and T. Schreiber. Analytical equation of the emulsion calibration curve of photographic photometry—1058(A)
Grey, David S. New series of microscope objectives: II. Preliminary investigation of catadioptric Schwarzschild systems—723
—— **and Paul H. Lee.** New series of microscope objectives: I. Catadioptric Newtonian systems—719
—— (see Blout, Elkan R.)—1052(A)
Griffin, P. M. (see McNally, J. R., Jr.)—1036
Grosch, H. R. J. Ray tracing with the selective sequence electronic calculator—1059(A)
Gross, Paul M. (see Scheraga, Harold A.)—410(L)
Grossman, H. H., E. W. Peterson, J. L., Saunderson, and V. J. Caldecourt. Optical and electrical alterations to a Michigan microphotometer—261
—— (see Peterson, E. W.)—1055(A)

Haber, Heinz. Mount for a Perot-Fabry interferometer without etalon ring—1050(L)
—— Torus grating—1055(A)
Hainer, R. M. (see McMahon, H. O.)—786
Halsey, R. M. (see Chapanis, Alphonse)—1057(A)
Hamly, D. H. Ridgeway color standards with a Munsell notation key—592, 633(A)

Hammad, A. Scattered and rescattered sunlight—157
Hanes, R. M. (see Bartlett, N. R.)—463
Hanson, W. T., Jr. (see Brewer, W. L.)—924
Harding, Samuel W. (see Coleman, Howard S.)—766, 771
Hardy, Arthur C., and F. Mansfield Young. Correction of slit-width errors—265, 638(A)
—— **and F. Mansfield Young.** Colorimetry by abridged spectrophotometry—460, 634(A)
Hare, G. (see Miller, W. C.)—377
Harle, G. A. Comparison of lens radii—718(L)
Harrison, George R. Production of diffraction gratings I. Development of the ruling art—413
—— Production of diffraction gratings: II. Design of eschelle gratings and spectrographs—522
—— Editorial comment—977
—— (see Jacobsen, Edward)—1054(A)
Hasler, M. F. Recent advances in the direct-reading analysis of high percentage alloys—1062(A)
——**, R. W. Lindhurst, J. W. Kemp, and M. C. Kraushaar.** New spectrometer for production control quantometer—1060(A)
Hass, Georg. Preparation of hard oxide films with precisely controlled thickness on evaporated aluminum mirrors—532, 632(A)
—— **and Noel W. Scott.** Silicon monoxide protected front-surface mirrors—179
Hazel, W. M. (see Fetterley, G. H.)—1060(A)
Hecht, Selig, Charles D. Hendley, Sylvia Frank, and Simon Shlaer. Contrast discrimination charts for demonstrating the effect of anoxia on vision—922
—— (see Hendley, Charles D.)—630(A), 870
Hendley, Charles D. and Selig Hecht. Colors of natural objects and terrains, and their relation to visual color deficiency—630(A), 870
—— (see Hecht, Selig)—922
Herman, Robert C. and Charles F. Meyer. Rise in brightness on infra-red sensitive phosphors—729
—— (see Silverman, S.)—216
Herzberger, M. and H. Jenkins. Color correction in optical systems and types of glass—1058(A)
Hett, J. H. and J. B. Gilstein. Pyrometer for measurement of instantaneous temperatures of flames—909
Hitchcock, William J. (see McNally, J. Rand, Jr.)—57
Hobbs, Marcus E. (see Scheraga, Harold A.)—410(L)
Hoerlin, Herman. Photographic action of x-rays in the 1.3 to 0.01A range—891
Holmes, Marian C. (see Middleton, W. E. Knowles)—582, 631(A)
Hopkins, R. E. Secondary color in optical relay systems—919, 1059(A)
—— **and Brian O'Brien.** Artificial sapphire for optical elements—1060(A)
Hornig, Donald F. Infra-red and Raman spectra of crystals—1061(T)
Horton, C. A. (see Brewer, W. L.)—924
Houghton, H. G. and W. R. Chalker. Scattering cross section of water drops in air for visible light—955
Hsü, Hsien-Yü (see Richartz, M.)—136
Huber, R. L. and A. B. Rakus. Photoelectric reflection-transmission densitometer—873
Hughes, Harold K. and R. W. Murphy. Emulsion calibration scale for quantitative spectroscopic analysis—501
Hulburt, E. O. Night sky brightness measurements in latitudes below 45°—211
—— Green segment seen from an airplane—409(L)
Humphreys, Curtis J. Extensions to the analysis of the infra-red spectra of the noble gases—1059(A)
Hunter, Richard S. Improved gloss recorder—1056(A)
Hurwitz, J. K. (see Convey, J.)—1061(A)
Imm, L. W. (see Davidson, H. R.)—633(A), 942
Ivanoff, A. Focusing wave-length for white light—718(L)
Ives, Herbert E. Book Review—297
—— Lorentz-type transformations as derived from performable rod and clock operations—757

Jacobsen, Edward and George R. Harrison. Ultrafrequency excitation of Hg 198 lamps for interferometer illumination—1054(A)
Jacquinot, P. and P. Rouard. International colloquium on solid thin films—1048(L)
Jean, J. N. and Brian O'Brien. Microwave test of a theory of the Stiles and Crawford effect—1057(A)
Jenkins, H. (see Herzberger, M.)—1058(A)
Jerrard, H. G. Formation of fringes in a babinet compensator—1031
Johnson, James S., Jr. and Ferd E. Williams. Thermoluminescence of manganese-activated zinc fluoride phosphors—629(A), 709
Jones, Ernest A. (see Kirby-Smith, J. S.)—780
Jones, Loyd, A. and H. R. Condit. Sunlight and skylight as determinants of photographic exposure. II. Scene structure, directional index, photographic efficiency of daylight, safety factors, and evaluation of camera exposure—94
—— **and H. R. Condit.** Errata: Sunlight and skylight as determinants of photographic exposure. I. Luminous density as determined by solar altitude and atmospheric conditions—135
—— **and H. R. Condit.** Errata: Sunlight and skylight as determinants of photographic exposure. I. Luminous density as determined by solar altitude and atmospheric conditions—790
Jones, R. Clark. New classification system for radiation detectors—327
—— Erratum: Ultimate sensitivity of radiation detectors—343
—— Factors of merit for radiation detectors—344
—— On the possibility of a spathic polarizer which transmits more than one-half of the incident unpolarized light—1058(A)
—— (see Shurcliff, W. A.)—912
Judd, Deane B. Color perceptions of deuteranopic and protanopic observers—252
—— Standard response functions for protanopic and deuteranopic vision—505(L)
—— Book review—765
——Comparison of direct colorimetry of titanium pigments with their indirect colorimetry based on spectrophotometry and a standard observer—945
——**and Lorenzo Plaza.** Tritanopia with abnormally heavy ocular pigmentation—1056(A)
Jurmain, J. H. (see Magrun, W.)—1060(A)

Kaczor, Emil and Katherine Chamberlain. Air interrupter for use with the A.R.L. spark source—637(A), 917
Katz, Amrom H. Camera shutters—1
Keck, Paul H. and Arthur T. Brice. Image contrast in phase-contrast microscopy—507
Kelly, F. M. (see Crawford, M. F.)—888(L)
Kemp, J. W. (see Hasler, M. F.)—1060(A)
King, Gilbert W. (see McMahon, H. O.)—786
Kirby-Smith, J. S., and Ernest A. Jones. Use of polytrifluorochloroethylene in infra-red and Raman spectroscopy—780
Kirkatrick, Paul. X-ray images by refractive focusing—796(L)
Kivenson, Gilbert, Albert Roth, and Myrtle Rider. Some new techniques in the construction of spectrographic absorption cells—484
Klein, Myron W. (see Smakula, Alexander)—445; Erratum—890(L)

Knoll, Henry A. Comment on "A note on the photo-pupil reflex"—954(L)
Kohn, Hedwig and H. Sponer. Absorption spectrum of 1,2,4-trichlorobenzene in the near ultraviolet—75
Koomen, M., R. Tousey, and R. Scolnik. Spherical aberration of the eye—370
Koppius, O. G. Detection of lead in air with the aid of a Geiger-Müller counter—294
Kornfeld, G. Herschel effect and the structure and stability of the photographic latent image—490
—— Latent-image distribution by x-ray exposures—1020
Kraushaar, M. C. (see Hasler, M. F.)—1060(A)
Kröger, F. A. Sodium and lithium as activators of fluorescence in zinc sulfide—670
—— (see Smit, N. W.)—661

Lamar, Edward S. Fraunhofer diffraction patterns of squares and rectangles—929
Lee, Bernard S. Oblique reflecting systems—487
Lee, Paul H. (see Grey, David S.)—719
Lindhurst, R. W. (see Hasler, M. F.)—1060(A)
Linfoot, E. H. and E. Wolf. On the corrector plates of Schmidt cameras—752
Longini, R. L. Optical characteristics of sheets of scattering materials—551
—— Intrinsic efficiency of the cathodoluminescence process —877
Loofbourow, John. Microspectroscopy—1052(T)
Lowe, D. S. (see Sponer, H.)—840
Luedecke, Walter D. (see Coleman, Howard S.)—864

MacAdam, David L. Colorimetric analysis of dye mixtures —22
—— Measurement of the influence of local adaptation on color matching—454, 631(A)
—— (see Brown, W. R. J.)—808
Magrun, W., M. Windle, and J. H. Jurmain. Comparative results of photographic and direct reading methods of analysis of high alloy steels—1060(A)
Mahoney, Marie M. (see Smith, Daniel)—86
Makas, A. S. (see Blake, R. P.)—1054(A)
—— (see West, C. D.)—791
Margenau, Henry. Book review—489
Marton, L. Electrons *vs.* protons—a comparison of microscopes—1052(T)
Matossi, Frank. On the utilization of complex optical constants—506(L)
—— Reflection and transmission formulas for a film on a backing plate—928
McKelvey, J. P. (see Rank, D. H.)—762
McMahon, H. O., R. M. Hainer, and Gilbert W. King. Low temperature infra-red transmission cell—786
McMath, Robert R. and Orren C. Mohler. Solar spectroscopy with a Cashman cell—903
McNally, J. Rand, Jr. Preliminary investigation of the spectra of uranium isotopes—271
—— Nomograph of HG 5461 structure as a function of etalon separation—1050(L)
——**, P. M. Griffin, and L. E. Burkhart.** Possibility of enhanced HG^{202} as a source of monochromatic light—1036
——**, Julius P. Molnar, William J. Hitchcock, and Norman F. Oliver.** High members of the principal series in caesium—57
Meggers, William F. and Bourdon F. Scribner. Emission spectra of technetium—1059(A)
Menzies, A. C. New Raman spectrograph and source—1061(A)
—— Infra-red spectrophotometer with cathode-ray display 1061(A)
Meyer, Charles F. (see Herman, Robert C.)—729
Middleton, W. E. Knowles. Effect of the angular aperture of a telephotometer on the telephotometry of collimated and non-collimated beams—576
—— **and Marian C. Holmes.** Apparent colors of surfaces of small subtense—A preliminary report—582, 631(A)
Miller, W. C., G. Hare, D. C. Strain, K. P. George, M. E. Stickney, and A. O. Beckman. New spectrophotometer employing a glass Fery prism—377
Mohler, Orren C. (see McMath, Robert R.)—903
Molby, Fred A. Index of refraction and coefficients of expansion of optical glasses at low temperatures—600
Molnar, Julius P. (see McNally, J. Rand, Jr.)—57
Morris, Fred J. (see Coleman, Howard S.)—515
Mouzon, J. C., and C. A. Dyer. Low temperature radiation pyrometry in industry—203
Mrozowski, S. Anomalous rotational isotope effect in mercury hydride—1061(A)
Mueller, F. W. H. Some remarks on gold treatment of photographic silver halide emulsions—494, 639(A)
Murphy, R. W. (see Hughes, Harold K.)—501
Murray, Allen E. Reflected light and ghosts in optical systems—30; Erratum—356

Nagy, Elemér. Optical and electrical properties of zinc silicate phosphors—42
Nail, N. R., F. Urbach, and D. Pearlman. New observations on superlinear luminescence—628(A), 690
—— (see Urbach, F.)—628(A), 675, 1011
Nelson, R. C. Direct recording of spectra in the region 1.2 μ to 3 μ using the lead sulfide photo-conductive cell—68
Newbound, Kenneth B. Refractive indices of water vapor and carbon dioxide at low pressure—835
Nickerson, Dorothy. Munsell renotations used to study color space of Hunter and of Adams—1055(A)
Nielsen, J. Rud. Aberrations in ellipsoidal mirrors used in infra-red spectrometers—59
Nottingham, Wayne B. Survey of present methods used to determine the optical properties of phosphors—641
Nusbaum, R. E. (see Sihvonen, Y. T.)—257

O'Brien, Brian. Comment on the note entitled "Retinal cones as dielectric antennas"—324(L)
—— (see Hopkins, Robert E.)—1060(A)
—— (see Jean, J. N.)—1057(A)
Ogle, Kenneth N. Theory of the induced effect in binocular vision—1057(A)
Oliver, Norman F. (see McNally, J. Rand, Jr.)—57
Osterberg H. Microscope imagery and interpretations—1052(T)
—— **and J. Ernest Wilkins, Jr.** Resolving power of a coated objective—553
—— **and Franklyn C. Wissler.** Resolution of two particles in a bright field by coated microscope objectives—558, 638(A)
Otero, J. M., L. Plaza, and F. Salaverri. Absolute thresholds and night myopia—167

Parkinson, W. W., Jr. and Ferd E. Williams. Vacuum ultraviolet monochromator for absorption and photoconductivity measurements on luminescent solids—627(A), 705
Patten, Stanley H. and Ferd E. Williams. Emission spectrum of manganese-activated magnesium germanate—629 (A), 702
Pearlman, D., P. E. Goddard, and F. Urbach. Simplified Lenard phosphors—628(A), 695
—— (see Nail, N. R.)—628(A), 690
—— (see Urbach, F.)—628(A), 675

Peck, E. R. (see Sittner, W. R.)—474, 544, 635(A)
Peckham, R. H. Measurement of the luminescence of fluoroscopic x-ray screens—626(A), 714
—— Visual acuity through various types and grades of sun glass lenses—1057(A)
Penner, S. S. Radiant heat transfer to receivers moving along the axis of a right circular cylindrical chamber—200(L)
Petersen, E. W., H. H. Grossman, J. L. Saunderson, and V. J. Caldecourt. Electrical tristimulus integrator—1055(A)
—— (see Grossman, H. H.)—261
Petrie, G. R. (see Coulman, C. E.)—612(L)
Pfund, A. H. High index refractometer—966
Pittenger, J. T. (see Shenstone, A. G.)—219
Pittman, M. A. (see Billings, Bruce H.)—978
Plank, William C. Non-intermittent motion picture projection—505(L)
Platt, John R. Further remarks on the Stiles-Crawford effect—614(L)
Plaza, Lorenzo (see Judd, Deane B.)—1056(A)
—— (see Otero, J. M.)—167
Plyler, Earl K. (see Tilton, Leroy W.)—1060(A)
Plymale, W. S., Jr. and L. H. Dawson. Photometric evaluation of luminous materials for naval uses—626(A), 712
Polster, Harry D. Reflection from a multilayer filter—1038
—— Dielectric interferometer filter—1054(A)
—— (see Gee, Alan E.)—1054(A)
Prescott, Rochelle (see Gayhart, E. L.)—546
Price, George R. Fluorescence studies of plutonium and neptunium—1054(A)
——**, Renato J. Ferretti, and Samuel Schwartz.** Fluorophotometric determination of uranium—1053(A)
——**, Renato J. Ferretti, and Samuel Schwartz.** Sensitive fluorophotometers—1053(A)

Rakus, A. B. (see Huber, R. L.)—873
Rank, D. H. and J. P. McKelvey. Study of the mechanism of modified Rayleigh scattering—762
——**, Paul Yoder, Jr., and Joseph Vrabel.** Sensitivity of a rapid test for high speed parabolic mirrors—36
Ray, Kamalesh. On the mechanism of optical polishing—92(L)
Richartz, M., and Hsien-Yü Hsü. Analysis of elliptical polarization—136
Rider, Myrtle (see Kivenson, Gilbert)—484
Riggs, Lorrin A., Richard N. Berry, and Matthew Wayner. Comparison of electrical and psychophysical determinations of the spectral sensitivity of the human eye—427
Rood, Joseph L. Some properties of thin evaporated films on glass—854
Rosenbaum, Alma (see Studer, Frank J.)—627(A), 685
Rosenberger, Harold E. (see Coleman, Howard S.)—515, 990
Roth, Albert (see Kivenson, Gilbert)—484
Rouard, P. (see Jacquinot, P.)—1048(L)
Rupert, C. S. and John Strong. Carbon arc as an infra-red source—1060(A)

Safonov, George and Robert Graham. Prismatic properties of ophthalmic lenses—406
Salaverri, F. (see Otero, J. M.)—167
Saunderson, J. L. (see Grossman, H. H.)—261
—— (see Peterson, E. W.)—1055(A)
Sayama, Yoshihiro. Optical theory of the spectral sensitivity of a caesium oxide photo-cathode—162
Saylor, Charles Proffer, Arthur T. Brice, and F. Zernike. Color phase contrast: requirements and applications—1053(A)
Schawlow, A. L. (see Crawford, M. F.)—888(L)
Scheraga, Harold A., Marcus E. Hobbs, and Paul M. Gross. Relative measurement of Kerr constants—410(L)
Schreiber, T. (see Green, Milton)—1058(A)
Schwartz, Samuel (see Price, George R.)—1053(A), 1053(A)
Scolnik, R. (see Koomen, M.)—370
Scott, F. R., R. H. Thompson, and R. T. Ellickson. Inertia effects in infra-red sensitive phosphors—64
Scott, Noel W. (see Hass, Georg)—179
Scribner, B. F. Effect of gaseous atmospheres on excitation in emission spectroscopy—1059(T)
—— (see Meggers, William F.)—1059(A)
—— **and J. T. Pittenger.** Cadmium spectra—219
Shlaer, Simon (see Hecht, Selig)—922
Shrader, R. E. Temperature-dependent structure of the emission spectra of two crystalline forms of the zinc silicate: Mn phosphor—629(A), 699
Shurcliff, William A. Multi-slit double monochromator using no moving parts—1048(L)
—— **and R. Clark Jones.** Trapping of fluorescent light produced within objects of high geometrical symmetry—912
—— **and E. I. Stearns.** New "offset" method of interpreting spectrophotometric curves—72
Sihvonen, Y. T., D. L. Fry, R. E. Nusbaum, and R. R. Baumgartner. Spectrographic analysis of high cobalt (vitallium) alloys—257
Silverman, Shirleigh. Determination of flame temperatures by infra-red radiation—275
—— **and R. C. Herman.** Infra-red emission spectra of the oxy-hydrogen and oxy-deuterium flames—216
—— (see Bullock, B. W.)—200(L)
Sinclair, D. A. Characteristics of pulsed arcs in spectrochemical analysis. Part I: zinc alloys—958
Sittner, W. R. and E. R. Peck. Spectra of argon, krypton, and xenon between 1.2 and 2.2 microns—474, 635(A)
—— **and E. R. Peck.** Recording interferometer for precision wave-length determinations—544
Smakula, Alexander and Myron W. Klein. Plastic deformation and crystal orientation of thallium halides—445; Erratum—890(L)
Smit, N. W. and F. A. Kröger. Luminescence of zinc sulfide activated by lead—661
Smith, Daniel and Marie M. Mahoney. Preparation and application of reproducible gloss standards—86
Sponer, H. and D. S. Lowe. Absorption spectrum of benzotrifluoride vapor in the near ultraviolet—840
—— (see Kohn, Hedwig)—75
Stearns, E. I. (see Gabel, Joseph W.)—481
—— (see Shurcliff, W. A.)—72
Stempel, Waldemar M. Erratum: A differential adjustment method of refining optical systems—199
Stephens, Robert E. (see Tilton, Leroy W.)—1060(A)
Stickney, M. E. (see Miller, W. C.)—377
Stockbarger, Donald C. Artificial fluorite—731
Strain, D. C. (see Miller, W. C.)—377
Strong, John. Resolving power limitations of grating and prism spectrometers—320
—— (see Rupert, C. S.)—1060(A)
Strong, H. M. (see Bundy, F. P.)—393; Addendum—698
Studer, Frank J. and Gorton R. Fonda. Optical properties of calcium silicate phosphors—655
—— **and Alma Rosenbaum.** Phosphorescence decay of halophosphates and other doubly activated phosphors—627(A), 685
Sweet, A. L. (see Bartlett, N. R.)—470

Tardy, P. A. (see Cornu, A. F.)—613(L)
Terrien, J. On the standard source for low level photometry—888(L)

Thompson, R. H. (see Scott, F. R.)—64
Tilton, Leroy, W., Earl K. Plyler, and Robert E. Stephens. Refractive index of silver chloride for visible and infra-red radiant energy—1060(A)
Timma, D. L. Spark spectra of elements 43 and 61—898
—— (see Brode, Wallace R.)—478
Tomkins, Frank S. and Mark Fred. Spectra of the heavy elements—357, 637(A)
Tousey, R. (see Koomen, M.)—370
Tyler, John E. Optimum absorption—264(L)

Urbach, F., N. R. Nail, and D. Pearlman. Asymptotic behavior of spontaneous and forced decay—628(A), 675
——**, N. R. Nail, and D. Pearlman.** Observation of temperature distributions and of thermal radiation by means of non-linear phosphors—1011
—— (see Nail, N. R.)—628(A), 690
—— (see Pearlman, D.)—628(A), 695

van Heel, A. C. S. High precision measurements with simple equipment—1054(T)
Vašiček, Antonin. Reflecting power of glass with a thin and with a thick film—409(L)
Vrabel, Joseph (see Rank, D. H.)—36

Wagman, Irving H. Book review—264
Wald, George. Eye and the camera—1057(T)
Walker, Marshall J. (see Coleman, Howard S.)—515
Warga, Mary E. Book review—911
Wayner, Matthew (see Riggs, Lorrin A.)—427
Weaver, K. S. Provisional standard observer for low level photometry—278
Webb, Julian H. Study of low intensity reciprocity law failure in photographic exposure—1058(A)
West, C. D. and A. S. Makas. Spectral dispersion of birefringence, especially of birefringent plastic sheets—791
—— (see Blake, R. P.)—1054(A)
Weyl, W. A. and A. I. Cramer. Photosensitivity of mechanical mixtures of non-sensitive compounds—889(L)
—— **and D. P. Enright.** Photosensitivity of metal halides as affected by adsorbed ions—889(L)
White, Harvey E. Book review—412
Wilber, D. T. Phosphorescent response to sinusoidal excitation—627(A), 673
Wilcock, W. L. On a paper by Vašiček concerning reflection from multilayer films—889(L)
Wilkins, J. Ernest, Jr. (see Osterberg Harold—553
Williams, Ferd E. Review of the interpretations of luminescence phenomena—648
—— (see Johnson, James S., Jr.)—629(A), 709
—— (see Parkinson, W. W., Jr.)—627(A), 705
—— (see Patten, Stanley H.)—629(A), 702
Williams, Franklin C. Objectives and methods of density measurement in color film sensitometry—1058(A)
Williams, Stanley B. Visibility on cathode-ray tube screens: viewing angle—782
—— (see Bartlett, N. R.)—463
Williamson, D. E. Infra-red interference filter used in calibration—613(L)
Windle, M. (see Magrun, W.)—1060(A)
Wissler, Franklyn C. (see Osterberg, Harold)—558, 638(A)
Wolf, E. (see Linfoot, E. H.)—752
Wolfe, R. A. (see Enns, J. H.)—298
Woodruff, J. F. Use of briquetted samples in the spectrochemical analysis of carbon and alloy steels and other metals—1061(A)
Woodson, Robert A. Fresnel diffraction near a narrow slit —1059(A)
Wooters, Glenn. Establishment of lens centering tolerances —1059(A)

Yoder, Paul, Jr. (see Rank, D. H.)—36
Young, F. Mansfield (see Hardy, Arthur C.)—265, 638(A)
—— (see Hardy, Arthur C.)—460, 634(A)

Zernike, Frits. New method for the accurate measurement of phase differences—1059(A)
—— (see Saylor, Charles Proffer)—1053(A)

JOURNAL OF THE OPTICAL SOCIETY OF AMERICA VOLUME 39, NUMBER 12 DECEMBER, 1949

Analytic Subject Index to Volume 39

References with (A) are to abstracts of papers presented at meetings of the Optical Society of America.
(L) designates Letters to the Editor.

Absorption, including absorption spectra
  Absorption spectrum of benzotrifluoride vapor in the near ultraviolet, H. Sponer and D. S. Lowe—840
  Absorption spectrum of 1,2,4-trichlorobenzene in the near ultraviolet, Hedwig Kohn and H. Sponer—75
  High members of the principal series in caesium, J. Rand McNally, Julius P. Molnar, William J. Hitchcock, and Norman F. Oliver—57
  Infra-red absorption analyses used in control of a pilot-plant process, D. L. Fry—402
  Infra-red absorption spectra of ten substituted methanes, Earle K. Plyler and W. S. Benedict—635(A)
  Optimum absorption, John E. Tyler—264(L)
  Presentation of absorption spectra data, Wallace R. Brode —1022
  Some new techniques in the construction of spectrographic absorption cells, Gilbert Kivenson, Albert Roth, and Myrtle Rider—484
  Vacuum ultraviolet monochromator for absorption and photoconductivity measurements on luminescent solids, W. W. Parkinson, Jr. and Ferd E. Williams—705, 627(A)
Announcements
  Electronics for spectroscopists—983
  Inauguration, George Eastman House—993

Announcements (continued)
  In memoriam:
    A. Herman Pfund—325
    Frank Benford—325
  Installation of the New England Section of the Optical Society of America, 566
  International Commission of Optics—486
  Inter-Society Color Council—Seventeenth Annual Meeting—56
  London Conference on Optical Instruments, July, 1950—1037
  Notice of election of officers of the Optical Society of America—326
  Physics Abstracts—277, 887
  Publication costs and a new format, editorial comment—93
  Symposium on fine particles and resolution—405
  Symposium on molecular structure and spectroscopy—202
  Symposium on spectroscopic light sources—186
  Table of sines and cosines to fifteen decimal places at hundredths of a degree—781

Biological applications
  Chromaticity confusions of color defectives, Dean Farnsworth—1056(A)
  Color perceptions of deuteranopic and protanopic observers, Deane B. Judd—252
  Comment on the note entitled "Retinal cones as dielectric antennas," Brian O'Brien—324(L)
  Physiological and pharmacological studies of blood from x-ray personnel, David I. Macht, Marcus Ostro, and Stanley H. Macht—632(A)
  Retina cones as dielectric antennas, G. Toraldo di Francia—324(L)
  Spectrophotometric studies of living human skin in the ultraviolet, Seibert Q. Duntley, Edward A. Edwards, and Nisson A. Finkelstein—1056(A)
  Standard response functions for protanopic and deuteranopic vision, Deane B. Judd—505(L)
  Tritanopia with abnormally heavy ocular pigmentation, Deane B. Judd and Lorenzo Plaza—1056(A)
Book reviews
  Absorption spectrophotometry, by G. F. Lothian, Wallace R. Brode—528
  Atomic energy levels—as derived from the analysis of optical spectra, prepared at the National Bureau of Standards, Harvey E. White—412
  Comparative list of color terms, compiled by Sidney M. Newhall and Josephine G. Brennan, Deane B. Judd—765
  High current carbon arc, by Wolfgang Finkelnburg, Henry Margenau—489
  Physical aspects of color, by P. J. Bouma, Herbert E. Ives—297
  Spectrographic analysis of soils, plants, and related materials, by R. L. Mitchell, Mary Warga—911
  Vision and the eye, by M. H. Pirenne, Irving H. Wagman—264

Color and colorimetry
  Apparent colors of surfaces of small subtense—a preliminary report, W. E. Knowles Middleton and Marian C. Holmes—582, 631(A)
  Calculation of subtractive color mixtures, H. R. Davidson—1056(A)
  Chromaticity confusions of color defectives, Dean Farnsworth—1056(A)
  Color correction in optical systems and types of glass, M. Herzberger and H. Jenkins—1058(A)
  Colorimetry by abridged spectrophotometry, Arthur C. Hardy and Mansfield Young—460, 634(A)
  Colorimetric analysis of dye mixtures, David L. MacAdam—22
  Colors of natural objects and terrains, and their relation to visual color deficiency, Charles D. Hendley and Selig Hecht—630(A), 870
  Color perceptions of deuteranopic and protanopic observers, Deane B. Judd—252
  Color phase contrast: requirements and applications, Charles Proffer Saylor, Arthur T. Brice, and F. Zernike—1053(A)
  Color translating ultraviolet microscopy and ultraviolet spectrophotometry, Elkan R. Blout and Miriam S. Flower—636(A)
  Comparison of color systems with respect to uniform visual spacing, Robert W. Burnham—387
  Comparison of direct colorimetry of titanium pigments with their indirect colorimetry based on spectrophometry and a standard observer, Deane B. Judd—945
  Continuous, automatic tristimulus integrator for use with the recording spectrophotometer, H. R. Davidson and L. W. Imm—633(A), 942
  Design of a daylight filter for color film sensitometry, R. H. Bingham—633(A)
  Diagnosing types of color deficiency by means of pseudoisochromatic tests, Alphonse Chapanis—242
  Electrical tristimulus integrator, E. W. Peterson, H. H. Grossman, J. L. Saunderson, and V. J. Caldecourt—1055(A)
  Measurement of the influence of local adaptation on color matching, David L. MacAdam—454, 631(A)
  Metameric colors and macular pigment, Walter C. Granville and Deane B. Judd—632(A)
  Methods of color translation, R. Clark Jones—636(A)
  Munsell renotations used to study color space of Hunter and of Adams, Dorothy Nickerson—1055(A)
  On some aspects of white, gray, and black, Ralph M. Evans—774
  Plochere color system: a descriptive analysis, W. E. Knowles Middleton—633(A)
  Ridgway color standards with a Munsell notation key, D. H. Hamly—592, 633(A)
  Secondary color in optical relay systems, R. E. Hopkins—919, 1059(A)
  Subtractive color reproduction. The approximate reproduction of selected colors, W. L. Brewer, W. T. Hanson, Jr., and C. A. Horton—924
  Tristimulus computation in the dyestuff and textile field, I. H. Godlove—633(A)
  Tritanopia with abnormally heavy ocular pigmentation, Deane B. Judd and Lorenzo Plaza—1056(A)
  Visual sensitivities to combined chromaticity and luminance differences, W. R. J. Brown and D. L. MacAdam—808

Densitometry
  Objectives and methods of density measurement in color film sensitometry, Franklin C. Williams—1058(A)
  Optical and electrical alterations to a Michigan microphotometer, H. H. Grossman, E. W. Peterson, J. L. Saunderson, and V. J. Caldecourt—261
  Photoelectric reflection-transmission densitometer, R. L. Huber and A. B. Rakus—873
Dispersion
  Spectral dispersion of birefringence, especially of birefringent plastic sheets, C. D. West and A. S. Makas—791

Electro-optics
  Electro-optic effect in uniaxial crystals of the type X H_2PO_4. I. Theoretical, Bruce H. Billings—797

Electro-optic effect in uniaxial crystals of the type XH_2PO_4. II. Experimental, Bruce H. Billings—802

Eye

Absolute thresholds and night myopia, J. M. Otero, L. Plaza, and F. Salaverri—167
Coefficient of specific resolution of the human eye for Foucault test objects viewed through circular apertures, Howard S. Coleman, Madeline F. Coleman, David L. Fridge, and Samuel W. Harding—766
Comment on the note entitled "Retinal cones as dielectric antennas," Brian O'Brien—324(L)
Comment on a "Note on the photo-pupil reflex," Henry A. Knoll—954(L)
Comparison of electrical and psychophysical determinations of the spectral sensitivity of the human eye, Lorrin A. Riggs, Richard N. Berry, and Matthew Wayner—427
Course of foveal light adaptation measured by the threshold intensity increment, Howard DeHaven Baker—172
Eye movements and the variation of visual acuity with test object orientation, W. R. J. Brown—1057(A)
Focusing wave-length for white light, A. Ivanoff—718(L)
Functional analysis of regional differences in the human fovea, Walter R. Miles—630(A)
Further remarks on the Stiles-Crawford effect, John R. Platt—614(L)
Microwave test of a theory of the Stiles and Crawford effect, J. N. Jean and Brian O'Brien—1057(A)
Note on the photo-pupil reflex, Jules de Launay—364
Prismatic properties of ophthalmic lenses, George Safonov and Robert Graham—406
Retina cones as dielectric antennas, G. Toraldo di Francia—324(L)
Spherical aberration of the eye, M. Koomen, R. Tousey, and R. Scolnik—370
Standard response functions for protanopic and deuteranopic vision, Deane B. Judd—505(L)
Steadiness of the eye, Lorrin A. Riggs and Floyd Ratliff—630(A)
Threshold gradient of rods and cones, in the dark-adapted and in the partially light-adapted eye, Louise L. Sloan—630(A)

Filters

Birefringent filter, John W. Evans—229, a correction—412
Design of a daylight filter for color film sensitometry, R. H. Bingham—633(A)
Dielectric interferometer filter, Harry D. Polster—1054(A)
Experimental study of Dennison-Hadley infra-red reflection filters, E. E. Barr—634(A)
Experimental study of Turner frustrated total reflection filters in the infra-red, B. H. Billings—634(A)
Frustrated total reflection filter for the infra-red, Bruce H. Billings and M. A. Pittman—978
Infra-red interference filter used in calibration, D. E. Williamson—613(L)
Infra-red transmitting filters, E. R. Blout, R. S. Corley, and P. L. Snow—634(A)
Reflection from a multilayer filter, Harry D. Polster—1038

Fluorescence and phosphorescence

Asymptotic behavior of spontaneous and forced decay, F. Urbach, N. R. Nail, and D. Pearlman—628(A), 675
Characteristics of fluorescent emission under near ultraviolet radiation, C. E. Barnett and L. D. Grady—627(A)
Correlation between cathodoluminescence efficiency and decay as a function of temperature, Richard H. Bube—628(A), 681
Emission characteristics of fluorescent pigments, C. E. Barnett and L. D. Grady—663
Emission spectrum of manganese-activated magnesium germanate, Stanley H. Patten and Ferd E. Williams—629(A), 702
Fluorescence studies of plutonium and neptunium, George R. Price—1054(A)
Inertia effects in infra-red sensitive phosphors, F. R. Scott, R. H. Thompson, and R. T. Ellickson—64
Intrinsic efficiency of the cathodoluminescence process, R. L. Longini—877
Luminescence of photo-conducting phosphors, G. F. J. Garlick and A. F. Gibson—935
Luminescence of zinc sulfide activated by lead, N. W. Smit and F. A. Kröger—661
Measurement of the luminescence of fluoroscopic x-ray screens, R. H. Peckman—626(A), 714
Multibanded emission spectra of zinc-cadmium sulfide phosphors, W. H. Byler—91(L)
New observations on superlinear luminescence, N. R. Nail, F. Urbach, and D. Pearlman—628(A), 690
Observation of temperature distributions and of thermal radiation by means of non-linear phosphors, F. Urbach, N. R. Nail, and D. Pearlman—1011
Optical and electrical properties of zinc silicate phosphors, Elemér Nagy—42, 628(A)
Optical properties of calcium silicate phosphors, Frank J. Studer and Gorton R. Fonda—655
Phosphorescence decay of halophosphates and other doubly activated phosphors, Frank J. Studer and Alma Rosenbaum—627(A), 685
Phosphorescent response to sinusoidal excitation, D. T. Wilber—627(A), 673
Photo-conductivity in crystal phosphors, Rudolf Frerichs—1053(A)
Photometric evaluation of luminous materials for naval uses, W. S. Plymale, Jr. and L. H. Dawson—626(A), 712
Review of the interpretations of luminescence phenomena, Ferd E. Williams—648
Rise in brightness of infra-red sensitive phosphors, Robert C. Herman and Charles F. Meyer—729
Simplified Lenard phosphors, D. Pearlman, P. E. Goddard, and F. Urbach—628(A), 695
Sodium and lithium as activators of fluorescence in zinc sulfide, F. A. Kröger—670
Some applications of non-linear phosphors, Franz Urbach, Nelson R. Nail, and Donald Pearlman—629(A)
Survey of present methods used to determine the optical properties of phosphors, Wayne B. Nottingham—641
Temperature-dependent structure of the emission spectra of two crystalline forms of the zinc silicate: Mn phosphor, R. E. Shrader—629(A), 699
Thermoluminescence of manganese-activated zinc fluoride phosphors, James S. Johnson, Jr. and Ferd E. Williams—629(A), 709
Vacuum ultraviolet monochromator for absorption and photo-conductivity measurements on luminescent solids, W. W. Parkinson, Jr. and Ferd E. Williams—627(A), 705
Visual sensitivities of combined chromaticity and luminance differences, W. R. J. Brown and D. L. MacAdam—808

Glass, properties of

Index of refraction and coefficients of expansion of optical glasses at low temperatures, Fred A. Molby—600

Illumination

Green segment seen from an airplane, E. O. Hulburt—409(L)
Night sky brightness measurements in latitudes below 45°, E. O. Hulburt—211

Illumination (continued)
Some variables influencing vernier acuity. I. Illumination and exposure time. II. Wave-length of illumination, Katherine Eleanor Baker—567
Ultrafrequency excitation of Hg 198 lamps for interferometer illumination, Edward Jacobsen and George R. Harrison—1054(A)

Infra-red
Aberrations in ellipsoidal mirrors used in infra-red spectrometers, J. Rud Nielsen—59
Carbon arc as an infra-red source, C. S. Rupert and John Strong—1060(A)
Determination of flame temperatures by infra-red radiation, Shirleigh Silverman—275
Direct recording of spectra in the region of 1.2μ to 3μ using the lead sulfide photo-conductive cell, R. C. Nelson —68
Experimental study of Dennison-Hadley infra-red reflection filters, E. E. Barr—634(A)
Experimental study of Turner frustrated total reflection filters in the infra-red, B. H. Billings—634(A)
Extensions to the analysis of the infra-red spectra of the noble gases, Curtis J. Humphreys—1059(A)
Frustrated total reflection filter for the infra-red, Bruce H. Billings and M. A. Pittman—978
Improvement in routine analysis with the Beckman I.R. 2 infra-red spectrophotometer by a slight mechanical modification, A. F. Cornu and P. A. Tardy—613(L)
Inertia effects in infra-red sensitive phosphors, F. R. Scott, H. R. Thompson, and R. T. Ellickson—64
Infra-red absorption analyses used in control of a pilot-plant process, D. L. Fry—402
Infra-red absorption spectra of the ten substituted methanes, Earl K. Plyler and W. S. Benedict—635(A)
Infra-red emission spectra of the oxy-hydrogen and oxy-deuterium flames, S. Silverman and R. C. Herman—216
Infra-red interference filter used in calibration, D. E. Williamson—613(L)
Infra-red microspectroscopy, Elkan R. Blout, George R. Bird, and David S. Grey—1052(A)
Infra-red spectrophotometer with cathode-ray display, A. C. Menzies—1061(A)
Infra-red transmitting filters, E. R. Blout, R. S. Corley, and P. L. Snow—634(A)
Low temperature infra-red transmission cell, H. O. McMahon, R. M. Hainer, and Gilbert W. King—786
Molecular-type dichroic film polarizers for 0.75 to 2.8μ-radiations, R. P. Blake, A. S. Makas, and C. D. West—1054(A)
Optical transmission of additively colored alkali halide crystals in the visible and near infra-red, H. Friedman and C. P. Glover—795(L)
Performance of a new double beam infra-red spectrophotometer, John U. White and Max D. Liston—634(A)
Photographic action of x-rays in the 1.3 to 0.01A range, Herman Hoerlin—891
Rapid scanning spectrometer for the near infra-red, B. W. Bullock and S. Silverman—634(A)
Reflectance and transmittance measurements of thin evaporated metallic films in the infra-red, Max Oldham—634(A)
Refractive index of silver chloride for visible and infra-red radiant energy, Leroy W. Tilton, Earl K. Plyler, and Robert E. Stephens—1060(A)
Rise in brightness of infra-red sensitive phosphors, Robert C. Herman and Charles F. Meyer—729
Spectra of argon, krypton, and xenon between 1.2 and 2.2 microns, W. R. Sittner and E. R. Peck—474, 635(A)
Use of polytrifluorochloroethylene in infra-red and Raman spectroscopy, J. S. Kirby-Smith and Ernest A. Jones—780

Intensity measurements
Effect of finite aperture on the fringe intensity distribution of Fabry Perot interferometers, Felix E. Geiger, Jr.—249
Influence of extraneous elements on line intensity. IV. Extraneous element effects in the direct-current arc, Wallace R. Brode and Donald L. Timma—478
Method of measuring high intensities at the focus of a parabolic reflector with large relative aperture, George E. Davis—541

Interference
Dielectric interferometer filter, Harry D. Polster—1054 (A)
Effect of finite aperture on the fringe intensity distribution of Fabry Perot interferometers, Felix E. Geiger, Jr.—249
Haidinger fringes in a basal section of calcite, Bruce H. Billings—39
Infra-red interference filter used in calibration, D. E. Williamson—613(L)
Instrumental and Doppler broadening in the Fabry Perot interference pattern of close doublets, P. M. Griffin and J. R. McNally, Jr.—636(A)
Interference phenomenon in the schlieren system, E. L. Gayhart and Rochelle Prescott—546
Recording interferometer for precision wave-length determinations, W. R. Sittner and E. R. Peck—544
Transmission and reflection coefficients of aluminum films for interferometry, M. F. Crawford, W. M. Gray, A. L. Schawlow, and F. M. Kelly—888(L)
Ultrafrequency excitation of Hg 198 lamps for interferometer illumination, Edward Jacobsen and George R. Harrison—1054(A)

Lenses and mirrors
Aberrations in ellipsoidal mirrors used in infra-red spectrometers, J. Rud Nielsen—59
Analysis of para-elliptic reflector, Benjamin Goldberg and Nels C. Benson—497, 631(A)
Comparison of lens radii, G. A. Harle—718(L)
Method of measuring the contrast rendition of telescopic systems, Howard S. Coleman, George W. Arnold, Jr., and Walter D. Luedecke—864
Method of measuring high intensities at the focus of a parabolic reflector with large relative aperture, George E. Davis—541
Oblique reflecting systems, Bernard S. Lee—487
On the preparation of hard oxide films with precisely controlled thickness on evaporated aluminum mirrors, Georg Hass—532, 632(A)
Prismatic properties of ophthalmic lenses, George Safonov and Robert Graham—406
Sensitivity of rapid test for high speed parabolic mirrors, D. H. Rank, Paul Yoder, Jr., and Joseph Vrabel—36
Seventy-two-inch high vacuum evaporator and its glow discharge equipment, Nels C. Benson, Georg Hass, and Noel W. Scott—632(A)
Silicon monoxide protected front-surface mirrors, Georg Hass and Noel W. Scott—179
Some notes on the designing of aspherical magnifiers for binocular vision, C. E. Coulman and G. R. Petrie—612(L)
X-ray optics: imperfections of optical flats and their effect on the reflection of x-rays, W. Ehrenberg—746

Letters to the Editor
Combustion studies with the orthicon spectrograph, J. T. Agnew, R. G. Franklin, R. E. Benn, and A. Bazarian—409

Comment on a "Note on the photo-pupil reflex," Henry A. Knoll—954
Comment on the note entitled "Retinal cones as dielectric antennas," Brian O'Brien—324
Comparison of lens radii, G. A. Harle—718
Focusing wave-length for white light, A. Ivanoff—718
Further remarks on the Stiles-Crawford effect, John R. Platt—614(A)
Green segment seen from an airplane, E. O. Hulburt—409
Improvement in routine analysis with the Beckman I.R. 2 infra-red spectrophotometer by a slight mechanical modification, A. F. Cornu and P. A. Tardy—613
Infra-red interference filter used in calibration, D. E. Williamson—613
International colloquium on solid thin films, P. Jacquinot and P. Rouard—1048
Light quanta and vision, Hl. de Vries—201
Mount for a Perot Fabry interferometer without etalon ring, Heinz Haber—1050
Multibanded emission spectra of zinc-cadmium sulfide phosphors, W. H. Byler—91
Multi-slit double monochromator using no moving parts, W. A. Shurcliff—1048
Nomograph of HG5461 structure as a function of etalon separation, J. R. McNally, Jr.—1050
Non-intermittent motion picture projection, William C. Plank—505
On a paper by Vašiček concerning reflection from multilayer films, W. L. Wilcock—889
On the mechanism of optical polishing, Kamalesh Ray—92
On the relative measurement of Kerr constants, Harold A. Scheraga, Marcus E. Hobbs, and Paul M. Gross—410
On the standard source for low level photometry, J. Terrien—888
On the utilization of complex optical constants, Frank Matossi—506
Optical transmission of additively colored alkali halide crystals in the visible and near infra-red, H. Friedman and C. P. Glover—795
Optimum absorption, John E. Tyler—264
Photosensitivity of mechanical mixtures of non-sensitive compounds, W. A. Weyl and A. I. Cramer—889
Photosensitivity of metal halides as affected by adsorbed ions, W. A. Weyl and D. P. Enright—889
Radiant heat transfer to receivers moving along the axis of a right circular cylindrical chamber, S. S. Penner—200
Rapid scanning spectrometer for oscillographic recording, B. W. Bullock and S. Silverman—200
Reflecting power of glass with a thin and with a thick film, Antonin Vašiček—409
Retina cones as dielectric antennas, G. Toraldo di Francia—324
Some notes on the designing of aspherical magnifiers for binocular vision, C. E. Coulman and G. R. Petrie—612
Standard response functions for protanopic and deuteranopic vision, Deane B. Judd—505
Transmission and reflection coefficients of aluminum films for interferometry, M. F. Crawford, W. M. Gray, A. L. Schawlow, and F. M. Kelly—888
X-ray images by refractive focusing, Paul Kirkpatrick—796

Light sources, properties and measurements
Air interrupter type spectrographic light source, J. H. Enns and R. A. Wolfe—298
Night sky brightness measurements in latitudes below 45°, E. O. Hulburt—211
Possibility of enhanced Hg^{202} as a source of monochromatic light, J .R. McNally, Jr., P. M. Griffin, and L. E. Burkhart—1036
Trapping of fluorescent light produced within objects of high geometrical symmetry, W. A. Shurcliff and R. Clark Jones—912
Ultraviolet light sources, Charles H. Matz and Dwight P. Merrill—635(A)

Meetings
Minutes of the thirty-third meeting of the Board of Directors of the Optical Society of America, Incorporated—615
Minutes of the thirty-fourth meeting of the Board of Directors of the Optical Society of America, Incorporated—1063
Proceedings of the winter meeting of the Optical Society of America—626
Proceedings of the thirty-fourth annual meeting of the Optical Society of America—1052

Microscopy
Color phase contrast: requirements and applications, Charles Proffer Saylor, Arthur T. Brice, and F. Zernike—1053(A)
Color translating ultraviolet microscopy and ultraviolet spectrophotometry, Elkan R. Blout and Miriam S. Flower—636(A)
Extension of Toraldo's theory of phase contrast, L. Ivan Epstein—1053(A)
Image contrast in phase-contrast microscopy, Paul H. Keck and Arthur T. Brice—507
Infra-red microspectroscopy, Elkan R. Blout, George R. Bird, and David S. Grey—1052(A)
Motion pictures of some optical and electrical effects in barium titanate crystals, Norman J. Field and A. P. DeBretteville, Jr.—1053(A)
New family of microscope objectives, David S. Grey—635(A)
New series of microscope objectives. I. Catadioptric Newtonian systems, David S. Grey and Paul H. Lee—719
New series of microscope objectives. II. Preliminary investigation of catadioptric Schwarzschild systems, David S. Grey—723
Resolution of two particles in a bright field by coated microscope objectives, Harold Osterberg and Franklyn C. Wissler—558, 638(A)
Resolving power of a coated objective. II., J. Ernest Wilkins—638(A)

Optical instruments
Analysis of para-elliptic reflector, Benjamin Goldberg and Nels C. Benson—497
Combustion studies with the orthicon spectrograph, J. T. Agnew, R. G. Franklin, R. E. Benn, and A. Bazarian—409(L)
Direct recording of spectra in the region $1.2\,\mu$ to $3\,\mu$ using the lead sulfide photo-conductive cell, R. C. Nelson—68
Effect of the angular aperture of a telephotometer on the telephotometry of collimated and non-collimated beams, W. E. Knowles Middleton—576
High index refractometer, A. H. Pfund—966
Improved gloss recorder, Richard S. Hunter—1056(A)
Low temperature infra-red transmission cell, H. O. McMahon, R. M. Hainer, and Gilbert W. King—786
Modified schlieren apparatus for large areas of field, Ralph A. Burton—907
New improved refractometer, A. H. Pfund, E. J. Weichel, and B. H. Billings—631(A)

Optical instruments (continued)

New spectrophotometer employing a glass Fery prism, W. C. Miller, G. Hare, D. C. Strain, K. P. George, M. E. Stickney, and A. O. Beckman—377

Oblique reflecting systems, Bernard S. Lee—487

On the relative measurement of Kerr constants, Harold A. Scheraga, Marcus E. Hobbs, and Paul M. Gross—410 (L)

Optical and electrical alterations to a Michigan microphotometer, H. H. Grossman, E. W. Peterson, J. L. Saunderson, and V. J. Caldecourt—261

Photoelectric reflection-transmission densitometer, R. L. Huber and A. B. Rakus—873

Prismatic properties of ophthalmic lenses, George Safonov and Robert Graham—406

Production of diffraction gratings. I. Development of the ruling art, George R. Harrison, 413

Production of diffraction gratings. II. The design of eschelle grating and spectrographs, George R. Harrison —522

Rapid mobile analyzer for minute amounts of lead in air, Henry Aughey—292

Rapid scanning spectrometer for oscillographic recording, B. W. Bullock and S. Silverman—200(L)

Ray tracing with the selective sequence electronic calculator, H. R. J. Grosch—1059(A)

Recording interferometer for precision wave-length determinations, W. R. Sittner and E. R. Peck—544

Reflected light and ghosts in optical systems, Allen E. Murray—30

Relation between entrance and exit pupils of telescopic systems, Irvine C. Garner—638(A)

Resolution of two particles in a bright field by coated microscope objectives, Harold Osterberg and Franklyn C. Wissler—558, 638(A)

Resolving power of a coated objective, Harold Osterberg and J. Ernest Wilkins, Jr.—553

Seventy-two-inch high vacuum evaporator and its glow discharge equipment, Nels C. Benson, Georg Hass, and Noel W. Scott—632(A)

Some new techniques in the construction of spectrographic absorption cells, Gilbert Kivenson, Albert Roth, and Myrtle Rider—484

Some notes on the designing of aspherical magnifiers for binocular vision, C. E. Coulman and G. R. Petrie—612(L)

Transmission of light from diffuse sources by periscope tubes, F. P. Bundy and H. M. Strong—393; Addendum —698

Optical materials

Artificial fluorite, Donald C. Stockbarger—731

Artificial sapphire for optical elements, Robert E. Hopkins and Brian O'Brien—1060(A)

Auxiliary working standard equivalent to magnesium oxide on a General Electric spectrophotometer,, Joseph W. Gabel and E. I. Stearns—481

Birefringent filter, John W. Evans—229

Comparison of lens radii, G. A. Harle—718(L)

Design of a daylight filter for color film sensitometry, R. H. Bingham—633(A)

Emulsion calibration scale for quantitative spectroscopic analysis, Harold K. Hughes and R. W. Murphy—501

Influence of magnification on resolving power of telescopic systems for Foucault test objects of different inherent contrast, Howard S. Coleman, Madeline F. Coleman, and Samuel W. Harding—771

Motion pictures of some optical and electrical effects in barium titanate crystals, Norman J. Field and A. P. DeBretteville, Jr.—1053(A)

On the mechanism of optical polishing, Kamalesh Ray—92(L)

Optical and electrical properties of zinc silicate phosphors, Elemér Nagy—42

Optical properties of calcium silicate phosphors, Frank J. Studer and Gorton R. Fonda—655

Preliminary measurements of the cold flow of silver chloride and thallium bromide-iodide, Lewis S. Combes, James R. Travis, and Stanley S. Ballard—635(A)

Spectral dispersion of birefringence, especially of birefringent plastic sheets, C. D. West and A. S. Makas, 791

Transmission and reflection coefficients of aluminum films for interferometry, M. F. Crawford, W. M. Gray, A. L. Schawlow, and F. M. Kelly—888(L)

Optical Society of America reports

Annual report of the Editor of Publications—615

Annual report of the Secretary of the Optical Society of America, Incorporated, for the calendar year 1948—616

Annual report of the Treasurer of the Optical Society of America—619

Optical testing

Coefficient of specific resolution of the human eye for Foucault test objects viewed through circular apertures, Howard S. Coleman, Madeline F. Coleman, David L. Fridge, and Samuel W. Harding—766

Contrast discrimination charts for demonstrating the effect of anoxia on vision, Selig Hecht, Charles D. Hendley, Sylvia Frank and Simon Shlaer—922

Differential adjustment method of refining optical system; Erratum, Waldemar M. Stempel—199

Experimental studies of the reduction of apparent contrast by water, Seibert Q. Duntley—629(A)

Measurement of meteorological range in water, Seibert Q. Duntley—630(A)

On the mechanism of optical polishing, Kamalesh Ray—92(L)

On the relative measurement of Kerr constants, Harold A. Scheraga, Marcus E. Hobbs, and Paul M. Gross—410 (L)

Preparation and application of reproducible gloss standards, Daniel Smith and Marie M. Mahoney—86

Optics, general

Artificial sapphire for optical elements, Robert E. Hopkins and Brian O'Brien—1060(A)

Coma of slightly decentered wide aperture systems, L. Ivan Epstein—631(A)

Electrical and optical properties of zinc silicate phosphors, Elemér Nagy—628(A)

Low temperature radiation pyrometry in industry, J. C. Mouzon and C. A. Dyer—203

New classification system for radiation detectors, R. Clark Jones—327

On the mechanism of optical polishing, Kamalesh Ray—92(L)

On the utilization of complex optical constants, Frank Matossi—506(L)

Optical characteristics of sheets of scattering materials, R. L. Longini—551

Optical properties of calcium silicate phosphors, Frank J. Studer and Gorton R. Fonda—655

Optical theory of the spectral sensitivity of a caesium oxide photo-cathode, Yoshihiro Sayama—162

Optical transmission of additively colored alkali halide crystals in the visible and near infra-red, H. Friedman and C. P. Glover—795(L)

Reflected light and ghosts in optical systems, Allen E. Murray—30

Relation between entrance and exit pupils of telescopic systems, Irvine C. Gardner—638(A)

Secondary color in optical relay systems, Robert E. Hopkins—1059(A)

Solar spectroscopy with a Cashman cell, Robert R. McMath and Orren C. Mohler—903

Some notes on the designing of aspherical magnifiers for binocular vision, C. E. Coulman and G. R. Petrie—612(L)

Spectral dispersion of birefringence, especially of birefringent plastic sheets, C. D. West and A. S. Makas—791

Transmission and reflection coefficients of aluminum films for interferometry, M. F. Crawford, W. M. Gray, A. L. Schawlow, and F. M. Kelly—888(L)

Transmission of light from diffuse sources by periscope tubes, F. P. Bundy and H. M. Strong—393; Addendum—698

X-ray optics: imperfections of optical flats and their effect on the reflection of x-rays, W. Ehrenberg—746

X-ray optics: the production of converging beams by total reflection, W. Ehrenberg—741

Optics, geometrical

Aberrations of slightly decentered optical systems, L. Ivan Epstein—847

Correction of slit-width errors, Arthur C. Hardy and F. Mansfield Young—265, 638(A)

Direct calculation of achromatized and corrected optical systems, Ernesto E. Geiger—193

Establishment of lens centering tolerances, Glenn Wooters—1059(A)

Fraunhofer diffraction patterns of squares and rectangles, Edward S. Lamar—929

Fresnel diffraction near a narrow slit, Robert A. Woodson—1059(A)

General theory of isoplanatism for finite aperture and field, Mario Di Jorio—305

New method for the accurate measurement of phase differences, Frits Zernike—1059(A)

Optical characteristics of sheets of scattering materials, R. L. Longini—551

Ray tracing with the selective sequence electronic calculator, H. R. J. Grosch—1059(A)

Resolution of two particles in a bright field by coated microscope objectives, Harold Osterberg and Franklyn C. Wissler—558, 638(A)

Resolving power of a coated objective, Harold Osterberg and J. Ernest Wilkins, Jr.—553

Transmission of light from diffuse sources by periscope tubes, F. P. Bundy and H. M. Strong—393; Addendum—698

Trapping of fluorescent light produced within objects of high geometrical symmetry, W. A. Shurcliff and R. Clark Jones—912

Optics, physical

Analysis of elliptical polarization, M. Richartz and Hsein-Yü Hsü—136

Anomalous rotational isotope effect in mercury hydride, S. Mrozowski—1061(A)

Formation of fringes in a babinet compensator, H. G. Jerrard—1031

Haidinger fringes in a basal section of calcite, Bruce H. Billings—39

Lorentz-type transformations as derived performable rod and clock operations, Herbert E. Ives—757

Measurement of meteorological range in water, Seibert Q. Duntley—630(A)

On the relative measurement of Kerr constants, Harold A. Scheraga, Marcus E. Hobbs, and Paul M. Gross—410(L)

On the utilization of complex optical constants, Frank Matossi—506(L)

Orientation of methylene blue molecules adsorbed on solids, Scott Anderson—49

Plastic deformation and crystal orientation of thallium halides, Alexander Smakula and Myron W. Klein—445; Erratum—890(L)

Remarks on the classical and quantum-mechanical treatment of partial polarization, U. Fano—859

Scattered and rescattered sunlight, A. Hammad—157

Scattering cross section of water drops in air for visible light, H. C. Houghton and W. R. Chalker—955

Study of the mechanism of modified Rayleigh scattering, D. H. Rank and J. P. McKelvey—762

Photoelectricity

Comparison of photographic and photoelectric measurements of atmospheric attenuation of brightness contrast, Howard S. Coleman and Harold E. Rosenberger—990

Photo-conductivity of crystal phosphors, Rudolf Frerichs—1053(A)

Photoelectric method of measuring the atmospheric attenuation of brightness contrast along a horizontal path for the visible region of the spectrum, Howard S. Coleman, Fred J. Morris, Harold E. Rosenberger, and Marshall J. Walker—515

Photoelectric reflection-transmission densitometer, R. L. Huber and A. B. Rakus—873

Photography, including cameras

Analytical equation of the emulsion calibration curve of photographic photometry, Milton Green and T. Schreiber—1058(A)

Camera shutters, Amrom H. Katz—1

Comparison of photographic and photoelectric measurements of atmospheric attenuation of brightness contrast, Howard S. Coleman and Harold E. Rosenberger—990

Dependence of the sensitivity of unsensitized photographic emulsions upon temperature, M. Biltz—994

Design of a daylight filter for color film sensitometry, R. H. Bingham—633(A)

Herschel effect and the structure and stability of the photographic latent image, G. Kornfeld—490

Latent image distribution by x-ray exposures, G. Kornfeld—1020

Non-intermittent motion picture projection, William C. Plank—505(L)

Objectives and methods of density measurement in color film sensitometry, Franklin C. Williams—1058(A)

On the corrector plates of Schmidt cameras, E. H. Linfoot and E. Wolf—752

Photogrammetric errors from camera lens decentering, P. D. Carman—632(A), 951

Photographic action of x-rays in the 1.3 to 0.01A range, Herman Hoerlin—891

Photographic spectral sensitometry with a biprism, Willoughby M. Cady and Gary Gordon—368

Photographing spectra in the vacuum ultraviolet, A. L. Schoen and Edwin S. Hodge—637(A)

Photosensitivity of mechanical mixtures of non-sensitive compounds, W. A. Weyl and A. I. Cramer—889(L)

Photosensitivity of metal halides as affected by adsorbed ions, W. A. Weyl and D. P. Enright—889(L)

Some remarks on gold treatment of photographic silver halide emulsions, F. W. H. Mueller—494, 639(A)

Study of low intensity reciprocity law failure in photographic exposure, Julian H. Webb—1058(A)

Sunlight and skylight as determinants of photographic exposure II. Scene structure, directional index, photographic efficiency of daylight, safety factors, and evaluation of camera exposure, Loyd A. Jones and H. R. Condit—94

Photometry

Analytical equation of the emulsion calibration curve of photographic photometry, Milton Green and T. Schreiber—1058(A)

Photometry (continued)
Multi-slit spectrometry, Marcel J. E. Golay—437
On the standard source for low level photometry, J. Terrien—888(L)
Orientation of methylene blue molecules adsorbed on solids, Scott Anderson—49
Photoelectric method of measuring the atmospheric attenuation of brightness contrast along a horizontal path for the visible region of the spectrum, Howard S. Coleman, Fred J. Morris, Harold E. Rosenberger, and Marshall J. Walker—515
Photometric evaluation of luminous materials for Naval uses, W. S. Plymale, Jr. and L. H. Dawson—626(A), 712
Preparation and application of reproducible gloss standards, Daniel Smith and Marie M. Mahoney, 86
Provisional standard observer for low level photometry, K. S. Weaver—278
Spectral dispersion of birefringence, especially of birefringent plastic sheets, C. D. West and A. S. Makas—791

Polarization
Analysis of elliptical polarization, M. Richartz and Hsien-Yü Hsü—136
Molecular-type dichroic film polarizers for 0.75 to 2.8 mμ radiations, R. P. Blake, A. S. Makas, and C. D. West—1054(A)
On the possibility of a spathic polarizer which transmits more than one-half of the incident unpolarized light, R. Clark Jones—1058(A)
Orientation of methylene blue molecules adsorbed on solids, Scott Anderson—49
Remarks on the classical and quantum-mechanical treatment of partial polarization, U. Fano—859

Pyrometry
Determination of flame temperatures by infra-red radiation, Shirleigh Silverman—275
Low temperature radiation pyrometry in industry, J. C. Mouzon and C. A. Dyer—203
Measurement of flame temperatures, Curtis J. Humphreys and Earle K. Plyler—639(A)
Observation of temperature distributions and of thermal radiation by means of non-linear phosphors, F. Urbach, N. R. Nail, and D. Pearlman—1011
Pyrometer for measurement of instantaneous temperatures of flames, J. H. Hett and J. B. Gilstein—909
Radiant heat transfer to receivers moving along the axis of a right circular cylindrical chamber, S. S. Penner—200(L)

Radiation
Conditions for blackbody radiation of gases, Wolfgang Finkelnburg—185
Emissivities of copper and aluminum, George Best—1009
Factors of merit for radiation detectors, R. Clark Jones—344
New classification system for radiation detectors, R. Clark Jones—327
On the ultimate sensitivity and practical performance of radiation detectors, P. B. Fellgett—970
Physiological and pharmacological studies of blood from x-ray personnel, David I. Macht, Marcus Ostero, and Stanley H. Macht—632(A)
Radiant heat transfer to receivers moving along the axis of a right circular cylindrical chamber, S. S. Penner—200(L)
Radiation slide rule and nomographs for the simplification of radiation calculations, Alfred H. Canada—639(A)
Scattered and rescattered sunlight, A. Hammad—157

Refraction
High index refractometer, A. H. Pfund—966
Index of refraction and coefficients of expansion of optical glasses at low temperatures, Fred A. Molby—600
New improved refractometer, A. H. Pfund and E. J. Weichel, and B. H. Billings—631(A)
Refractive indices of water vapor and carbon dioxide at low pressure, Kenneth B. Newbound—835
X-ray images by refractive focusing, Paul Kirkpatrick—796(L)

Spectrographic analysis
Air interrupter for use with the A.R.L. spark source, Emil Kaczor and Katherine Chamberlain—917, 637(A)
Air interrupter type spectrographic light source, J. H. Enns and R. A. Wolfe—298
Characteristics of pulsed arcs in spectrochemical analysis. Part I. Zinc alloys, D. A. Sinclair—958
Comparative results of photographic and direct reading methods of analysis of high alloy steels, W. Magrun, M. Windle, and J. H. Jurmain—1060(A)
D. c. arc source and automatic controller, G. H. Fetterley and W. M. Hazel—1060(A)
Detection of lead in air with the aid of a Geiger-Müller counter, O. G. Koppius—294
Emission spectra of technetium, William F. Meggers and Bourdon F. Scribner—1059(A)
Emulsion calibration paper for quantitative spectroscopic analysis, Harold K. Hughes and R. W. Murphy—637(A)
Extension to the analysis of the infra-red spectra of the noble gases, Curtis J. Humphreys—1059(A)
Fluorophotometric determination of uranium, George R. Price, Renato J. Ferretti, and Samuel Schwartz—1053(A)
Improvement in routine analysis with the Beckman I.R. 2 infra-red spectrophotometer by a slight mechanical modification, A. F. Cornu and P. A. Tardy—613(L)
Influence of extraneous elements on line intensity. IV. Extraneous element effects in the direct-current arc, Wallace R. Brode and Donald L. Timma—478
Introductory study of the spectral characteristics of ferrous alloys, J. Convey and J. K. Hurwitz—1061(A)
Laboratory-cast pin sample for the spectrographic analysis of copper-base alloys, E. W. Palmer, J. P. Irwin, and C. C. Fogg—637(A)
Presentation of adsorption spectra data, W. R. Brode—1022
Quantitative spectrographic analysis of the rare earth elements. III. Determination of major constituents in complex mixtures, Velmer A. Fassel—187
Rapid mobile analyzer for minute amounts of lead in air, Henry Aughey—292
Recent advances in the direct-reading analysis of high percentage alloys, M. F. Hasler—1062(A)
Sensitive fluorophotometers, George R. Price, Renato J. Ferretti, and Samuel Schwartz—1053(A)
Spectra of the heavy elements, Frank S. Tomkins and Mark Fred—357, 637(A)
Spectrographic analysis of high cobalt (vitallium) alloys, Y. T. Sihvonen, D. L. Fry, R. E. Nusbaum, and R. R. Baumgartner—257
Some new techniques in the spectrochemical analysis of non-metallic samples, M. F. Hasler and C. E. Harvey—638(A)
Use of briquetted samples in the spectrochemical analysis of carbon and alloy steels and other metals, J. F. Woodruff—1061(A)

Spectroscopy; spectrometry; spectrophotometry
Aberrations in ellipsoidal mirrors used in infra-red spectrometers, J. Rud Nielsen—59

Absorption spectrum of benzotrifluoride vapor in the near ultraviolet, H. Sponer and D. S. Lowe—840

Absorption spectrum of 1,2,4-trichlorobenzene in the near ultraviolet, Hedwig Kohn and H. Sponer—75

Analysis of elliptical polarization, M. Richartz and Hsien-Yü Hsü—136

Auxiliary working standard equivalent to magnesium oxide on a General Electric spectrophotometer, Joseph W. Gabel and E. I. Stearns—481

Cadmium spectra, A. G. Shenstone and J. T. Pittenger—219

Colorimetry by abridged spectrophotometry, Arthur C. Hardy and F. Mansfield Young—460, 634(A)

Color translating ultraviolet microscopy and ultraviolet spectrophotometry, Elkan R. Blout and Miriam S. Flower—636(A)

Combustion studies with the orthicon spectrograph, J. T. Agnew, R. G. Franklin, R. E. Benn, and A. Bazarian—409(L)

Correction of slit-width errors, Arthur C. Hardy and F. Mansfield Young—265, 638(A)

Detection of lead in air with the aid of a Geiger-Müller counter, O. G. Koppius—294

Direct recording of spectra in the region of 1.2μ to 3μ using the lead sulfide photo-conductive cell, R. C. Nelson—68

Emission spectra of technetium, William F. Meggers and Bourdon F. Scribner—1059(A)

Emission spectrum of manganese-activated magnesium germanate, Stanley H. Patten and Ferd E. Williams—702, 629(A)

Emulsion calibration scale for quantitative spectroscopic analysis, Harold K. Hughes and R. W. Murphy—501

Experimental study of Dennison-Hadley infra-red reflection filters, E. E. Barr—634(A)

Experimental study of Turner frustrated total reflection filters in the infra-red—634(A)

Extensions to the analysis of the infra-red spectra of the noble gases, Curtis J. Humphreys—1059(A)

Further classification of the spectrum of singly-ionized uranium, J. R. McNally, Jr. and G. R. Harrison—636(A)

Image orthicon in spectroscopy, R. E. Benn, W. S. Foote, and C. T. Chase—529

Improvement in routine analysis with the Beckman I.R. 2 infra-red spectrophotometer by a slight mechanical modification, A. F. Cornu and P. A. Tardy—613(L)

Influence of extraneous elements on line intensity. IV. Extraneous element effects in the direct-current arc, Wallace R. Brode and Donald C. Timma—478

Infra-red absorption spectra of ten substituted methanes, Earle K. Plyler and W. S. Benedict—635(A)

Infra-red emission spectra of the oxy-hydrogen and oxy-deuterium flames, S. Silverman and R. C. Herman—216

Infra-red interference filter used in calibration, D. E. Williamson—613(L)

Infra-red microspectroscopy, Elkan R. Blout, George R. Bird and David S. Grey—1052(A)

Infra-red spectrophotometer with cathode-ray display, A. C. Menzies—1061(A)

Laboratory-cast pin sample for the spectrographic analysis of copper-base alloys, E. W. Palmer, J. P. Irwin, and C. C. Fogg—637(A)

Multibanded emission spectra of zinc-cadmium sulfide phosphors, W. H. Byler—91(L)

Multi-slit double monochromator using no moving parts, W. A. Shurcliff—1048(L)

Multi-slit spectrometry, Marcel J. E. Golay—437

New "offset" method of interpreting spectrophotometric curves, W. A. Shurcliff and E. I. Stearns—72

New Raman spectrograph and source, A. C. Menzies—1061(A)

New spectrophotometer employing a glass Fery prism, W. C. Miller, G. Hare, D. C. Strain, K. P. George, M. E. Stickney, and A. O. Beckman—377

New spectrometer for production control quantometer, M. F. Hasler, R. W. Lindhurst, J. W. Kemp, and M. C. Kraushaar—1060(A)

Nomograph of HG5461 structure as a function of etalon separation, J. R. McNally, Jr.—1050(L)

Optical and electrical properties of zinc silicate phosphors, Elemér Nagy—42

Optical theory of the spectral sensitivity of a caesium oxide photo-cathode, Yoshihiro Sayama—162

Optimum absorption, John E. Tyler—264(L)

Orientation of methylene blue molecules adsorbed on solids, Scott Anderson—49

Out of focus diffraction patterns, L. Ivan Epstein—226

Performance of a new double beam infra-red spectrophotometer, John U. White and Max D. Liston—634(A)

Permanence of gloss standards issued to check the photometric scale of spectrophotometers, Kasson S. Gibson and Marion A. Belknap—1055(A)

Photoelectric method of measuring the atmospheric attenuation of brightness contrast along a horizontal path for the visible region of the spectrum, Howard S. Coleman, Fred J. Morris, and Harold E. Rosenberger, and Marshall J. Walker—515

Photographing spectra in the vacuum ultraviolet, A. L. Schoen and Edwin S. Hodge—637(A)

Photographic spectral sensitometry with a biprism, Willoughby M. Cady and Gary Gordon—368

Preliminary investigation of the spectra of uranium isotopes, J. Rand McNally, Jr.—271

Presentation of absorption spectra data, Wallace R. Brode—1022

Production of diffraction gratings. I. Development of the ruling art, George R. Harrison—413

Production of diffraction gratings. II. The design of echelle gratings and spectrographs, George R. Harrison—522

Quantitative spectrographic analysis of the rare earth elements. III. Determination of major constituents in complex mixtures, Velmer A. Fassel—187

Rapid mobile analyzer for minute amounts of lead in air, Henry Aughey—292

Rapid scanning spectrometer for oscillographic recording, B. W. Bullock and S. Silverman—200(L)

Rapid scanning spectrometer for the near infra-red, B. W. Bullock and S. Silverman—634(A)

Reflectance and transmittance measurements of thin evaporated metallic films in the infra-red, Max S. Oldham—634(A)

Resolution of two particles in a bright field by coated microscope objectives, Harold Osterberg and Franklyn C. Wissler—558, 638(A)

Resolving power limitations of grating and prism spectrometers, John Strong—320

Resolving power of a coated objective, Harold Osterberg and J. Ernest Wilkins, Jr.—553

Solar spectroscopy with a Cashman cell, Robert R. McMath and Orren C. Mohler—903

Some new techniques in the construction of spectrographic absorption cells, Gilbert Kivenson, Albert Roth, and Myrtle Rider—484

Spark spectra of elements 43 and 61, D. L. Timma—898

Spectral dispersion of birefringence, especially of birefringent plastic sheets, C. D. West and A. S. Makas—791

Spectroscopy (continued)
- Spectral reflectance measurements in the ultraviolet, Nisson A. Finkelstein—1056(A)
- Spectra of argon, krypton, and xenon between 1.2 and 2.2 microns, W. R. Sittner and E. R. Peck—474, 635(A)
- Spectrographic analysis of high cobalt (vitallium) alloys, Y. T. Sihvonen, D. L. Fry, R. E. Nusbaum, and R. R. Baumgartner—257
- Spectrophotometric studies of living human skin in the ultraviolet, Seibert Q. Duntley, Edward A. Edwards, and Nisson A. Finkelstein—1056(A)
- Torus grating, Heinz Haber—1055(A)
- Use of polytrifluorochloroethylene in infra-red and Raman spectroscopy, J. S. Kirby-Smith and Ernest A. Jones—780

Thin Films on Glass
- Achromatic anti-reflection films, Paul Leurgans—639(A)
- Infra-red transmitting filters, E. R. Blout, R. S. Corley, and P. L. Snow—634(A)
- International colloquium on solid thin films, P. Jacquinot and P. Rouard—1048(L)
- Method for measuring extremely small non-uniformities in the optical thickness of evaporated films, Alan E. Gee and Harry D. Polster—1044
- On a paper by Vašiček concerning reflection from multilayer films, W. L. Wilcock—889(L)
- On the preparation of hard oxide films with precisely controlled thickness on evaporated aluminum mirrors, Georg Hass—532, 632(A)
- Reflectance and transmittance measurements of thin evaporated metallic films in the infra-red, Max S. Oldham—634(A)
- Reflecting power of glass with a thin and with a thick film, Antonin Vašiček—409(L)
- Reflection and transmission formulas for a film on a backing plate, Frank Matossi—928
- Seventy-two-inch high vacuum evaporator and its glow discharge equipment, Nels C. Benson, Georg Hass, and Noel W. Scott—632(A)
- Some properties of thin evaporated films on glass, Joseph L. Rood—854
- Thickness non-uniformities in evaporated films, A. E. Gee and H. D. Polster—1054(A)

Transmission
- Infra-red transmitting filters, E. R. Blout, R. S. Corley and P. L. Snow—634(A)
- Low temperature infra-red transmission cell, H. O. McMahon, R. M. Hainer, and Gilbert W. King—786
- Optical transmission of additively colored alkali halide crystals in the visible and near infra-red, H. Friedman and C. P. Glover—795(L)
- Radiant heat transfer to receivers moving along the axis of a right circular cylindrical chamber, S. S. Penner—200(L)
- Transmission of light from diffuse sources by periscope tubes, F. P. Bundy and H. M. Strong—393; Addendum—698

Ultraviolet
- Absorption spectrum of benzotrifluoride vapor in the near ultraviolet, H. Sponer and D. S. Lowe—840
- Absorption spectrum of 1,2,4-trichlorobenzene in the near ultraviolet, Hedwig Kohn and H. Sponer—75
- Characteristics of fluorescent emission under near ultraviolet, C. E. Barnett and L. D. Grady—627(A)
- Color translating ultraviolet microscopy and ultraviolet spectrophotometry, Elkan R. Blout and Miriam S. Flower—636(A)
- New series of microscope objectives: II. Preliminary investigation of catadioptric Schwarzschild systems, David S. Grey—723
- Photographing spectra in the vacuum ultraviolet, A. L. Schoen and Edwin S. Hodge—637(A)
- Spectral reflectance measurements in the ultraviolet, Nisson A. Finkelstein—1056(A)
- Spectrophotometric studies of living human skin in the ultraviolet, Seibert Q. Duntley, Edward A. Edwards, and Nisson A. Finkelstein—1056(A)
- Ultraviolet characteristics of the high pressure xenon arc, William Baum and Lawrence Dunkelman—1055(A)
- Ultraviolet light sources, Charles H. Matz and Dwight P. Merrill—635(A)
- Vacuum ultraviolet monochromator for absorption and photo-conductivity measurements on luminescent solids, W. W. Parkinson, Jr. and Ferd E. Williams—627(A), 705

Vision, visibility; visual phenomena
- Chromaticity confusions of color defectives, Dean Farnsworth—1056(A)
- Color perceptions of deuteranopic and protanopic observers, Deane B. Judd—252
- Colors of natural objects and terrains, and their relation to visual color deficiency, Charles D. Hendley and Selig Hecht—630(A), 870
- Contrast discrimination charts for demonstrating the effect of anoxia on vision, Selig Hecht, Charles D. Hendley, Sylvia Frank, and Simon Shlaer—922
- Diagnosing types of color deficiency by means of pseudo-isochromatic tests, Alphonse Chapanis—242
- Experimental studies of the reduction of apparent contrast by water, Seibert Q. Duntley—629(A)
- Eye movements and the variation of visual acuity with test object orientation, W. R. J. Brown—1057(A)
- Further remarks on the Stiles-Crawford effect, John R. Platt—614(L)
- Green segment seen from an airplane, E. O. Hulburt—409(L)
- Light quanta and vision, Hl. de Vries—201(L)
- Measurement of meteorological range in water, Seibert Q. Duntley—630(A)
- Microwave test of a theory of the Stiles-Crawford effect, J. N. Jean and Brian O'Brien—1057(A)
- Photopic thresholds for red light in an unselected sample of color deficient individuals, Alphonse Chapanis and R. M. Halsey—1057(A)
- Some notes on the designing of aspherical magnifiers for binocular vision, C. E. Coulman and G. R. Petrie—612(L)
- Standard response functions for protanopic and deuteranopic vision, Deane B. Judd—505(L)
- Theory of the induced effect in binocular vision, Kenneth N. Ogle—1056(A)
- Tritanopia with abnormally heavy ocular pigmentation, Deane B. Judd and Lorenzo Plaza—1056(A)
- Visibility on cathode-ray tube screens. Effect of size and shape of pip, N. R. Bartlett, S. B. Williams, and R. M. Hanes—463
- Visibility on cathode-ray tube screens: Signals on a P-7 screen exposed for different intervals, N. R. Bartlett and A. L. Sweet—470
- Visibility on cathode-ray tube screens: Viewing angle, Stanley B. Williams—782
- Visual acuity through various types and grades of sun glass lenses, R. H. Peckham—1057(A)
- Visual sensitivities to combined chromaticity and luminance differences, W. R. J. Brown and D. L. MacAdam—808

2

5

n-
id

L.

on

he
ls,

rc,

P.

nd
ls,
),

ns-

rs,

on
rig

ect
ey,

lo-

ast

est

R.

:—

Q.

ect,

ple
and

for
:—

pic

eth

on,

and
M.

P-7
and

gle,

sun

nce
808